รายงานวิจัยฉบับสมบูรณ์

โครงการ

กลไกการควบคุมการแสดงออกของยีนที่เกี่ยวข้อง ในกระบวนการสร้างไวเทลโลจีนินในกุ้งกุลาดำ

Molecular mechanism controlling expression of genes that are involved in vitellogenesis in *Penaeus monodon*

โดย

รองศาสตราจารย์อภินันท์ อุดมกิจ

สถาบันชีววิทยาศาสตร์โมเลกุล มหาวิทยาลัยมหิดล

31 กรกฎาคม 2561

สัญญาเลขที่ BRG5880005

รายงานวิจัยฉบับสมบูรณ์

โครงการ

กลไกการควบคุมการแสดงออกของยีนที่เกี่ยวข้อง ในกระบวนการสร้างไวเทลโลจีนินในกุ้งกุลาดำ

Molecular mechanism controlling expression of genes that are involved in vitellogenesis in *Penaeus monodon*

โดย

รองศาสตราจารย์อภินันท์ อุดมกิจ

สถาบันชีววิทยาศาสตร์โมเลกุล มหาวิทยาลัยมหิดล

สนับสนุนโดยสำนักงานกองทุนสนับสนุนการวิจัยและ

มหาวิทยาลัยมหิดล

(ความเห็นในรายงานนี้เป็นของผู้วิจัย สกว. และมหาวิทยาลัยมหิดลไม่จำเป็นต้องเห็นด้วยเสมอไป)

บทคัดย่อ

รหัสโครงการ: BRG5880005

ชื่อโครงการ: กลไกการควบคุมการแสดงออกของยีนที่เกี่ยวข้องในกระบวนการสร้างไวเทลโลจีนินในกุ้งกุลาดำ

ชื่อนักวิจัย: อภินันท์ อุดมกิจ
สถาบันชีววิทยาศาสตร์โมเลกุล
มหาวิทยาลัยมหิดล ศาลายา
นครปฐม 73170
E-mail: apinunt.udo@mahidol.ac.th

ระยะเวลาโครงการ: 31 กรกฎาคม 2558 ถึง 30 กรกฎาคม 2561

การสังเคราะห์ไวเทลโลจีนินเป็นกระบวนการสำคัญสำหรับการพัฒนารังไข่ในกุ้ง ซึ่งถูกควบคุมด้วยฮอร์โมนยับยั้งการพัฒนารังไข่ (GIH) ที่สร้างจากปมประสาทในก้านตา อย่างไรก็ตามกลไกการควบคุมการสร้างไวเทลโลจีนินโดยฮอร์โมน GIH ยังไม่มีการศึกษาในรายละเอียด โครงการนี้จึงมีวัตถุประสงค์เพื่อศึกษาการควบคุมการแสดงออกของยีนที่สร้าง GIH และไวเทลโลจีนิน (Vg) และศึกษาผลของ GIH ต่อการแสดงออกของยีนในรังไข่ว่ามีความสัมพันธ์กับการสร้างไวเทลโลจีนินอย่างไร โดยการโคลนชิ้นดีเอ็นเอทางปลาย 5’ ของยีน *GIH* และยีน *Vg* ซึ่งเป็นส่วนที่ควบคุมการแสดงออกของยีน พบว่าบริเวณดังกล่าวมีลำดับนิวคลีโอไทด์ที่เป็นบริเวณจับของ transcription factors หลายชนิด ที่น่าสนใจคือบริเวณจับของตัวตอบรับนิวเคลียร์ retinoid-X receptor (RXR) ซึ่งพบทั้งในลำดับนิวคลีโอไทด์ทางปลาย 5’ ของยีน *GIH* และยีน *Vg* อย่างไรก็ตามสามารถยืนยันการจับของโปรตีน RXR กับบริเวณจับที่ปลาย 5’ ของยีน *Vg* เท่านั้น การยับยั้งการแสดงออกของยีน *PmRXR* ในแม่พันธุ์กุ้งด้วยอาร์เอ็นเอสายคู่ที่จำเพาะส่งผลให้มีการแสดงออกของยีน *Vg* ในรังไข่ลดลง แสดงให้เห็นว่าการจับของโปรตีน PmRXR บนบริเวณจับทางปลาย 5’ ของยีน *Vg* น่าจะช่วยให้มีการกระตุ้นการแสดงออกของยีน *Vg* นอกจากนี้ยังพบว่าการยับยั้งการแสดงออกของยีน *GIH* ส่งผลต่อระดับการแสดงออกของยีนหลายชนิดในรังไข่ของกุ้ง หนึ่งในนั้นได้แก่ยีนที่สร้างโปรตีน calreticulin (CRT) ซึ่งมีการแสดงออกที่ลดลงในสภาวะที่ยีน *GIH* ถูกยับยั้ง CRT เป็นโปรตีนที่สามารถจับกับตัวตอบรับนิวเคลียร์ และขัดขวางการทำงานของตัวตอบรับนิวเคลียร์ การทดลองนี้พบว่าเมื่อการแสดงออกของยีน *PmCRT* ถูกยับยั้งจะทำให้มีระดับการแสดงออกของยีน *Vg* ที่สูงขึ้น และสามารถยืนยันการจับกันระหว่างโปรตีน PmRXR และ PmCRT ได้ ซึ่งผลการทดลองทั้งหมดแสดงให้เห็นว่า การ

แสดงออกของยีน *Vg* ถูกควบคุมด้วยโปรตีน PmRXR และ PmCRT การศึกษาที่ผ่านมาพบว่าในแม่พันธุ์กุ้งระยะ previtellogenic ที่ยังไม่มีการพัฒนารังไข่ จะมีระดับฮอร์โมน GIH สูง ซึ่งจะมีโปรตีน CRT ที่สามารถจับกับ RXR ทำให้ RXR ไม่สามารถจับกับบริเวณจับบนยีน *Vg* ได้ ส่งผลให้ไม่มีการแสดงออกของยีน *Vg* เมื่อกุ้งมีการพัฒนารังไข่จะมีระดับฮอร์โมน GIH ลดลง ซึ่งส่งผลให้ CRT ลดลง และไม่สามารถขัดขวางการจับของ RXR กับบริเวณจับบนยีน *Vg* ทำให้มีการกระตุ้นการแสดงออกของยีน *Vg* และส่งผลให้มีการพัฒนารังไข่ได้ ผลงานวิจัยจากโครงการนี้ทำให้ทราบถึงกลไลในการควบคุมการแสดงออกของยีนไวเทลโลจีนิน ซึ่งจะเป็นประโยชน์ต่อการพัฒนาวิธีการกระตุ้นการวางไข่ในแม่พันธุ์กุ้งต่อไป

คำสำคัญ กุ้ง gonad-inhibiting hormone ไวเทลโลจีนิน regulatory factor การพัฒนารังไข่

Abstract

Project Code: BRG5880005

Project Title: Molecular mechanism controlling expression of genes that are involved in vitellogenesis in *Penaeus monodon*

Investigator: Assoc. Prof. Apinunt Udomkit

Institute of Molecular Biosciences

Mahidol University, Salaya Campus

Nakhon Pathom 73170

E-mail Address: apinunt.udo@mahidol.ac.th

Project Period: 31 July 2015 – 30 July 2018

Vitellogenin synthesis or vitellogenesis is an essential process required for ovarian maturation in crustaceans. Vitellogenesis is negatively regulated by an eyestalk neuropeptide called a gonad-inhibiting hormone (GIH). However, the mechanism through which GIH regulates vitellogenin (Vg) expression is not well studied so far. This study is aimed at investigation of transcriptional regulation of *Vg* expression and study the effect of GIH on expression of genes in the ovary of *Penaeus monodon* that may be related to the regulation of Vg synthesis. Identification of the 5' regulatory sequence of *GIH* and *Vg* genes revealed several potential binding sites for the retinoid-x-receptor (RxR), a nuclear receptor that is shown to stimulate ovarian development in carb. However, the result from electrophoretic mobility shift assay showed that RXR binds to *Vg* but not to *GIH* 5' regulatory sequence. Suppression of *RXR* expression by specific double-stranded RNA resulted in a decrease level of *Vg* transcript suggesting that the binding of RXR to its response element upstream of *Vg* gene is probably required for *Vg* expression. In addition, the result from suppression subtractive hybridization has identified calrecticulin (PmCRT) as one of down-regulated genes in the ovary of GIH-knockdown shrimp. The binding of calreticulin to steroid receptor prevents the binding of the receptor to its response element to regulate gene expression. The result in this study showed that PmCRT knockdown shrimp showed an increased *Vg* expression level. Furthermore, in vitro pull-down assay revealed the binding between RXR and CRT. Taken together, these results suggest that PmCRT may be an inhibitory mediator of vitellogenin synthesis by interfering the binding of RxR to its binding site on *Vg* 5' regulatory sequence. This project therefore provides an insight into the control mechanism of

viellogenesis, which will be useful for development of hormonal manipulation strategy to achieve maximum reproductive performance of the shrimp.

Keywords shrimp; gonad-inhibiting hormone; vitellogenin; regulatory factors; ovarian maturation

Executive summary

Project Code: BRG5880005

Project Title: Molecular mechanism controlling expression of genes that are involved in vitellogenesis in *Penaeus monodon*

Investigator: Assoc. Prof. Apinunt Udomkit

Institute of Molecular Biosciences

Mahidol University, Salaya Campus

Nakhon Pathom 73170

E-mail Address: apinunt.udo@mahidol.ac.th

Project Period: 31 July 2015 – 30 July 2018

Enhancement of reproductive maturation in captive shrimp broodstock is important for shrimp aquaculture. Although, it is known that vitellogenin synthesis, the process that is crucial for ovarian maturation in shrimp is controlled by a gonad-inhibiting hormone (GIH), its detailed mechanism is not well established. This study is aimed at investigation of transcriptional regulation of vitellogenin (*Vg*) gene expression and study the effect of GIH on expression of genes in the ovary of the black tiger shrimp, *Penaeus monodon* that may be related to the regulation of Vg synthesis.

In order to understand the regulation of *GIH* and *Vg* gene, the 5' upstream sequences of both genes were obtained by genome walking strategy. Identification of the 5' regulatory sequence of *GIH* and *Vg* genes revealed potential binding sites of several transcription factors. One of these are the putative binding sites of a retinoid-x-receptor (RxR), a nuclear receptor that is shown to stimulate ovarian development in the carb. The recombinant DNA binding domain of PmRXR was produced and was shown by electrophoretic mobility shift assay to be able to binds only with the 5' regulatory sequence of *Vg* gene, but not with that of the *GIH* gene. Therefore, only the role of PmRXR on *Vg* gene expression was further investigated. Suppression of *PmRXR* expression by specific double-stranded RNA (dsRNA) resulted in a decrease level of *Vg* transcript suggesting that the binding of PmRXR to its response element upstream of *Vg* gene is probably required for *Vg* expression.

In addition, the effect of GIH on expression of genes in the ovary was studied by suppression subtractive hybridization (SSH) between GIH-knockdown shrimp and the control shrimp. GIH-knockdown was carried out by specific dsRNA, and the increase in *Vg*

expression levels in GIH-knockdown shrimp was confirmed by RT-PCR. The results form SSH revealed several genes, the expression of ahich were either up- or down-regulated under GIH-knockdown condition. Among these genes, calrecticulin (*PmCRT*) is one of the down-regulated genes in the ovary of GIH-knockdown shrimp. The binding of calreticulin to steroid receptor prevents the binding of the receptor to its response element to regulate gene expression. The possible function of *PmCRT* in regulating *Vg* expression was determined by specific knockdown of *PmCRT* by dsRNA. The result showed that in *PmCRT*-knockdown shrimp, the expression levels of *Vg* was up-regulated by 30% when compared with the control shrimp, suggesting a negative effect of *PmCRT* on *Vg* expression. Since our results suggest that PmRXR may bind to its response element on *Vg* genes to induce *Vg* gene expression, we further investigated whether PmCRT regulates *Vg* expression by interfere with the binding of PmRXR to its response elements. In order to verify this, the recombinant N-terminal domain of PmCRT was produced, and used in the *in vitro* pull-down assay to investigate the binding between PmCRT and PmRXR. The result revealed that both proteins could be detected in the pull-down complex suggesting that PmCRT could bind to PmRXR.

Taken together, our results suggest that in immature or pre-vitellogenic female shrimp where the *GIH* is expressed at high levels, *PmCRT* should also be highly expressed. PmCRT could therefore bind to PmRXR and prevents the binding of PmRXR to its response elements on the 5' upstream regulatory sequence of *Vg* gene resulting in low *Vg* expression levels. By contrast, in the early-vitellogenic female shrimp, the expression of *GIH* was reduced, and thus PmCRT expression should also be down-regulated, PmRXR can bind to its response element and induce *Vg* expression.

This project therefore provides an insight into the control mechanism of viellogenesis, which will be useful for development of hormonal manipulation strategy to achieve maximum reproductive performance of the shrimp.

Introduction

Vitellogenesis is a principal process during ovarian maturation in crustaceans. Vitellogenesis can be divided into two phases: the synthesis of vitellogenin (Vg), a yolk precursor and the accumulation of a yolk protein or vitellin into oocytes. In the black tiger shrimp *Penaeus monodon*, Vg is synthesized in both the ovary and hepatopancreas like in other penaied shrimps (Avarre et al., 2003; Phiriyangkul and Utarabhand, 2006; Tsang et al., 2003; Tseng et al., 2001; Tsutsui et al., 2000; Xie et al., 2009). Following its synthesis, Vg is proteolytically cleaved into smaller subunits and deposited into developing oocytes before undergoing further biochemical modifications into vitellin, a major source of nutrient during embryogenesis (Wilder et al., 2010).

A cDNA encoding vitellogenin was cloned and characterized in a number of penaeid shrimps e.g. *Penaeus japonicus* (Tsutsui et al., 2000), *Litopenaeus vannamei* (Raviv et al., 2006, *Penaeus merguiensis* (Phiriyangkul and Utarabhand, 2006), *Fenneropenaeus chinensis* (Xie et al., 2009) and *P. monodon* (Tseng et al., 2001). The expression of *Vg* in penaeid shrimps was found in both the ovary and hepatopancreas. On the other hand, the genome of *Metapenaeus ensis* contains two different genes that encode for MeVg1 and MeVg2. While MeVg1 was expressed in both tissues as the Vg in other shrimps, MeVg2 was demonstrated to be a hepatopnacreas-specifc form. (Tsang et al., 2003). The presence of two types of Vg was also reported in the Pandalus shrimp, *Pandalopsis japonica* where one type showed hepatopancreas-specific expression similar to that of *M. ensis* (Jeon et al., 2010). The ovary and hepatopancreas may have unequal contribution to vitellogenesis as *Vg* was expressed at different levels in both tissues. Therefore, the regulation of *Vg* gene expression may be distinct in the ovary and the hepatopancreas.

The information about the promoter and regulatory regions of *Vg* gene is still very limited. Only the 5' flanking region of *MeVg2* gene was reported so far. In addition to TATA element and binding sites of general transcription factors such as SP1and GATA, several clusters of heat shock factor binding site (HSE) were also identified in the 5' flanking region of *MeVg2* gene (Chan et al., 2014). The heat shock cognate 70 (Hsc70) was suggested to be a molecular chaperone that negatively regulates *MeVg2* expression through the formation of a repressor complex with heat shock factor (HSF). Similarly, MeVg1 was also demonstrated to be under the control of Hsp90. Because the expression of *MeHsp90* in the immature ovary was induced by the addition of estradiol-17β, it was suggested that *Vg* expression in *M. ensis* is probably regulated by estrogen hormone similar to that in vertebrates (Wu and Chu, 2008).

This was supported by the occurrence of several vertebrate type-steriod hormones such as estradiol-17β, progesterone, testosterone, and 17α-hydroxyprogesterone (Fingerman et al., 1993; Cardoso et al., 1997).

Vitellogenesis in crustaceans is influenced by two major hormones: a gonad-inhibiting hormone and a gonad-stimulating hormone. A substance containing gonad-stimulating activity was found to reside in the thoracic ganglia. Yano, 1992 and Yano et al., 1998 showed that vitellogenesis in the shrimp could be induced by either implantation of thoracic ganglion or injection of ganglia extract. Nevertheless, a protein responsible for this gonad-stimulating activity has not yet been identified so far. By contrast, a gonad-inhibiting hormone (GIH) is well characterized in a number of crustaceans (Soyez et al., 1991; Edomi et al., 2002; Treerattrakool et al., 2008; Nagaraju, 2011). GIH is a member of the CHH hormone family that is synthesized and stored in the X-organ-sinus gland neurosecretory system in the eyestalk. Other members of the CHH family include crustacean hyperglycemic hormone (CHH), molt-inhibiting hormone (MIH) and mandibular organ-inhibiting hormone (MOIH). It is generally known that eyestalk ablation can stimulate ovarian maturation in the shrimp (Browdy, 1992). Our group demonstrated previously that *Vg* gene expression as well as ovarian maturation of *P. monodon* was induced when the *GIH* expression was suppressed by a specific double-stranded RNA (dsRNA) (Treerattrakool et al., 2008; Treerattrakool et al., 2011). These results suggest that GIH is an eyestalk factor that retards ovarian maturation via inhibition of vitellogenin expression. The inhibitory role of GIH on vitellogenesis was also supported by the detection of GIH levels in the hemolymph of an American lobster (Homarus americanus) that showed a high level of hemolymph GIH during immature and previltellogenic stages before declining in later stages of vitellogenesis (de Kleijn et al., 1998). Our recent study in *P. monodon* also showed a similar pattern of hemolymph GIH levels during vitellogenesis (Urtgam et al., 2015). However, the detailed mechanism through which GIH regulates *Vg* expression is not well studied.

At present, the control of *GIH* expression in the shrimp has not been investigated. Only a few studies on the structure and the promoter region of the other genes encoding hormones in the CHH family were reported. Binding sites of transcription factors such as CAAT-binding factor and AP1 were found in the 5' flanking sequences of CHH, MIH and MOIH genes (Gu and Chang, 1998; Gu et al., 2000; Lu et al., 2000; Wiwegweaw et al., 2006). In addition, the presence of a binding site for cyclic AMP responsive element binding protein (CREB) upstream of the genes encoding CHH family members implies that the

expression of these genes is mediated by cAMP via the cAMP/PKA signaling pathway. These findings suggest that the genes in the CHH family are probably under the control of similar mechanisms.

One of the major problems in shrimp fry production in the hatcheries is the reduced reproductive performance of the captive broodstock. Consequently, elimination of GIH synthesis site by eyestalk ablation has been used to induce ovarian maturation and spawning (Browdy, 1992). However, the repeated spawning after eyestalk ablation eventually resulted in deterioration in both the quality and quantity of eggs (Benzie, 1998). Furthermore, eyestalk ablation is considered an unethical practice, the issue that becomes more concern in the shrimp trading worldwide. Since the black tiger shrimp, *Penaeus monodon* is one of the important farmed species in Thailand, an in-depth knowledge about the mechanism underlying ovarian maturation in *P. monodon* is therefore necessary for future development of an alternative method to induce ovarian maturation in the female broodstock. The understanding of the control mechanism of viellogenesis will be useful for hormonal manipulation methods to achieve maximum reproductive performance of the shrimp.

Objectives

1. to study a promoter and regulatory sequences of *GIH* and *Vg* genes of *P. monodon*
2. to identify and characterize regulatory sequence-binding factors that may regulate *GIH* and *Vg* genes
3. to investigate the effect of GIH on the control of vitellogenin gene expression

Materials and Methods

Identification of putative promoter and regulatory sequences of *GIH* and *Vg* genes

To identify a promoter and regulatory sequences of *GIH* and *Vg* genes of *Penaeus monodon*, the 5' upstream sequences of both genes were cloned and analyzed for the presence of a putative promoter and regulatory sequences. The genomic DNA from shrimp abdominal muscle tissue was used for genome walking using the Universal GenomicWalkerTM kit (CLONTECH, Palo Alto, USA) to obtain the 5' unknown DNA fragment harboring the sequence upstream of transcriptional region of both genes. Briefly, the genomic DNA approximately 2.5 μg/reaction were digested to generate blunt-ended genomic fragments by 4 different restriction enzymes (*Dra*I, *Eco*RV, *Hpa*I, *Sna*BI). Then, each digested genomic DNA was ligated into the Genome Walker Adapter, which was referred to as a Genomic Walker library. The 5' unknown flanking sequences of *GIH* and *Vg*

genes were amplified from each genome walker library with adapter primers and gene specific primers, and subsequently cloned in to pGEMT Easy vector. The nucleotide sequences of these 5' upstream DNA fragments were determined by the ABI PRISMTM BigDye Terminator Cycle Sequencing Kit (Applied Biosystems, Foster City, USA). The prediction of the putative promoter and regulatory sequences in the 5' upstream fragment was performed by TF sitescan software on the MIRAGE www server (http://www.ifti.org/ cgibin/ifti/Tfsitescan.pI) compared to PROMH (G) software on the softberry www server (http://linux1. softberry.com/ all.htm), and the transcription start site was predicted by NNPP program (http://www.fruitfly.org).

Preparation of nuclear protein extracts for determination of the binding of nuclear factors to the 5' upstream regulatory sequences of *GIH* and *Vg* genes

To validate the binding of nuclear factors on the predicted regulatory sequences, an electrophoretic mobility shift assay (EMSA) was performed. For the factors binding to the *GIH* regulatory sequence, the nuclear extract was prepared from shrimp eyestalk ganglia that is the synthesis site of GIH. The nuclear extract from the ovary was prepared for determining the binding factors of *Vg* regulatory sequence. The extraction method of Dimaruo et al., 2013 (BMC Research Notes 2012, 5:513) was followed with some modifications. The concentration of proteins in each extract was analyzed by Bradford protein assay (BIO-RAD) according to the manufacture's protocol, and the protein patterns were determined on 15 % SDS-PAGE. The present of histone proteins in the nuclear extract was confirmed by western blot analysis with 1:10,000 polyclonal anti-human histone 3 (Abcam; ab1791).

Identification of regulatory sequence-binding factors that bind to the promoter region of *GIH* and *Vg* genes

To identify the binding of nuclear factors on the predicted regulatory sequences of GIH and Vg genes, an electrophoretic mobility shift assay (EMSA) was performed. The nuclear factors that bind to the regulatory sequences were excised from SDS-PAGE and characterized by tandem mass spectrometry.

3' end labeling of the DNA fragments with biotin

In order to prepare DNA probe for EMSA, biotin 3' end DNA labeling was performed using biotin 3' end DNA labeling kit (Thermo Scientific). The procedure of this kit is optimized for labeling 5 pmol of 3'-OH ends in each reaction. Firstly, 2 U/µl of working TdT was prepared by diluting 1 µL of 20 U/µl TdT stock with 2 µL 5xTdT reaction buffer and 7 µL of ultrapure water. Then, the reaction of labeling was prepared by mixing 5 pmol of purified DNA with 1xTdT reaction buffer, 0.5 µM of Biotin-11-UTP, 0.2 U/µl of diluted

TdT, and the total volume was adjusted to 50 µl by ultrapure water. After mixing the reaction gently, the reaction was incubated at 37ºC for 30 minutes, and, 2.5 µl of 0.2 M EDTA was added to stop reaction. Then, 50 µl of chloroform:isoamyl alcohol (1:1) was added into the reaction followed by centrifugation at 13,000 rpm for 2 minutes. Finally, the upper phase was transferred to the new tube and use as DNA probe for EMSA.

Electrophoretic mobility shift assay (EMSA)

The DNA-protein binding reaction between 2 µg of nuclear extracts (eyestalk nuclear protein for *GIH* regulatory fragment (GIH-TF) probe, ovarian nuclear protein for *Vg* regulatory fragment (Vg-TF) probe and muscle nuclear protein for negative control) and 10 fmol of each probe were mixed with 1x binding buffer, 100 ng of poly dI-dC, and the reaction volume was adjusted to 8.0 µl by ultrapure water. The reactions were incubated at room temperature for 30 min. For competition assay, 50 to 200-fold of an unlabeled DNA fragment was added to the reaction and incubated at room temperature 10 minutes before the addition of the DNA probe. In addition, an unrelated probe, 550 bp of actin DNA fragment, was used as a non-specific competitor. Two microliters of 5x loading dye buffer were added to the binding the reaction before the reaction was applied on native polyacrylamide gel followed by running in 0.5xTBE buffer at 100 V for 1 hr. Then, the DNA-protein complex in the gel was transferred to a nylon membrane in 0.5xTBE buffer for 90 minutes at 4O°C. Finally, the membrane was subjected to detection by LightShift® Chemiluminescent EMSA Kit (Thermo Scientific) according to the manufacture's protocol.

Identification of the regulatory sequence-binding factors of GIH and Vg genes

In order to identify the factors that bind to the regulatory sequences of *GIH* and *Vg* genes, the binding complexes were analyzed on SDS-PAGE. The bands of proteins presented in the complexes were excised and characterized by tandem mass spectrometry (LC MS/MS) at Proteomic center, faculty of Medical technology, Mahidol University. Then, their amino acid sequences were analyzed by Mascot search software server against NCBI and Swissprot databases.

Functional study of Retenoid X receptor (RXR) in regulating the expression of *GIH* and *Vg* genes

Because the putative binding sites of RXR were identified in the regulatory sequences of both *GIH* and *Vg* genes, its cDNA was cloned and characterized. In addition, the function of PmRXR in regulating the expression of *GIH* or *Vg* genes will be studied by *in vivo* RNA silencing by specific dsRNA.

cDNA cloning of PmRXR coding region

Total RNA was extracted from the ovary of previtellogenic female *P. monodon* using Trizol Reagent (Invitrogen, USA) following the manufacturer's protocol. RNA quality was determined by ND-1000 spectrophotometer, and RNA integrity was detected by electrophoresis on 1.2% agarose gel. The first strand cDNA was synthesized by using PRT-oligo-dT16 primer, and reverse transcriptase followed the condition: 25°C for 5 min, 42 °C for 60 min, and 70°C for 15 min. To amplify an open reading frame (ORF) of PmRXR, specific primers were designed from the conserved sequences of RXR of other penaeid shrimps (29). The PCR reaction contained 1 µl of first stand cDNA, 0.3 mM of dNTPs, 1x long range buffer, 1.75 mM MgCl2, 0.5 µM Pm-CDSRXR-F primer, 0.5 µM PmCDSRXR-R primer, 1.25 U KAPA LongRange DNA polymerase, and adjusted to 25 µl by distilled water. The PCR reaction was performed with the following parameters: 94°C for for 2 min; 35 cycles (94°C for 15 sec; 55°C, 15 sec; 68°C, 2 min); and a final extension at 72°C for 3 min. The specifically amplified product was ligated into the pGEM®-T easy vector (Promega) and used to transform into Escherichia coli DH5α. The nucleotide sequence of PmRXR was determined by automated DNA sequencing (1st BASE Laboratories Sdn Bhd, Malaysia). An ORF was identified using the ORF finder available from NCBI database.

Expression profile of PmRXR in P. monodon

To detect the expression of PmRXR in shrimp tissues, total RNA was extracted from tissues of pre-vitellogenic stage female shrimp; brain, eyestalk, thoracic ganglion, abdominal ganglion, heart, muscle, gill, hepatopancreas, and ovary. One microliter of cDNA form these tissues were used to amplify PmRXR with primers RXR-F and RXR-R, whereas an internal control actin was amplified with actin-F and actin-R primers. In addition, to determine PmRXR expression upon ovarian maturation, the expression of PmRXR in the ovary at different stages was determined by RT-qPCR using KAPA SYBR® FAST qPCR kit (KAPABIOSYSTEMS, USA) according to the manufacture's protocol. The relative gene transcript levels were calculated using $2^{-\Delta\Delta Ct}$ method using EF-1α as an internal control.

Functional study of PmRXR in regulating the expression of GIH or Vg genes

The function of PmRXR in regulating the expression of *GIH* or *Vg* genes was studied by RNA interference approach. Firstly, the dsRNA targeting *PmRXR* (dsRXR) was produced as a stem-loop precursor; a cDNA encoding PmRXR was used to design specific dsRNA targeting a ligand-binding domain, and produced in a bacteria expression system. Briefly, the DNA template of the 480 bp stem-loop of dsRNA was amplified with primers SL-eRXR F-XbaI, and SL-eRXR R-BamHI. Another DNA template for the 400 bp stem of dsRNA, was

amplified with primers ST-eRXR F-XhoI and ST-eRXR R-BamHI. The stem-loop fragment was first cloned into pET17b vector at *Xba* I and *Bam*H I sites, following by the stem at *Xho* I and *Bam*H I. Then, the recombinant eRXR-pET17b expression cassette was used to transform *E. coli* strain DH5-α. The expression of a stem-loop specific dsRNA targeting *PmRXR* was carried out by 0.4 mM IPTG induction in 2xYT medium for 4 hr at 37°C with shaking. The extraction of stem-loop dsRNA was performed by Tri-solution in the presence of RNaseA before dissolved in 150 mM NaCl and stored at -30°C until use. Determination of the concentration and purity of dsRNA was monitor by agarose gel electrophoresis. The quality of dsRNA was verified by RNase digestion assay.

To test whether *PmRXR* has any effect on the expression of *GIH* and *Vg* gene or not, the expression of *GIH* and *Vg* were determined upon *PmRXR* knockdown in female shrimp. Previtellogenic female wild shrimp or vitellogenic female shrimp were divided into three group; shrimp injected with NaCl as a negative control; shrimp injected with dsRXR (2.5 μg/g body weight of shrimp); and shrimp injected with dsGFP (2.5 μg/g body weight). Then, the eyestalk and ovary of shrimp in each group were dissected on days 5 or day 10 after injection and used for isolation of total RNA. The first strand cDNA was synthesized, and suppression of *PmRXR* transcript in the eyestalk ganglia and ovary were determined by semi-quantitative RT-PCR using cDNA obtained as described above comparing with that of the control NaCl and dsGFP injected shrimp. The effect of PmRXR-knockdown on *GIH* expression in the eyestalk or *Vg* expression in the ovary was also determined by semi-quantitative RT-PCR.

Determination of the binding of PmRxR to the 5' upstream region of *Vg* gene

Construction of recombinant plasmid expressing recombinant PmRxR/MBP-6xhis fusion protein

The DNA fragment encoding the DNA-binding domain of PmRxR (DBD-RXR) were obtained by PCR for expression of recombinant proteins in a reaction containing 10 ng of FL-RXR/pGEM plasmid, 0.3 mM of dNTPs, 1x long range buffer, 1.75 mM $MgCl_2$, 0.5 μM DBD-RXR F-XhoI primer, 0.5 μM DBD-RXR R-KpnI primer, 1.25 U KAPA LongRange DNA polymerase, and adjusted 25 μl by distilled water. The PCR reaction was performed with the following parameters: 94°C for for 2 min; 35 cycles of 94°C for 15 sec; 55°C, 15 sec; 68°C, 2 min, and a final extension at 72°C for 3 min.

The PCR fragment of DBD-RXR were ligated to pGEM-T easy (Promega), and transformed to *E. coli* DH5-α strain then, the positive transformants were determined by

digestion with *Xho* I and *Kpn* I restriction enzymes. The DBD-RXR fragment was then sub-cloned into pSY7 expression plasmid that had been digested with same enzymes. The ligated product was transformed to *E. coli* DH5-α stain, and the nucleotide sequences of the transformant clones were determined by automated DNA sequencing (1st BASE Laboratories Sdn Bhd, Malaysia). The positive clone was re-transformed to *E. coli* stain BL21 DE3)pLysS).

Expression and purification of recombinant DBD-RXR protein

A single colony of *E. coli* BL21 DE3(pLysS) harboring the DBD-RXR-pSY7 recombinant plasmid was inoculated into 10 ml of LB broth containing of 300 µg/µl kanamycin and 34 µg/µl chloramphenicol. The cultures were incubated overnight at 37 ^{o}C, 250 rpm, then diluted at 1:50 in 100 ml of LB broth containing of the same antibiotics as above. The culture was grown at 30 ^{o}C until OD_{600} reached 0.4-0.6. Then, the culture was induced by 0.4 mM IPTG, and incubated at 30 ^{o}C for 4 h. After that, the cells were harvested at 6,000 rpm for 15 min, 4 ^{o}C. The supernatant was discarded, and cell pellet was kept at -30 ^{o}C until used.

The recombinant DBD-RXR/MBP-6xhis fusion protein expressed from DBD-RXR-pSY7, and MBP-6xhis protein from pSY7 plasmid were purified using HisTrapFF columns (GE Healthcare). Approximately 100 OD of DBD-RXR/MBP-6xhis, and MBP-6xhis expressed *E. coli* lysates were purified in 1 ml column, which was equilibrated with binding buffer (20 mM sodium phosphate, 0.5 M NaCl, 20–40 mM imidazole, pH 7.4). The histidine bound column was washed with binding buffer for at least 3 times. After wash, the protiens were eluted from the column with a series of elution buffer (20 mM sodium phosphate, 0.5 M NaCl, 100- 500 mM imidazole, pH 7.4). The purified proteins were analyzed with 15% SDS-PAGE and western blotting using 1:8,000 anti-6xhis monoclonal antibody (Abcam).

Determination of the binding between recombinant DBD-RXR and VgTF probes

To verify the binding of RXR on the predicted regulatory sequence of *Vg* gene, an electrophoretic mobility shift assay (EMSA) was performed. Based on previously studied, the truncated probe fragments of *Vg* upstream regions, VgTF1 and VgTF3, that contain putative RXR binding sites formed large complexes with the ovary nuclear extract. These probes were therefore used to verify the binding of recombinant DBD-RXR. The DNA-protein binding reactions containing 0 to 4 µg of recombinant DBD-RxR/MBP-6x his were added to 10 fmol of each probe mixed with 1X binding buffer, 100 ng of poly dI-dC, and adjusted the volume to 8.0 µl by ultrapure water. The reactions were incubated at room temperature for 30 minutes. After the addition of 2.0 µl of 5X loading dye buffer to the binding reactions and

mixed well, the reactions were applied on native polyacrylamide gel followed by running in 0.5X TBE buffer at 100 V for 1 hour. Then, the DNA-protein complex in the gel was transferred to a nylon membrane in 0.5X TBE buffer for 90 minutes at 4oC. Finally, the membrane was subjected to detection by LightShift® Chemiluminescent EMSA Kit (Thermo Scientific) according to the manufacture's protocol.

Investigation of the effect of *GIH* on gene expression profile in the ovary

A change in gene expression in the ovary that may act downstream of GIH was determined by suppression substractive hybridization (SSH) between *GIH*-knockdown shrimp and the control shrimp. Furthermore, a role of potential genes that may be involved in the regulation of *Vg* gene expression will be further studied by RNAi technology.

To test whether GIH has any effect on global gene expression in shrimp ovary or not, previtellogenic female shrimp (approximately 20 g) was divided into two groups; shrimp injected with .3 μg/g shrimp body weight of GIH-dsRNA kindly provide by Dr. Supattra Treerattrakool, Mahidol University, and control shrimp that were injected with GFP-dsRNA for five days. Then, the ovaries were dissected and homogenized in TRI-REAGENT® (Molecular Research Center). The first strand cDNA was synthesized by using PRT-oligo-dT12 primer, and reverse transcriptase followed the condition: 25°C for 5 min, 42 °C for 60 min, and 70 °C for 15 min. The suppression of GIH transcript in the eyestalk ganglia and the expression of *Vg* gene in the ovary of the GIH-dsRNA inject shrimp was determined by semi-quantitative RT-PCR comparing with that of the control (GFP-dsRNA injected) shrimp.

Examination of global gene expression in the ovary under GIH-knockdown condition

In order to study the genes downstream of GIH that may be involved in the regulatory pathway of *Vg* gene expression, changes in gene expression in the ovary of the GIH-knockdown shrimp was determined by suppression subtractive hybridization (SSH), using a PCRTM cDNA subtraction kit (Clonetech) according to the manufacture's protocol. The cDNA from the *GIH*-knockdown shrimps were used as tester or driver cDNAs, to determine genes that are up-regulated or down-regulated upon GIH knock-down, respectively. The cDNA fragments obtained from each subtractive library were cloned, and their nucleotide sequences were determined and processed by removing the unwanted vector and primer sequences using Bio-Edit program. The homolog sequences were searched on the blastn and blastx program at NCBI GenBank database (http://www.ncbi.nlm.nih.gor/BLAST) for clone annotation. The significant matches were accepted at E-values lower than 1×10^{-7}.

Validation of the expression in response to Vg expression under the GIH knockdown condition

Candidate genes in SSH experiment that are involved in ovarian maturation were selected for RT-qPCR to verify their expression under *GIH* suppression. The qPCR was performed using an appropriate amount of cDNA for each gene with the specific oligonucleotide primers using KAPA SYBR® FAST qPCR kit (KAPABIOSYSTEMS, USA). Furthermore, the expression of candidate genes that are involved in reproduction were determined upon ovarian maturation stages.

Functional characterization of Calreticulin gene during in Vg synthesis

Cloning of cDNA encoding calreticulin of P. monodon (PmCRT)

One of the candidate down-regulated gene under *GIH*-knockdown condition is calreticulin (*PmCRT*). To determine the open reading frame (ORF) of *PmCRT,* the specific primer was designed from (53). The amplification of *PmCRT* cDNA was performed in the reaction containing 1 µl of first-stranded ovary cDNA, 0.3 mM of dNTPs, 1x long range buffer, 1.75 mM MgCl2, 0.5 µM PmCRT-F primer, 0.5 µM PmCRT-R primer, 1.25 U KAPA LongRange DNA polymerase, and adjusted the volume to 25 µl by distilled water. The PCR reaction was carried out with the following temperature cylces: 94°C for for 2 min; 35 cycles of 94°C for 15 sec; 55°C, 15 sec; 68°C, 2 min; and a final extension at 72°C for 3 min. The specifically amplified product was cloned, and their sequences were determined and analyzed on NCBI database.

Construction of PmCRT:pGEX-4X-1 recombinant plasmid

In order to express recombinant protein PmCRT, the DNA fragment encoding N-terminal domain of PmCRT was obtained by PCR using specific primer to N-terminal domain. The PCR fragment of N-ter PmCRT was digest with *Eco*RI and *Bam*H I restriction enzyme and ligated to pGEX-4x that had been digested with same enzymes. The ligated product was transformed to *E. coli* stain DH5-α, and the candidate recombinant clones were subjected to DNA sequencing. The correctly clone was re-transformed to *E. coli* BL21 (DE3)pLysS.

Protein expression and protein fraction analysis

A single colony of *E. coli* BL21 (DE3)pLysS containing N-ter PmCRT:pGEX-4X-1 recombinant plasmid was inoculated into 3 ml of LB broth containing of 100 µg/µl amplicillin and 34 µg/µl chloramphenicol. The culture was incubated at 37 ºC, 250 rpm for overnight. Then, the culture was diluted at 1:50 in 10 ml of LB broth containing of the same

antibiotics as above. The culture was grown at 30 ^{o}C until OD_{600} reached 0.5-0.6. Then, the culture was induced by 0.4 mM IPTG under the control of T7 promoter, and incubated at 37 ^{o}C for 4 h. After that, 1 OD_{600} of bacterial cell was collected and packed by centrifuged at 13,000 rpm for 1 min. The supernatant was collected as soluble fraction, and the pellet was collected as inclusion protein fraction, and was resolved by 15% SDS-PAGE. The recombinant proteins in both fractions were verified by western blot analysis using anti-GST monoclonal antibody.

Investigation of protein-protein interaction between CRT and RXR by MBP-amylose pull-down assay

To investigate binding between PmCRT and PmRXR, *in vitro* pull-down was performed. Approximate 10 OD_{600} cell of soluble DBD-RXR/MBP-6x histidine recombinant protein was immobilized into 50 ul slurry of amylose resin (NEB). After that, 10 OD_{600} cell of soluble N ter-CRT/GST was then added into the immobilized, DBD-RXR/MBP-6x histidine or MBP-6x histidine alone in binding buffer (1x PBS, 2mM DTT, and 1X Protease inhibitor). The reaction tubes were rotated for 2 hour in a cold room, and washed several times to remove non-specific binding. The protein binding complexes were eluted out with elution buffer (50 mM Tris-HCl, 10 mM maltose, pH 7.4). The pull-down proteins were analyzed with 15% SDS-PAGE and western blotting against 1:5,000 dilution of anti-GST (Abcam) monoclonal antibody and 1:4,000 of anti-6x histidine monoclonal antibody (Abcam).

Functional study of CRT in regulating the expression of *Vg* gene by RNAi technology

The function of PmCRT in regulating the expression of *Vg* genes was performed by RNA interference approach. Firstly, the dsRNA targeting *PmCRT* (N-terminal domain coding region) was produced and tested for its efficiency to knockdown *PmCRT* expression.

CRT-dsRNA production

A cDNA encoding PmCRT was used to design specific dsRNA targeting N-terminal domain. Briefly, the DNA template for the 511 bp stem-loop of dsRNA was amplified with primers SL-NCRT F-XbaI, and SL-NCRT R-BamHI. Another DNA template for the 431 bp stem of dsRNA, was amplified with primers ST-NCRT F-EcoRI and ST-NCRT R-BamHI. The stem-loop fragment was first cloned into pET17b vector at *Xba*I and *Bam*HI sites, following by the stem at *Eco*RI and *Bam*HI. Then, the recombinant NCRT-pET17b expression cassette was used to transform *E. coli* strain DH5-α performed to DNA sequencing. The correct recombinant plasmid was transformed to *E. coli* strain HT115. The

expression of stem-loop specific dsRNA targeting *CRT* genes was carried out by 0.4 mM IPTG induction in 2XYT medium for 4 hr at 37°C with shaking. The hair-pin dsRNA was extracted by Tri-solution before dissolved in 150 mM NaCl and stored at -30°C until use. Determination of the concentration and purity of dsRNAs was monitored by agarose gel electrophoresis. The quality of hair-pin dsRNAs was verified by RNAse digestion assay.

In vivo PmCRT silencing by specific dsRNA and its effect on Vg expression

To test whether *PmCRT* has any effect on *Vg* gene expression, the expression of *Vg* was determined upon CRT-knockdown in female shrimp. Vitellogenic female shrimp (approximately 250 g) was divided into two group; shrimp injected with NaCl as a negative control and shrimp injected with dsCRT (2.5 μg/ g body weight of shrimp). Then, the ovary of shrimp in each group were dissected on days 3 and 7 after injection and used for isolation of total RNA. The first strand cDNA was synthesized, and suppression of *PmCRT* transcript in the ovary was determined by semi-quantitative RT-PCR. The effect on *Vg* expression in in the ovary was also determined by semi-quantitative RT-PCR in *PmCRT* knockdown shrimps.

Results

Putative promoter and regulatory elements of *GIH* and *Vg* genes

Construction of genome walking library and amplification of GIH and Vg upstream sequences

Genomic DNA was extracted from muscle tissue of *P. monodon* by chloroform/ isoamyl alcohol extraction. Approximately 4-6 μg of genomic DNA was obtained from 200 mg tissues. Verification of the genomic DNA on agarose gel revealed a major band above the 23 kb band of the lambda/ Hind III marker (Fig. 1A) indicating good quality of the genomic DNA that was mostly intact and could be used for genome walking. The genomic DNA was then digested with four blunt-end generating restriction enzymes; *Dra* I, *Eco*R V, *Hpa* I and *Sna*B I in separate reactions (Fig. 1B). The digested DNA fragments in each reaction were ligated to the Genome Walker Adaptor, and the pool of adaptor-ligated DNA fragments was called a genome walker library. Then each genome walker library was amplified with Adaptor primer and gene-specific primer (GSP) which is *GIH*-specific or *Vg*-specific reverse primer designed from the sequence near the 5' end of *GIH* or *Vg* cDNA sequence, respectively in order to obtain the 5' upstream DNA sequence of each gene. The results in Fig. 2 showed that a band at about 150 bp, 500 bp and two bands at approximately 1.2 and 1.3 kb were obtained from *Dra* I, *Eco*R V and *Hpa* I libraries, respectively for *GIH* gene, whereas two bands approximately 1 kb and a major band around 1.6 kb were obtained from *Eco*R V and *Sna*B I libraries, respectively for *Vg* gene.

Amplification and characterization of GIH promoter and regulatory sequences

The amplified DNA fragments were cloned into pGEMT Easy vector. The result of the four bands obtained by GIH-specific primer confirmed that each band contained the 5' upstream sequence of *GIH* genes. The two bands from *Hpa* I library (*Hpa* IA and *Hpa* IB) shared the same nucleotide sequence in the proximal region but they were different in the distal region. To verify whether these two fragments were really the upstream sequence of GIH gene, specific primers were designed from the sequence at or near the 5' end of each fragment and used to amplify genomic DNA together with the reverse primer located in GIH coding sequence. Only the primer from *Hpa* IA could amplify the fragment at the expected size at approximately 1.2 kb while no band was obtained from the *Hpa* IB primers (Fig. 3).

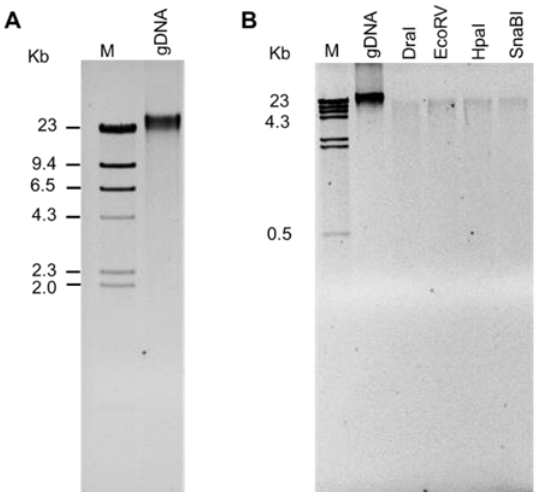

Fig. 1 *P. monodon*' s genomic DNA. Genomic DNA (gDNA) was extracted from muscle tissue of *P. monodon* (A) and digested separately with *Dra* I, *Eco*R V, *Hpa* I and *Sna*B I. The DNA were analyzed by 0.6% agarose gel electrophoresis. M is λ/Hind III DNA marker.

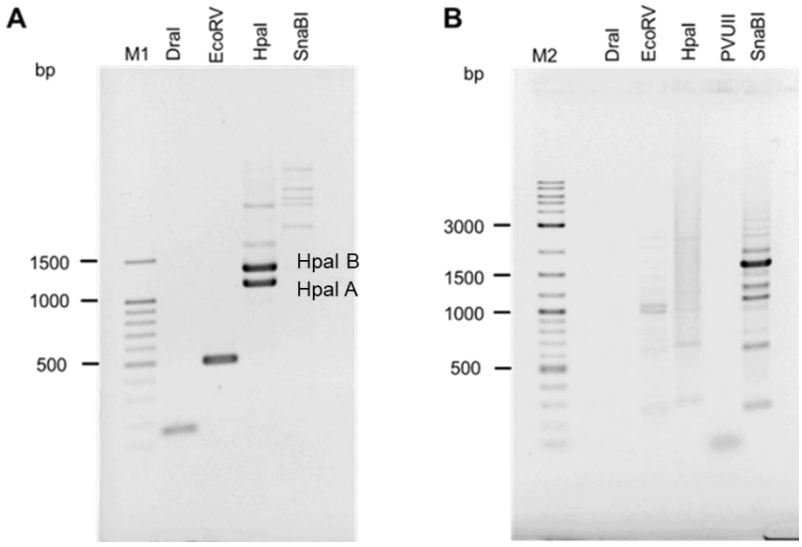

Fig. 2 Amplification of 5' upstream region of *GIH* (A) and *Vg* (B) genes from *P. monodon*'s genome walker libraries. The four genome walker libraries were amplified with *GIH*-specific primer or *Vg*-specific primer and adaptor primer. *Pvu* II library was also included in the amplification of *Vg* upstream sequence. M1 is 100 bp DNA ladder and M2 is 1kb plus 100 bp DNA ladder.

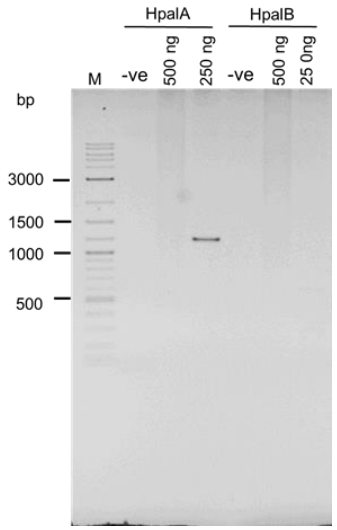

Fig. 3 Verification of the 5' upstream sequence of *GIH* gene. The *Hpa* IA fragment was confirmed to be the 5' upstream sequence of *GIH* gene by amplification of *P. monodon* genomic DNA with the primer designed approximately 215 bp downstream of the 5' of *Hpa* IA and the reverse primer in the coding region (about 205 bp downstream of ATG start codon) of GIH cDNA fragment. The *Hpa* IB was confirmed with the primer designed from the 5'end of the *Hpa* IB fragment and the same reverse primer in GIH coding region as used for verification of *Hpa* IA fragment. M is 1 kb plus 100 bp DNA ladder, and –ve represent the reaction without genomic DNA template as negative control of PCR.

Since the Hpa IA fragment contains the longest nucleotide sequence of the 5' UTR of *GIH* gene, the putative promoter and regulatory sequences in the *Hpa* IA fragment were predicted by TF sitescan software on the MIRAGE www server (http://www.ifti.org/cgibin/ifti/ Tfsitescan.pI) compared to PROMH (G) software on the softberry www server (http://linux1. softberry.com/all.htm), and the transcription start site was predicted by NNPP program (http://www.fruitfly.org) (Fig. 4). The criteria to determine the putative promoter and regulatory sequences based on the consensus elements composing of at least 5 nucleotides that hit with high threshold score (E < e-3) by both programs. The result revealed a TATA box at -30 to -24 position from the predicted transcription start site. Putative biding sites for several transcriptional factors were predicted in this fragment such as CAAT, SP1, CREB, heat chock element (HSE), Pit-1, Oct-1 and retinoid-X receptor (RXR).

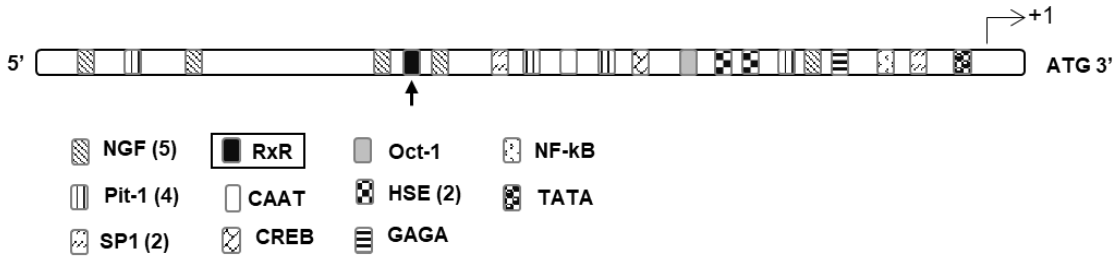

Fig. 4 Putative promoter region of *P. monodon*' s *GIH* gene. The putative transcription initiation site was predicted using NNPP program (http://www.fruitfly.org), and transcription factor binding sites in the 5' upstream sequence of P. monodon's GIH gene were predicted by TF sitescan software on the MIRAGE (http://www.ifti.org) and PROMH (G) software. Only the sites that were predicted by both softwares are indicated in this figures.

Amplification and characterization of Vg promoter and regulatory sequences

The major band around 1.6 kb obtained by *Vg* gene specific primers and adaptor primers from SnaBI library were purified and cloned into pGEMT Easy vector. Nucleotide sequences of three clones were determined and showed similar sequences. This 5' upstream genomic sequence was further analyzed for the present of a promoter and regulatory sequences on computational databases using the same prediction softwares and criteria as described for *GIH* promoter fragment. Several putative binding sites were present on *Vg* putative promoter fragment include TATA box, GATA, heat shock factor-binding element (HSE), and RXR as shown as a diagram in Fig 5. In addition, the position of a putative transcription start site was predicted by Neural Network (NNPP) programs (http://www.fruitfly.org/seq_tools/promoter.html). The putative transcription start site was located at position 186 nucleotides upstream from ATG start codon by a score of 0.83 (cut-off = 0.80).

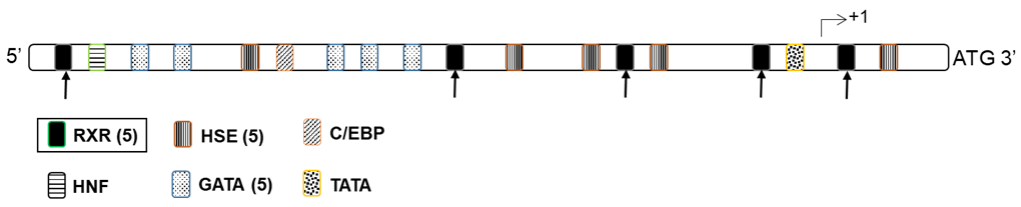

Fig. 5 Putative promoter region of *P. monodon*'s *Vg* gene. The putative transcription initiation site and transcription factor binding sites in the 5' upstream sequence of *P. monodon*'s *Vg* gene were predicted with the same softwares used to predict the sites on *GIH* promoter fragment.

Preparation of nuclear protein extracts for determination of the binding of putative factors on the 5' upstream regulatory sequences of *GIH* and *Vg* genes

In order to detect the binding of putative regulatory factors to the 5' upstream regulatory sequences of *GIH* and *Vg* genes, nuclear protein extract was prepared from eyestalk ganglia and ovary tissues, respectively. The cytoplasmic fractions were also collected as negative control. Because *GIH* and *Vg* are not expressed in shrimp muscle tissue, both cytosolic and nuclear fractions of abdominal muscle tissue were also collected as negative control. The protein pattern was determined on 15 % SDS-PAGE followed by silver staining. Fig. 6 shows the different protein patterns between muscle, eyestalk ganglion, and ovary extracts. The protein patterns of the nuclear and cytoplasmic fractions of each tissue were also different. Furthermore, small bands size around 10-20 kDa were found in the nuclear fractions from all tissues. These bands were expected to represent histone proteins and could be used as a marker for the nuclear fraction.

In order to validate the success of nuclear protein extraction, cytosolic and nuclear protein fractions were resolved by 15% SDS-PAGE. The proteins were loaded 500 ng of each fraction and transferred from gel onto a membrane for immunological analysis by using polyclonal antibody against human histone 3 (Accession no. P68431) that is highly conserved with shrimp histone 3 (Accession no. P83864) as a protein maker of the nuclear fraction (Fig. 7). The result showed the present of positive bands around 15 and 17 kDa in the nuclear fractions of ovary and eyestalk tissues and faint band around 15 kDa in the nuclear fraction of muscle, whereas these signals were not presented in the cytoplasmic fractions of any tissue. This result suggested that the nuclear fractions were obtained with good quality and purity enough for using to determine regulatory factors in protein-DNA interaction assay.

Identification and characterization of regulatory sequence-binding factors that bind to the promoter region of *GIH* and *Vg* genes

To identify the binding of nuclear factors on the predicted regulatory sequence of GIH and *Vg* genes by electrophoretic mobility shift assay (EMSA), the regulatory sequences of *GIH* and *Vg* genes were divided into three (GIH-TF1-3) and four (Vg-TF1-4) fragments of approximately 350-400 bp, respectively These fragments were obtained by PCR as shown in Fig. 8.

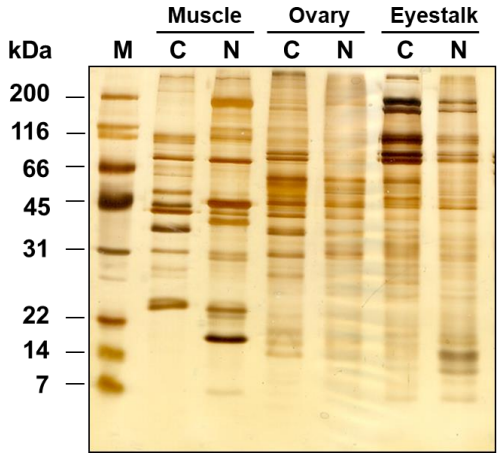

Fig. 6 Protein patterns of cytoplasmic and nuclear extracts from *P. monodon*'s muscle, ovary, and eyestalk ganglion tissues. The cytoplasmic proteins (C) and nuclear proteins (N) were prepared from muscle, ovary, and eyestalk ganglion tissues, and 300 ng of each sample were analyzed on 15 % SDS-PAGE followed by silver staining. Lane M is Broad range protein ladder.

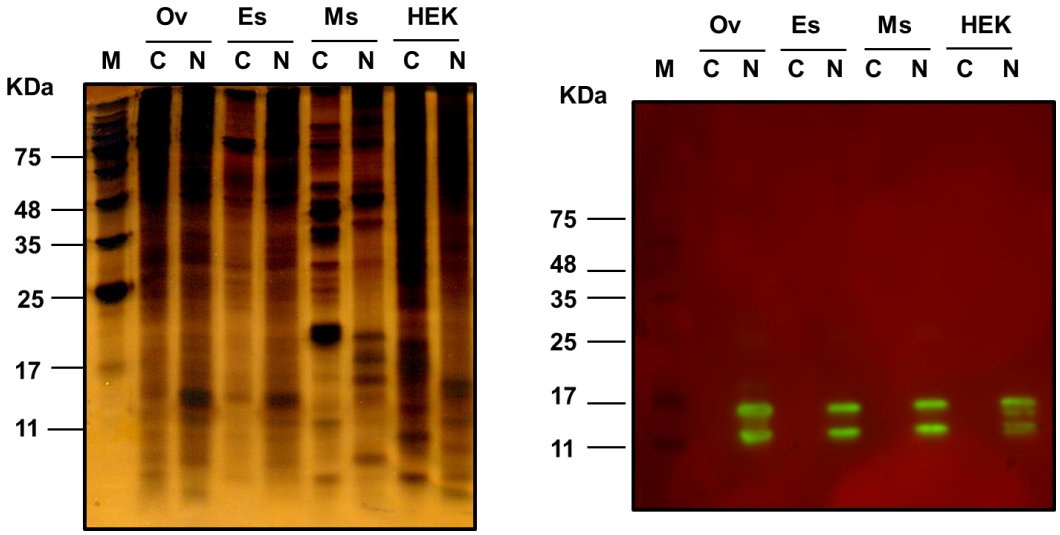

Fig. 7 Verification of the nuclear protein extracts from *P. monodon* tissues by immunological analysis using polyclonal anti-histone 3. The cytoplasmic proteins (C) and nuclear proteins (N) were prepared form muscle (Ms) ovary (Ov), and eyestalk ganglion (ES) tissues, and 500 ng of each sample were analyzed on 15 % SDS-PAGE followed by silver staining (A) and immunodetection using 1:10,000 anti-histone 3 (Abcam; ab1791) and exposed on CCD for 1-5 min. Lane M is Tricolor protein ladder (7B). The extracts from HEK cells (HEK) were used as positive control.

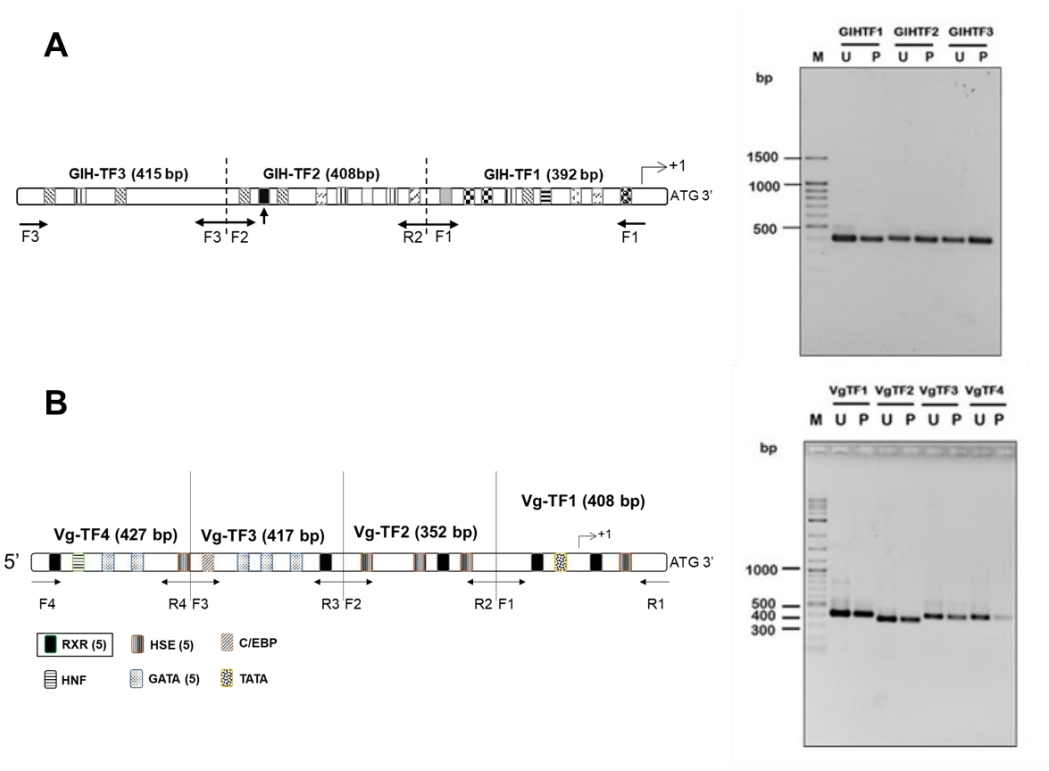

Fig. 8 Diagram and amplification of 5' regulatory sequences of *GIH* (A) and *Vg* (B) genes. Three fragments encompassing the regulatory sequence of *GIH* genes (GIH-TF1-3) were obtained by PCR while four fragments encompassing the regulatory sequence of *Vg* genes (Vg-TF1-4) were obtained. The PCR products of each fragment before (U) and after purification (P) were analyzed on 1.2 % agarose gel electrophoresis comparing with loading 100 ng of 100 bp DNA ladder in lane M.

After purification, 5 pmol of each DNA fragment were labeled with biotin-11-UTP at 3' end by the activity of TdT. The labeled efficiency and probe sensitivity were determined by dot blot analysis by comparing a signal of standard biotinylated DNA fragments and oligo DNA labeled probe control. While the signal of the standard biotinylated DNA fragment could be detected down to 1.6 fmole, the oligo DNA labeled probe control and the labeled fragments of *GIH* and *Vg* regulatory sequences showed the lowest detectable signal at approximately 6.2 fmole (Fig. 9). Therefore, approximately 10 fmole of each labeled fragment will be used for DNA-protein interaction detection by EMSA.

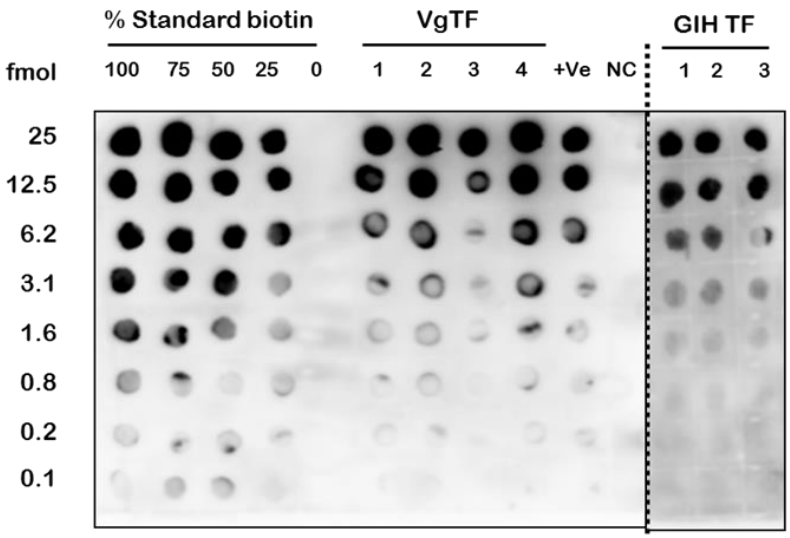

Fig. 9 Determination of the efficiency and sensitivity of biotinylated DNA probes. The labeling efficiency and sensitivity of 3' biotinylated DNA probes were determined by dot blot analysis compared to the standard biotin at different amounts and percentages of labeling. The amounts of GIH-TF1-3 and Vg-TF1-4 were varied from 25 to 0.2 fmol. Ppositive oligo-DNA (+Ve), and unlabeled oligo-DNA (NC) were included.

Electrophoretic mobility shift assay (EMSA)

To identify the binding of nuclear factors on the predicted regulatory sequence of *GIH* and *Vg* genes, an electrophoretic mobility shift assay (EMSA) was performed. Fig. 10 showed the shift band of 3'-labeled GIH-TF1, 2 and 3 fragments in the reactions containing 2 µg of eyestalk nuclear proteins when compared with the free probes or the reaction containing muscle nuclear proteins. To confirm the specific binding between eyestalk nuclear proteins and the three GIH-TF probes, unlabelled fragment of each probe at 50, 100, and 200-fold excess were used as the specific competitive inhibitor. The results showed that the ratio between the shift bands of probe-proteins complex and the free probes decreased as the amount of specific competitor increased. Whereas the non-specific competitor actin fragment could not compete or showed only little competitive effect to the binding between probes and nuclear proteins. Similar results were obtained for the binding reaction between Vg TF1 and 3, and ovary nuclear proteins (Fig. 10), which showed the shift bands of the complexes between Vg-TF probes and 2.0 µg of ovary nuclear proteins, but not with the muscle nuclear protein. These results suggest that the complex formation between the probes and nuclear extracts is specific.

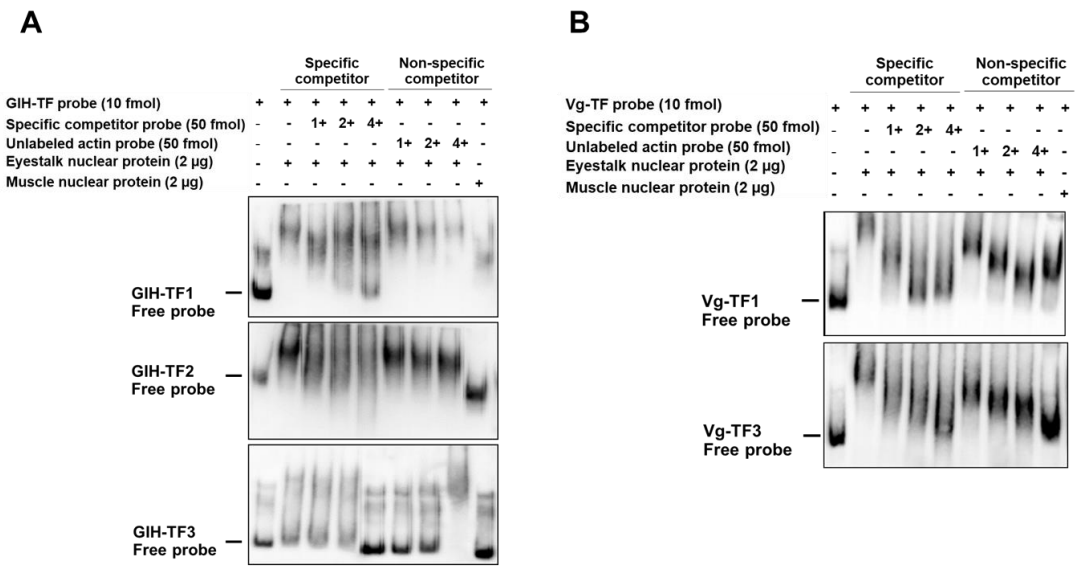

Fig. 10 Validation of binding specificity between nuclear proteins and 5' upstream fragments of *GIH* and *Vg* genes

The specificity of the binding between (A) 10 fmol of biotin-labelled 5' upstream fragments of *GIH* gene (GIH-TF1, GIH-TF2 and GIH-TF3) and 2 µg of eyestalk nuclear protein extract and (B) 10 fmol of biotin-labelled 5' upstream fragments of *Vg* gene (Vg-TF1 and Vg-TF3) and 2 µg of ovary nuclear protein extract (B) was determined by the addition of 50, 100, and 200-fold of unlabeled GIH-TF or Vg-TF DNA fragments (specific competitor) and unlabeled actin DNA fragment (non-specific competitor). Muscle nuclear extract was included as a negative binding reaction.

Based on the present of large complex of eyestalk nuclear extract bounded GIH-TF2 and ovary nuclear extract bounded Vg-TF3, these complexes were analyzed on SDS-PAGE. The proteins presented in these complexes were identified by LC MS/MS. Table 1 showed that most of the nuclear proteins identified in GIH-TF2 and Vg-TF3 complexes were the proteins associated with shrimp immunity. Some of protein such as Tudor staphylococal nuclease and NF-kB transcription factor relish could be transcriptional regulator of the gene expression that are involved in growth or program cell death. However, the candidate proteins identified from the DNA-protein complexed are not correlated with any predicted binding motifs on *GIH* and *Vg* promoter regions. This may be because of the lack of potential shrimp regulatory proteins in the database.

Table 1 Proteins that were identified in the DNA-protein complexes formed between eyestalk or ovary nuclear extract and 5' upstream of *GIH* or *Vg* genes

Probe	Predicted protein	Species	score	Mass (KDa)	Matches
GIH TF2	Prophenol oxidase	*Penaeus monodon*	31	79.68	1
Vg TF3	Tudor staphylococcal nuclease	*Penaeus monodon*	19	10.3	3
	Glutathione peroxidase	*Penaeus monodon*	25	15.89	3
	NF-kB transcription factor relish	*Penaeus monodon*	22	134.21	2
	β-actin	*Penaeus monodon*	63	42.32	2

Molecular cloning and characterization of a cDNA encoding retinoid X receptor of *P. monodon* (*PmRXR*)

Cloning of a cDNA encoding PmRXR

Among the candidate proteins whose binding sites were predicted on the upstream promoter of both *GIH* and *Vg* genes, a retinoid-X receptor (RXR) is of interest. The retinoid X receptor (RXR) belongs to the nuclear hormone receptor (NR) superfamily class II that functions as a transcription factor by forming a homodimer, or a heterodimer with another NR such as ecdysone receptor (EcR) and modulates molting, apoptosis, and reproduction in invertebrates. However, there is no information whether RXR regulates *Vg* or *GIH* gene expression in the shrimp so far. Therefore, a cDNA encoding PmRXR was cloned. In order to clone *PmRXR* cDNA, the specific primers designed from RXR of other Penaeid shrimps could successfully amplify a 1.2 Kb DNA fragment from the ovary cDNA of *P. monodon* (Fig. 11). The PCR product was cloned and subjected to DNA sequencing. Analysis of the cDNA revealed a 1,314 bp open reading frame (ORF) encoding a putative 326 amino acids PmRXR. The six domains of PmRXR were predicted by NCBI database including the candidate functional domains of nuclear protein receptors; a DNA binding domain and a ligand binding domain as shown in Fig. 12.).

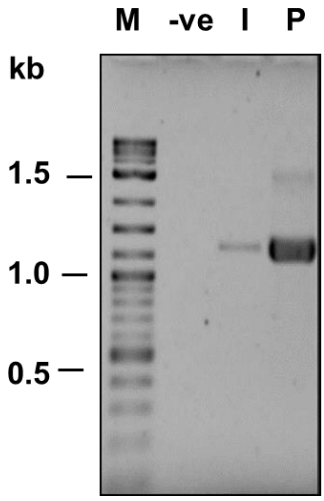

Fig. 11 PCR product of retinoid X receptor (*PmRxR*) cDNA of *P. monodon*
The PCR products of *PmRxR* ORF using cDNA from ovary of immature (I) and previtellogenic (P) *P. monodon* were determined on 1.2 % agarose gel electrophoresis comparing to 100 ng of 2-log DNA ladder in lane M. A negative control reaction (-ve) was performed in the absence of cDNA template.

Furthermore, phylogenetics tree indicated that PmRxR was a member of RxR family in penaeid shrimp that was separated from USP protein (RxR homologue protein) in insects (Fig 13).

Transcriptional profile of PmRxR

The expression of *PmRxR* in *P. monodon*'s tissues including, brain, eyestalk, thoracic ganglia, abdominal ganglia, muscle, gills, heart, hepatopancreas, and ovary from adult previtellogenic female shrimp were determined by RT-PCR. The result showed that *PmRxR* transcripts were found in all tissues (Fig. 14A) indicating ubiquitous expression of *PmRxR* in the shrimp. In addition, to determine whether *PmRxR* expression is related to ovarian maturation or not, the *PmRxR* transcript level was determined in different ovarian maturation stages by RT-qPCR. The result in Fig. 14B showed that *PmRxR* mRNA transcript levels were concurrently up-regulated during ovarian maturation. The result suggests that *PmRxR* might be a factor that control ovarian development in *P. monodon*.

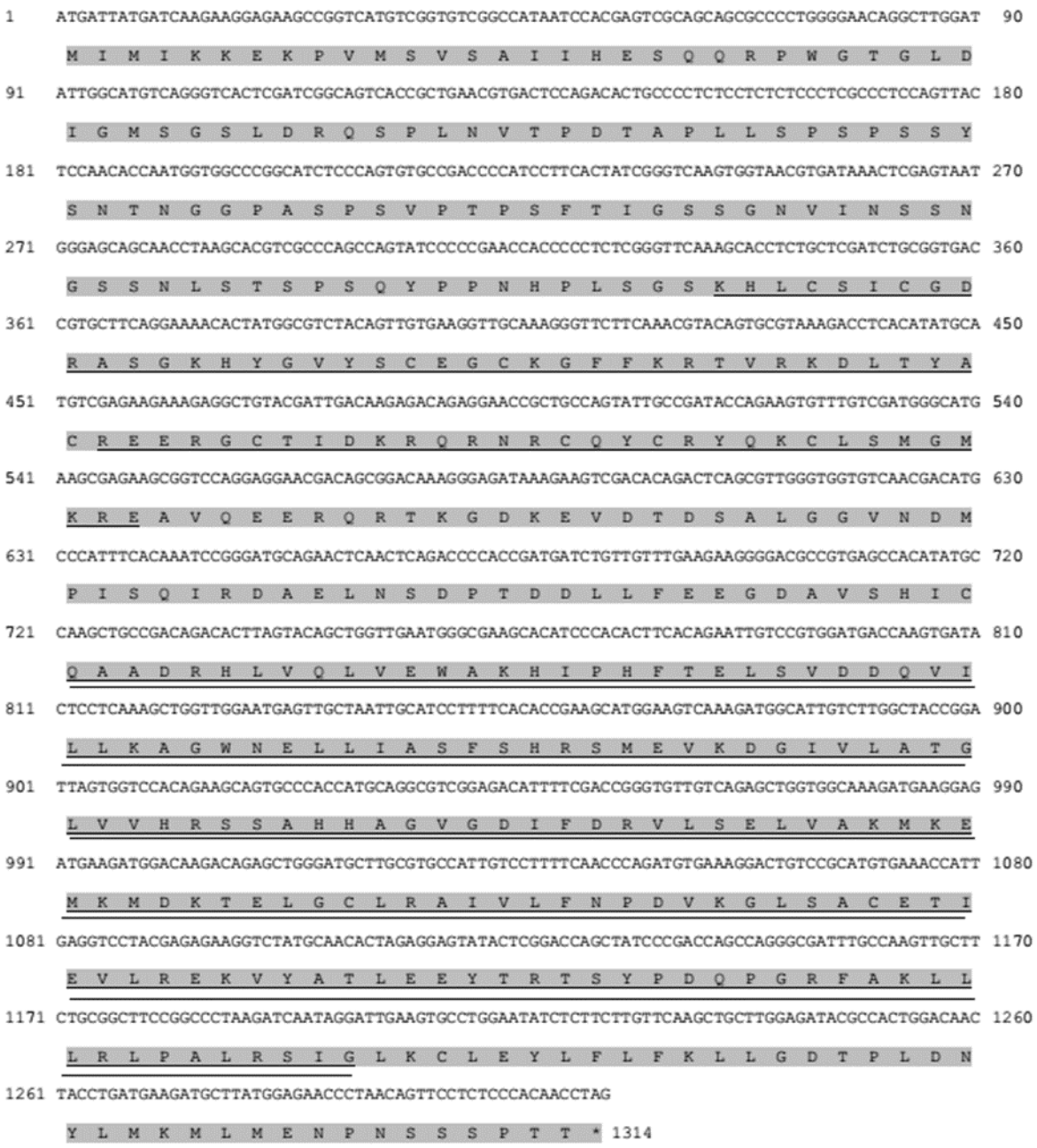

Fig. 12 Analysis of nucleotide and deduced amino acid sequences of retinoid-X receptor in *P. monodon* (PmRxR)

The nucleotide sequence is presented with the corresponding deduced amino acid (highlighted in gray). The conserved DNA binding domain of RxR was underlined, and the ligand binding domain was double underlined whereas the asterisk represents the stop codon.

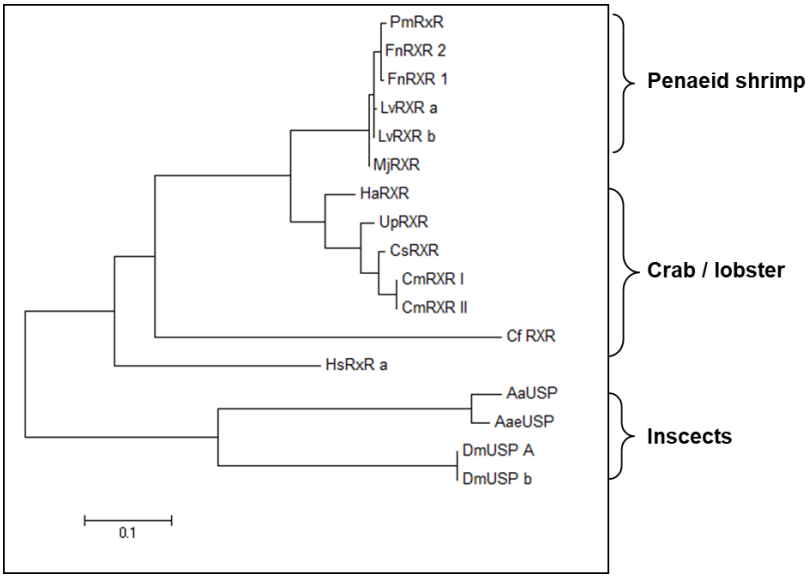

Fig. 13 Phylogenetic tree of nucleotide and deduced amino acid sequences of retinoid-X receptor in *P. monodon* (Pm-RXR)

Phylogenetic tree showing the relationship between PmRXR and RXR in other crustaceans and its homologs (USP) in insects was constructed using Mega 7 program,

Functional study of RxR in regulating the expression of GIH and Vg genes

The functions of PmRxR in regulating the expression of *GIH* and *Vg* genes were studied by RNA interference. The cDNA encoding PmRxR was used to design specific double-stranded RNA (dsRNA) targeting a ligand-binding domain (dsRXR), produced in a bacteria expression system, and verified by RNase digestion assay (Fig. 15).

Invetigation of dsRNA-mediated PmRxR knockdown in *P. monodon* by RT-PCR on day 10 after dsRXR injection showed about 75% and 50% significant suppression in *PmRXR* expression levels in previtellogenic and vitellogenic shrimp, respectively compared to NaCl treated shrimp, while the unrelated dsRNA (dsGFP) did not have effect on *PmRXR* expression (Fig. 16, open bars). In addition, the expression of Vg in PmRXR-knockdown shrimp was significantly reduced when compared to the control groups (Fig. 16, black bars). So, these results suggested that RxR might positively control *Vg* synthesis in the ovary of *P. monodon*.

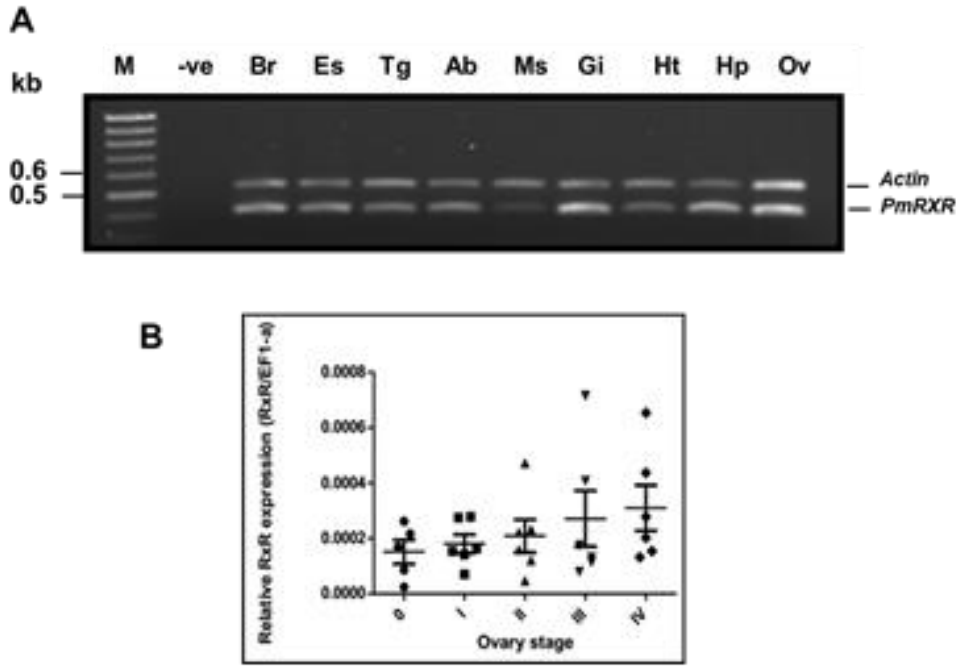

Fig. 14 Expression profile of *PmRXR* in shrimp

(A) Expression of *PmRXR* in brain (Br), eyestalk (ES), thoracic nerve (Tg), abdominal ganglia (Ab), muscle (M), gill(Gi), heart (Ht), hepatopancreas (Hp) and ovary (Ov) of *P. monodon* was determined by RT-PCR using specific primers for the LBD region of PmRXR. The actin transcript was amplified as an internal control. (B) The expression levels of *PmRXR* in the ovary at immature stage (o), pre-vitellogenic stage (I), early-vitellogenic stage (II), late vitellogenic stage (III) and ripe stage (IV) were determined by qPCR using the ovarian cDNA as a template from. The relative amounts of gene transcripts were calculated to that of EF1-α, and analyzed by $2^{-\Delta\Delta Ct}$ method.

Furthermore, dsRXR could also suppress *PmRxR* expression approximately 45% in the eyestalk of previtellogenic female shrimp on day 10 post-injection compared with expression in the control shrimp. However, the level of *GIH* expression in the eyestalk of RXR-knockdown shrimp was not significantly different from the control groups (Fig. 17). So, this result suggested that PmRxR might not be involved in the control of GIH expression in shrimp eyestalk.

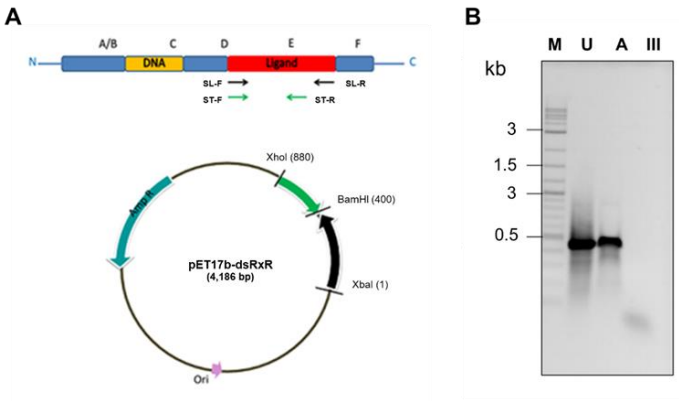

Fig. 15 Production and verification of PmRXR-specific dsRNA (dsRxR)

The physical map of dsRxR producing plasmid pET17b-dsRxR is shown in (A) The quality of dsRxR was determined by RNase digestion assay. The untreated dsRNA (U), and RNase A (A), and RNase III (III) treated dsRxR were analyzed on 1.2 % agarose gel electrophoresis comparing with 100 ng of 2-log DNA ladder in lane M.

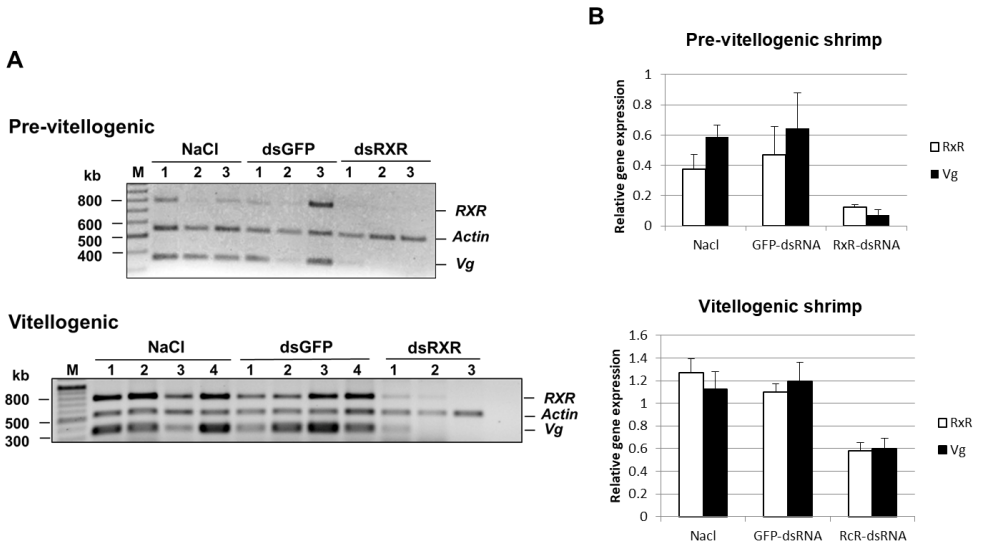

Fig. 16 Determination of *PmRXR* knockdown by dsRxR and its effect on *Vg* expression in the ovary of *P. monodon*

(A) *PmRXR* knockdown in the ovary of pre-vitellogenic and vitellogenic female *P. monodon* showed inhibition of *Vg* gene expression in PmRXR knockdown shrimp (dsRXR) compared to NaCl and dsGFP treated control shrimp on day 10 post-dsRNA injection. (B) Relative expression levels of *PmRXR* and *Vg* compared to that of actin as measured by the intensities of the bands in (A) and calculated by ScionImage program .

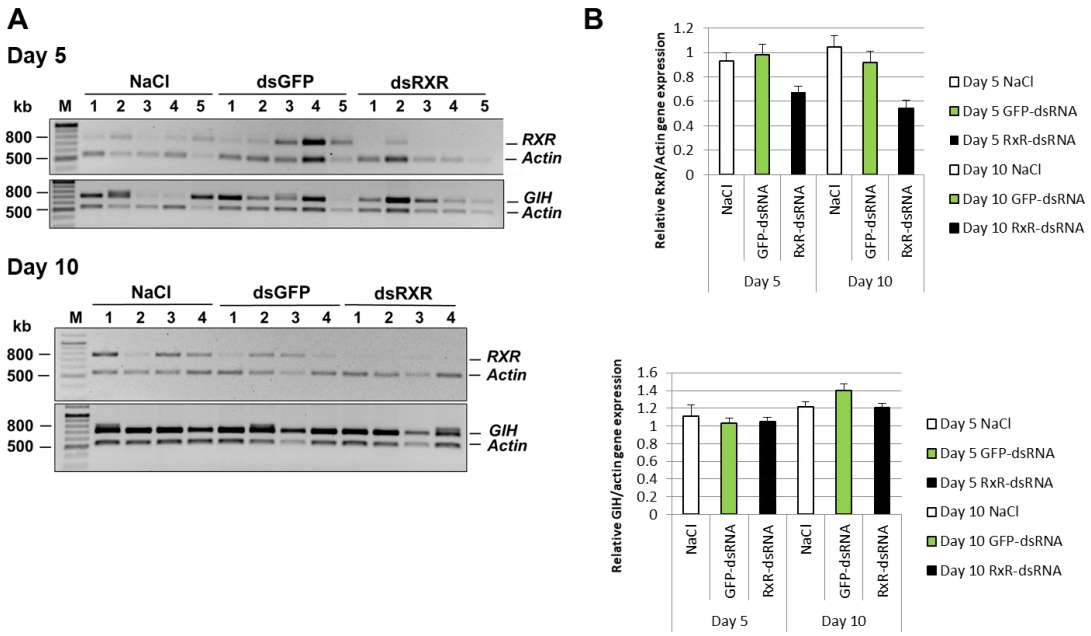

Fig. 17 Determination of *PmRXR* knockdown by dsRxR and its effect on *GIH* expression in the eyestalk of *P. monodon*

(A) *PmRXR* and *GIH* expression in the eyestalk of dsRXR-injected female *P. monodon* was determined by RT-PCR on day 5 and day 10 post-injection compared with that in NaCl and dsGFP injected shrimps (A). Relative expression
levels of *PmRXR* and *GIH* compared to that of actin as measured by the intensities of the bands in (A) and calculated by ScionImage program (B).

Determination of PmRXR that bind to the promoter region of *Vg* gene.

Construction of DNA-binding domain of RXR (DBD-RXR) expression plasmid

To validate the binding of PmRXR on the 5' upstream region of *Vg* gene, the recombinant DBD-RxR was produced for DNA-protein interaction study by electrophoretic mobility shift assay (EMSA). The recombinant DBD-RxR protein was produced as an MBP/6xhistidine tagged protein. The DBD-RxR/MBP-6xhis, (56 kDa) was successfully produced in *E. coli*. Over-expressed protein was obtained by IPTG induction at 30 ^{o}C for 4 hr (Fig. 18), and these recombinant proteins were expressed in the soluble form as determined by SDS-PAGE analysis. The DBD-RxR/MBP-6x his was successfully purified by immobilized metal affinity chromatography by eluted with 100-200 mM Imidazole (Fig. 19), and confirmed by western

blot analysis (Fig. 20). The protein was further used for validation of the binding with their responsive elements on *Vg* gene, and for studying protein-protein interaction with PmRxR protein partner.

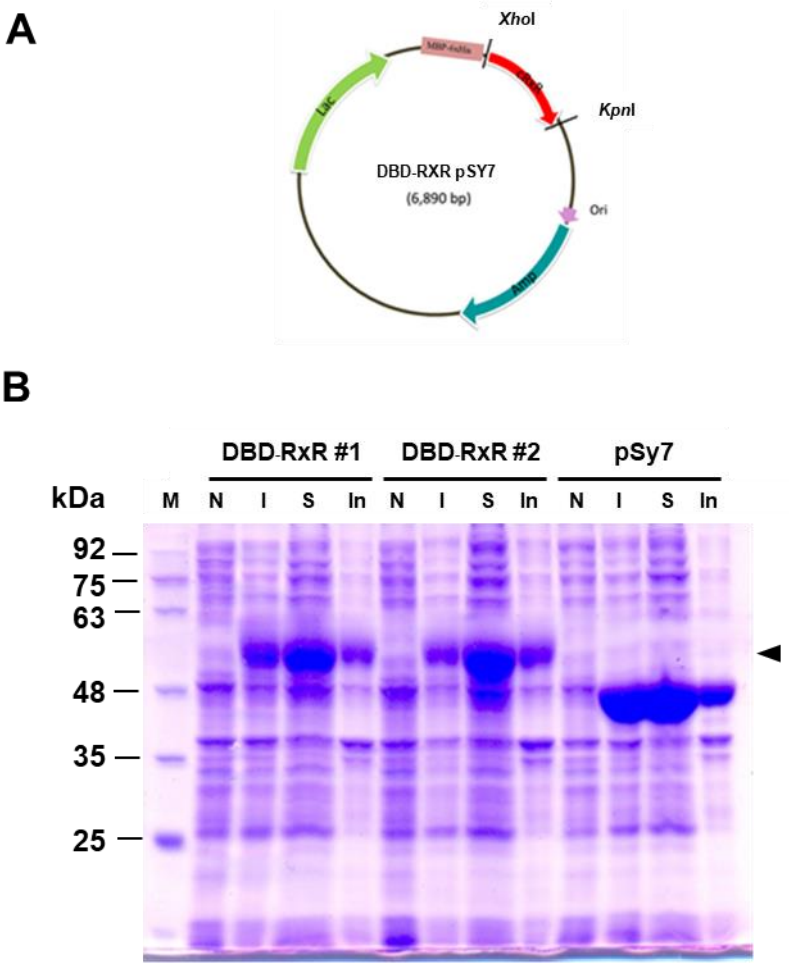

Fig. 18 Production of DBD-RXR/MBP-6xhis fusion protein by bacterial expression system.

(A) Physical map of the recombinant DBD-RXR pSy7 plasmid for the expression of recombinant DBD-RXR-MBP-6x histidine fusion protein. (B) SDS-PAGE analysis of over-expression of the positive transformants (DBD-RXR#1 and #2) containing DBD-RXR pSy7 compared between non induction (N) and 0 IPTG induction (I). The presence of the reombinent DBD-RXR fusion protein (arrow head) in the soluble fraction (S), and inclusion fraction (In) were also determined. The protein expressed from pSY7 plasmid alone was also included as a control.

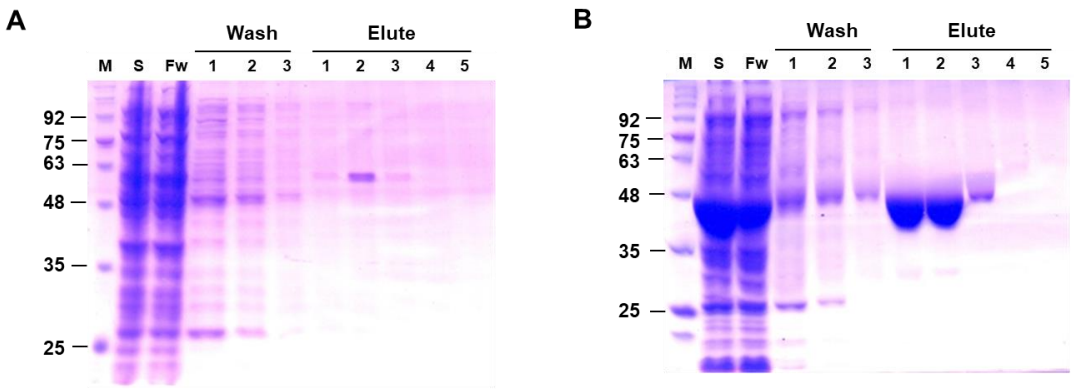

Fig. 19 Purification of DBD-RXR/MBP-6x his fusion protein by immobilized metal affinity chromatography.

SDS-PAGE analysis of protein purification pattern of the recombinant DBD-RXR/ MBP-6x his (A), and MBP-6x his (B) by HisTrapFF column. Approximately 1 OD of soluble protein (S), flow-through (Fw), wash (1-3), and elute (1-5 representing 100-500 Imidazole eluent) were loaded compared to Pre-stain protein ladder

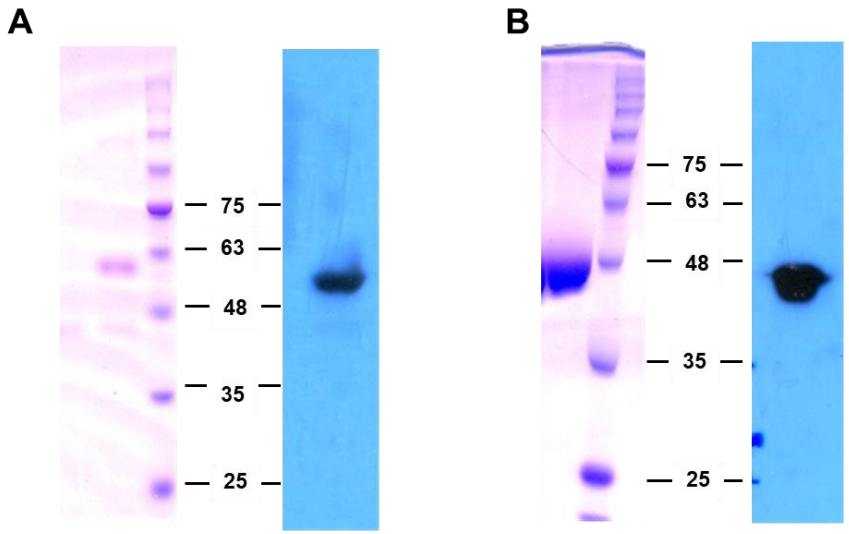

Fig. 20 Western blot analysis of DBD-RXR/MBP-6x his fusion protein, and MBP-6x histidine

Approximately 1 OD of the recombinant DBD-RXR/MBP-6x his (A), and MBP/6x his (B) were confirmed by western blotting using 1:8,000 dilution of anti-6x histidine monoclonal antibody.

Electrophoretic mobility shift assay (EMSA)

The Vg-TF1 and Vg-TF3 probes that contain putative RXR binding sites, and produced large complexes with ovary nuclear extract were used to verify the binding of RXR by EMSA. The optimization of binding condition was performed with different amounts between 0 to 4 μg of DBD-RXR/MBP-6x his and 10 fmol of Vg-TF1 and Vg-TF3 probes. The Vg-TF1 probe showed a shifted band when at least 3 μg of DBD-RXR/MBP-6x his was added to the reaction, while Vg-TF3 probe showed only slightly shifted bands (Fig.21).

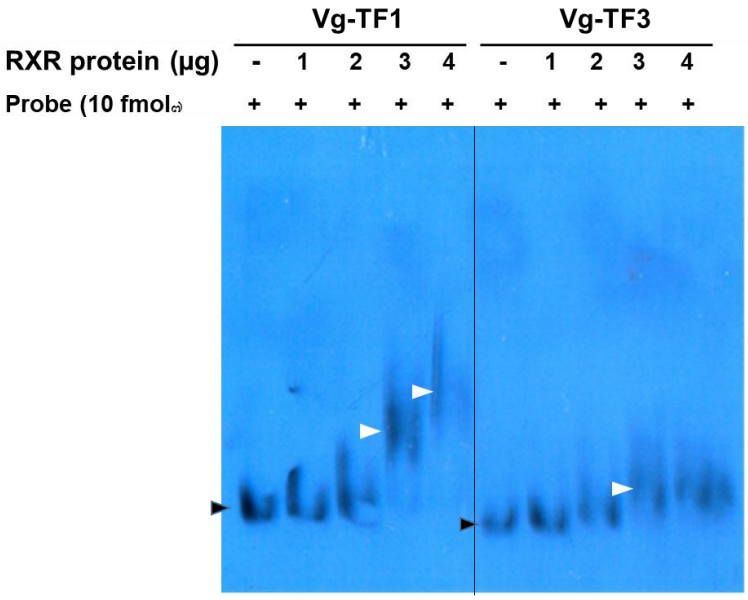

Fig. 21 Optimization of binding between recombinant DBD-RXR protein and Vg TF1 and Vg-TF3 probes

The binding between various amounts from 0 to 4 μg of DBD-RXR/MBP 6x to 10 fmol of VgTF1 and VgTF3 (B) probes was determined by EMSA. The DNA-protein biding reactions were separated on native polyacrylamide gel electrophoresis, transferred to a nylon membrane and detected with LightShift® Chemiluminescent EMSA Kit. Black arrows indicate the free probes, and white arrows show the shifted bands.

Investigation of the effect of *GIH* on gene expression profile in the ovary

A change in gene expression in the ovary that may act downstream of GIH was determined by suppression substractive hybridization (SSH) between GIH-knockdown shrimp and the

control shrimp. First, the suppression of *GIH* expression by GIH-dsRNA (dsGIH) and its consequence on induction of *Vg* gene expression was confirmed.

Verification of GIH knockdown by dsGIH

The suppression of *GIH* transcript in the eyestalk ganglia and the expression of *Vg* gene in the ovary of the dsGIH inject shrimp was determined by semi-quantitative RT-PCR comparing with that of the control (dsGFP-injected) shrimp. The result in Fig. 22 showed that after injected with dsGIH for 5 days, the expression of *GIH* in the eyestalk was significantly suppressed more than 83% of that in the control shrimp. Moreover, the expression of *Vg* gene in these *GIH*-knockdown shrimp were significantly induced by more than two fold. This result indicated that silencing of *GIH* by dsGIH was effective, and the cDNA from these shrimp can be used in SSH to determine gene that were differentially expressed under *GIH* knockdown condition.

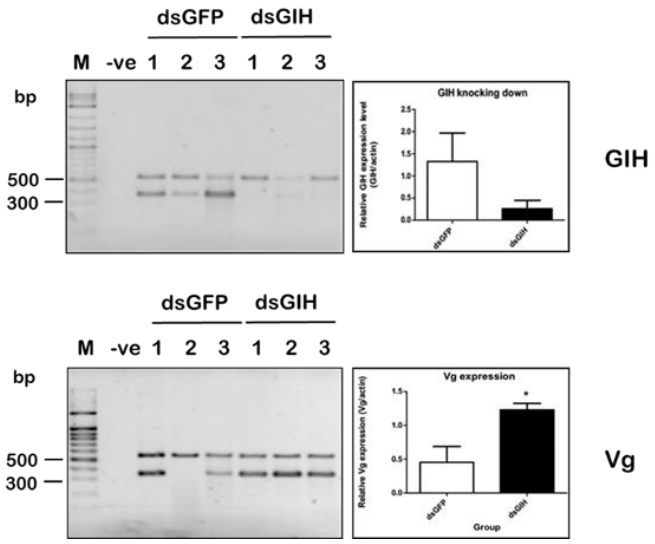

Fig. 22 Determination of *GIH* and *Vg* transcript levels under *GIH* knockdown condition

Previtellogenic female *P. monodon* (approximately 20 g body weight) were injected with dsGFP (control) or dsGIH, and the expression of *GIH* in the eyestalk and *Vg* in the ovary was determined by RT-PCR on day 5 after dsRNA injection. A reaction in the absence of DNA template was used as a negative control (-ve). The RT-PCR products for each gene were analyzed on 1.5 % agarose gel electrophoresis comparing to 2-log DNA. The relative intensity of the RT-PCR product bands between *GIH* or *Vg* gene and the internal control actin in each shrimp in both groups was measured by Scion Image software and present in a bar graph as mean±SD.

Identification of differential gene expression in the ovary under GIH deprivation

The nucleotide sequences of the cDNA fragments of the positive clones obtained from each subtractive library were determined, and the homolog sequences were searched on the blastn and blastx program at NCBI GenBank database for clone annotation. The significant matches were accepted at E-values lower than 1×10^{-7}. For the forward library (representing up-regulated genes under GIH-knockdown), nucleotide sequences of 10^2 positive clones matched to 37 unique sequences in NCBI GenBank database. The genes that were up-regulated upon *GIH* knockdown were categorized based on their functions as shown in table 2. These include ribosomal RNA, gene encoding protein in several pathways such as ovarian development, focal adhesion, energy/lipid metabolism, signaling transduction pathway, cell cycle/transcription factor/protein repair enzyme, and protein folding. The expression of genes involving in ovarian development such as *peritrophin I* (*Per I*), *thrombospondin II* (*TSP II*), and *Vg* were validated under *GIH* suppressed condition (Fig. 23). Their expression profile during ovarian development in female shrimp (Fig. 24A) showed the higher levels of expression when the ovary developed into vitellogenic stages.

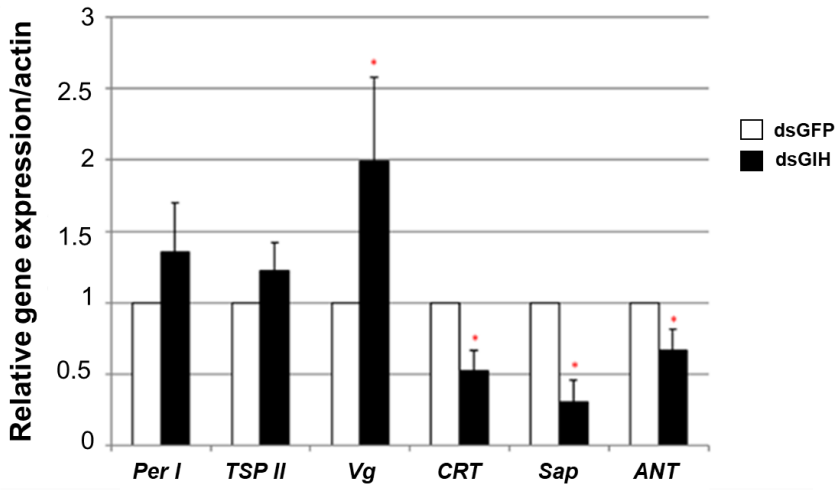

Fig. 23 Expression of selected genes from SSH libraries

Expression levels of *peritrophin I* (*Per I*), *thrombospondin II* (*TSP II*), *vitellogenin* (*Vg*) from the forward library and *calreticulin* (*CRT*), *saposin* (*Sap*), *Adenine nucleotide translocase* (*ANT*) from the reverse library in the *GIH*-knockdown shrimp (black bars) were determined by RT-PCR, and the expression was calculated in relative to that of control shrimp injected with dsGFP (open bars) and presented in a bar graph. The experiments were done in triplicate. Data is presented as mean ± SEM (n=3). Asterisk indicates significant differences between data at $p< 0.05$.

For the reverse library, nucleotide sequences of 81 positive clones matched to 32 unique sequences in the NCBI GenBank database. These genes (considered as down-regulated upon *GIH* knockdown) were categorized according to their functions as shown in table 3 including ribosomal RNA, and genes that are involved in ovarian development, glycoprotein metabolism/ energy metabolism, calcium signaling pathway, protein trafficking/protein folding, and protein synthesis. The genes involving in reproductive system such as *calreticulin* (*CRT*) and energy metabolism such as *saposin* (*Sap*), and *Adenine nucleotide translocase* (*ANT*) were validated for down-regulated expression under *GIH*-suppressed condition (Fig. 23). In addition, determination of their expression during ovarian development revealed the decreased expression levels in vitellogenic ovary compared to that in the immature of pre-vitellogenic ovary (Fig. 24B).

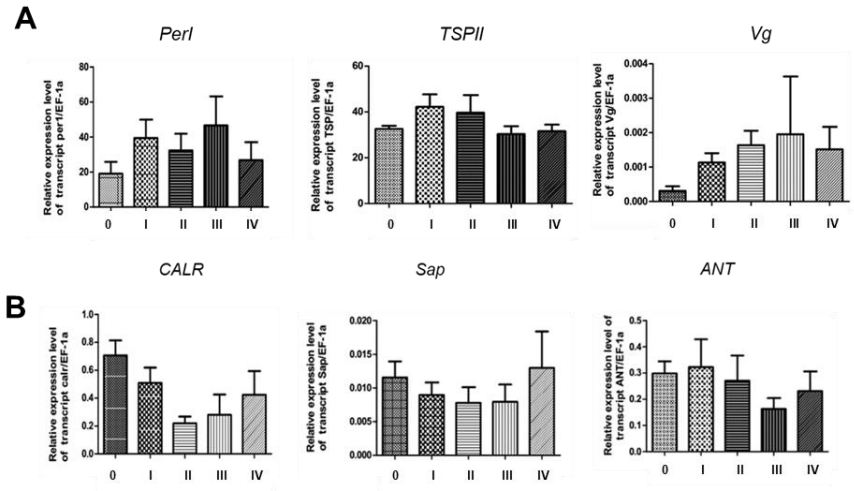

Fig. 24 Expression of candidate genes that changes upon *GIH*-knockdown in the ovary of female *P. monodon* during ovarian maturation.

The expression levels of genes in the ovary that were up- (A) or down- (B) regulated upon *GIH*-knockdown at different ovarian developmental stages; immature stage (o), pre-vitellogenic stage (I), early-vitellogenic stage (II), late vitellogenic stage (III) and ripe stage (IV) of female *P. monodon* were determined by RT-qPCR. The relative amounts of gene transcripts were calculated to that of EF1-α were analyzed by $2^{-\Delta\Delta Ct}$ method. Data present as mean ± SEM (n=3-4).

Functional characterization of *PmCRT* during Vg synthesis

In this study, *calreticulin* (*CRT*) gene was significantly down-regulated upon *GIH* knock-down. CRT can bind to steroid receptor on a DNA binding domain (KXGFFKR) motif, and prevents the binding of the receptor to its responsive element to regulate gene expression in vertebrate. Interestingly, the PmRxR whose binding site was found in the regulatory sequence of *GIH* and *Vg* genes also contains the KGFFKR sequence at position 136-141. It is therefore possible that CRT is an inhibitory mediator of Vg synthesis by interfering the binding of RxR to its binding site on *Vg* 5' upstream sequence. To proof this hypothesis, the protein-protein interaction between CRT and RXR and their function in vitellogenin synthesis was determined.

Expression of the PmCRT recombinant protein

Approximately 1.2 Kb of *PmCRT* cDNA was successfully obtained from previtellogenic ovary using specific primer of *P. monodon* CRT that was previously reported. The PCR product was cloned and subjected to DNA sequencing. Analysis of the cDNA showed that *CRT* contained 1314 bp ORF encoding putative 437 amino acids with three functional domains as show in Fig. 25.

Furturemore, to proof whether CRT interacts with RXR in controlling Vg synthesis, the recombinant protein of N-terminal domain of PmCRT was produced using a recombinant GST-tagged system. The PmCRT-Nter/GST protein (rPmCRT-Nter, 46 kDa) was successfully produced in *E. coli*. Overexpressed protein was obtained by IPTG induction at 30 ^{o}C for 4hr (Fig. 26), and rPmCRT-Nter/GST was expressed in the soluble form as determined by SDS-PAGE analysis and confirm by western blot analysis. The rPmCRT-NTer/GST was affinity purified before using to study protein-protein interaction with rPmRxR.

In vitro pull-down assay

To investigate whether CRT can bind to RXR, a putative regulator of *Vg* gene, an amylose resin in vitro pull-down assay was used to determine the binding between N-ter CRT/GST and DBD-RxR/MBP-6xhis. The SDS-PAGE analysis showed that both the band of N-ter CRT/GST (50 KDa) and DBD-RxR/MBP-6xhis (56 KDa) were presented in the eluted fraction indicating that the N-terminal domain of CRT possibly binds to DBD of RxR protein but did not present in the eluted fraction between DBD-RxR and GST or MBP and GST reaction (Fig 27), suggesting that N-ter CRT possibly interact to RxR via the site in the DNA binding domain of RXR.

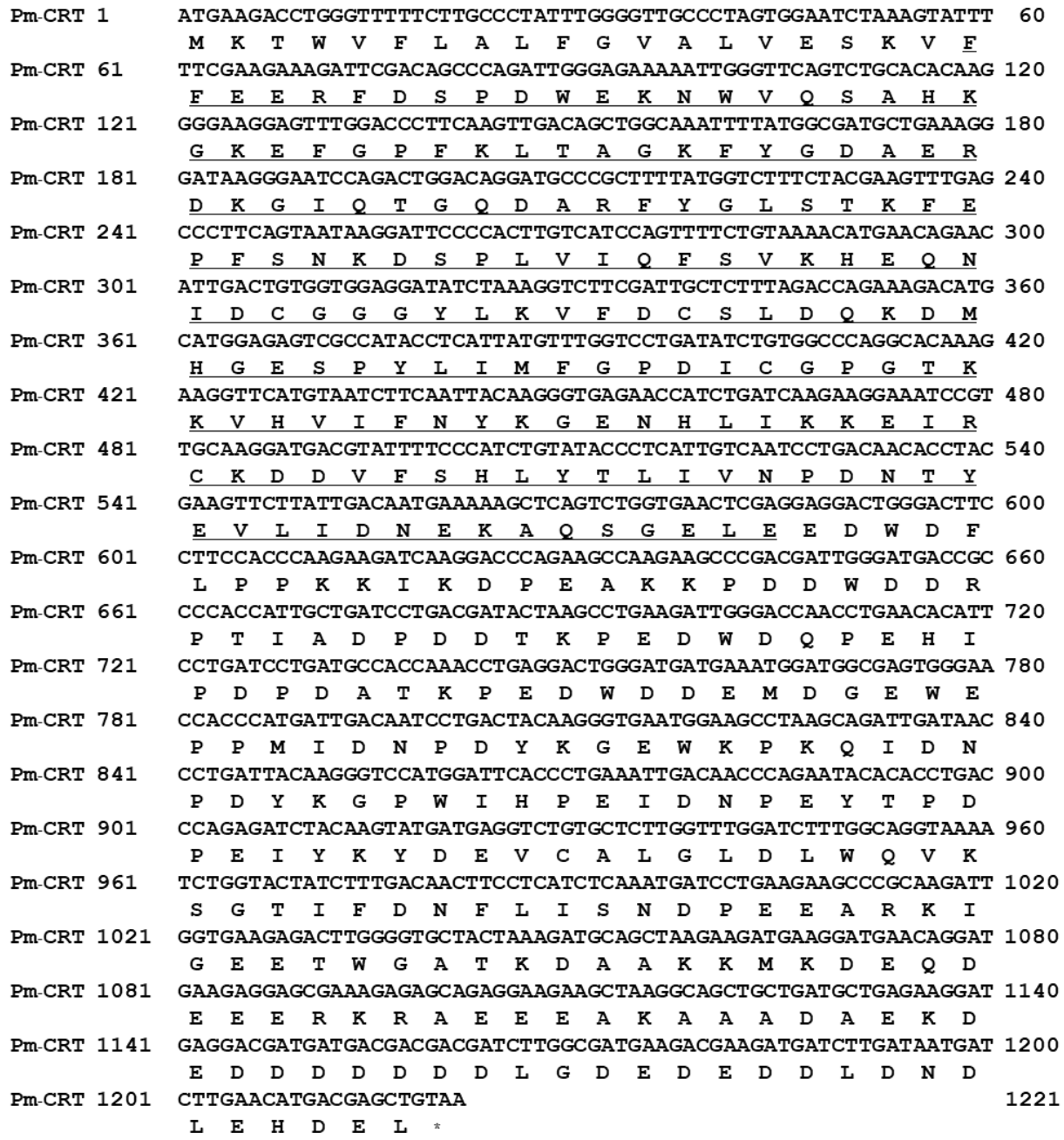

Fig. 25 Analysis of nucleotide and deduced amino acid sequences of *P. monodon*'s calreticulin (PmCRT)

The nucleotide sequence of *PmCRT* is presented with the corresponding deduced amino acids in a one-letter code. The conserved N terminal domain of PmCRT is underlined whereas the asterisk represents the stop codon.

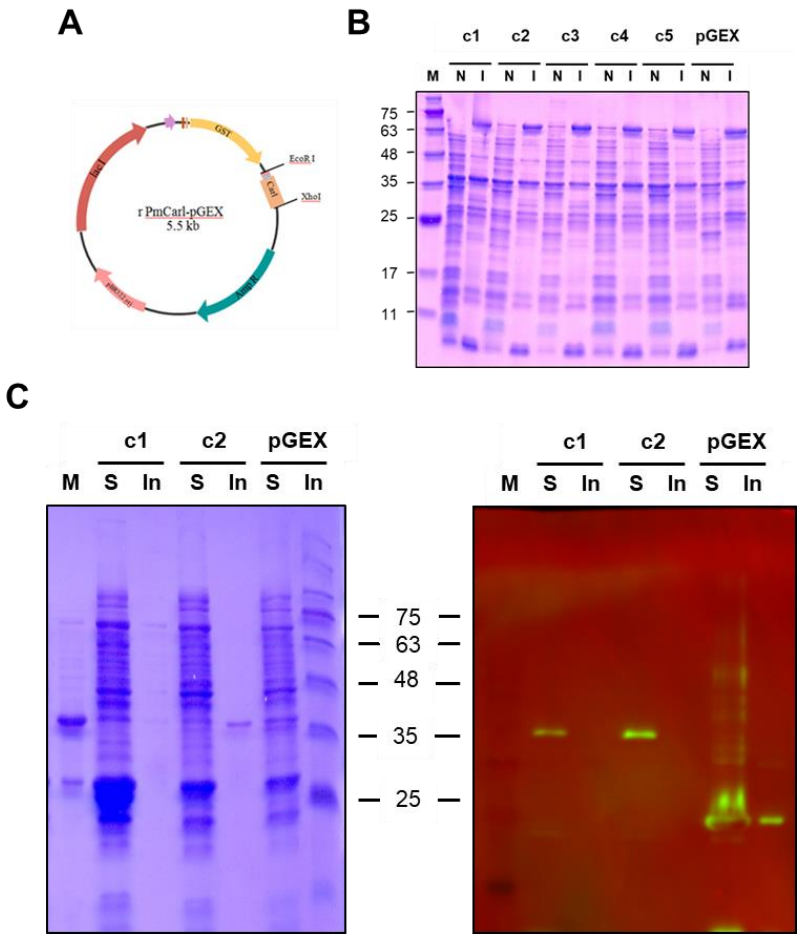

Fig. 26 Production of recombinant CRT-Nter/GST fusion protein in *E. coli*

(A) Physical map of expression plasmid for N-terminal domain of PmCRT (CRT-Nter/GST fusion). (B) Overexpression of positive transformants (C1 to c5) containing PmCRT-Nter/pGEX-4X-1 compared between non-induction (N) and 0.4 mM IPTG induction. (C) Analysis of soluble (S) and inclusion (In) fractions of proteins from clone c1 and c2 by SDS-PAGE analysis (left panel), and verification of CRT-Nter/GST by western blot using anti-GST antibody.

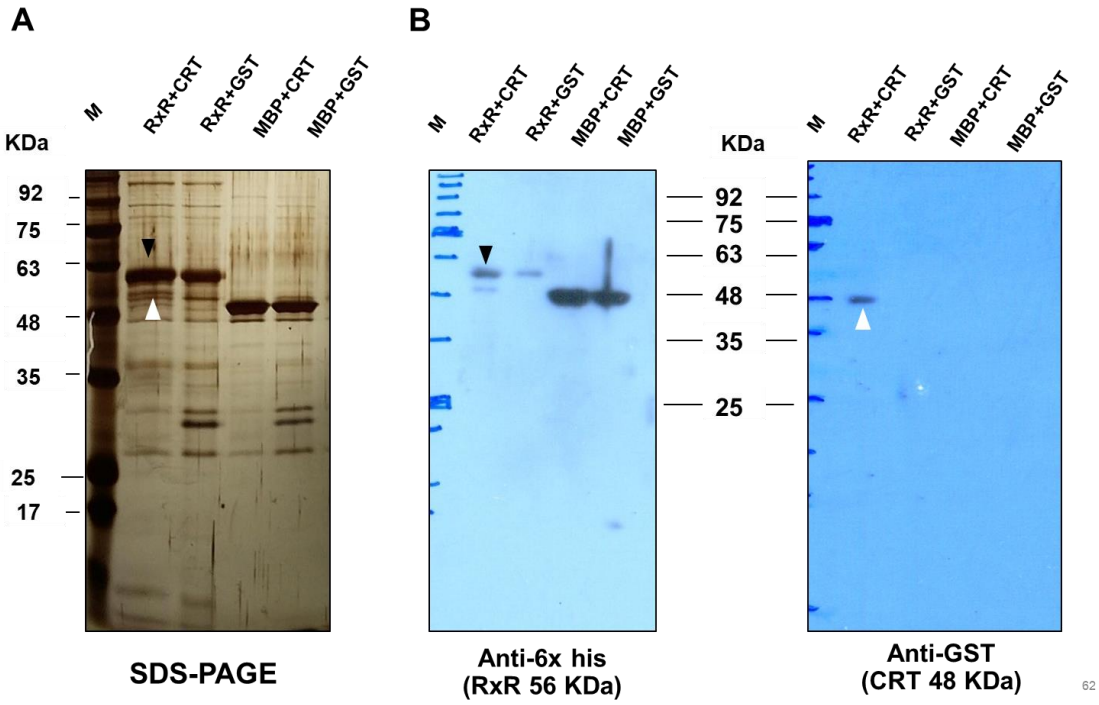

Fig. 27 *In vitro* pull-down assay between DBD-RxR/MBP-6x his and N ter-CRT/GST

The pull-down reactions between DBD-RxR/MBP-6x his and N ter-CRT/GST (RXR+CRT), DBD-RxR/MBP-6x his and GST (RXR+GST), MBP and N ter-CRT/GST (MBP+CRT) and MBP and GST (MBP+GST) were analyzed by (A) SDS-PAGE analysis with silver staining and (B) western blot analysis using to anti-6x histidine (left panel) and anti-GST (right panel). The white arrowheads indicate the band of N ter-CRT/GST (approximately 50 KDa), and the black arrowheads indicate DBD-RxR/MBP-6x his (approximately 56 KDa).

Functional study of *PmCRT* in regulating *Vg* expression

The function of *PmCRT* in regulating the expression of *Vg* gene was studied by RNA interference. The cDNA encoding *PmCRT* was used to design specific dsRNA targeting an N-terminal domain of PmCRT. The dsCRT was produced in *E. coli* expression system, and verified by RNase digestion assay (Fig. 28). Injection of the dsCRT into previtellogenic *P. monodon* could slightly suppress *PmCRT* expression on day 3 after injection, but showed approximately 46 % suppression of *PmCRT* expression on day 7 after dsRNA injection compared to the control shrimp. In addition, *Vg* expression level in the ovary of CRT-knockdown shrimp was increased by approximately 30 % compared to the control group (Fig

29). This result suggests that PmCRT possibly controls vitellogenesis by inhibiting *Vg* gene expression in the ovary.

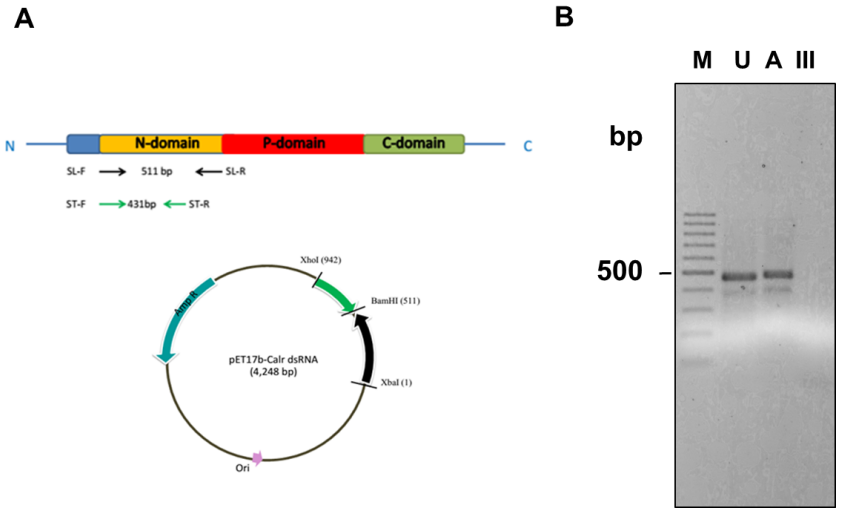

Fig. 28 Production and verification of dsCRT

(A) Diagram showing the location of the stem and stem-loop fragment for N-terminal domain of PmCRT and physical map of recombinant plasmid for dsCRT expression. (B) The quality of dsCRT (431 bp) was determined by RNase digestion assay. The untreated dsRNA (U), RNase A treated (A), and RNase III (III) were analyzed on 1.2 % agarose gel electrophoresis comparing with loading 100 ng of 2-log DNA ladder in lane M.

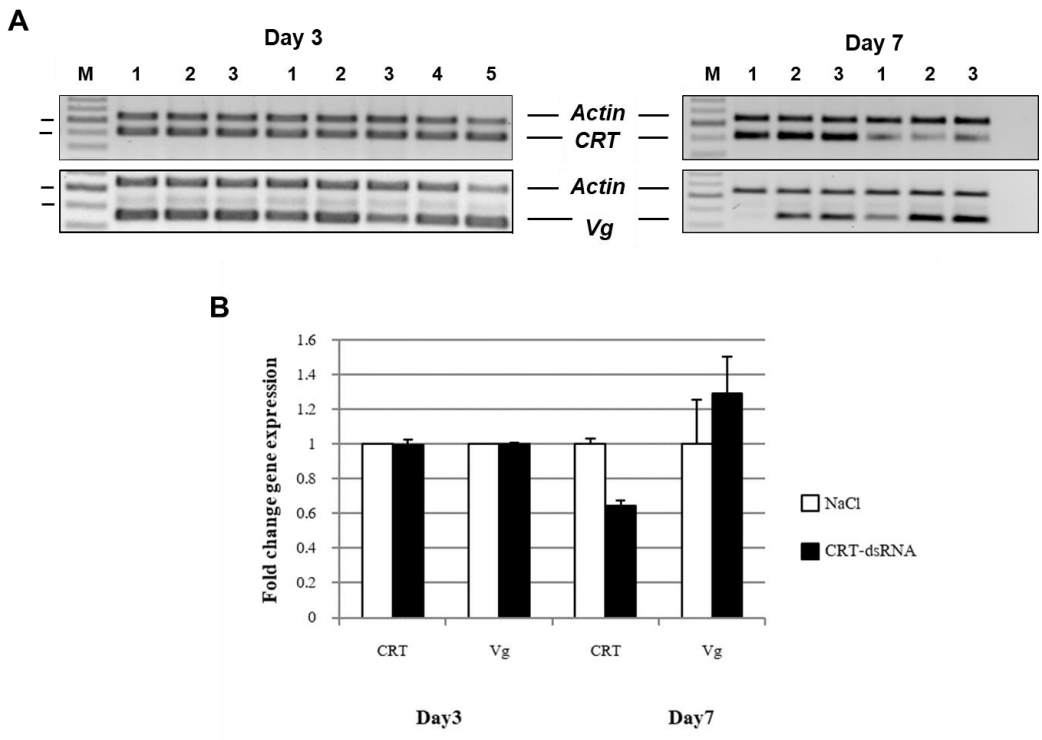

Fig. 29 Determination of *PmCRT* knockdown by dsCRT and its effect on *Vg* expression in the ovary of *P. monodon*

The expression of *PmCRT* in the ovary of previtellogenic female *P. monodon* was suppressed by dsCRT, and the expression of *Vg* in CRT-knockdown shrimp was determined by RT-PCR compared to NaCl treated control shrimp on day 3 and day 7 post-dsRNA injection (A). The relative fold changes of the expression of each gene were calculated from the intensities of the bands in (A) and showed as bar graphs (B).

Discussion

Ovarian maturation of female shrimp is one of the important factors that influence shrimp production. This process is known to be mediated by an eyestalk neuropeptide hormone called gonad-inhibiting hormone (GIH) that negatively regulates vitellogenesis, a central process during ovarian maturation (Ohira et al., 2006). However, the mechanism of vitellogenesis regulation by GIH is still not well understood. In this study, the promoter and regulatory region of *GIH* and vitellogenin (*Vg)* genes were identified and characterized in order to understand their regulation. Genome walking and regulatory element prediction by computer programs identified putative promoter and putative binding sites of several transcription factors, among which five putative binding sites of retinoid X receptor (RXR)

were found on the 5' upstream regulatory region of *Vg* gene, and one on the 5' region of *GIH* gene.

RXR belongs to a family of nuclear receptor proteins; it is the most commonly fond nuclear receptors that target multiple signaling pathways. RXR is important for several physiological processes in arthropods such as embryonic development (Wang et al., 2007), molting (Eichner et al., 2015; Tang et al., 2014) and ovarian maturation (Asazuma et al., 2007; Hopkins et al., 2008; Nagaraju et al., 2011). RXR contains six domains including DNA-binding domain) that contains two C2C2 zinc-finger motifs and the ligand-binding domain (LBD) that are present in all nuclear receptors (Dawson and Xia, 2012). In crustaceans, methyl farnesoate (MF), a hormone that is known to regulate reproductive maturation (Nagaraju, 2007), has been proposed as a natural ligand that binds with high affinity to RXR (Hopkins et al., 2008). MF also synergized with ecdysteroids to increase the activation of transcription mediated by the RXR–EcR heterodimeric complex (Wang YH & LeBlanc, 2009; Wang et al. 2007).

In this study, a cDNA encoding RXR of *P. monodon* was successfully cloned. The expression of PmRXR in the ovary showed an increasing trend with higher ovarian developmental stages suggesting that PmRXR possible play a role in ovarian maturation. The deduced amino acid sequence of PmRXR contained six domains including the candidate functional domains of nuclear protein receptors; a DNA binding domain and a ligand binding domain, and was phylogenetically grouped with other shrimp RXR. To verify whether PmRXR binds to its putative binding sites on *Vg* 5' regulatory region, the recombinant protein of the DNA binding domain (DBD) of PmRXR was produced and purified. The result form EMSA showed that the recombinant DBD-RXR can bind to the Vg-TF1 fragment of *Vg* regulatory region that contains two putative RXR binding site. Thus binding of PmRXR to its responsive elements upstream of *Vg* gene may control *Vg* expression in *P. monodon*.

In order to understand how GIH influence the expression of reproduction-related genes in the ovary, *GIH* suppression in previtellogenic female shrimp was performed by specific dsRNA (dsGIH) to knockdown *GIH* transcripts. The *GIH*-knockdown shrimp showed an increase in *Vg* expression level similar to previous report by Treerattrakool et al., 2008. The suppression substractive hybridization (SSH) between the total RNA of GIH-knockdown shrimp and the control shrimp resulted in up- and down-regulaion of several genes. One of the interesting gene is calreticulin (*CRT*), the expression of which in the ovary is reduced upon GIH knockdown.

Calreticulin (CRT) is a calcium binding protein that has multi-functions in animals and plants (Cabezón et al., 2008). CRT can bind specifically to a KXGFFKR motif found in the DNA binding domain (DBD) of steroid hormone receptors (Laudet et al., 1992). The binding of the amino-terminal region of CRT with the DBD of glucocorticoid receptor and androgen receptor prevent the binding of the receptors to their response elements (Burns et al., 1994; Dedhar et al., 1994). In addition, overexpression of the calreticulin gene led to a decrease in the expression of genes under retinoic acid receptor (RAR) stimulation in B16 mouse melanoma cells (Desai et al., 1996).

The result in this study showed that the knockdown of *PmCRT* expression in *P. monodon* by specific dsRNA resulted in an increased *Vg* expression level by 30% of that in the control shrimp. Our result further demonstrated the protein-protein interaction between the DNA binding domain of RXR and the N-terminal domain of CRT. These results together with the presence of RXR binding sites in the regulatory region of *Vg* gene of *P. monodon* may imply that CRT interacts with RXR, and thus interfere with the binding of RXR to its response elements on *Vg* regulatory region to control *Vg* gene expression in shrimp ovary.

In summary, our present works provide insight into the detailed mechanism of the control of vitellogenesis via the interaction of nuclear receptor and calreticulin. The influence of GIH on calreticulin expression suggests a linkage between the eyestalk neuropeptide and this control mechanism, however the mode of action of GIH on vitellogenesis remains to be investigated.

References

Asazuma H, Nagata S, Kono M, Nagasawa H. Molecular cloning and expression analysis of ecdysone receptor and retinoid X receptor from the kuruma prawn, *Marsupenaeus japonicus*. Comp. Biochem. Physiol. B. 2007;148:139–150.

Avarre JC, Michelis R, Tietz A, Lubzens E. Relationship between vitellogenin and vitellin in a marine shrimp *Penaeus semisulcatus* and molecular characterization of vitellogenin complementary DNAs. Biol Reprod. 2003;69:355-364.

Browdy CL. A review of the reproductive biology of Penaeus species: perspectives on controlled shrimp maturation system for high quality nauplii production. in: Proceeding of the Special Session on Shrimp farming (Wyban, J., Ed) 1992. pp. 22-51. Baton Rouge, LA.

Burns K, Duggan B, Atkinson EA, Famulski KS, Nemer M, Bleackley

RC, Michalak M. Modulation of gene expression by calreticulin binding to the glucocorticoid receptor. Nature. 1994;367:476–480.

Cardoso AM, Barros CMF, Correia AJF, Cardoso JM, CortezA, Carvalho F, Baldaia L. Identification of vertebrate type steroid hormones in the shrimp *Penaeus japonicus* by tandem mass spectrometry and sequential product ion scanning. J. Am. Soc. Mass Spectrom. 1997;8:365–370.

Chan SM, He JG, Chu KH, Sun CB. The Shrimp Heat Shock Cognate 70 Functions as a negative regulator in vitellogenin gene expression. Biol Reprod. 2014;14:1-11.

Dawson MI, Xia Z. The retinoid X receptors and their ligands. Biochim Biophys Acta. 2012;1821(1):21-56.

Dedhar S, Rennie PS, Shago M, Hagesteijn C-Y L, Yang H, Filmus J. Inhibition of nuclear hormone receptor activity by calreticulin. Nature. 1994;367:480-483.

de Kleijn DPV, Janssen KPC, Waddy SL, Hegeman R, Lai W Y, Martens GJM, Van Herp F. Expression of the crustacean hyperglycemic hormones and the gonad-inhibiting hormone during the reproductive cycle of the female American lobster *Homarus americanus*. J. Endocrinol. 1998;156:291-298.

Desai D, Michalak M, Singh NK, Nilesi RM. Inhibition of retinoic acid receptor function and retinoic acid-regulated gene expression in mouse melanoma cells by calreticulin. J Biol Chem. 1996;271:15153–15159.

Edomi P, Azzoni E, Mettulio R, Pandolfelli N, Ferrero EA, Giulianini PG. Gonad-inhibiting hormone of the Norway lobster (*Nephrops norvegicus*): cDNA cloning, expression, recombinant protein production, and immunolocalization. Gene. 2002;284:93-102.

Eichner C. et al. Characterization of a novel RXR receptor in the salmon louse (*Lepeophtheirus salmonis*, Copepoda) regulating growth and female reproduction. BMC genomics 2015;16:81.

Fingerman M, Nagabhushanam R, Sarojini R. Vertebrate-type hormones in crustaceans: localization, identification and functional significance. Zool Sci. 1993;10:13-29.

Gu P-L, Chan S-M. The shrimp hyperglycemic hormone-like neuropeptide is encoded by multiple copies of genes arranged in a cluster. FEBS Lett. 1998;441:397-403.

Gu P-L, Yu KL, Chan S-M. Molecular characterization of an additional shrimp hyperglycemic hormone: cDNA cloning, gene organization, expression and biological assay of recombinant proteins. FEBS Lett. 2000;472:122-128.

Hopkins PM, Durica D, Washington T. RXR isoforms and endogenous retinoids in the fiddler crab, Uca pugilator. Comp Biochem Physiol A. 2008;151:602–614.

Jeon JM, Lee SO, Kim KS, Baek HJ, Kim S, Kim IK, Mykles DL, Kim HW. Characterization of two vitellogenin cDNAs from a Pandalus shrimp (*Pandalopsis japonica*):

expression in hepatopancreas is down-regulated by endosulfan exposure. Comp Biochem Physiol B Biochem Mol Biol. 2010;157:102-12

Laudet V, Hänni C, Coll J, Catzeflis F, Stéhelin D. Evolution of the nuclear receptor gene superfamily. EMBO J. 1992;11(3):1003–1013.

Lu W, Wainwright G, Webster SG, Rees HH, Turner PC. Clustering of mandibular organ-inhibiting hormone and moult-inhibiting hormone genes in the crab, *Cancer pagurus*, and implications for regulation of expression. Gene. 2000;253:197-207.

Nagaraju GPC. Is methyl farnesoate a crustacean hormone? Aquaculture. 2007;272: 39–54

Cabezón C, Cabrera G, Paredesa R, Ferreira A, Galanti N. Echinococcus granulosus calreticulin:molecular characterization and hydatid cyst localization. Mol Immunol. 2008; 45:1431–1438.

Nagaraju GPC. Reproductive regulators in decapods crustaceans: an overview. J Exp Biol. 2011;214:3-16.

Nagaraju, GPC, Rajitha B, Borst DW. Molecular cloning and sequence of retinoid X receptor in the green crab *Carcinus maenas*: a possible role in female reproduction. J Endocrinol. 2011;210:379–390.

Ohira T, Okumura T, Suzuki M, Yajima Y, Tsutsui N, Wilder MN & Nagasawa H. Production and characterization of recombinant vitellogenesis-inhibiting hormone from the American lobster, *Homarus americanus*. Peptides. 2006;27:1251-1258.

Phiriyangkul P, Utarabhand P. Molecular characterization of a cDNA encoding vitellogenin in the banana shrimp, *Penaeus (Litopenaeus merguiensis* and sites of vitellogenin mRNA expression. Mol Reprod Dev. 2006;73:410-423.

Soyez D, Van Deijnen JE, Martin M. Isolation and characterization of a vitellogenesis-inhibiting factor from sinus glands of the lobster, *Homarus americanus*. J Exp Zool. 1987;244(3):479-484.

Tang J, Zhu DF, Cui XY, Xie X, Qiu, XE. Molecular cloning, characterization and expression analysis of the retinoid X receptor in the swimming crab, *Portunus trituberculatus* (Miers, 1876) (Decapoda, Portunidae). Crustaceana. 2014;87:312–327.

Treerattrakool S, Panyim S, Chan SM, Withyachumnarnkul B, Udomkit A. Molecular characterization of gonad-inhibiting hormone of *Penaeus monodon* and elucidation of its inhibitory role in vitellogenin expression by RNA interference. FEBS J. 2008;275:970-980.

Treerattrakool S, Panyim S, Udomkit A. Induction of ovarian maturation and spawning in *Penaeus monodo*n broodstock by double-stranded RNA. Mar Biotechnol. 2011;13:163-169.

Tsang WS, Quackenbush LS, Chow BK, Tiu SH, He JG, Chan SM. Organization of the shrimp vitellogenin gene: evidence of multiple genes and tissue specific expression by the ovary and hepatopancreas. Gene. 2003;303:99-109.

Tseng DY, Chen YN, Kou GH, Lo CF, Kuo CM. Hepatopancreas is the extraovarian site of vitellogenin synthesis in black tiger shrimp, *Penaeus monodon*. Comp Biochem Physiol. 2001;129A:909-917.

Tsutsui N, Kawazoe I, Ohira T, Jasmani S, Yang WJ, Wilder MN, Aida K. Molecular characterization of a cDNA encoding vitellogenin and its expression in the hepatopancreas and ovary during vitellogenesis in the Kuruma prawn, *Penaeus japonicus*. Zool Sci. 2000;17:651-660.

Urtgam S, Treerattrakool S, Roytrakul S, Wongtripop S, Prommoon J, Panyim S, Udomkit A. Correlation between gonad-inhibiting hormone and vitellogenin during ovarian maturation in the domesticated *Penaeus monodon*. Aquaculture. 2015; 437**:**1-9.

Wang YH & LeBlanc GA. Interactions of methyl farnesoate and related compounds with a crustacean retinoid X receptor. Molecular and Cellular Endocrinology 2009:309;109–116.

Wang YH, Wang G, LeBlanc GA. Cloning and characterization of the retinoid X receptor from a primitive crustacean Daphnia magna. Gen. Comp. Endocrinol. 2007;150:309–318.

Wilder MN, Okumura T, Tsutsui N. Reproductive mechanisms in crustacean focusing on selected prawn species: vitellogenin structure, processing and synthetic control. Aqua-BioSci Monogr. 2010;3:73-110.

Tsang WS, Quackenbush LS, Chow BK, Tiu SH, He JG, Chan SM. Organization of the shrimp vitellogenin gene: evidence of multiple genes and tissue specific expression by the ovary and hepatopancreas.Gene. 2003;303:99-109.

Wiwegweaw A, Udomkit A, Panyim S. Molecular structure and organization of crustacean hyperglycemic hormone genes of *Penaeus monodon*. J Biochem Mol Biol. 2004;37(2):177-184.

Wu LT, Chu KH. Characterization of heat shock protein 90 in the shrimp *Metapenaeus ensis*: Evidence for its role in the regulation of vitellogenin synthesis. Mol Reprod Dev. 2008;75(5):952-9.

Xie S, Sun L, Liu F, Dong B. Molecular characterization and mRNA transcript profile of vitellogenin in Chinese shrimp, *Fenneropenaeus chinensis*. Mol Biol Rep. 2009;36:389-397.

Yano I. Effect of thoracic ganglion on vitellogenin secretion in kuruma prawn, *Penaeus japonicus*. Bull Natl Res Inst. Aquaculture. 1992;21:9-14.

Yano I, Tsukimura B, Sweeney JN, Wyban JA. Induced ovarian maturation of *Penaeus vannamei* by implantation of lobster ganglion. J World Aquacult Soc. 1988;19:201-209.

Outputs

1. Sathapondecha P, Panyim S, Udomkit A. A novel function of bursicon in stimulation of vitellogenin expression in black tiger shrimp, *Penaeus monodon*. Aquaculture. 2015;446:80-87.
2. Sathapondecha P, Panyim S, Udomkit A. An essential role of Rieske domain oxygenase Neverland in the molting cycle of black tiger 1 shrimp, *Penaeus monodon*. Comp Biochem Physiol-A. 2017;213:11-19.
3. Sathapondecha P, Panyim S, Udomkit A. *In vitro* study of a putative role of gonad-inhibiting hormone in oocyte growth stimulation in *Penaeus monodon*. Aquaculture Res. 2017;48: 5846–5853.
4. Ho T, Panyim, S, Udomkit A. Suppression of Argonautes compromises viral infection in *Penaeus monodon*. Submitted to Developmental and Comparative Immunology (under revision).
5. Sukthaworn S, Panyim, S, Udomkit A. Piwi controls transposon expression and spermatogenesis in *Penaeus monodon*. Submitted to Aquaculture (under review).

Appendices

Reprints

1. Sathapondecha P, Panyim S, Udomkit A. A novel function of bursicon in stimulation of vitellogenin expression in black tiger shrimp, *Penaeus monodon*. Aquaculture. 2015;446:80-87.

2. Sathapondecha P, Panyim S, Udomkit A. An essential role of Rieske domain oxygenase Neverland in the molting cycle of black tiger 1 shrimp, *Penaeus monodon*. Comp Biochem Physiol-A. 2017;213:11-19.

3. Sathapondecha P, Panyim S, Udomkit A. *In vitro* study of a putative role of gonad-inhibiting hormone in oocyte growth stimulation in *Penaeus monodon*. Aquaculture Res. 2017;48: 5846–5853.

Manuscripts

1. Ho T, Panyim, S, Udomkit A. Suppression of Argonautes compromises viral infection in *Penaeus monodon*. Submitted to Developmental and Comparative Immunology (under revision).

2. Sukthaworn S, Panyim, S, Udomkit A. Piwi controls transposon expression and spermatogenesis in *Penaeus monodon*. Submitted to Aquaculture (under review).

Aquaculture 446 (2015) 80–87

Contents lists available at ScienceDirect

Aquaculture

journal homepage: www.elsevier.com/locate/aqua-online

A novel function of bursicon in stimulation of vitellogenin expression in black tiger shrimp, *Penaeus monodon*

Ponsit Sathapondecha [a], Sakol Panyim [a,b], Apinunt Udomkit [a,*]

[a] Institute of Molecular Biosciences, Mahidol University, Salaya Campus, Nakhon Pathom 73170, Thailand
[b] Department of Biochemistry, Faculty of Science, Mahidol University, Rama VI Road, Bangkok 10400, Thailand

ARTICLE INFO

Article history:
Received 28 February 2015
Received in revised form 23 April 2015
Accepted 25 April 2015
Available online 2 May 2015

Keywords:
Cystine knot
Vitellogenesis
Shrimp
Gonad-stimulating hormone
Gonadotropins

ABSTRACT

Bursicon is a cystine knot glycoprotein hormone that is composed of two subunits; alpha and beta. Bursicon plays several physiological roles in insects and crustaceans such as cuticle tanning, wing expansion and molting process. Because of its structural similarity with vertebrate gonadotropins, this study therefore aimed to investigate a novel function of bursicon in vitellogenin (Vg) stimulation in reproductive female shrimp, *Penaeus monodon*. Full-length cDNAs encoding the alpha and beta subunits of bursicon in *P. monodon* (Pmbursα and Pmbursβ) were obtained by rapid-amplification of cDNA ends. Both *Pmbursα* and *Pmbursβ* mRNA levels were dominantly expressed in subesophageal ganglia and thoracic ganglia. The expression of *Pmbursα* and *Pmbursβ* in subesophageal ganglia was significantly increased in early-vitellogenic stage of ovarian development suggesting a possible role of bursicon in vitellogenesis. To study the function of bursicon in shrimp reproduction, recombinant Pmbursα (rbursα), Pmbursβ (rbursβ) and Pmbursαβ (rbursαβ) were successfully expressed in the methylotrophic yeast, *Pichia pastoris*. A treatment of shrimp ovarian cells with recombinant Pmburs showed that only rbursαβ could induce the expression of *Vg* mRNA. In addition, injection of rbursαβ into female *P. monodon* broodstock caused an increase of *Vg* mRNA expression in the ovary as well as stimulated ovarian development. This study provides the first evidence for a reproductive role, most likely as an invertebrate neuropeptide gonad-stimulating hormone, of the heterodimeric bursicon in *P. monodon*.

Statement of relevance

Useful information for improvement of shrimp reproduction.

1. Introduction

Oocyte development is an important physiological process in female reproduction. In crustaceans, the oocyte development can be divided into two major phases; primary vitellogenesis and secondary vitellogenesis. The primary vitellogenesis involves oocyte growth and follicular development whereas the secondary vitellogenesis precedes by the synthesis and accumulation of vitellogenin (Vg), a precursor of yolk protein, and oocyte maturation (Charniaux-Cotton, 1985). Vitellogenesis in both phases is regulated by several factors such as peptide hormones, steroid hormones and neurotransmitters. A neuropeptide gonad-inhibiting hormone (GIH) is well-characterized in its function of vitellogenesis inhibition in several crustaceans including *Penaeus monodon*, *Litopenaeus vannamei* and *Homarus americanus* (Chen et al., 2014; de Kleijn et al., 1994; Treerattrakool et al., 2008). In contrast, a putative gonad-stimulating hormone (GSH) is believed to be synthesized and secreted from brain and/or thoracic ganglia of crustaceans. For instances, the injection of thoracic ganglia extract prepared from vitellogenic female shrimp, *Penaeus japonicus*, resulted in an increase in the hemolymph Vg level (Yano, 1992). In addition, ovarian maturation in *Penaeus vannamei* was induced after the injection of brain extract from vitellogenic female American lobster, *H. americanus* (Yano and Wyban, 1992). In addition, in the red swamp crayfish, *Procambarus clarkii*, oocyte growth could be stimulated by a neurotransmitter serotonin in the ovarian explants that was co-incubated with brain or thoracic ganglia, but not in the serotonin-treated ovarian explants alone (Sarojini et al., 1996). This result suggested that serotonin stimulated the secretion of a putative GSH from brain and thoracic ganglia that was required for oocyte growth. These evidences suggested the existence of putative GSH in the brain and thoracic ganglia of crustaceans though none has been identified and characterized so far.

In vertebrates, gonad development is controlled by gonadotropins such as follicle-stimulating hormone (FSH), luteinizing hormone (LH) and chorionic gonadotropin (CG) (Burger et al., 2004). These hormones are heterodimeric glycoprotein hormone composing of alpha and beta subunits. Each subunit forms a conserved cystine knot-containing tertiary structure (Boime and Ben-Menahem, 1999; Milton and Peter,

* Corresponding author. Tel.: +66 2 441 9003 7x1236; fax: +66 2 441 9906.
E-mail address: apinunt.udo@mahidol.ac.th (A. Udomkit).

http://dx.doi.org/10.1016/j.aquaculture.2015.04.027
0044-8486/

2000). The function of FSH and LH are known to stimulate follicular development, steroid hormone production, and ovulation (Ulloa-Aguirre and Timossi, 1998; Weghofer et al., 2007). In crustaceans, the existence of vertebrate gonadotropin-like hormone in brain and thoracic ganglia was demonstrated by a number of studies. The FSH and LH-like peptide were detected in the brain and thoracic ganglia tissues of the swimming crab, *Portunus trituberculatus* using the monoclonal antibody against human FSH or LH (Huang et al., 2008). Moreover, FSH-like peptide in the hemolymph of *Marsupenaeus japonicas* was also detected by ELISA, and its level was increased in vitellogenic stage of ovarian development suggesting the involvement of FSH-like peptide in gonad-stimulation in the shrimp (Ye et al., 2011). Nevertheless, a vertebrate gonadotropin-like peptide in crustaceans has not yet been identified.

An invertebrate cystine knot glycoprotein, bursicon (burs) was first discovered in the blowflies and was demonstrated for its role in cuticle tanning (Fraenkel and Hsiao, 1965). Since then, diverse functions of bursicon have been elucidated such as wing expansion (Huang et al., 2007; Nathan et al., 2008) and development in insects (Loveall and Deitcher, 2010), and cuticle hardening during the molting cycle of crustaceans (Chung et al., 2012; Webster et al., 2013; Wilcockson and Webster, 2008). Bursicon is a heterodimeric protein comprising of alpha (bursα) and beta (bursβ) subunits. Both subunits are mainly synthesized at thoracic ganglia in crustaceans (Chung et al., 2012; Sharp et al., 2010; Webster et al., 2013; Wilcockson and Webster, 2008) and at ventral nervous tissues in insects (Honegger et al., 2011; Luo et al., 2005). Each burs subunit contains a cystine knot conserved sequence C–X–G–X–C, which forms a cystine knot structure by 3 disulfide bonds similar to that of other cystine knot growth factors such as vertebrate gonadotropins and transforming growth factor (Avsian-Kretchmer and Hsueh, 2004; Honegger et al., 2008). This structural homology of bursicon to other growth factors therefore suggests its possible roles in growth and reproductive processes.

This study is aimed to investigate a reproductive function of bursicon in female black tiger shrimp, *P. monodon*. A full-length cDNA of both *P. monodon bursα* (*Pmbursα*) and *bursβ* (*Pmbursβ*) was cloned, and the correlation between their expression and ovarian development was investigated. A recombinant *P. monodon*'s bursicon was expressed in the yeast *Pichia pastoris* and was used to demonstrate its function in gonad-stimulation in the shrimp.

2. Material and methods

2.1. RNA extraction and cDNA synthesis

Adult female black tiger shrimp, *P. monodon* were provided from Shrimp Genetic Improvement Center, Suratthani, Thailand. All animal experiments were carried out in accordance with animal care and use protocol of the Mahidol University Animal Care and Use Committee. Shrimp tissues were freshly isolated from the shrimp that had been anesthetized on ice, and the total RNA was extracted by Ribozol reagent (Ameresco, USA) according to the manufacturer's protocol. The RNA concentration was measured by Nanodrop (ND-1000, Thermoscientific). The total RNA was treated with 0.5 U DNase I (Thermoscientific) at 37 °C for 15 min, then heated at 65 °C for 5 min before converting into the first-stranded cDNA. The cDNA synthesis was primed with an oligo-dT primer in a reaction containing 1X reverse transcriptase buffer (Promega), 3 mM $MgCl_2$, 0.5 mM dNTP and 1 μl Impromp II reverse transcriptase (Promega). The reverse transcription reaction was incubated at 25 °C for 5 min, 42 °C for 60 min and 70 °C for 10 min. The cDNA was kept at −20 °C until use.

2.2. Cloning of full-length PmBursα and PmBursβ cDNAs

The nucleotide sequence of *L. vannamei* EST clone (Accession No. FE173462) that showed high homology to bursα of *Homarus gammarus* (Accession No. HM113369) was aligned with that of bursα of *H. gammarus*, *Carcinus maenas* and *Callinectes sapidus*, and the conserved sequences were selected to design specific primers for obtaining Pmbursα partial nucleotide sequence. While the conserved sequences among the translated amino acid sequence of bursβ of *H. gammarus*, *C. maenas* and *C. sapidus* was used to design degenerate primers to obtain partial sequence of Pmbursβ (data not shown). These partial nucleotide sequences of Pmbursα and Pmbursβ were used to design specific primers for the cloning of full-length cDNA encoding each subunit as described below.

A full-length cDNA of PmBursα and PmBursβ was obtained by rapid amplification of cDNA ends (RACE). In 3′ RACE, the cDNA synthesized from thoracic ganglia RNA was used to amplify with PmBursα-F1 or PmBursβ-F1 and oligo-dT (PRT) primers in a PCR reaction mixture containing 1X *Taq* DNA polymerase buffer with 2 mM $MgCl_2$, 0.2 mM dNTP, 0.2 μM primers and 1 U *Taq* DNA polymerase (New England Laboratory). The PCR reaction was performed at 94 °C for 3 min, then 35 cycles of 94 °C for 30 s, 60 °C for 30 s and 72 °C for 30 s followed by a final extension at 72 °C for 5 min. The PCR product was used as a template in nested PCR with PmBursα-F2 or PmBursβ-F2 and PM1 primers with the same temperature profile. For 5′ RACE, two microgram of thoracic ganglia RNA was used to synthesize the first-stranded cDNA with PmBursα-R1 or PmBursβ-R1 primer. The cDNA was 3′-tailed with dATP by terminal deoxynucleotidyl transferase (TdT) reaction composing of 1X TdT buffer, 0.2 mM dATP and 1 U TdT (Promega). The reaction was incubated at 37 °C for 30 min, then 65 °C for 5 min. The poly A-tailed cDNA was used as a template in the PCR with PmBursα-R2 or PmBursβ-R2 and oligo-dT primer pair. The PCR product was subsequently used to amplify with nested primers (PmBursα-R3 or PmBursβ-R3 and PM1 primer pair). These PCR products were ligated to pGemT-easy vector (Promega), and used to transform into *Escherichia coli* DH5α. The nucleotide sequences of the cloned cDNAs were determined by 1st-Base company, Malaysia. Nucleotide sequences of all primers were shown in Table 1.

2.3. Expression of Pmbursα and Pmbursβ in shrimp tissues

Determination of mRNA levels was performed by quantitative real-time RT-PCR. The cDNA from different tissues of adult female *P. monodon* was used as a template in a PCR mixture that was composed

Table 1
List of nucleotide sequence of primers used in this study.

Primer	Sequence (5′ → 3′)	Experiment
PRT	CCGGAATTCAAGCTTCTAGAGGATCCTTTTTTTTTTT TTTTTT	cDNA, RACE
PM1	CCGGAATTCAAGCTTCTAGAGGATCC	RACE
Pmbursβ-F1	TGCAACCATCCGTCAACACTC	3′RACE,qPCR
Pmbursβ-F2	GGATTCCTGAAGGACTGCC	3′RACE
Pmbursβ-R1	AGTGGGATCGAACTCCTTATCGG	5′RACE.qPCR
Pmbursβ-R2	GGCAGTCCTTCAGGAATCC	5′RACE
Pmbursβ-R3	GAGTGTTGACGGATGGTTGC	5′RACE
matPmbursβ-F	CCGCTCGAGAAAAGACACACCTACGGCTCAGAATG	Protein expression
matPmbursβ-R	GCTTCTAGATTATCGGATCGAATTCCCGCAC	Protein expression
Pmbursα-F1	TGCATGTGTTGCCAGGAGTC	3′RACE
Pmbursα-F2	CGCCCATTGACTGCATGTG	3′RACE,qPCR
Pmbursα-R1	GAGATCACAGGTCGGCAACG	5′RACE.qPCR
Pmbursα-R2	AAGGGCGTGGTGGTCATTAC	5′RACE
Pmbursα-R3	AAGTTGGCGATCTCCTGCG	5′RACE
matPmbursα-F	CCGCTCGAGAAAAGAGACGAATGCTCCCTGACG	Protein expression
matPmbursα-R	GCTTCTAGATTACTTCAGGAATGGGACG	Protein expression
EF1α-F	GAACTGCTGACCAAGATCGACAGG	qPCR
EF1α-R	GAGCATACTGTTGGAAGGTCTCCA	qPCR
Vg-F	TCCATCTGCAGCACCAATCTTCGC	qPCR
Vg-R	GCAACAGCCTTCATTCTGATGCCA	qPCR
5′ AOX1	GACTGGTTCCAATTGACAAGC	PCR
3′ AOX1	GCAAATGGCATTCTGACATCC	PCR

of 1X SYBR fast ABI Prism® qPCR (KAPA Biosystem) and 0.25 μM of each gene-specific primer shown in Table 1. The PCR reaction was carried out in real-time PCR machine (realplex^4, Eppendorf) with the temperature profile of 95 °C for 3 min, then 40 cycles of 95 °C for 5 s and 60 °C for 30 s. Subsequently, the melting curve analysis was performed by incubation of the PCR product at 95 °C for 30 s, 60 °C for 30 s and 95 °C for 30 s. The Ct value of the target gene and reference gene (Elongation factor 1α, *EF1α*) was calculated for its copy number from the standard curve of each gene that was constructed from the Ct values of the amplification of each gene at different copy numbers ranging from 10^2 to 10^8 copies. The relative expression of the target gene was presented as a ratio of its copy number to that of the reference gene.

2.4. Construction of recombinant PmBursα, PmBursβ and PmBursαβ expression vector

The nucleotide sequences encoding mature peptide of either Pmbursα or PmBursβ were amplified with matPmbursα-F and matPmbursα-R or matPmbursβ-F and matPmbursβ-R primer pairs, respectively (Table 1). The cDNA from subesophageal ganglia was used as a template in a PCR reaction mixture containing of 1X *Pfu* polymerase buffer with 1.5 mM $MgCl_2$, 0.2 mM dNTP, 0.2 μM each primer and 1 U *Pfu* polymerase (Promega). The PCR reaction was performed at 94 °C for 3 min, then 35 cycles of 94 °C for 30 s, 60 °C for 30 s and 72 °C for 1 min. The PCR product of the mature Pmbursα and Pmbursβ coding sequences were digested with *Xho* I and *Xba* I prior to ligation to pPICZαA plasmid (Invitrogen) that had been digested with the same restriction enzymes to produce pmatPmbursα and pmatPmbursβ recombinant plasmids. Both recombinant plasmids were individually transformed into *E. coli* DH5α. The nucleotide sequences of the cloned fragments were determined by automated DNA sequencing (1st Base Company, Malaysia). To construct a dual expression plasmid containing both matPmbursα and matPmbursβ expression cassettes, the pmatPmbursα plasmid was linearized with *Bam*H I and dephosphorylated by alkaline phosphatase enzyme. Due to the size of the matPmbursβ expression cassette excised with *Bam*H I and *Bgl* II was very close to that of the vector backbone, the matPmbursβ expression cassette was excised from the pmatPmbursβ plasmid by digestion with *Bgl* II, *Bam*H I and also with *Nco*I that cut within the vector backbone sequence in order to eliminate the backbone such that the matPmbursβ expression cassette would be purified more easily. The matPmbursβ cassette was then ligated into the linearized pmatPmBursα with T4 ligase enzyme. The resulting recombinant plasmid, pmatPmbursαβ, was verified by restriction enzyme analysis with *Eco*R I, *Bgl* II and *Bam*H I enzymes. Approximately 50 ng of pmatPmBursα and pmatPmbursβ were linearized with *Dra* I as well as 500 ng of undigested pmatPmbursαβ prior to transformation into the *P. pastoris* KM71 by electroporation using a condition of 2 kV and 25 μF. The transformants were cultured on YPD (1% w/v yeast extract, 2% w/v peptone and 2% w/v D-glucose) containing 100 μg/ml zeocin (Invitrogen) agar. The genomic DNA of *P. pastoris* recombinants was extracted following Lõoke et al., 2011. Integration of each matPmburs expression cassette into the yeast genomic was then verified by PCR with 5′AOX1 and 3′AOX1 primers (Table 1).

2.5. Expression and purification of recombinant Pmburs in P. pastoris

The expression of Pmburs proteins from recombinant *P. pastoris* KM71 was induced by methanol induction. A single colony of recombinant *P. pastoris* KM71 was cultured in YPD medium containing 100 μg/ml zeocin at 30 °C for 2 days. The starter culture was inoculated in BMGY medium (1% w/v yeast extract, 2% w/v peptone, 100 mM phosphate buffer pH 6.0, 1% v/v glycerol, 0.67% w/v YNB and 0.00004% w/v biotin) at the OD_{600} of 0.1. The yeast culture was incubated at 30 °C for 12–13 h until the OD_{600} reached 6–8. Approximately 30–35 OD_{600}/ml of *P. pastoris* culture were induced in BMMY medium (1% w/v yeast extract, 2% w/v peptone, 100 mM phosphate buffer pH 6.0, 3% v/v methanol, 0.67% w/v YNB and 0.0004% w/v biotin) at 30 °C for 2 days. The culture medium was then collected, and recombinant Pmburs proteins were subsequently precipitated by 40–50% saturated ammonium sulfate. The ammonium sulfate precipitated proteins were further purified by anion exchange chromatography by dissolving in 20 mM Tris pH 7.4 and subjected into a Hitrap Q HP column (GE Healthcares). After washing the column with 20 mM Tris pH 7.4, a step-wise elution was performed with 20 mM Tris pH 7.4 containing different concentration of NaCl ranging from 0.1 to 0.5 M. The purified rPmbursα and rPmbursβ were identified by liquid chromatography and mass spectrometry (LC-MS/MS). Analysis of dimeric formation of the purified recombinant Pmburs was performed by SDS-PAGE either with or without the reducing agent, β-mercaptoethanol and native polyacrylamide gel.

2.6. Functional assay of recombinant Pmburs proteins in P. monodon

The function of Pmburs in the stimulation of vitellogenin expression was studied both in the primary culture of ovarian cells and in the shrimp. To prepare the ovarian cells, previtellogenic ovaries were freshly isolated from adult female *P. monodon*, excised into small pieces and rinsed with the culture medium (Leibovitz's L-15 powder, 0.5% w/v NaCl, 1% w/v D-glucose, 3.33% w/v lactalbumin, 10% v/v FBS, 10% v/v shrimp meat extract) containing 100 U penicillin/streptomycin. The ovary pieces were washed several times in the culture medium containing 1000 U and 2000 U penicillin/streptomycin, and subsequently chopped by scissors until homogeneous suspension was obtained. Approximately 7.5×10^5 oocyte cells were seeded in 1 ml culture medium at 28 °C. After seeded the cells for overnight, the culture medium was discarded and replaced with fresh culture medium containing 200 ng of either rbursα, rbursβ or rbursαβ whereas the Tris/NaCl buffer (20 mM Tris pH 7.4, 200 mM NaCl) was added to the control cells. This amount of recombinant protein was based on twice amount of the bursicon in hemolymph at ecdysis stage of the crab, *C. maenas* (Webster et al., 2013). After treatment for 24 h, approximately 1 ml of ovarian cells was collected to determine *Vg* expression levels. The culture medium of the remaining 24-h treated ovarian cells was then replaced with 500 μl of the fresh culture medium containing the same concentration of the recombinant proteins, and cultured for another 24 h before collecting the cells. Total RNA was extracted from the cells that were treated with each rPmburs protein for 24 and 48 h as well as from the control cells, and the *Vg* mRNA level was determined by real-time RT-PCR as described above.

For *in vivo* study, previtellogenic female shrimp (~90 g) were injected with 6 μg of rbursαβ (equivalent to approx. 60 ng/g shrimp body weight) or Tris/NaCl buffer. Two days later, the shrimp were injected for the second time with the same treatment. Ovaries were isolated on day 4 after the first injection to determine for *Vg* mRNA expression by real-time RT-PCR using EF1α as an internal control as described previously. The developmental stage of the ovary was observed by the appearance of the ovary through the dorsal skeleton under the torchlight as described by Tan-Fermin and Pudadera, 1989.

3. Results and discussion

3.1. Characterization of Pmbursα and Pmbursβ cDNAs

A heterodimeric glycoprotein hormone, bursicon has been identified and characterized in several insects such as *Calliphora erythrocephala*, *Drosophila melanogaster*, *Anopheles gambiae* and *Bombyx mori* (Fraenkel and Hsiao, 1965; Honegger et al., 2011; Huang et al., 2007; Luo et al., 2005) and crustaceans including *H. gammarus*, *C. maenas* and *C. sapidus* (Chung et al., 2012; Sharp et al., 2010; Wilcockson and Webster, 2008).

Total RNA from thoracic ganglia was used as a source for cDNA cloning of *P. monodon*'s bursicon in this study because bursicon was commonly found in the thoracic ganglia of several crustaceans. The full-length cDNA encoding Pmbursα and Pmbursβ in *P. monodon* (GenBank accession no. KP191597 and KP191598, respectively) were

successfully obtained by RACE technique. The *Pmbursα* cDNA contains a 423 bp open reading frame coding for a putative signal peptide and a mature peptide of 20 and 121 amino acids, respectively. A 432 bp open reading frame of *Pmbursβ* cDNA encodes 29 amino acids residues of a signal peptide and a 115 amino acids mature peptide of Pmbursβ. An alignment of the deduced amino acid sequences of Pmbursα and Pmbursβ to those of other arthropods indicated high levels of similarity (Fig. 1A and B). Pmbursα and Pmbursβ share the highest identity of 84% and 83%, respectively to that of *H. gammarus*. The amino acid sequences of both Pmburs subunit peptides contain 11 conserved cysteine residues including a conserved sequence of cystine knot-containing proteins, C–X–G–X–C, that is found in other cystine knot growth factors such as vertebrate gonadotropins and transforming growth factor (Avsian-Kretchmer and Hsueh, 2004; Honegger et al., 2008). In addition, three intra-molecular disulfide bridges were found in both bursicon subunits which were paired between C1 and C7, C3 and C9, and C4 and C10 (Fig. 1). Structurally, two of these disulfide bonds form a knot-ring and another pass through the ring resulting in three-loop formation. This was similar to other cystine knot-containing proteins including glycoprotein hormone family, transforming growth factor beta and bone morphogenetic protein (BMP) antagonist (Roch and Sherwood, 2014). Moreover, additional disulfide bond between C2 and C8 formed a seat-belt like structure, which was similar to that of human CGβ (Hearn and Gomme, 2000) and *Drosophila* bursicon (Luo et al., 2005).

3.2. Expression of bursicon mRNAs in *P. monodon*

Bursicon peptide was detected in the ventral nerve cord of insects by immunohistostaining (Luo et al., 2005), whereas the mRNA detection by either semi-quantitative RT-PCR or *in situ* hybridization demonstrated

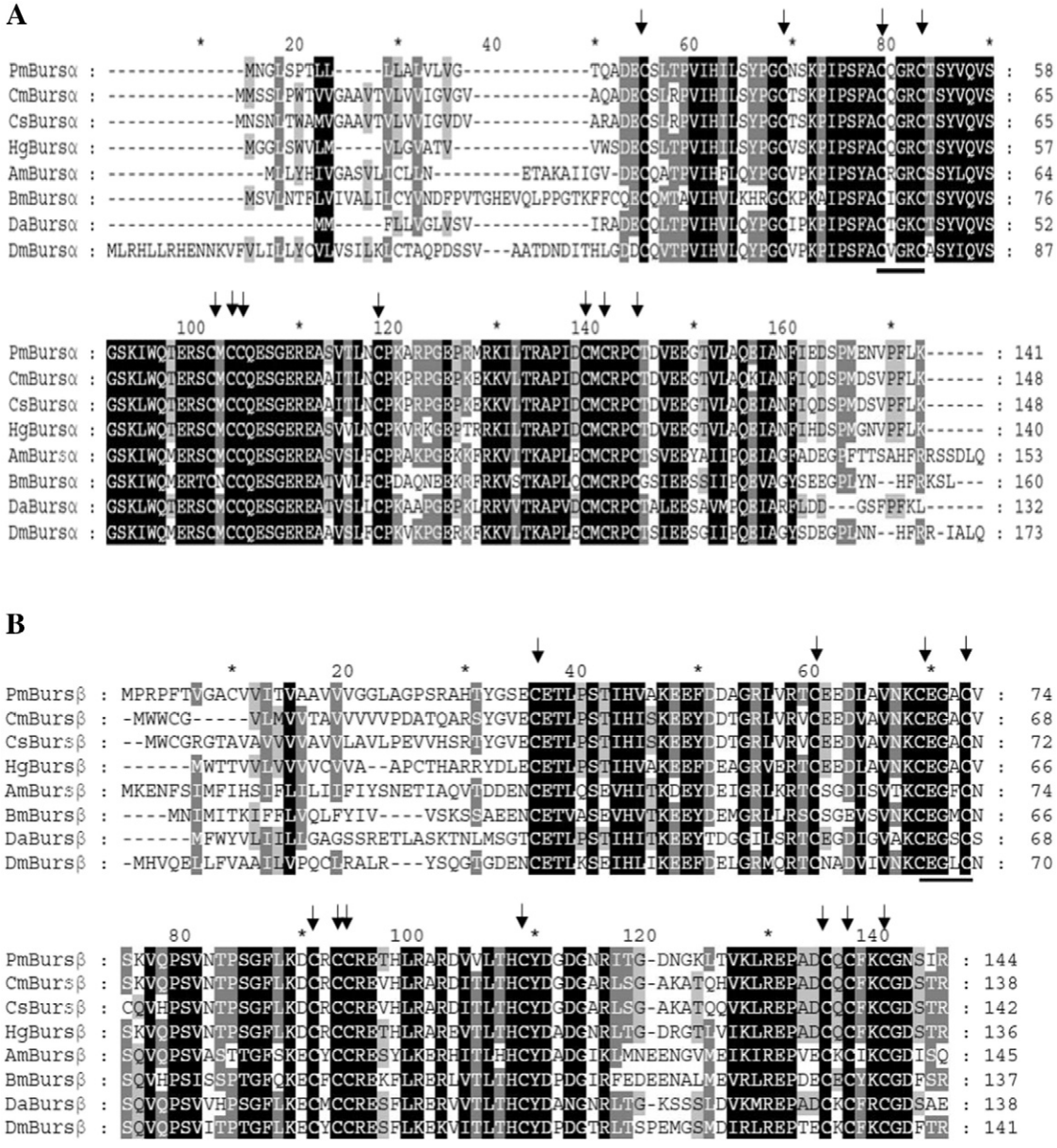

Fig. 1. Alignment of deduced amino acid sequences of bursα and bursβ. The deduced amino acid sequence of Pmbursα (A) and Pmbursβ (B) were aligned with those of other insects and crustaceans by Clustal X program. The sequences include bursicons of *C. maenas* (Cmbursα: EU139428 and Cmbursβ: EU139429), *C. sapidus* (Csbursα: EU677191 and Csbursβ: EU677190), *H. gammarus* (Hgbursα: HM113369 and Hgbursβ: HM113370), *Apis mellifera* (Ambursα: NM_001098234 and Ambursβ: NM_001040262), *B. mori* (Bmbursα: NM_001098375 and Bmbursβ: NM_001043824), *Daphnia arenata* (Dabursα: EU139431 and Dabursβ: EU139430) and *D. melanogaster* (Dmbursα: NM_142726 and Dmbursβ: NM_135868). The amino acids that were identical in all sequences are highlighted in black. The lesser degrees of identity are highlighted in different shades of gray. Arrows indicate conserved cysteine residues in cystine knot proteins. The conserved sequence of cystine knot protein is underlined.

the expression of both bursicon subunits in the thoracic ganglia of crustaceans (Chung et al., 2012; Sharp et al., 2010; Wilcockson and Webster, 2008). Similarly, the quantitative real-time PCR detection of bursicon mRNA in *P. monodon* revealed that both *Pmbursα* and *Pmbursβ* mRNA were dominantly expressed in subesophageal ganglia and thoracic ganglia whereas the expression in other tissues including eyestalk, brain, hepatopancreas, gills, ovary and muscle was not detectable (Fig. 2). This indicated a common source of bursicon production in crustaceans. In addition, the mRNA expression level of *Pmbursα* and *Pmbursβ* in subesophageal ganglia and each node of thoracic ganglia of previtellogenic female shrimp were determined. The result showed that both *Pmbursα* and *Pmbursβ* transcripts were expressed at higher level in subesophageal ganglia than in the thoracic ganglia, and that each node of thoracic ganglia expressed similar levels of *Pmbursα* and *Pmbursβ* transcripts (Fig. 3). This is similar to the mRNA expression of bursicon in the lobster, *H. gammarus* where no difference in the expression level in each node of either thoracic ganglia or abdominal nerve cords was reported (Sharp et al., 2010).

In order to investigate the correlation between bursicon expression and ovarian development in the shrimp, the expression of both *Pmbursα* and *Pmbursβ* in subesophageal ganglia of female *P. monodon* at different stages of ovarian development was determined by real-time RT-PCR. The result in Fig. 4 showed that *Pmbursα* and *Pmbursβ* expression was significantly increased approximately two-folds in early vitellogenic shrimp compared with that in pre-vitellogenic ovary (Fig. 4). The expression of *Pmbursα* and *Pmbursβ* in higher stages of ovarian development was then reduced again to the levels similar to that in previtellogenic stage. This result implicated that bursicon may play a role during early vitellogenesis in the shrimp. Although no direct evidence for the reproduction-related function of bursicon has been shown so far, our expression study of *bursicon* during ovarian developmental cycle in *P. monodon* together with its cystine knot structure that is conserved among vertebrate gonadotropins, which is involved in gonad-stimulation (Roch and Sherwood, 2014) suggesting that bursicon may play a role in reproduction of female shrimp, particularly in vitellogenin synthesis during ovarian development.

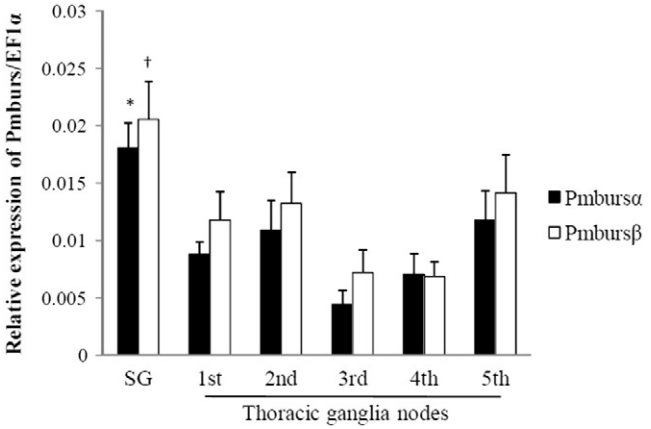

Fig. 3. Expression pattern of *Pmburs* mRNA in the ganglia of shrimp. Relative expression of *Pmbursα* (black bar) and *Pmbursβ* (open bar) in subesophageal ganglia and each node of thoracic ganglia of female *P. monodon* at previtellogenic stage of ovarian development were determined by real-time RT-PCR. The relative expression levels of *Pmburs* to that of *EF1α* are represented as mean ± SEM (n = 7). Asterisk and cross depict significant difference at $p < 0.05$ between groups by random complete block design ANOVA and pair-wise comparison with Tukey's HSD test of *Pmbursα* and *Pmbursβ*, respectively.

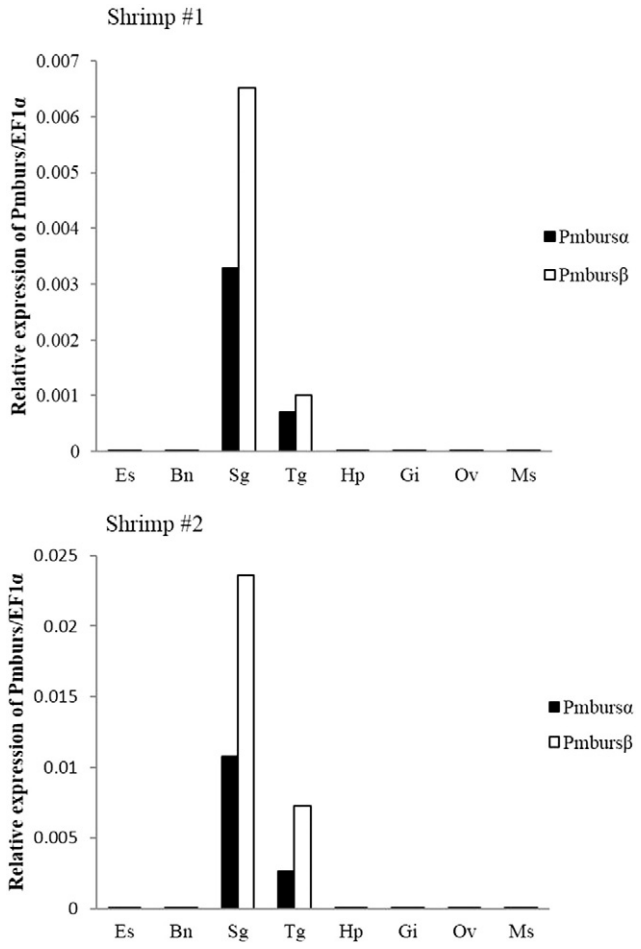

Fig. 2. Determination of *Pmburs* mRNA expression in various shrimp tissues. The *Pmbursα* (black bar) and *Pmbursβ* (open bar) mRNA expression were determined in *P. monodon* tissues including eyestalk (Es), brain (Bn), subesophageal ganglia (Sg), thoracic ganglia (Tg), hepatopancreas (Hp), gill (Gi), ovary (Ov) and muscle (Ms) by real-time RT-PCR. The expression in two shrimp is shown individually. The values are shown as relative expression level of *Pmburs* to that of *EF1α*.

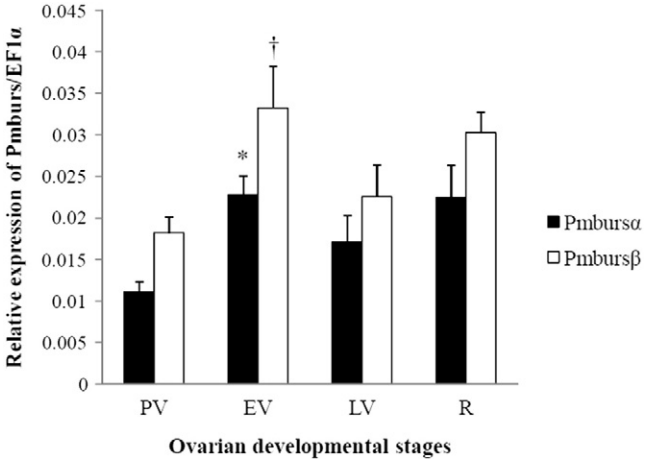

Fig. 4. Expression pattern of *Pmburs* mRNA in subesophageal ganglia at different stages of ovarian development. The subesophageal ganglia of female broodstock shrimp at each stage of ovarian development was determined for *Pmbursα* (black bar) and *Pmbursβ* (open bar) mRNA level by real-time RT-PCR. The ovarian stages are composed of previtellogenic (PV), early vitellogenic (EV), late vitellogenic (LV) and ripe stages (R). The relative expression levels of *Pmburs* to that of *EF1α* are represented as mean ± SEM (n = 7–9). Asterisk and cross depict significant difference at $p < 0.05$ between groups by one-way ANOVA and pair-wise comparison with Tukey's HSD test of *Pmbursα* and *Pmbursβ*, respectively.

3.3. Production of recombinant P. monodon's bursicon in P. pastoris

To study the function of bursicon in *P. monodon*, recombinant proteins of Pmbursα (rbursα) and Pmbursβ (rbursβ) were expressed in the yeast, *P. pastoris* either individually to produce a homodimeric form of each subunit or co-expressed together to produce a heterodimeric Pmbursαβ (rbursαβ). Because the homodimeric form of either bursα or bursβ could occur after expression in mammalian cells system (An et al., 2012; Luo et al., 2005), therefore the expression cassette of Pmbursα and Pmbursβ was cloned into the same plasmids for heterodimeric rbursαβ expression instead of *in vitro* dimerization of both rbursα and rbursβ subunits so as to prevent self-formation of homodimeric proteins. After ammonium sulfate precipitation, the expressed rbursα, rbursβ and rbursαβ were further purified by anion exchange Hitrap Q HP column (GE Healthcares). Only rbursβ and rbursαβ could be purified by anion exchange chromatography whereas rbursα seemed to be unstable under the condition used in the purification step, and thus could not be recovered after purification. Accordingly, the anion exchange purified rbursβ and rbursαβ and the ammonium sulfate precipitated rbursα were used in further studies.

Analysis by SDS-PAGE indicated that rbursα was expressed as two bands at the molecular weight of 16–18 kDa, which was similar to *Drosophila* bursα expressed in HEK293 cells (Luo et al., 2005), while a single band of rbursβ was presented at approximately 20 kDa.

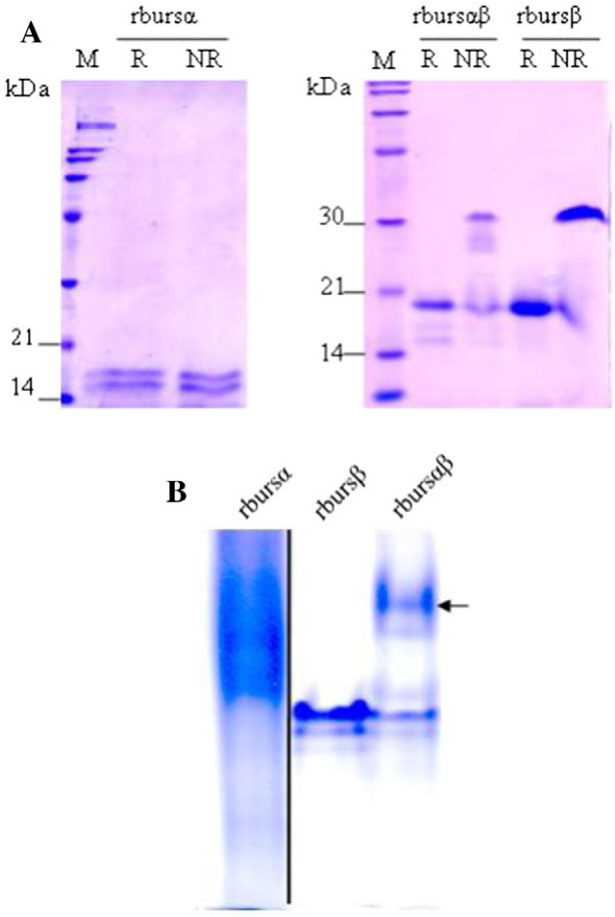

Fig. 5. Analysis of recombinant Pmburs peptides on polyacrylamide gel electrophoresis. Approximately 2 μg of rbursα, rbursβ and rbursαβ were analyzed by denaturing SDS-PAGE and native gel. The purified recombinant peptides treated with (R) or without (NR) reducing agent were separated on 15% SDS-PAGE (A). Analysis of the purified recombinant Pmburs in the native gel were performed by 7.5% polyacrylamide gel electrophoresis without SDS (B). M is a broad-range protein marker (Bio-rad). An arrow shows a heterodimer of rbursαβ.

The rbursαβ showed the band pattern corresponding to that of both rbursα and rbursβ (Fig. 5A). The protein bands of both rbursα and rbursβ were verified by LC-MS/MS, and the result revealed similarity to bursicons of the crab, *C. maenas* with 14% and 9% coverage, respectively (data not shown). When analyzed under reduced and non-reduced conditions, a protein band of rbursβ appeared at higher molecular weight of approximately 32 kDa under the non-reduced condition compared with that under the reduced condition (Fig. 5A) suggesting the formation of a homodimeric rbursβ via an intermolecular disulfide bond. The expected size of the homodimeric rbursβ was not well correlated with that of the monomeric form could possibly due to the difference in the structure of the monomer subunit or post-translational modifications, particularly glycosylation. Under the non-reduced condition, the strong intramolecular disulfide bonds might still hold the cystine knot structure of each monomer subunit of the homodimeric rbursβ, whereas the monomeric form under reduced condition did not retain the cystine knot structure. In contrast to rbursβ, rbursα showed the same protein pattern under both conditions suggesting that rbursα might not form a homodimer. However, when analyzed by native gel, rbursα appeared to be slightly larger than rbursβ (Fig. 5B) implying that rbursα was presented as homodimer that was likely formed by a non-disulfide bond.

In addition, the co-expression of rbursα and rbursβ resulted in the formation of rbursαβ heterodimer as recognized under the non-reduced condition (Fig. 5A). However, the homodimer of rbursβ and the free rbursα subunits were also present. The formation of rbursαβ when both subunits were co-expressed was confirmed by the presence of an extra band, as indicated by an arrow in Fig. 5B, in the native gel that did not appear in either rbursα or rbursβ alone. The expression of recombinant shrimp bursicon in *P. pastoris* suggested either homodimeric or heterodimeric formation of recombinant bursicon similar to the recombinant *Drosophila* bursicon expressed in HEK293 cells (An et al., 2012; Luo et al., 2005), except that the formation of shrimp rbursα homodimer might not occur by disulfide bond. This was probably due to the difference in the expression system and translational modification in different host systems.

3.4. Reproductive function of P. monodon bursicon

In order to study a possible involvement of bursicon in the reproduction in female *P. monodon*, its effect on vitellogenin expression and oocyte development were investigated. Vitellogenin (Vg), a precursor

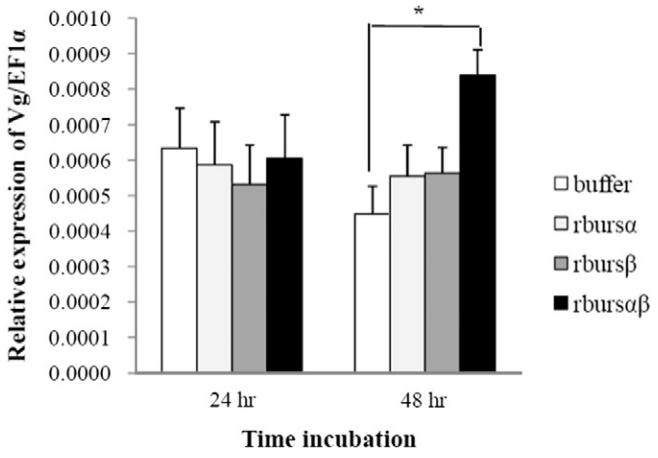

Fig. 6. Effect of recombinant Pmburs on vitellogenin mRNA expression in ovarian cells. The primary ovarian cells were treated with approximately 200 ng/ml rbursα, rbursβ, rbursαβ or Tris/NaCl buffer, and incubated at 28 °C for 24 and 48 h. After incubation, *Vg* mRNA level in the ovarian cells were determined by real-time RT-PCR. The relative expression levels of *Vg* to that of *EF1α* is presented as mean ± SEM of three independent experiments. Asterisk represents significant difference at $p < 0.05$ between groups by two-way ANOVA and pairwise comparison with Duncan's test.

of yolk protein, was used as a biomarker to determine the effect of bursicon on gonad stimulation. In primary ovarian cells, *Vg* mRNA levels after the treatment with rbursα, rbursβ or rbursαβ for 24 h did not change significantly when compared to that of the control cells. However, the *Vg* mRNA expression level was significantly elevated approximately two-folds in rbursαβ-treated ovarian cells at 48 h after treatment whereas the cells treated with rbursα or rbursβ still expressed the same level of *Vg* to the control cells (Fig. 6). This study indicated that only the heterodimeric rbursαβ, but not rbursα or rbursβ homodimer alone could stimulate *Vg* expression in ovarian cells of *P. monodon*. This effect of Pmburs on Vg stimulation is analogous to that of putative gonad-stimulating hormone from the brain and thoracic ganglia extracts previously reported in a few decapods (Thangaraj and Prakash Vincent, 2004; Yano, 1992; Yano and Wyban, 1992). The up-regulation of *Vg* induced by bursicon at 48 h after treatment might suggest that bursicon is required to mediate the stimulation of vitellogenesis. Although there was no evidence revealing downstream process activated by bursicon in crustaceans, one of the roles of other glycoprotein hormones, especially FSH was to regulate the expression and increase the activity of a steroidogenic enzyme aromatase that converts androgens to estrogens (Erickson and Hsueh, 1978; Hearn and Gomme, 2000; Parakh et al., 2006). Moreover, vertebrate steroid hormone such as 17β-estradiol was also demonstrated to stimulate Vg synthesis in the oocyte of *M. japonicus* (Yano and Hoshino, 2006) as well as increase Vg level in the hemolymph of the crayfish, *Cherax albidus* (Coccia et al., 2010). It is therefore possible that bursicon may regulate *Vg* expression in crustacean ovary via steroidogenesis. It was demonstrated that serotonin, a neurotransmitter that is known to stimulate ovarian maturation in crustacean (Kulkarni et al., 1992; Vaca and Alfaro, 2000; Wongprasert et al., 2006) exert its function via stimulating the release of GSH from brain and/or thoracic ganglia (Sarojini et al., 1995, 1996). Whether or not serotonin also takes part in bursicon stimulation is not known and awaits further investigation.

To study the function of bursicon in the shrimp, previtellogenic female *P. monodon* were injected with rbursαβ or Tris/NaCl buffer twice on day 0 and day 2. The effect of rbursαβ on gonad stimulation was then investigated on day 4. The result in Fig. 7A showed that *Vg* mRNA expression in the ovary was significantly elevated more than three-folds in the rbursαβ-injected shrimp compared with that in the buffer-injected shrimp. Consistent with the *Vg* expression, approximately 75% of the buffer-injected shrimp were retained in previtellogenic stage whereas the majority (>60%) of the shrimp injected with rbursαβ could develop to late vitellogenic and mature stages (Fig. 7B). These results suggested that bursicon plays a role in ovarian maturation by stimulating Vg synthesis in *P. monodon*. This biological function is related to the elevated mRNA expression level of *Pmburs* in subesophageal ganglia at early vitellogenic stage of ovarian development. Concentration of circulating bursicon in the hemolymph at different molting stages was studied in the crabs, and the highest level (~4000 fmol/ml in *C. maenas* and ~100 fmol/ml in *C. sapidus*) was found at ecdysis stage (Chung et al., 2012; Webster et al., 2013). This suggests that the effective hemolymph concentrations of bursicon could be different between different species. However, because rbursαβ was produced as a mixture with monomeric and homodimeric forms the effective concentration of rbursαβ that caused up-regulation of *Vg* expression and ovarian development in *P. monodon* is presently not known, and further study with a higher purity of rbursαβ should be performed.

The effect of Pmburs on ovarian maturation is similar to that of a number of mammalian gonadotropins in crustaceans. For example, FSH and LH showed stimulating effect on the ovary of the sand shrimp, *Crangon crangon* (Żukowska-Arendarczyk, 1981). In the fresh water prawn *Macrobrachium lamerrii*, injection of FSH led to an increase in follicle cell number and size as well as the accumulation of yolk granules in the oocytes (Sarojini et al., 1988). The human chorionic gonadotropin (hCG) also had the influence on gonad maturation and spawning in *Penaeus semisulcatus* (Aktas and Kumlu, 2005).

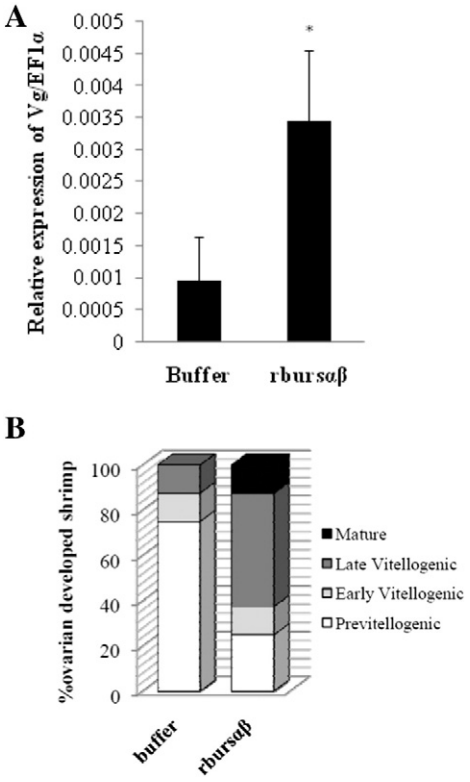

Fig. 7. Effect of recombinant bursαβ on vitellogenin expression in shrimp. Female *P. monodon* broodstock (approximately 90 g body weight) at previtellogenic stage of ovarian development were injected twice with approximately 60 ng/g bogy weight shrimp of rbursαβ or Tris/NaCl buffer on day 0 and 2. (A) The relative *Vg* mRNA expression to that of *EF1α* in the ovary was determined by real-time RT-PCR. An asterisk represents significant difference at $p < 0.05$ by Mann–Whitney U test. The values were presented as mean ± SEM (n = 8). (B) Ovarian developmental stage of individual shrimp in each group was observed and determined by morphology of the ovary. The results are presented as a percentage of shrimp at each ovarian developmental stage to the total number of shrimp in each group.

In addition, mode of action of gonadotropins involves the binding of the hormones to their specific receptors, a leucine-rich repeated G protein-coupled receptor (GPCR), which triggers adenylyl cyclase activation resulting in an increase of cAMP and subsequently activates protein kinase A (Milton and Peter, 2000). Interestingly, a specific bursicon receptor was identified in *D. melanogaster* to be a leucine-rich repeated GPCR type 2, and binding of recombinant bursicon to the receptor triggered cAMP production resulting in cuticle tanning stimulation (Luo et al., 2005). Besides, the expression of the bursicon-specific receptor was found in nervous tissues (Diao and White, 2012), epidermis (Davis et al., 2007) and muscle (Harwood et al., 2014). Similarly, the FlyAtlas database revealed that the bursicon receptor was expressed in several tissues including brain, thoracic ganglia, fat body, ovary and testis in adult *D. melanogaster* (Chintapalli et al., 2007). The ubiquitous expression of bursicon receptor in those tissues conformed to the multiple roles of bursicon including cuticle tanning (Fraenkel and Hsiao, 1965), wing expansion (Huang et al., 2007; Nathan et al., 2008) and development (Loveall and Deitcher, 2010). Accordingly, the expression of bursicon receptor found in the ovary might suggest another role of bursicon on an ovarian developmental process. These evidences imply that Pmburs might induce vitellogenin expression via similar signaling pathway to that used by gonadotropin to trigger ovarian maturation.

In conclusion, our study demonstrated for the first time the reproductive function of bursicon in the shrimp. Its structural similarity to vertebrate gonadotropins as well as its effect on the stimulation of *Vg* expression suggests that Pmburs is an invertebrate gonadotropin

homolog, and is likely one of putative gonad-stimulating factors in *P. monodon*.

Acknowledgments

We thank Ms. Somjai Wongtripop (Shrimp Genetic Improvement Center, Thailand) for providing shrimp samples. This study was supported by the Thailand Research Fund (Basic Research Grant to AU and DPG5680001 to SP), the Office of the Higher Education Commission and Mahidol University under the National Research Universities Initiative, and Mahidol University Research Grant. PS is the recipient of the student fellowship by the Royal Golden Jubilee Ph. D. program (PHD/0188/2553) under the Thailand Research Fund and Mahidol University.

References

Aktas, M., Kumlu, M., 2005. Gonadal maturation and spawning in *Penaeus semisulcatus* de Hann, 1844 by hormone injection. Turk. J. Zool. 29, 193–199.

An, S., Dong, S., Wang, Q., Li, S., Gilbert, L.I., Stanley, D., Song, Q., 2012. Insect neuropeptide bursicon homodimers induce innate immune and stress genes during molting by activating the NF-κB transcription factor relish. PLoS One 7, e34510.

Avsian-Kretchmer, O., Hsueh, A.J.W., 2004. Comparative genomic analysis of the eight-membered ring cystine knot-containing bone morphogenetic protein antagonists. Mol. Endocrinol. 18, 1–12.

Boime, I., Ben-Menahem, D., 1999. Glycoprotein hormone structure—function and analog design. Recent Prog. Horm. Res. 54, 271–288.

Burger, L.L., Haisenleder, D.J., Dalkin, A.C., Marshall, J.C., 2004. Regulation of gonadotropin subunit gene transcription. J. Mol. Endocrinol. 33, 559–584.

Charniaux-Cotton, H., 1985. Vitellogenesis and its control in malacostracan crustacea. Am. Zool. 25, 197–206.

Chen, T., Zhang, L.P., Wong, N.K., Zhong, M., Ren, C.H., Hu, C.Q., 2014. Pacific white shrimp (*Litopenaeus vannamei*) vitellogenesis-inhibiting hormone (VIH) is predominantly expressed in the brain and negatively regulates hepatopancreatic vitellogenin (VTG) gene expression. Biol. Reprod. 90 (47) (41-10).

Chintapalli, V.R., Wang, J., Dow, J.A.T., 2007. Using FlyAtlas to identify better *Drosophila melanogaster* models of human disease. Nat. Genet. 39, 715–720.

Chung, J.S., Katayama, H., Dircksen, H., 2012. New functions of arthropod bursicon: inducing deposition and thickening of new cuticle and hemocyte granulation in the blue crab, *Callinectes sapidus*. PLoS One 7, e46299.

Coccia, E., de Lisa, E., Di Cristo, C., Di Cosmo, A., Paolucci, M., 2010. Effect of estradiol and progesterone on the reproduction of the freshwater crayfish *Cherax albidus*. Biol. Bull. 218, 36–47.

Davis, M.M., O'Keefe, S.L., Primrose, D.A., Hodgetts, R.B., 2007. A neuropeptide hormone cascade controls the precise onset of post-eclosion cuticular tanning in *Drosophila melanogaster*. Development 134, 4395–4404.

de Kleijn, D.P.V., Sleutels, F.J.G.T., Martens, G.J.M., Van Herp, F., 1994. Cloning and expression of mRNA encoding prepro-gonad-inhibiting hormone (GIH) in the lobster *Homarus americanus*. FEBS Lett. 353, 255–258.

Diao, F., White, B.H., 2012. A novel approach for directing transgene expression in *Drosophila*: T2A-Gal4 in-frame fusion. Genetics 190, 1139–1144.

Erickson, G.F., Hsueh, A.J., 1978. Stimulation of aromatase activity by follicle stimulating hormone in rat granulosa cells *in vivo* and *in vitro*. Endocrinology 102, 1275–1282.

Fraenkel, G., Hsiao, C., 1965. Bursicon, a hormone which mediates tanning of the cuticle in the adult fly and other insects. J. Insect Physiol. 11, 513–556.

Harwood, B.N., Draper, I., Kopin, A.S., 2014. Targeted inactivation of the rickets receptor in muscle compromises *Drosophila* viability. J. Exp. Biol. 217, 4091–4098.

Hearn, M.T.W., Gomme, P.T., 2000. Molecular architecture and biorecognition process of the cystine knot protein superfamily: part I. The glycoprotein hormones. J. Mol. Recognit. 13, 223–278.

Honegger, H., Dewey, E., Ewer, J., 2008. Bursicon, the tanning hormone of insects: recent advances following the discovery of its molecular identity. J. Comp. Physiol. A. 194, 989–1005.

Honegger, H., Estévez-Lao, T.Y., Hillyer, J.F., 2011. Bursicon-expressing neurons undergo apoptosis after adult ecdysis in the mosquito *Anopheles gambiae*. J. Insect Physiol. 57, 1017–1022.

Huang, J., Zhang, Y., Li, M., Wang, S., Liu, W., Couble, P., Zhao, G., Huang, Y., 2007. RNA interference-mediated silencing of the bursicon gene induces defects in wing expansion of silkworm. FEBS Lett. 581, 697–701.

Huang, H., Ye, H., Li, S., Wang, G., 2008. Immunocytological evidence for the presence of vertebrate FSH- and LH-like substances in the brain and thoracic ganglion of the swimming crab, *Portunus trituberculatus*. Prog. Nat. Sci. 18, 1453–1457.

Kulkarni, G.K., Nagabhushanam, R., Amaldoss, G., Jaiswal, R.G., Fingerman, M., 1992. *In vivo* stimulation of ovarian development in the red swamp crayfish, *Procambarus clarkii* (Girard), by 5-hydroxytryptamine. Invertebr. Reprod. Dev. 21, 231–239.

Lõoke, M., Kristjuhan, K., Kristjuhan, A., 2011. Extraction of genomic DNA from yeasts for PCR-based applications. Biotechniques 50, 325–328.

Loveall, B., Deitcher, D., 2010. The essential role of bursicon during *Drosophila* development. BMC Dev. Biol. 10, 92.

Luo, C., Dewey, E., Sudo, S., Ewer, J., Hsu, S., Honegger, H., Hsueh, A., 2005. Bursicon, the insect cuticle-hardening hormone, is a heterodimeric cystine knot protein that activates G protein-coupled receptor LGR2. Proc. Natl. Acad. Sci. U. S. A. 102, 2820–2825.

Milton, T.W.H., Peter, T.G., 2000. Molecular architecture and biorecognition process of the cystine knot protein superfamily: part I. The glycoprotein hormones. J. Mol. Recognit. 13, 223–278.

Nathan, C.P., Diao, F., Kuan, H., Wang, H., Dewey, E.M., Honegger, H.-W., Benjamin, H.W., 2008. Bursicon functions within the *Drosophila* central nervous system to modulate wing expansion behavior, hormone secretion and cell death. J. Neurosci. 28, 14379–14391.

Parakh, T.N., Hernandez, J.A., Grammer, J.C., Weck, J., Hunzicker-Dunn, M., Zeleznik, A.J., Nilson, J.H., 2006. Follicle-stimulating hormone/cAMP regulation of aromatase gene expression requires β-catenin. Proc. Natl. Acad. Sci. U. S. A. 103, 12435–12440.

Roch, G.J., Sherwood, N.M., 2014. Glycoprotein hormones and their receptors emerged at the origin of metazoans. Genome Biol. Evol. 6, 1466–1479.

Sarojini, R., Jayalakshmi, K., Sambasivarao, S., Nagabhushanam, R., 1988. Stimulation of oogenesis in the freshwater prawn, *Macrobrachium lamerri* by prostagalndin E_2 and follicle stimulating hormone. Indian J. Fish. 25, 283–287.

Sarojini, R., Nagabhushanam, R., Fingerman, M., 1995. Mode of action of the neurotransmitter 5-hydroxytryptamine in stimulating ovarian maturation in the red swamp crayfish, *Procambarus clarkii*: an in vivo and in vitro study. J. Exp. Zool. 271, 395–400.

Sarojini, R., Nagabhushanam, R., Fingerman, M., 1996. In vitro inhibition by dopamine of 5-hydroxytryptamine-stimulated ovarian maturation in the red swamp crayfish, *Procambarus clarkii*. Experientia 52, 707–709.

Sharp, J.H., Wilcockson, D.C., Webster, S.G., 2010. Identification and expression of mRNAs encoding bursicon in the plesiomorphic central nervous system of *Homarus gammarus*. Gen. Comp. Endocrinol. 169, 65–74.

Tan-Fermin, J.D., Pudadera, R.A., 1989. Ovarian maturation stages of the wild giant tiger prawn, *Penaeus monodon* Fabricius. Aquaculture 77, 229–242.

Thangaraj, M., Prakash Vincent, S.G., 2004. Assessment of vitellogenin stimulating activity in extracts of brain and sub-oesophageal ganglia of tiger shrimp, *Penaeus monodon*. Indian J. Fish. 51, 133–138.

Treerattrakool, S., Panyim, S., Chan, S.M., Withyachumnarnkul, B., Udomkit, A., 2008. Molecular characterization of gonad-inhibiting hormone of *Penaeus monodon* and elucidation of its inhibitory role in vitellogenin expression by RNA interference. FEBS J. 275, 970–980.

Ulloa-Aguirre, A., Timossi, C., 1998. Structure-function relationship of follicle-stimulating hormone and its receptor. Hum. Reprod. Update 4, 260–283.

Vaca, A.A., Alfaro, J., 2000. Ovarian maturation and spawning in white shrimp, *Penaeus vannamei*, by serotonin injection. Aquaculture 182, 373–385.

Webster, S.G., Wilcockson, D.C., Mrinalini, Sharp, J.H., 2013. Bursicon and neuropeptide cascades during the ecdysis program of the shore crab, *Carcinus maenas*. Gen. Comp. Endocrinol. 182, 54–64.

Weghofer, A., Schnepf, S., Barad, D., Gleicher, N., 2007. The impact of luteinizing hormone in assisted reproduction: a review. Curr. Opin. Obstet. Gynecol. 19, 253–257.

Wilcockson, D.C., Webster, S.G., 2008. Identification and developmental expression of mRNAs encoding putative insect cuticle hardening hormone, bursicon in the green shore crab *Carcinus maenas*. Gen. Comp. Endocrinol. 156, 113–125.

Wongprasert, K., Asuvapongpatana, S., Poltana, P., Tiensuwan, M., Withyachumnarnkul, B., 2006. Serotonin stimulates ovarian maturation and spawning in the black tiger shrimp *Penaeus monodon*. Aquaculture 261, 1447–1454.

Yano, I., 1992. Effect of thoracic ganglion on vitellogenin secretion in kuruma prawn, *Penaeus japonicus*. Bull. Natl. Res. Inst. Aquac. 21, 9–14.

Yano, I., Hoshino, R., 2006. Effect of 17 β-estradiol on the vitellogenin synthesis and oocyte development in the ovary of kuruma prawn (*Marsupenaeus japonicus*). Comp. Biochem. Physiol. A 144, 18–23.

Yano, I., Wyban, J.A., 1992. Induced ovarian maturation of *Penaeus vannamei* by injection of lobster (*Homarus americanus*) brain extract. Bull. Natl. Res. Inst. Aquac. 21, 1–7.

Ye, H., Ma, J., Lin, Q., Wang, G., 2011. Occurrence of follicle-stimulating hormone-like substance in the kuruma prawn, *Marsupenaeus japonicus*, during ovarian maturation. Mar. Biol. Res. 7, 304–309.

Żukowska-Arendarczyk, M., 1981. Effect of hypophyseal gonadotropins (FSH and LH) on the ovaries of the sand shrimp *Crangon crangon* (Crustacea: Decapoda). Mar. Biol. 63, 241–247.

Comparative Biochemistry and Physiology, Part A 213 (2017) 11–19

Contents lists available at ScienceDirect

Comparative Biochemistry and Physiology, Part A

journal homepage: www.elsevier.com/locate/cbpa

An essential role of Rieske domain oxygenase Neverland in the molting cycle of black tiger shrimp, *Penaeus monodon*

Ponsit Sathapondecha[a], Sakol Panyim[b,c], Apinunt Udomkit[b,*]

[a] Department of Molecular Biotechnology and Bioinformatics, Faculty of Science, Prince of Songkla University, Hat Yai, Songkhla 90112, Thailand
[b] Institute of Molecular Biosciences, Mahidol University, Salaya Campus, Nakhon Pathom 73170, Thailand
[c] Department of Biochemistry, Faculty of Science, Mahidol University, Rama VI Road, Bangkok 10400, Thailand

ARTICLE INFO

Keywords:
Rieske domain oxygenase
Cholesterol 7-desaturase
Cholesterol 7,8-dehydrogenase
Ecdysteroid biosynthesis
Molt
Shrimp

ABSTRACT

Molting is an important process for development and growth in arthropods. In crustaceans, molt is regulated by ecdysteroids or molting hormones that are synthesized in Y-organs. However, ecdysteroid biosynthesis pathway in crustaceans and its participating enzymes have not been well studied so far. In this study, a Rieske domain oxygenase, the enzyme that acts as cholesterol 7,8-dehydrogenase by converting cholesterol to 7-dehydrocholesterol in the first step of the ecdysteroid biosynthesis was characterized in black tiger shrimp, *Penaeus monodon*. A full-length cDNA of *P. monodon*'s Rieske domain oxygenase Neverland (PmNvd) was successfully cloned. The expression of *PmNvd* was dominantly found in the Y-organ, and changed during molting period. The *PmNvd* mRNA level was low in intermolt and early premolt stages, then dramatically increased in the mid premolt stage suggesting its role in molt regulation. The function of *PmNvd* in the molting process was investigated by RNAi approach. Silencing of *PmNvd* transcript in shrimp by specific double-stranded RNA (dsNvd) led to prolonged molt duration with abnormal molting progression, i.e. the molting process got stuck at early premolt stage. In addition, 20-hydroxyecdysone titer in the hemolymph of dsNvd-injected shrimp was significantly reduced compared with that in NaCl-injected shrimp. These evidences suggested a crucial role of PmNvd in molt progression, particularly during the initiation of premolt phase via the regulation of ecdysteroid production.

1. Introduction

Molt or ecdysis is a physiological process that is critical for growth in arthropods. In penaeid shrimp, the molting stages can be classified based on morphological changes on epidermal tails (Promwikorn et al., 2004). Ecdysis or shading of old exoskeleton occurred with several physiological changes, including high rate of water uptake and absorption of many ions such as Mg^{2+} and Ca^{2+} (Phlippen et al., 2000). The molting cycle can be divided into postmolt (stages A, B), intermolt (stage C), premolt (stage D) and molting or ecdysis (E). Each stage can be divided into sub-stages according to physical changes of the cuticle as can be clearly observed at the tip of uropod under light microscope (Promwikorn et al., 2004).

In crustaceans, the molting process is controlled by several hormonal factors, particularly ecdysteroids or molting hormones and molt-inhibiting hormone (MIH) (Nakatsuji and Sonobe, 2004; Nakatsuji et al., 2006). Ecdysteroids are important steroid hormones that play a crucial role in molting process in ecdysozoa animals. In insect, ecdysteroids are synthesized in prothoracic gland, whereas crustacean ecdysteroids are synthesized in Y-organs. In addition to their role in the molting process, ecdysteroids are also involved in other physiological processes including oogenesis, longevity and neuronal activity (Uryu et al., 2015). By contrast, crustacean neuropeptide hormone MIH plays a role in the inhibition of ecdysteroid production by suppressing the uptake of cholesterol, an ecdysteroid precursor in the Y-organ (Nakatsuji et al., 2009; Kang and Spaziani, 1995a, 1995b; Spaziani and Wang, 1993). Moreover, MIH was also shown to inhibit a secretion of ecdysteroids from Y-organs (Nakatsuji et al., 2006; Nakatsuji and Sonobe, 2004; Mattson and Spaziani, 1985).

Ecdysteroids are secreted into hemolymph as an inactive form. The inactive ecdysteroids are then catalyzed to an active form in periphery tissues such as epidermis (Mykles, 2011). There are several derivatives of ecdysteroids including ecdysone (E), 3-dehydroecdysone, ponasterone and 20-hydroxyecdysone (20-HE) depending on ecdysteroid biosynthetic process of each organism (Mykles, 2011). For example, 20-HE and E were mainly found in shrimp, *P. monodon* (Kuo and Lin, 1996), *Litopenaeus vannamei* (Blais et al., 1994) and *Macrobrachium rosenbergii* (Okumura and Aida, 2000), whereas ponasterone and 20-HE

* Corresponding author.
E-mail address: apinunt.udo@mahidol.ac.th (A. Udomkit).

http://dx.doi.org/10.1016/j.cbpa.2017.08.004
Received 3 May 2017; Received in revised form 8 August 2017; Accepted 15 August 2017
Available online 24 August 2017

Table 1
List of oligo-nucleotide used in this study.

Name	Propose	Sequence (5′ → 3′)
dPmNvd-F1	Partial sequence	TNGAYGCYTACTGCCCGCA
dPmNvd-R1	Partial sequence	GTCDGCNCCRTTYTCDGG
PmNvd-F2	Partial sequence	AGATGTCCATACCATGGTTGG
PmNvd-F3	3′RACE	GCTATTCAGAGGGTCTGATGGC
PmNvd-F4	3′RACE and qPCR	GCTCCTGTGCCCACATTC C
PmNvd-R2	5′RACE and qPCR	GGGAATCTCCTGAATATGTGCG
PmNvd-R3	5′RACE	CTT CAT GGT AGG TCC TTC CGC
FullPmNvd-F	PCR	ACTCCAGGATCATCATTTGTCG
FullPmNvd-R	PCR	GCATTATTTCCATGAGGCAGCG
*Xba*I-stNvd-F	dsNvd	GCTCTAGAAGGGACGACTTCCGCAATG
*Eco*RI-stNvd-R	dsNvd	CGGAATTCGGACGA TCTTCTGCCTGA GG
*Xho*I-stLNvd-F	dsNvd	CCGCTCGAGAGGGACGACTTCCGCAATG
*Eco*RI-stLNvd-R	dsNvd	CGGAATTCACTTGAGGATTTGGCGGTCC
PRT	cDNA synthesis	CCGGAATTCAAGCTTCTAGAGGATCCTTTTTTTTTTTTTTTT
PM1	RACE	CCGGAATTCAAGCTTCTAGAGGATCC
EF1α-F	qPCR	GAACTGCTGACCAAGATCGACAGG
EF1α-R	qPCR	GAGCATACTGTTGGAAGGTCTCCA
Actin-F	PCR	GACTCGTACGTGGGCGACGAGG
Actin-R	PCR	AGCAGCGGTGGTCATCTCCTGCTC

```
   1  GAGTCACTTAGATCCTGCGTCCAGCCTCAGATATCGGTTATCACGTGTTTATTTTTGTGCAGTTGGCTAAAGGAACTCCA
  81  GGATCATCATTTGTCGACGTAGGTGGACATGCAAATAGAAGATCTTGGACGCAAGTGCTGATCACTGTCATTACTCCAGC
 161  ATGACTATCATTGTATCCCTTGTCTCCTACCTGACCACCATGTCCTGGCCAGGGGATCGCTGGACTCTCGCCGCCCGGGA
       M  T  I  I  V  S  L  V  S  Y  L  T  T  M  S  W  P  G  D  R  W  T  L  A  A  R  D
 241  CGCACTCTCAGCACCGTGGACTGTTGAGTTGCTTTGGACTTTGCTGCCCTATGCGCTCGGCCTCCTCCTCGCTGCCGTCT
         A  L  S  A  P  W  T  V  E  L  L  W  T  L  L  P  Y  A  L  G  L  L  L  A  A  V
 321  TGTACCGCCACGCCTTCATTCCTCTGGATCGGGTCAGGAGAGTAACGGAGATTGGATGGGGTTGCATAGCTGCAGATGAC
       L  Y  R  H  A  F  I  P  L  D  R  V  R  R  V  T  E  I  G  W  G  C  I  A  A  D  D
 401  AAGAGGCCCATCGCCGAGCGTATCAGGGAGATTCAGCGGCCCAGGAAGATTGGGCAACTTCCTCCTGTCTATCCCAATGG
        K  R  P  I  A  E  R  I  R  E  I  Q  R  P  R  K  I  G  Q  L  P  P  V  Y  P  N  G
 481  GTGGTTTGCTGTGACCGAGTCCAGAAAGGTCAAGGTGGAACAGGTGATTCAGGTGCAAGTGTTCGGGGAGACGCTGGCGG
         W  F  A  V  T  E  S  R  K  V  K  V  E  Q  V  I  Q  V  Q  V  F  G  E  T  L  A
 561  TGTTTCGGAGTAAGGACGGCACAGCACACGTAACGGACGCTTACTGTCCCCATATGGGCGCCAACATGGCAGTAGGCGGT
       V  F  R  S  K  D  G  T  A  H  V  T  D  A  Y  C  P  H  M  G  A  N  M  A  V  G  G
 641  GTGGTAAAAGGAGACTGTCTTGAGTGTCCCTTTCATGGTTGGCTATTCAGAGGGTCTGATGGCTCCTGTGCCCACATTCC
        V  V  K  G  D  C  L  E  C  P  F  H  G  W  L  F  R  G  S  D  G  S  C  A  H  I  P
 721  ATATTCAAGTAAAGCTGTGCCTAAGACGGCTAATGTAAAGCGATGGGAGTCACGCGAAGTAAACGGTCGCATATACGTGT
         Y  S  S  K  A  V  P  K  T  A  N  V  K  R  W  E  S  R  E  V  N  G  R  I  Y  V
 801  GGTACGACGCAGAGGGACGACTTCCGCAATGGCACATCCCTGAAATCGGCCACATCACCCGCGGAGAGTGGTCCTACCGC
       W  Y  D  A  E  G  R  L  P  Q  W  H  I  P  E  I  G  H  I  T  R  G  E  W  S  Y  R
 881  GGAAGGACCTACCATGAAGTCCTCGCACATATTCAGGAGATTCCCGAGAATGGAGCAGACATGGCCCACCTAGGACACTT
        G  R  T  Y  H  E  V  L  A  H  I  Q  E  I  P  E  N  G  A  D  M  A  H  L  G  H  L
 961  GCACGTGCCTAACATTTTAAAAGGAAACGATTTGAGGGACGCATTTGCCAACAACCAGGCAATGGACTTAGCTGAGCATG
         H  V  P  N  I  L  K  G  N  D  L  R  D  A  F  A  N  N  Q  A  M  D  L  A  E  H
1041  CGTGGAACGGTGAGTGGCGAGCCCGTGAGTCTCCAGAATCCCATATGGCTGAACTGGTCATGACGCACTCTCTCTCCTTC
      A  W  N  G  E  W  R  A  R  E  S  P  E  S  H  M  A  E  L  V  M  T  H  S  L  S  F
1121  ATCGGCGGCAAGTTCAAGCTTTTCAAGATGACTGTCAGGGCCGAACAAATTGGGCCAGGCATCGTGCACCTGCATTTCGA
        I  G  G  K  F  K  L  F  K  M  T  V  R  A  E  Q  I  G  P  G  I  V  H  L  H  F  D
1201  CACCGGGCTCGGCGCCGGCATCCTTATCCAGACCGTCACGCCCATCGAGCCCCTCAGGCAGAAGATCGTCCATGAGTTCT
         T  G  L  G  A  G  I  L  I  Q  T  V  T  P  I  E  P  L  R  Q  K  I  V  H  E  F
1281  ACACTTCGAGCACCTTCTTCGCCCCATACGCCAAGTTTGTCCTTCTCTGCGAAGCCTACCACTTGGAGCGCGATATCATG
       Y  T  S  S  T  F  F  A  P  Y  A  K  F  V  L  L  C  E  A  Y  H  L  E  R  D  I  M
1361  ATCTGGAACAGCAAAGTCTACCAGTCGCAGCCGTTGTTGGTGGCAGAGGACCGCCAAATCCTCAAGTTCCGCCGATGGTA
        I  W  N  S  K  V  Y  Q  S  Q  P  L  L  V  A  E  D  R  Q  I  L  K  F  R  R  W  Y
1441  CAACCAGTTCTACTCGGAGAACAGTCCAAAGTTCAACTTCAGGAAAGAGTCATTCGAGTGGTGA
        N  Q  F  Y  S  E  N  S  P  K  F  N  F  R  K  E  S  F  E  W  *
1505  TGCGCGTACCCAGTGGCGCTGCCTCATGGAAATAATGCTATTCTGTCTTCGCACTTTCCACACACACGGGAGGTAAAGGA
1585  CATGTGTGTGAAAAGTTGGATGCTATTCATGACAACAAGAAACCATTTCTTGTGACAGTTTGATCATCTTGAAGACGTTA
1665  GTGATAGCTGTGTACTGTAGAACCGTACCCACGAGAAGCCAAGTAACTTCGAAATTATCATTC
```

Fig. 1. Nucleotide and deduced amino acid sequences of PmNvd (GenBank Accession No. KU360639). The full-length *PmNvd* cDNA of 1727 nucleotides is shown with its deduced 447 amino acid residues as one-lettered symbols underneath the corresponding codons. The region used for dsRNA design is highlighted, where underlined nucleotides represent the stem region of the dsRNA. An asterisk indicates the stop codon.

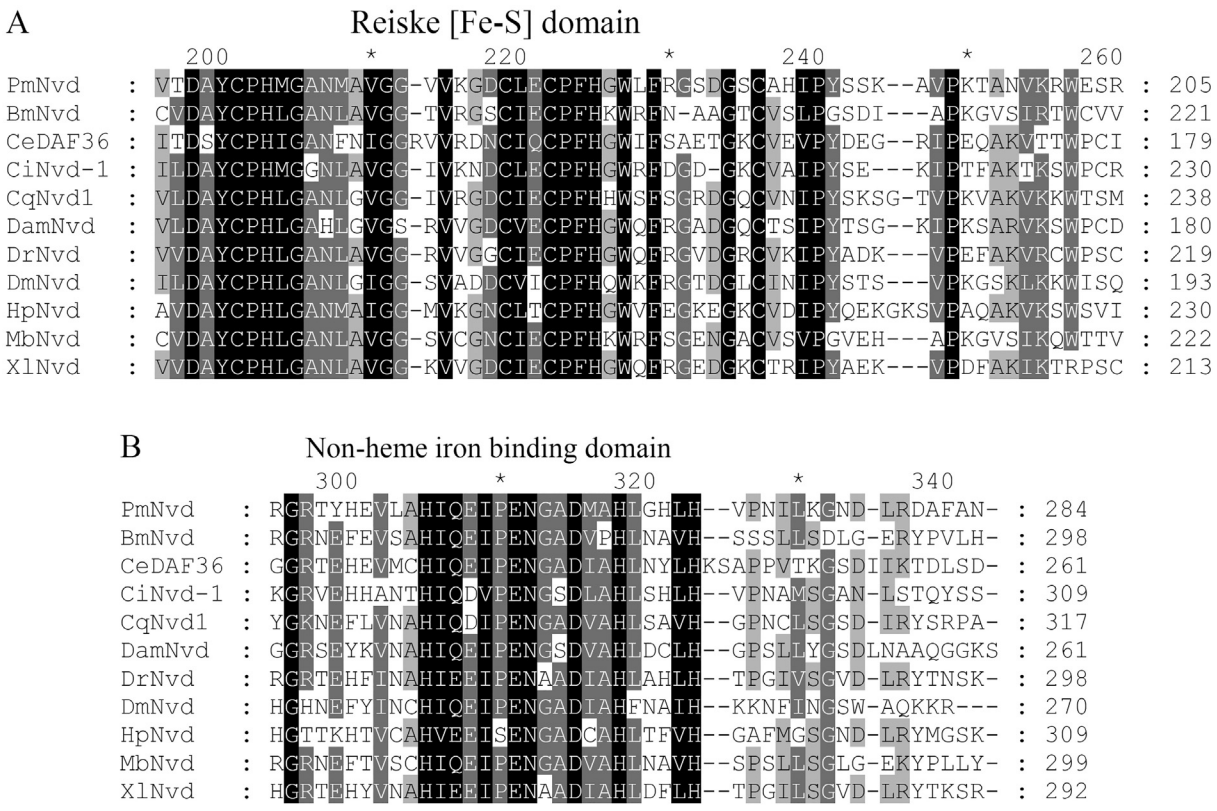

Fig. 2. Alignment of conserved domains of amino acid sequences of invertebrate Rieske domain oxygenase Neverland. The Rieske [Fe-S] domain (A) and non-heme iron binding domain (B) of the deduced amino acids of *P. monodon*'s Nvd (Accession No. KU360639) are compared with the same conserved domain of Nvd from other invertebrates including *B. mori* (Accession No. NM_001044161; BmNvd), *C. elegans* (Accession No. NM_073228; CeDAF36), *Ciona intestinalis* (Accession No. AB607952; CiNvd-1), *Culex quinquefasciatus* (Accession No. XM_001847974; CqNvd), *D. magna* (Accession No. AB839171; DamNvd), *Danio rerio* (Accession No. AB607951; DrNvd), *D. melanogaster* (Accession No. NM_001104200; DmNvd), *Mamestra brassicae* (Accession No. AB649116; MbNvd), *Hemicentrotus pulcherrimus* (Accession No. AB607954; HpNvd) and *Xenopus laevis* (Accession No. AB607950; XlNvd) using ClustalW software. The conserved amino acid residues were highlighted in black, and amino acids with lesser similarity levels are shaded in gray.

or 3-dehydro-20-HE were major ecdysteroids found in several crabs such as *Carcinus maenas* (Lachaise et al., 1981), *Callinectes sapidus* (Chung, 2010) and *Menippe mercenaria* (Rudolph et al., 1992).

Ecdysteroid biosynthesis involves several chemical reactions catalyzed by ecdysteroidogenic enzymes including Rieske domain oxygenase Neverland (Nvd) and the Halloween gene family of cytochrome P450s (Mykles, 2011). Nvd acts as a cholesterol 7,8-dehydrogenase (Yoshiyama-Yanagawa et al., 2011) or cholesterol 7-desaturase (Wollam et al., 2011) which converts cholesterol to 7-dehydrocholesterol (7dC) in an early ecdysteroid biosynthetic pathway. Subsequently, 7dC was catalyzed to 5β-ketodiol by a series of Halloween P450 enzymes; CYP307A1/Spook (Spo), CYP307A2/Spookier (Spok) and CYP6T3 (Mykles, 2011; Niwa and Niwa, 2014; Rewitz et al., 2007). These catalytic steps are collectively called the “Black Box” as the intermediates in between are unknown. The 5β-ketodiol is further converted to ecdysone by another set of Halloween genes family including CYP306A1/Phantom (Phm), CYP302A1/Disembodied (Dib), and CYP315A1/Shadow (Sad) (Niwa and Niwa, 2014). The ecdysone is secreted into the hemolymph of arthropods and moves to peripheral tissues where it is finally converted to an active ecdysteroids, 20-HE by a CYP314A1/Shade (Shd) enzyme (Petryk et al., 2003).

Nvd is found in several organisms such as roundworms and arthropods as well as vertebrates (Lang et al., 2012; Sumiya et al., 2014; Wollam et al., 2011; Yoshiyama-Yanagawa et al., 2011; Yoshiyama et al., 2006). It has been shown to be essential for larval development in *Drosophila* as the development of *Drosophila* larva was arrested upon *Nvd* silencing, and eventually led to larval death (Yoshiyama et al., 2006). Recent study showed that *Nvd* plays an important role in the molting process of the water flea, *Daphnia magna*. *Nvd1* knockdown in *D. magna*'s embryo led to a defect in embryonic molting and development (Sumiya et al., 2016). Since the function of *Nvd* in decapod crustaceans has not been characterized so far, this study is aimed at characterization of an ecdysteroidogenic enzyme, *Nvd* and functional analysis in the molting process in *P. monodon*.

2. Materials and methods

2.1. RNA isolation and cDNA synthesis

P. monodon were kindly provided by Shrimp Genetics Improvement Center, Surat Thani, Thailand. All Shrimp were reared in 10 ppt seawater for one week before experiments began. Shrimp were anesthetized on ice prior to tissue collection. Total RNA was extracted from freshly collected shrimp tissues by RiboZol reagent (AMRESCO, USA) following the manufacturer's protocol. Two micrograms of RNA sample were treated with a mixture of 1 × RQ1 buffer and 1 U of RQ1 RNase free DNase (Promega, USA) by incubating at 37 °C for 10 min in order to eliminate contaminating genomic DNA. Subsequently, the RQ1-treated RNA sample was mixed with oligo-dT primer (PRT), heated at 70 °C for 3 min, and then placed on ice prior to the addition of 1 × Improm®-II buffer, 3.0 mM $MgCl_2$, 0.5 mM dNTP and 1 μl of Improm-II reverse transcriptase (Promega, USA). The reverse transcription reaction was performed at 25 °C for 5 min, 42 °C for 60 min and 70 °C for 10 min. The cDNA was kept at − 20 °C until used.

2.2. Cloning of a full-length cDNA of Rieske-domain oxygenase Neverland of P. monodon (PmNvd)

In order to obtain a partial nucleotide sequence of *PmNvd*, deduced amino acid sequences of Nvd from several insects and a sequence from

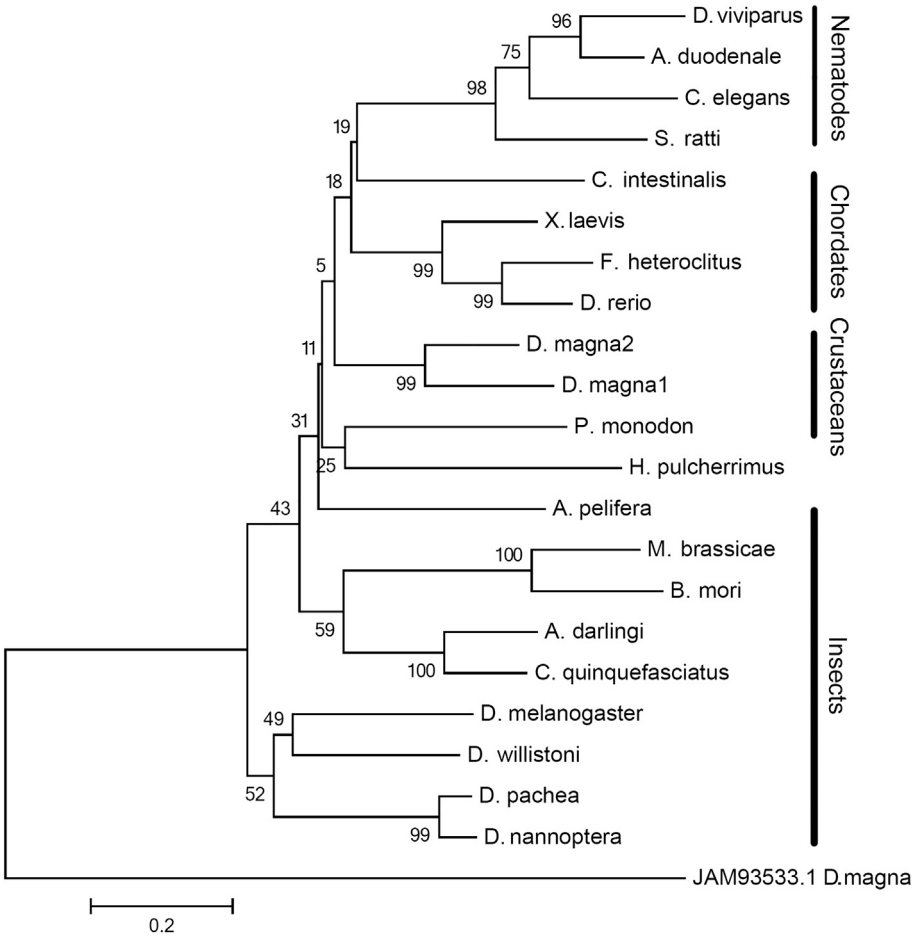

Fig. 3. Phylogenetic analysis of PmNvd. The full sequences of deduced amino acids of Nvd from several organisms were used to construct the phylogenetic tree. The sequences were aligned by MUSCLE multiple sequence alignment. The phylogenetic tree was generated by a Neighbor-Joining method based on the Poisson correction model using MEGA 6.06 software. The phylogeny test was performed by a bootstrap method at 1000 replicates. The tree is drawn to scale with branch length representing the number of substitutions per site. The amino acid sequences of Nvd include PmNvd, *Aedes darlingi* (Accession No. ETN63840), *Ancylostoma duodenale* (Accession No. KIH60101), *Apis melifera* (Accession No. BAJ54122), *B. mori* (Accession No. NP_001037626), *C. elegans* (Accession No. NM_073228), *C. intestinalis* (Accession No. BAK39961), *C. quinquefasciatus* (Accession No. EDS27493), *D. magna* Nvd1 and Nvd2 (Accession No. BAQ02388 and BAQ02389, respectively), *D. melanogaster* (Accession No. NP_001097670), *D. nannoptera* (Accession No. AFD97359), *D. pachea* (Accession No. AFU25035), *D. rerio* (Accession No. BAK39960), *D. willistoni* (Accession No. XP_002070225), *Dictyocaulus viviparus* (Accession No. KJH52421), *Fundulus heteroclitus* (Accession No. JAQ79933), *H. pulcherrimus* (Accession No. BAK39963), *M. brassicae* (Accession No. BAN66310), *Strongyloides ratti* (Accession No. CEF66692) and *X. laevis* (Accession No. BAK39959) The iron-sulfur protein's *D. magna* (Accession No. JAM93533) was used as an outgroup.

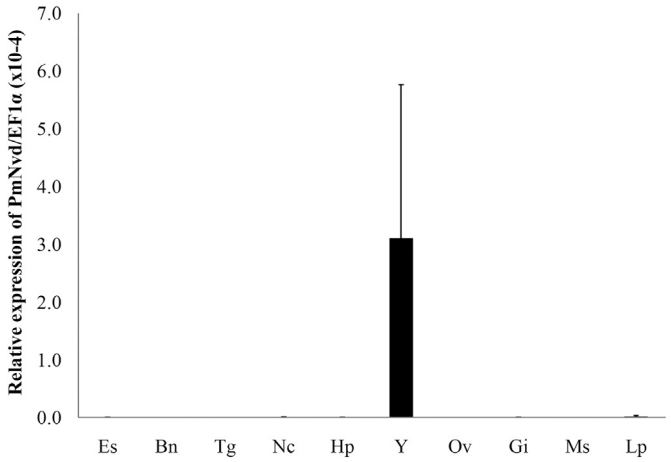

Fig. 4. Expression of *PmNvd* mRNA in *P. monodon* tissues. The mRNA expression level of *PmNvd* in various shrimp tissues including eyestalk (Es), brain (Bn), thoracic ganglia (Tg), nerve cord (Nc), hepatopancreas (Hp), Y-organ (Y), ovary (Ov), gills (Gi), muscle (Ms) and lymphoid organ (Lp) were determined by qRT-PCR, and presented as relative expression levels compared with that of *EF1α* of the same sample. The expression profiles from two adult female shrimp were shown. Bars and error bars represent mean and SEM, respectively.

L. vannamei EST database that shows high similarity to insect *Nvd* (GenBank Accession No. FE178330) were used to design primers for RT-PCR amplification. Y-organs cDNA of *P. monodon* was used as a template to amplify a partial *PmNvd* cDNA with the degenerate primers dPmNvd-F1 and dPmNvd-R1 (Table 1). Then, nested PCR was performed by amplifying the 1st PCR product with PmNvd-F2 and dPmNvd-R1 primers. The PCR reactions composing of 1 × standard *Taq* polymerase buffer (NEB Laboratory, USA), 0.2 mM dNTP, 0.2 μM each primers and 1 U *Taq* polymerase (NEB Laboratory, USA). The PCR reactions were performed at 95 °C for 3 min, then 35 cycles of 95 °C for 30 s, 50 °C for 30 s and 68 °C for 30 s, and final extension at 68 °C for 5 min. After obtaining the *PmNvd* partial nucleotide sequence, the 3′ and 5′ regions of *PmNvd* cDNA were amplified by rapid amplification of cDNA ends (RACE). For 3′ RACE, the oligo-dT-primed Y-organ cDNA was amplified with PmNvd-F3 and PRT primers, and the PCR product was further used to amplify with nested primers (PmNvd-F4 and PM1). For 5′ RACE, two microgram of Y-organ total RNA was used to synthesize the first-stranded cDNA with PmNvd-R1 primer designed from the partial cDNA sequence. The 3′ end of the first-stranded cDNA was tailed with dATP in a mixture of 1 × TdT buffer (Promega) and 0.4 mM dATP. The sample was heated at 94 °C for 3 min and placed on ice. Then, approximately 20 U TdT (Promega) was added to the mixture, and the reaction was performed at 37 °C for 30 min, followed by 65 °C for 10 min. The A-tailed cDNA was used as a template in the PCR reaction with PmNvd-R2 and PRT primers. The first PCR product was subsequently used as a template for nested PCR with PmNvd-R3 and PM1. The overlapping DNA sequences of the 3′ and 5′ RACE PCR products were verified by amplification of a full-length *PmNvd* cDNA with FullPmNvd-F and FullPmNvd-R primers by KAPA long Range DNA polymerase (KAPA Biosystems). The nucleotide sequences of all primers were shown in Table 1.

2.3. Determination of PmNvd mRNA expression in shrimp by quantitative reverse transcription PCR (qRT-PCR)

In order to determine expression level of *PmNvd* in shrimp, several

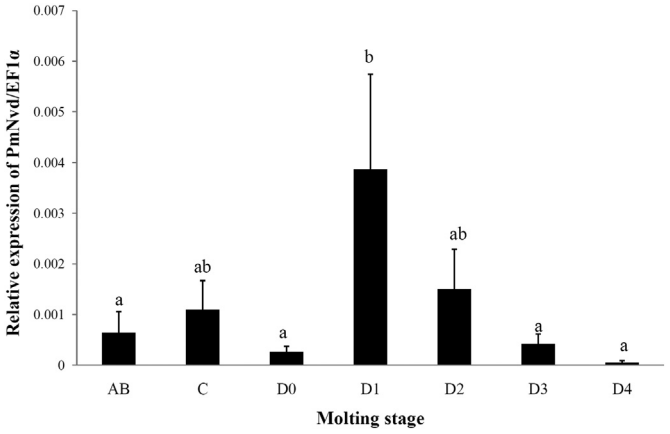

Fig. 5. Expression of *PmNvd* mRNA in the Y-organs at different molting stages. The Y-organs isolated from approximately 10 g *P. monodon* at different molting stages (n = 4–8 each) were used to determine the *PmNvd* expression level by qRT-PCR. Shrimp molting stages are characterized by physical changes of the cuticle at the tip of uropod as observed under light microscope (Promwikorn et al., 2004) as follows: postmolt (A, B) - the complete formation of setal cones; intermolt (C) – rigid integument and formation of the new cuticle is completed; early premolt (D0) - starting of the retraction of the epidermal tissue from the cuticle; premolt (D1–D3) - clear zone between the setal cones and the epidermis is clearly recognized at D1 and getting wider from D1 to D3, the edge of the epidermis becomes wavy at D2, and the white thin layer is clearly seen at the edge of the epidermis in D3; late premolt (D4) - serrated edge of the epidermis, light-reflecting at the edge of the white layer and epidermis present a paralleled-band pattern. Bars and error bars represent mean of relative expression levels compared with that of *EF1α* of the same sample and SEM, respectively. Different alphabets represent significant difference between groups ($p < 0.05$) as analyzed by ANOVA and pair-wise comparison by Tukey HSD.

tissues including eyestalk, brain, thoracic ganglia, abdominal nerve cord, hepatopancreas, Y-organ, ovary and muscle were isolated from two previtellogenic female shrimp at premolt stage, and the expression of *PmNvd* in these tissues was determined by qRT-PCR. The Y-organ from juvenile shrimp (approximately 10 g) at different stages of molt (n = 4–8 each) which was classified by changing pattern of tail fan epidermis under light microscope (Promwikorn et al., 2004) were used to determine expression profile of *PmNvd* during the molting cycle. The first-stranded cDNA from each tissue was added with a mixture of 1 × SYBR® FAST Master Mix (KAPA Biosystems) and 0.4 μM PmNvd-F4 and PmNvd-R2. The PCR reaction was performed at 95 °C for 3 min, then 40 cycles of 95 °C for 5 s and 60 °C for 30 s in a realtime PCR machine (Realplex^4, Eppendorf). Subsequently, the PCR product was analyzed for a melting curve with a temperature profile of 95 °C for 30 s, 60 °C for 30 s, 95 °C for 30 s. Elongation factor 1 alpha (*EF1α*) was used as an internal control. The efficiency of *PmNvd* and *EF1α* specific primers were 101% and 100%, respectively. Relative quantification was performed using a standard curve constructed by amplifying serial dilution of known amount of purified PCR products (10^2–10^8 copies) of either *PmNvd* or *EF1α*.

2.4. Construction and expression of double-stranded RNA specific to PmNvd (dsNvd)

The *PmNvd*-specific double-stranded RNA was produced as a stem-loop (small hairpin) precursor in *Escherichia coli* using pET17b plasmid as an expression vector. The template of stem and stem-loop fragments were amplified with specific primers tagged with restriction enzyme sites: *Xba*I-stNvd-F and *Eco*RI-stNvd-R for amplification of the stem fragment and *Xho*I-stLNvd-F and *Eco*RI-stLNvd-R for the stem-loop fragment (Table 1). After amplification, the stem and stem-loop fragments were sequentially cloned into pET17b vector at the corresponding restriction sites, in a sense and antisense direction relative to the T7 promoter, respectively. The recombinant plasmid was then transformed into *E. coli* DH5α. After verification of the nucleotide sequence by automated DNA sequence (1st BASE Company, Malaysia), the correct recombinant plasmid was re-transformed into *E. coli* HT115 for dsRNA expression. The *E. coli* HT115 carrying the expression plasmid for dsNvd was cultured in LB medium containing 100 μg/ml ampicillin and 25 μg/ml tetracycline overnight at 37 °C. The culture was inoculated at a dilution of 1:50 in the desired volume of LB medium, then the bacterial culture was incubated at 37 °C, 250 rpm for 1.5–2 h until its OD_{600} reached 0.4–0.6. Subsequently, the culture was induced with 0.4 mM IPTG for 4 h prior to extraction of dsNvd by ethanol method (Posiri et al., 2013). Briefly, the bacteria cells were collected and re-suspended in PBS pH 7.4. Ethanol was added to a final concentration of 75% and incubated at room temperature for 5 min. Then the cells were centrifuged at 5000*g* for 5 min, and the pellet was re-suspended with 150 mM NaCl and incubated at room temperature for 1 h. The supernatant containing dsNvd was collected by centrifuged at 13,000 rpm for 10 min. The dsNvd was verified by RNase digestion assay with either 0.1 μg/ml RNase A or 1 U RNase III (Invitrogen) by incubation at 37 °C for 5 min and analyzed on agarose gel electrophoresis.

2.5. Effect of PmNvd depletion on molt duration

Firstly, the effect of dsNvd on *PmNvd* silencing in *P. monodon* was determined. Approximately 10 g shrimp was injected with either NaCl or dsNvd at 2.5 $\mu g \cdot g^{-1}$ shrimp. Then, the Y-organ was isolated on days 3 and 6 after dsRNA injection, and *PmNvd* expression was determined by semi-quantitative RT-PCR with PmNvd-F4 and PmNvd-R2 primers. Actin transcript was amplified with Actin-F and Actin-R primers as an internal control. To study the function of PmNvd during the molting cycle, shrimp at intermolt stage was injected with 2.5 $\mu g \cdot g^{-1}$ shrimp of dsNvd twice, on day 0 and day 3, and the molting stage and molt duration of the shrimp were recorded compared to that of the control shrimp that were injected with NaCl.

2.6. Detection of 20-hydroxyecdysone (20-HE) titers in shrimp hemolymph by reverse phase high performance-liquid chromatography (RP-HPLC)

Shrimp at intermolt stage were injected with 2.5 $\mu g \cdot g^{-1}$ shrimp of dsNvd or NaCl (n = 9 each), and the hemolymph ecdysteroid titers were measured by reverse-phase HPLC (RP-HPLC). Approximately 200–400 μl of hemolymph from individual shrimp was collected in 100 μl of anticoagulant (10 mM Tris pH 7.4, 250 mM sucrose and 100 mM sodium citrate). The hemolymph from shrimp in the same group was pooled, and then hemocytes were removed by centrifugation at 800*g* for 10 min. The plasma was then extracted with 75% methanol followed by centrifugation at 13,000 rpm for 10 min. The supernatant was collected and dried by evaporation. The sample was dissolved in 35% methanol and subsequently subjected into Sep-Pak C-18 cartridge (Waters). The hemolymph ecdysteroids eluted with 100% methanol were dried by evaporation and re-dissolved in 10–15 μl of 35% methanol. Five microliters of the sample were injected into the Acclaim® RLSC C-18 (2.2 μm, 2.1 × 100 mm, Dionex) column connected with HPLC machine (Ultimate 3000 UHPLC, Dionex). The chromatography was performed by gradient elution with 35% to 60% methanol for 20 min at a flow rate of 0.3 ml/min. The signals were detected by UV absorbance at wavelength of 240 nm. The 20-HE (Abcam) at different concentrations (25–200 ng/μl) that was eluted at retention time of approximately 8.8 min was used to construct a standard curve. The peak area was calculated by Chameleon® software version 6.8.

3. Results

3.1. Cloning of a full-length cDNA of PmNvd

A 1727 bp full-length cDNA of Rieske domain oxygenase Neverland of *P. monodon* (*PmNvd*) was successfully cloned (GenBank Accession

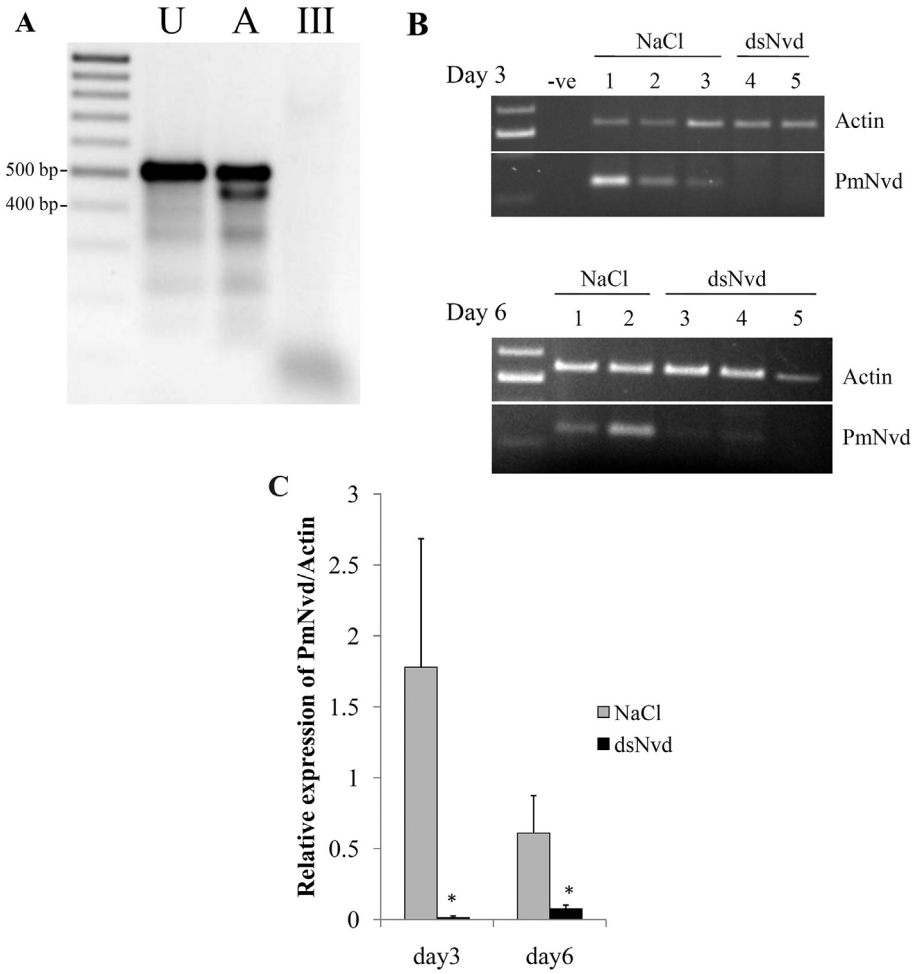

Fig. 6. Production and efficiency of *PmNvd*-specific dsRNA (A). The integrity of *PmNvd*-specific dsRNA (dsNvd) expressed in *E. coli* HT115 was verified by RNase digestion. The dsNvd digested with RNase A (A), RNase III (III) or water as a negative control (U) was separated in agarose gel compared with a DNA ladder marker. (B) The efficiency of *PmNvd* knockdown in shrimp was determined on days 3 and 6 after dsNvd injection. The *PmNvd* transcript in the Y-organ of shrimp injected with dsNvd or NaCl was determined by semi-quantitative RT-PCR. *Actin* was used as an internal control. Numbers represent individual shrimp, and –ve is a negative control of PCR reaction. (C) Relative expression of *PmNvd* to *actin* calculated from the intensity of RT-PCR products of both transcripts is shown in a bar graph. Bars and error bars represent means and SEM, respectively. Asterisks indicate a significant difference at $p < 0.05$ between groups analyzed by *t*-test.

No. KU360639). It was composed of a 160 bp 5′UTR, a 1341 bp coding region for a putative 447 amino acids and a 226 bp 3′ UTR (Fig. 1). The deduced PmNvd contains a signal peptide at the first 14 amino acid residues and a transmembrane motif ^{33}WxxF^{59} as predicted by SOSUI (Gomi et al., 2004). In addition, the Rieske [2Fe-2S] domain motif ^{107}AxxG^{209} with the highly conserved sequence C-X-H-X$_{16–17}$-C-X$_2$-H was predicted by pfam, and a non-heme iron-binding motif E-X$_3$-D-X$_2$-H-X$_4$-H was predicted by COACH server (Yang et al., 2013a, 2013b). An amino acid sequence alignment, particularly the Rieske domain (Fig. 2A) and the non-heme iron binding domain, indicated that the deduced PmNvd was highly similar to Rieske domain oxygenase Neverland of other species such as *Bombyx mori*, *Drosophila melanogaster* and *Caenorhabditis elegans* (Fig. 2B). Furthermore, phylogenetic analysis in Fig. 3 revealed that PmNvd was separated from Nvd of insects, nematodes and chordates. It was clustered in the same group as Nvd of the sea urchin, *Hemicentrotus pulcherrimus*, but on separate branch from Nvd1 and Nvd2 of the planktonic crustacean *D. magna*.

3.2. Determination of PmNvd mRNA expression in shrimp tissues

In order to determine the expression of *PmNvd* mRNA in the shrimp, *PmNvd* transcript levels in various tissues were detected by qRT-PCR. The result in Fig. 4 showed that *PmNvd* expression was mainly found in the Y-organ but not in other tissues i.e., eyestalk, brain, thoracic ganglia, hepatopancreas, gills, muscle and lymphoid. Furthermore, investigation of *PmNvd* expression in the Y-organ at different stages of the molting cycle showing that *PmNvd* was expressed at low level in the shrimp at intermolt (C) and early premolt (D0) stages (Fig. 5). A dramatic increase of *PmNvd* expression occurred at the premolt stage D1 prior to a slight decline at later premolt stages, D2 and D3. Subsequently, the expression level of *PmNvd* dropped to the basal level at late premolt stage (D4) and after ecdysis.

3.3. Effect of PmNvd knockdown on molting duration

In order to study the function of PmNvd in shrimp, a double-stranded RNA targeting *PmNvd* coding sequence (dsNvd) was expressed in *E. coli* HT115 as a small hairpin precursor. An approximately 500 bp small-hairpin dsNvd was validated for dsRNA characteristic by RNase digestion. The result in Fig. 6A suggested that the single-stranded loop region of the small hairpin dsNvd was digested by RNase A resulting in a 459 bp of dsNvd, whereas the dsNvd was completely digested with RNase III, thus confirming its double-stranded structure. The knockdown efficiency of dsNvd was further determined by monitoring *PmNvd* expression in the Y-organ of the shrimp after injected with dsNvd. Fig. 6B–C revealed that *PmNvd* transcript in the dsNvd-injected shrimp was significantly suppressed to an undetectable level by RT-PCR on day 3 after dsNvd injection compared with that in NaCl-injected shrimp. Moreover, *PmNvd* expression in dsNvd-injected shrimp began to recover partially on day 6.

The effect of *PmNvd* depletion on molt duration was further investigated by following the progress of molting cycle of *PmNvd* knockdown shrimp. Since the *PmNvd* transcript level in dsNvd-injected shrimp seemed to recover after day 3, the shrimp in this experiment were injected with dsNvd twice on days 0 and 3 to assure effective *PmNvd* silencing. Approximately 80% of shrimp were arrested at early premolt stage (D0) on day 3 after the first injection with 2.5 $\mu g \cdot g^{-1}$ shrimp dsNvd, while approximately 90% of NaCl-injected shrimp could

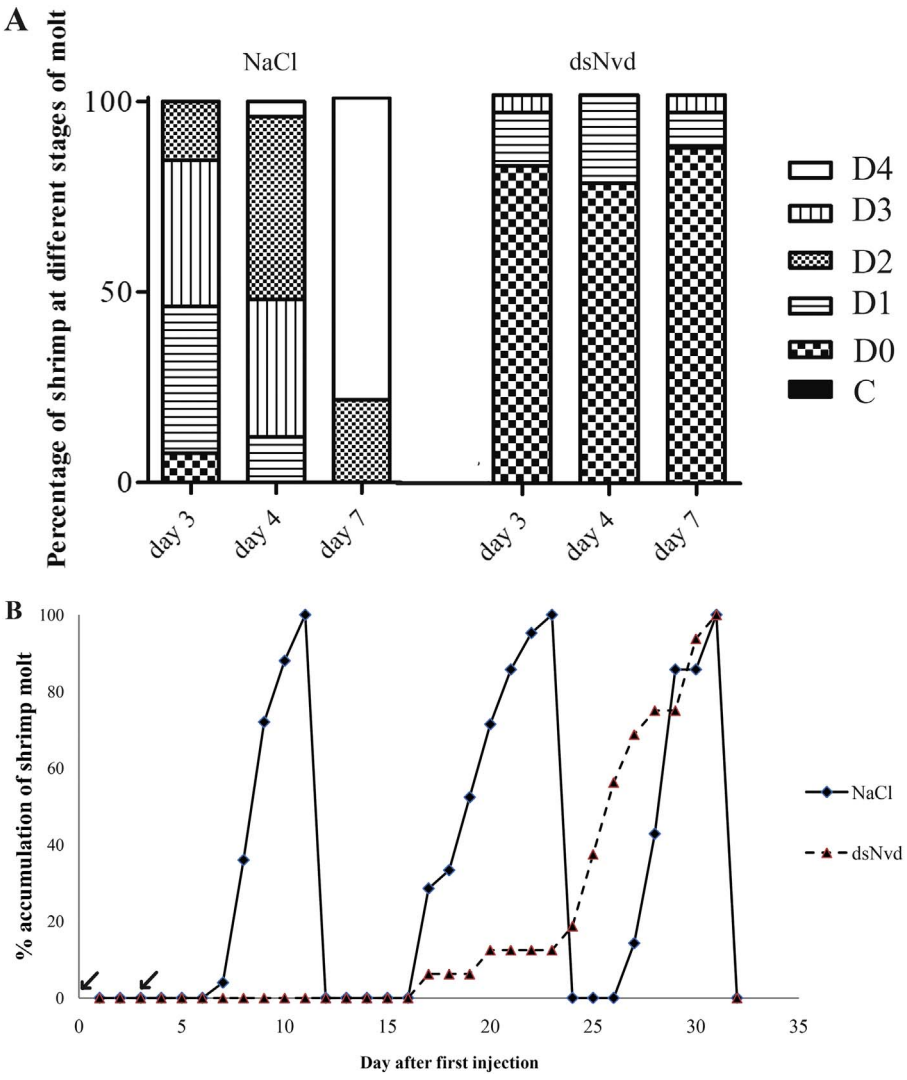

Fig. 7. Effect of *PmNvd* silencing on molt progression and molt duration. Approximately 10 g *P. monodon* was injected with dsNvd (n = 22) or NaCl (n = 25) twice on days 0 and day 3. (A) The numbers of shrimp in each group that were in different stages of molt (depicted by different filled patterns) were recorded on days 3, 4 and 7 and presented as the percentage compared to the total numbers of shrimp in that group. (B) The duration of molting cycle of shrimp is presented as the percentage of accumulated number of shrimp that molted in each day after dsNvd injection. Solid and dash lines represent NaCl and dsNvd-injected shrimp, respectively. Arrows indicate the day on which the shrimp were injected with dsNvd or NaCl.

proceed to later premolt stages (D1-D3) (Fig. 7A). Moreover, about 80% of dsNvd-injected shrimp remained at early premolt stage (D0) on day 7 after injection while the majority of NaCl-injected shrimp continuously progressed to late premolt stage (D4). Interestingly, approximately 80% of dsNvd-injected shrimp were arrested at early premolt stage for approximately 12 days after the second injection whereas all NaCl-injected shrimp had completed the first round of the molting cycle (Fig. 7B). Nevertheless, molting of the dsNvd-injected shrimp started to progress gradually after 15 days post injection and could eventually molt in an average of 26.1 ± 3.8 days (Fig. 7B) while the control shrimp had already molted for three cycles with the average molting duration of 9.0 ± 1.1, 10.3 ± 1.4 and 9.8 ± 0.8 days, respectively (Fig. 7B).

3.4. Hemolymph ecdysteroid titer upon PmNvd knockdown

In order to examine whether the interruption of the molting cycle by *PmNvd* depletion is related to ecdysteroid production or not, ecdysteroid (20-HE) titers in the hemolymph of *PmNvd* knockdown shrimp were determined by RP-HPLC. On day 3 after dsRNA injection, most of the shrimp in both dsNvd-injected group and the control group were at intermolt (C) and early premolt (D0) stages, and some (approximately 20%) of the control shrimp were in premolt stage D1 (Fig. 8A). Ecdysteroid titers of the shrimp in both groups were measured. The peak corresponding to the same retention time of 20-HE standard was calculated for 20-HE equivalent of ecdysteroid titers (Fig. 8B). The result showed that the hemolymph 20-HE in dsNvd-injected shrimp was retained in lower level at 9.9 ± 4.7 ng/ml compared with that in NaCl-injected shrimp (47.3 ± 7.5 ng/ml) as shown in Fig. 8C.

4. Discussion

Rieske domain containing oxygenase Neverland (Nvd) functions in converting cholesterol to 7-dehydrocholesterol (7dC) in the early ecdysteroid biosynthetic pathway. Nvd were present in both vertebrates such as *Ciona intestinalis*, *Danio rerio* and *Xenopus laevis* (Yoshiyama-Yanagawa et al., 2011) and invertebrates such as *D. magna* (Sumiya et al., 2014), *Drosophila* spp. (Lang et al., 2012) and *B. mori* (Yoshiyama et al., 2006) including the DAF-36 of *C. elegans* (Wollam et al., 2011; Yoshiyama-Yanagawa et al., 2011). However, Nvd has not been identified in shrimp so far. In this study, the full-length *Nvd* cDNA was successfully obtained from a marine shrimp, *P. monodon*, and its deduced amino acid sequence revealed a high similarity to Nvd of other organisms (Fig. 2). Nvd was demonstrated to be located at microsomal membrane in CHO cells (Yoshiyama-Yanagawa et al., 2011) and *Sf*9 cells (Wollam et al., 2011), and thus, is most likely localized to endoplasmic reticulum. The presence of a putative transmembrane motif in PmNvd structure may also indicate its localization at microsomal membrane. Furthermore, the Rieske domain (2Fe-2S motif) and non-heme Fe^{2+} binding domain of PmNvd were highly conserved among

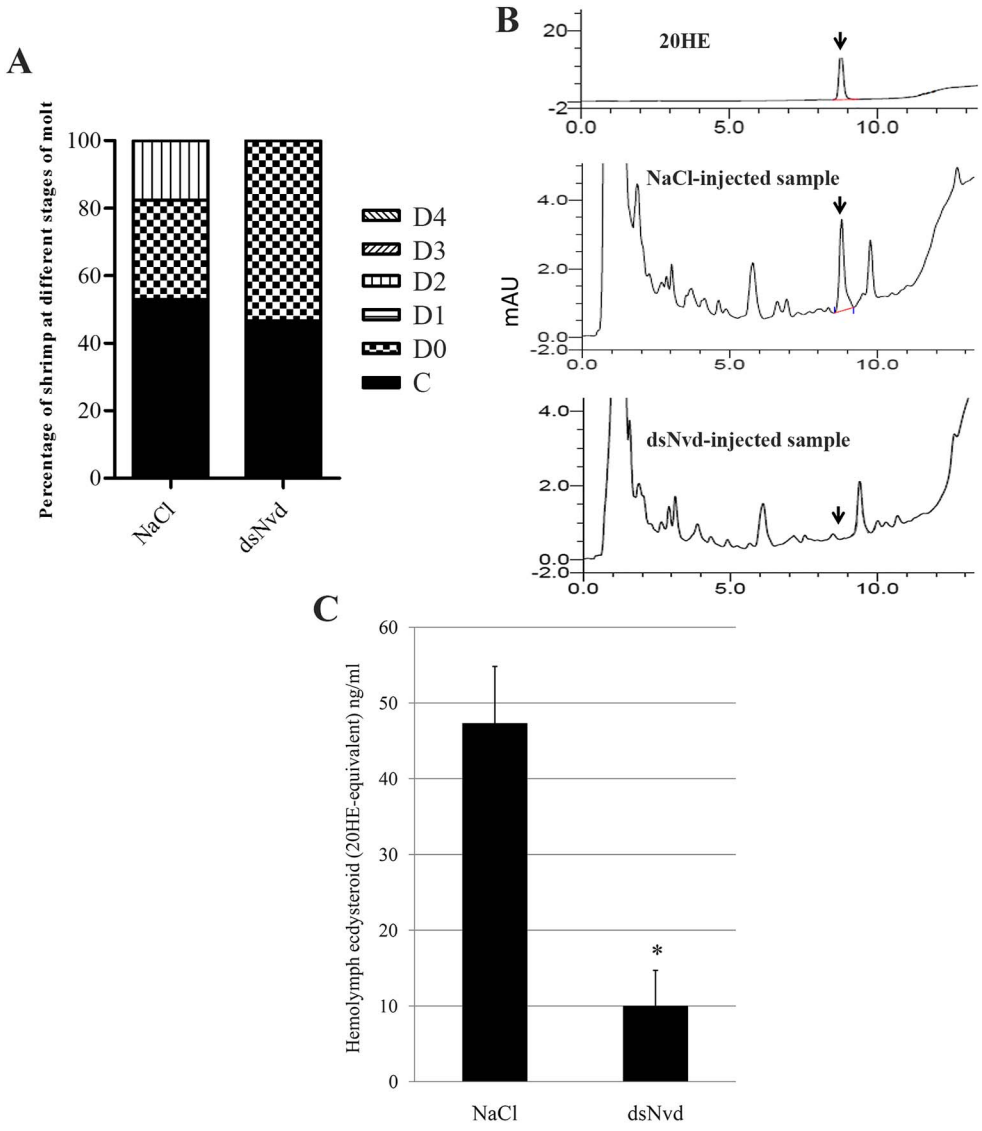

Fig. 8. Effect of *PmNvd* depletion on hemolymph ecdysteroid titer. *P. monodon* (~10 g) at intermolt stage was injected with dsNvd (n = 12) or NaCl (n = 18). (A) After injection for 3 days, the molt stage of shrimp was recorded and presented as a percentage compared to total numbers of shrimp in that group. (B) The ecdysteroid titers in shrimp hemolymph were measured by RP-HPLC. The chromatogram of 20-HE in the standard, hemolymph from NaCl- or dsNvd injected shrimp was indicated as a peak eluted at 8.8 min retention time at the absorbance of 240 nm. (C) Pooled hemolymph from 3 shrimp in each group was used for the calculation of 20-HE levels from the peak area of RP-HPLC. Bars and error bars represent mean and SEM, respectively. Asterisk is significant difference at $p < 0.05$ analyzed by t-test.

that in other species (Fig. 2). The phylogenetic analysis revealed that Nvd of *P. monodon* is more closely related to that of sea urchin than that of *D. magna*, and distinguish from that of insects, chordates and nematodes, suggesting that *P. monodon*'s Nvd evolutionarily diverged from *D. magna* and other organisms.

Nvd is expressed in the prothoracic gland in insects such as *B. mori* and *D. melanogaster* as well as in the ring gland of *D. melanogaster* embryo (Yoshiyama et al., 2006) which is a source of ecdysteroid production, while *DAF-36*, a Nvd homolog of *C. elegans*, is expressed in the intestinal cytoplasm and head mesodermal cells (Rottiers et al., 2006). In *D. magna*, Nvd is mainly found in the gut, but less in ovary and other tissues (Sumiya et al., 2014). In *P. monodon*, *PmNvd* was dominantly expressed in the Y-organ, a source of ecdysteroid synthesis in crustaceans, but not found in ovaries (Fig. 4). This is similar to the expression of *Phantom* (*Phm*), one of the ecdysteroidogenic enzymes, that was specifically expressed in the Y-organ of kuruma prawn, *Marsupenaeus japonicus* (Nakatsuji et al., 2006). Furthermore, Nvd of a crayfish, *Pontastacus leptodactylus*, was also found in Y-organ's transcriptome data (Tom et al., 2013). These results suggest the existence of ecdysteroidogenic pathway in the Y-organ of penaeid shrimp. According to phylogenetic analysis in Fig. 3, PmNvd is diverse from Nvd of *D. magna* and insects. This may explain different sources of ecdysteroid biosynthesis among insects, shrimp and *D. magna* that are from different evolutionary patterns. In addition, *PmNvd* in the Y-organ was expressed at the highest level in premolt stage of the molting cycle (Fig. 4). This is also similar to an increase of *M. japonicus*'s *Phm* expression during premolt stage (Nakatsuji et al., 2006). Moreover, *Nvd* expression in insects was increased before ecdysis in the 4th and 5th instar larvae of *B. mori* and *D. melanogaster* (Yoshiyama et al., 2006). The expression profile of *Nvd* is in accordance with the highest level of hemolymph ecdysteroids that was also found in the premolt stage in several crustaceans including *P. monodon* (Kuo and Lin, 1996), *P. vannamei* (Blais et al., 1994), *C. sapidus* (Chung, 2010), *C. maenas* (Styrishave et al., 2008), *Emerita asiatica* (Gunamalai et al., 2004), *Armadillidium vulgare* (Suzuki et al., 1996) and *Homarus americanus* (Snyder and Chang, 1991). The relationship between *Nvd* expression and ecdysteroid production at premolt stage suggested a possible role of PmNvd in ecdysteroid biosynthesis.

In this study, the role of PmNvd in the molting cycle was demonstrated by *PmNvd* knockdown in the shrimp. The *PmNvd*-specific dsRNA was successfully produced in the bacterial system, and it could completely suppress *PmNvd* transcript in the Y-organ within 3 days after injection into shrimp (Fig. 6B-C). Interestingly, molting progression in *PmNvd*-depleted shrimp was arrested at early premolt stage (D0) resulting in a delay of the molt duration (Fig. 7). Similarly, silencing of *Nvd* in *D. melanogaster* larvae also led to developmental arrest into pupae stage and eventually death (Yoshiyama et al., 2006). The development of the larvae could not be recovered by cholesterol

administration (Lang et al., 2012; Yoshiyama et al., 2006). However, it was rescued by the treatment with 7dC in concurrence with an increased ecdysteroid titer (Yoshiyama et al., 2006) suggesting the function of Nvd in the conversion of cholesterol to 7dC at the early step of ecdysteroid production. Furthermore, a dramatic decrease of hemolymph 20-HE titer in dsNvd-injected shrimp (Fig. 8B) indicated that PmNvd is basically involved in ecdysteroid biosynthesis. The arrest of molting progression at the early premolt stage upon *PmNvd*-depletion conformed to *PmNvd* expression profile that increased in the premolt stage (Fig. 5). This result suggested that there was a checkpoint of the molting process between early premolt and premolt stages that is dependent of hemolymph ecdysteroids titer. In addition, several studies reported the important role of Nvd in embryonic development and metamorphosis. For example, depletion of *Nvd* in *D. magna* resulted in lethal embryo (Sumiya et al., 2016) similar to that in *D. melanogaster* larvae (Yoshiyama et al., 2006). Therefore, Nvd is required for the progression in the premolt stage of ecdysis during both metamorphosis and growth via the regulation of ecdysteroid production.

5. Conclusion

Our study investigated a crucial function of an ecdysteroidogenic enzyme, Rieske domain oxygenase Neverland of *P. monodon* in molting process. The full length *PmNvd* cDNA was obtained, and its expression in the Y-organ was at the highest level in mid-premolt stage. The reduction of *PmNvd* by specific dsRNA caused a delay of molt duration with the arrestment of molt progression at early premolt stage. This together with the suppression of 20HE production in *PmNvd*-silent shrimp suggest that PmNvd functions during premolt stage by regulating hemolymph ecdysteroid titers, most likely by suppressing the early step in ecdysteroid synthesis as in other organisms.

Acknowledgement

The authors thank Miss Somjai Wongtripop (Shrimp Genetics Improvement Center, Surat Thani, Thailand) for providing the shrimp samples. We are thankful to Ms. Chawewan Chimwai and Ms. Pannee Thongboonsong for their technical assistance. This study was supported by Thailand Research Fund (BRG5880005) to AU, DBG5980011 to SP) and Mahidol University Research grant.

References

Blais, C., Sefiani, M., Toullec, J.-Y., Soyez, D., 1994. In vitro production of ecdysteroids by Y-organs of *Penaeus vannamei* (Crustacea, Decapoda). Correlation with hemolymph titers. Invertebr. Reprod. Dev. 26, 3–11.

Chung, J.S., 2010. Hemolymph ecdysteroids during the last three molt cycles of the blue crab, *Callinectes sapidus*: quantitative and qualitative analyses and regulation. Arch. Insect Biochem. Physiol. 73, 1–13.

Gomi, M., Sonoyama, M., Mitaku, S., 2004. High performance system for signal peptide prediction: SOSUIsignal. Chem-Bio. Inf. J. 4, 142–147.

Gunamalai, V., Kirubagaran, R., Subramoniam, T., 2004. Hormonal coordination of molting and female reproduction by ecdysteroids in the mole crab *Emerita asiatica* (Milne Edwards). Gen. Comp. Endocrinol. 138, 128–138.

Kang, B.K., Spaziani, E., 1995a. Uptake of high-density lipoprotein by Y-organs of the crab, *Cancer antennarius*. I. Characterization in vitro and effects of stimulators and inhibitors. Arch. Insect Biochem. Physiol. 30, 61–75.

Kang, B.K., Spaziani, E., 1995b. Uptake of high-density lipoprotein by Y-organs of the crab, *Cancer antennarius*. II. Formal characterization of receptor-mediation with isolated membranes. Arch. Insect Biochem. Physiol. 30, 77–91.

Kuo, C.M., Lin, W.W., 1996. Changes in morphological characteristics and ecdysteroids during the moulting cycle of tiger shrimp, *Penaeus monodon* Fabricus. Zool. Stud. 352, 118–127.

Lachaise, F., Goudeau, M., Hetru, C., Kappler, C., Hoffmann, J.A., 1981. Ecdysteroids and ovarian development in the shore crab, *Carcinus maenas*. H-S Z Physiol. Chem. 362, 521–529.

Lang, M., Murat, S., Clark, A.G., Gouppil, G., Blais, C., Matzkin, L.M., Guittard, É., Yoshiyama-Yanagawa, T., Kataoka, H., Niwa, R., Lafont, R., Dauphin-Villemant, C., Orgogozo, V., 2012. Mutations in the Neverland gene turned *Drosophila pachea* into an obligate specialist species. Science 337, 1658–1661.

Mattson, M., Spaziani, E., 1985. Characterization of molt-inhibiting hormone (MIH) action on crustacean Y-organ segments and dispersed cells in culture and a bioassay for MIH activity. J. Exp. Zool. 236, 93–101.

Mykles, D.L., 2011. Ecdysteroid metabolism in crustaceans. J. Steroid Biochem. Mol. Biol. 127, 196–203.

Nakatsuji, T., Sonobe, H., 2004. Regulation of ecdysteroid secretion from the Y-organ by molt-inhibiting hormone in the American crayfish, *Procambarus clarkii*. Gen. Comp. Endocrinol. 135, 358–364.

Nakatsuji, T., Sonobe, H., Watson, R.D., 2006. Molt-inhibiting hormone-mediated regulation of ecdysteroid synthesis in Y-organs of the crayfish (*Procambarus clarkii*): involvement of cyclic GMP and cyclic nucleotide phosphodiesterase. Mol. Cell. Endocrinol. 253, 76–82.

Nakatsuji, T., Lee, C.Y., Watson, R.D., 2009. Crustacean molt-inhibiting hormone: structure, function, and cellular mode of action. Comp. Biochem. Physiol. A Physiol. 152, 139–148.

Niwa, R., Niwa, Y.S., 2014. Enzymes for ecdysteroid biosynthesis: their biological functions in insects and beyond. Biosci. Biotechnol. Biochem. 78, 1283–1292.

Okumura, T., Aida, K., 2000. Fluctuations in hemolymph ecdysteroid levels during the reproductive and non-reproductive molt cycles in the giant freshwater prawn *Macrobrachium rosenbergii*. Fish. Sci. 66, 876–883.

Petryk, A., Warren, J.T., Marques, G., Jarcho, M.P., Gilbert, L.I., Kahler, J., Parvy, J.P., Li, Y., Dauphin-Villemant, C., O'Connor, M.B., 2003. Shade is the *Drosophila* P450 enzyme that mediates the hydroxylation of ecdysone to the steroid insect molting hormone 20-hydroxyecdysone. Proc. Natl. Acad. Sci. U. S. A. 100, 13773–13778.

Phlippen, M.K., Webster, S.G., Chung, J.S., Dircksen, H., 2000. Ecdysis of decapod crustaceans is associated with a dramatic release of crustacean cardioactive peptide into the hemolymph. J. Exp. Biol. 203, 521–536.

Posiri, P., Ongvarrasopone, C., Panyim, S., 2013. A simple one-step method for producing dsRNA from *E. coli* to inhibit shrimp virus replication. J. Virol. Methods 188, 64–69.

Promwikorn, W., Kirirat, P., Thaweethamsewee, P., 2004. Index of molt staging in the black tiger shrimp (*Penaeus monodon*). Songklanakarin J. Sci. Technol. 26, 765–772.

Rewitz, K.F., O'Connor, M.B., Gilbert, L.I., 2007. Molecular evolution of the insect Halloween family of cytochrome P450s: phylogeny, gene organization and functional conservation. Insect Biochem. Mol. Biol. 37, 741–753.

Rottiers, V., Motola, D.L., Gerisch, B., Cummins, C.L., Nishiwaki, K., Mangelsdorf, D.J., Antebi, A., 2006. Hormonal control of *C. elegans* dauer formation and life span by a Rieske-like oxygenase. Dev. Cell 10, 473–482.

Rudolph, P.H., Spaziani, E., Wang, W.L., 1992. Formation of ecdysteroids by Y-organs of the crab, *Menippe mercenaria*. Gen. Comp. Endocrinol. 88, 224–234.

Snyder, M.J., Chang, E.S., 1991. Ecdysteroids in relation to the molt cycle of the American lobster, *Homarus americanus*: I. Hemolymph titers and metabolites. Gen. Comp. Endocrinol. 81, 133–145.

Spaziani, E., Wang, W.L., 1993. Biosynthesis of ecdysteroid hormones by crustacean Y-organs: conversion of cholesterol to 7-dehydrocholesterol is suppressed by a steroid 5α-reductase inhibitor. Mol. Cell. Endocrinol. 95, 111–114.

Styrishave, B., Lund, T., Andersen, O., 2008. Ecdysteroids in female shore crabs *Carcinus maenas* during the moulting cycle and oocyte development. J. Mar. Biol. Assoc. UK 88, 575–581.

Sumiya, E., Ogino, Y., Miyakawa, H., Hiruta, C., Toyota, K., Miyagawa, S., Iguchi, T., 2014. Roles of ecdysteroids for progression of reproductive cycle in the fresh water crustacean *Daphnia magna*. Front. Zool. 11, 1–12.

Sumiya, E., Ogino, Y., Toyota, K., Miyakawa, H., Miyagawa, S., Iguchi, T., 2016. Neverland regulates embryonic moltings through the regulation of ecdysteroid synthesis in the water flea *Daphnia magna*, and may thus act as a target for chemical disruption of molting. J. Appl. Toxicol. 36 (11), 1476–1485.

Suzuki, S., Yamasaki, K., Fujita, T., Mamiya, Y., Sonobe, H., 1996. Ovarian and hemolymph ecdysteroids in the terrestrial isopod *Armadillidium vulgare* (Malacostracan Crustacea). Gen. Comp. Endocrinol. 104, 129–138.

Tom, M., Manfrin, C., Giulianini, P.G., Pallavicini, A., 2013. Crustacean oxi-reductases protein sequences derived from a functional genomic project potentially involved in ecdysteroid hormones metabolism - a starting point for function examination. Gen. Comp. Endocrinol. 194, 71–80.

Uryu, O., Ameku, T., Niwa, R., 2015. Recent progress in understanding the role of ecdysteroids in adult insects: germline development and circadian clock in the fruit fly *Drosophila melanogaster*. Zool. Lett. 1, 1–9.

Wollam, J., Magomedova, L., Magner, D.B., Shen, Y., Rottiers, V., Motola, D.L., Mangelsdorf, D.J., Cummins, C.L., Antebi, A., 2011. The Rieske oxygenase DAF-36 functions as a cholesterol 7-desaturase in steroidogenic pathways governing longevity. Aging Cell 10, 879–884.

Yang, J., Roy, A., Zhang, Y., 2013a. Protein-ligand binding site recognition using complementary binding-specific substructure comparison and sequence profile alignment. Bioinformatics 29, 2588–2595.

Yang, J., Roy, A., Zhang, Y., 2013b. A semi-manually curated database for biologically relevant ligand-protein interactions. Nucleic Acids Res. 41, 1096–1103.

Yoshiyama, T., Namiki, T., Mita, K., Kataoka, H., Niwa, R., 2006. Neverland is an evolutionally conserved Rieske-domain protein that is essential for ecdysone synthesis and insect growth. Development 133, 2565–2574.

Yoshiyama-Yanagawa, T., Enya, S., Shimada-Niwa, Y., Yaguchi, S., Haramoto, Y., Matsuya, T., Shiomi, K., Sasakura, Y., Takahashi, S., Asashima, M., Kataoka, H., Niwa, R., 2011. The conserved Rieske oxygenase DAF-36/Neverland is a novel cholesterol-metabolizing enzyme. J. Biol. Chem. 286, 25756–25762.

Received: 14 December 2016 | Revised: 29 April 2017 | Accepted: 29 April 2017

DOI: 10.1111/are.13407

ORIGINAL ARTICLE

WILEY Aquaculture Research

In vitro study of a putative role of gonad-inhibiting hormone in oocyte growth stimulation in *Penaeus monodon*

Ponsit Sathapondecha[1] | Sakol Panyim[2,3] | Apinunt Udomkit[2]

[1]Department of Molecular Biotechnology and Bioinformatics, Faculty of Sciences, Prince of Songkla University, Songkla, Thailand

[2]Institute of Molecular Biosciences, Mahidol University, Nakhon Pathom, Thailand

[3]Department of Biochemistry, Faculty of Science, Mahidol University, Bangkok, Thailand

Correspondence
Apinunt Udomkit, Institute of Molecular Biosciences, Mahidol University, Nakhon Pathom, Thailand.
Email: apinunt.udo@mahidol.ac.th

Funding information
Thailand Research Fund, Grant/Award Number: BRG5880005, DBG5980011; Mahidol University Research Grant; the Office of the Higher Education Commission and Mahidol University under the National Research Universities Initiative; the Royal Golden Jubilee Ph.D. Program

Abstract

Ovarian development in crustacean is controlled by several factors, among which a neuropeptide gonad-inhibiting hormone (GIH) is known to inhibit vitellogenin (Vg) synthesis in the ovary. It has been postulated that GIH may control Vg synthesis by inhibiting the release of gonad-stimulating factor (GSF) from brain and thoracic ganglia. To prove this hypothesis, this study was primarily aimed to investigate the influence of GIH on the release of GSF from thoracic ganglia of *Penaeus monodon*. Our result showed that GIH did not suppress the release of putative GSF from thoracic ganglia by calcium ionophore A23187 as the induction of oocyte growth in the ovary explants that were cocultured with thoracic ganglia in the presence of A23187 was not affected by the addition of recombinant GIH protein. In addition and interestingly, when the ovary explants were incubated with the recombinant GIH alone, the oocyte growth was increased at the rate comparable to that induced by A23187 in the presence of thoracic ganglia. Hence, our in vitro study demonstrated that the stimulation of GSF released from thoracic ganglia is independent of GIH, and that the GIH has a dual function in oocyte growth stimulation and inhibition of Vg synthesis in the early stage of ovarian development. This expands our knowledge on the regulation of ovarian development in shrimp by GIH. Further in vivo studies in this novel aspect of GIH function will be useful for the improvement of shrimp ovarian maturation in the future.

KEYWORDS
gonad-stimulating factor, oocyte growth, *Penaeus monodon*, vitellogenin

1 | INTRODUCTION

Ovarian development is an important process in female reproduction. In general, primary oocytes that are mitotically divided from oogonia are arrested at prophase I to prepare for oocyte maturation (Von Stetina & Orr-Weaver, 2011). In crustaceans, there are two major phases in ovarian development; primary vitellogenesis that involves oocyte growth and follicular development and secondary vitellogenesis comprising vitellogenin (Vg) synthesis and accumulation, and cortical rod formation in later phase (Charniaux-Cotton, 1985). In penaeid shrimps, the ovary at previtellogenic stage of development contained small oocyte cells, particularly chromatin nucleolar oocytes (CNOs) and perinucleolar oocytes (POs). The PO is larger than CNO in size, and their nucleoli are located at nuclear membrane. Some PO cells are surrounded by follicle cells. In vitellogenic ovary, Vg is initially synthesized in ovarian follicle cells and accumulated in the oocyte cells leading to an increase in their size. Cortical rods are formed in fully grown oocytes (Ayub & Ahmed, 2002). Moreover, *Vg* is also expressed and secreted from hepatopancreas and accumulated in the ovary (Tseng, Chen, Kou, Lo & Kuo, 2001).

Hormonal control of ovarian development in shrimp is mediated by several factors such as peptide hormones, steroid hormones and neurotransmitters (Subramoniam, 2011). There were several reports about the existence of gonad-stimulating factor (GSF) in the brain and thoracic ganglia of crustaceans during the past two decades. For

example, injection of thoracic ganglia extract in kuruma prawn, *Penaeus japonicus* caused an increase of Vg in haemolymph (Yano, 1992). Vitellogenesis in *Paratya compressa* was also stimulated by both brain and thoracic ganglia extract (Takayanagi, Yamamoto & Takeda, 1986). In addition, the release of putative GSF from brain and thoracic ganglia could be stimulated by calcium ionophore (A23187) as demonstrated either in ovarian explants or by in vivo injection in the crayfish *Procambarus clarkii* (Sarojini, Nagabhushanam & Fingerman, 1995). However, the actual molecule responsible for this gonad-stimulating activity has not been identified and characterized so far.

On the other hand, vitellogenesis is inhibited by gonad-inhibiting hormone (GIH), a neuropeptide belonging to the crustacean hyperglycemic hormone (CHH) family (Chang, 2001). GIH is mainly expressed in the X-organ sinus gland complex of eyestalk ganglia and was shown to function in inhibition of *Vg* expression in several decapod crustaceans including *Homarus americanus*, *Nephrops norvegicus*, *Penaeus monodon* and *Litopenaeus vannamei* (Chen et al., 2014; De Kleijn, Sleutels, Martens & Van Herp, 1994; Edomi et al., 2002; Treerattrakool, Panyim, Chan, Withyachumnarnkul & Udomkit, 2008). Moreover, neutralization of rGIH by monoclonal antibody against *P. monodon*'s GIH also stimulated *Vg* expression in primary ovarian cells (Treerattrakool, Boonchoy, Urtgam, Panyim & Udomkit, 2014). GIH level in the haemolymph of *H. americanus* was highest in previtellogenic stage and declined in vitellogenic stages of ovarian development (De Kleijn et al., 1998), which was in agreement with that in *P. monodon* (Urtgam et al., 2015). These supported the function of GIH in suppression of *Vg* synthesis in previtellogenic ovary. In addition, previtellogenic stage is the phase at which oocyte growth occurs; therefore, this brings into question whether or not GIH inhibits the release or synthesis of GSF (Nagaraju, 2011), and may it play any role in oocyte growth during previtellogenic stage.

Therefore, this study aimed to investigate a role of GIH in suppressing the release of putative GSF from thoracic ganglia. In addition, the function of GIH in oocyte growth in previtellogenic ovary will also be studied.

2 | MATERIALS AND METHODS

2.1 | Expression and purification of recombinant GIH (rGIH) in yeast expression system

Recombinant yeast, *Pichia pastoris* KM71, containing the nucleotide sequence encoding for a mature GIH peptide in its genome was kindly provided by Dr. Supattra Treerattrakool. The expression and purification of the recombinant GIH (rGIH) were carried out as described by Treerattrakool et al. (2014). Briefly, *P. pastoris* KM71 carrying the expression cassette for rGIH was cultured in YPD (1% yeast extract, 2% peptone and 2% D-glucose) containing 100 μg/ml zeocin at 30°C for 2 days. The starter culture was inoculated at 0.1 OD_{600}/ml in BMGY medium (1% w/v yeast extract, 2% w/v peptone, 100 mM phosphate buffer pH 6.0, 1% v/v glycerol, 0.67% w/v YNB and 0.4 μg/ml biotin) and incubated at 30°C for 12–13 hr until an OD_{600} of 6–8 was obtained. Then, the expression of rGIH was induced in BMMY medium (1% w/v yeast extract, 2% w/v peptone, 100 mM phosphate buffer 6.0, 3% v/v methanol, 0.67% w/v YNB and 0.4 μg/ml biotin) at 30°C for 2 days. The culture medium was collected and precipitated with 40%–50% saturated ammonium sulphate to obtain rGIH. The precipitated rGIH was dissolved with 20% acetonitrile and subjected to solid-phase extraction using a Sep-Pak C-18 column (Waters). The purified rGIH was eluted in a fraction of 40% acetonitrile in 0.1% TFA. The purified rGIH was then evaporated and dissolved in PBS before use.

2.2 | Validation of rGIH activity to inhibit vitellogenin (*Vg*) mRNA expression in primary ovarian cells

The ovary was freshly isolated from previtellogenic female shrimp *P. monodon* (~100 g body weight) and immediately rinsed in culture medium (Leibovitz's L-15 medium (Gibco), 1% w/v D-glucose, 0.5% w/v NaCl, 3.33% w/v lactalbumin, 10% v/v FBS, 10% v/v shrimp meat extract) containing 100 U penicillin/streptomycin. The ovary was cut into small pieces and washed several times in the culture medium containing 1000 U and 2000 U of penicillin and streptomycin, respectively. After washing, pieces of ovary were minced until homogenous in the culture medium. Approximately 7.5×10^5 oocyte cells in 1 ml culture medium were seeded in each well of a 24-well plate and incubated overnight at 28°C. The culture medium was then replaced with fresh culture medium containing 200 ng of rGIH; the amount that was about twofold higher than that previously used to demonstrate the dose-dependent inhibition of rGIH on *Vg* expression by Treerattrakool et al. (2014) to ensure substantial *Vg* suppression in this study. After 24 hr, 500 μl of culture medium was discarded, and 500 μl of fresh culture medium containing the same concentration of rGIH was added and further incubated for 24 hr. The cells that were cultured with the addition of PBS instead of rGIH were used as a control. The primary ovarian cells were collected at 24 hr and 48 hr after treatment, and total RNA was extracted using RiboZol™ reagent (AMERESCO) according to the manufacturer's protocol. The expression of vitellogenin (*Vg*) in each sample was determined by reverse transcription real-time PCR as described below.

2.3 | Quantification of *Vg* mRNA expression by reverse transcription real-time PCR (RT-qPCR)

Relative RT-qPCR was performed to determine *Vg* mRNA level. Total RNA samples were first treated with DNase I to eliminate the contaminated genomic DNA. One microgram of the RNA was incubated with 1× DNase I buffer and 1 U DNase I (Thermo Scientific) at 37°C for 15 min, followed by 65°C for 5 min. Then, the DNase I-treated RNA was used to synthesize first-stranded cDNA with an oligo-dT primer. The sample was preheated at 70°C for

5 min, and then the reverse transcription mixture containing 1× ImProm-II™ buffer, 3 mM $MgCl_2$, 0.4 mM dNTP and 1 μl ImProm-II™ reverse transcriptase (Promega) was added. The reaction was carried out in the following temperature profile; 25°C for 5 min, 42°C for 60 min and 70°C for 10 min. The cDNA was next used as a template in 1× SYBR® FAST Master Mix (KAPA Biosystems) and 0.25 μM Vg-specific primers (Vg-F; 5′-TCCATCTGCAGCAC CAATCTTCGC-3′ and Vg-R; 5′-GCAACAGCCTTCATTCTGATGCCA 3′). The reaction was carried out in a real-time PCR machine (RealPlex^4, Eppendorf) by incubating at 95°C for 3 min, then 40 cycles of 95°C for 5 s and 60°C for 30 s. The melting curve was performed at 95°C for 3 min, then 60°C for 30 s and 95°C for 3 min. Reference genes including elongation factor 1 alpha (EF1α), elongation factor 2, tubulin and calreticulin were analysed for appropriate reference gene by using Normfinder software (data not shown). EF1α was selected as a reference gene to normalize *Vg* expression using EF1α-specific primers (EF1α-F; 5′-GAACTGCT GACCAAGATCGACAGG-3′ and EF1α-R; 5′-GAGCATACTGTTG GAAGGTCTCCA-3′). The PCR products of both *Vg* and *EF1α* were purified by gel extraction kit (QIAGEN), and serial dilutions of the known amount of *Vg* and *EF1α* PCR product (10^2–10^8 copies) were used as a template to construct a standard curve. The copy number of *Vg* and *EF1α* in each sample was calculated by comparing its C_t value with that of the standard curve. The relative expression of *Vg* to *EF1α* was calculated from *Vg* copies normalized with *EF1α* copies. Each sample was amplified in duplicate.

2.4 | Effect of rGIH on calcium ionophore (A23187)-induced release of putative gonad-stimulating factor (GSF) from thoracic ganglia

Ovary explant culture was used as a system to determine the effect of rGIH on GSF-induced oocyte growth stimulation. To prepare the ovary explants, the ovary freshly isolated from previtellogenic female shrimp was excised into small pieces (approximately 3 × 3 × 3 mm^3), washed in M199 medium (Gibco) containing 1000 U and 2000 U penicillin and streptomycin and modified salts (232 mM NaCl, 15 mM $MgSO_4$, 10 mM KCl, 16 mM $CaCl_2$, 1 mM $NaHCO_3$ and 50 mM Hepes pH 7.4). The previtellogenic ovary explants were divided into two groups; the ovary explants that were cultured alone and the ovary explants that were cultured with thoracic ganglia from vitellogenic shrimp. Both groups were subjected to four treatments by the addition of different substances as follows: the first treatment was added with PBS, the second and third treatments with 200 ng of rGIH and 5 μM calcium ionophore A23187 (Sigma), respectively, and the last treatment with the combination of 200 ng of rGIH and 5 μm A23187 in 1 ml of culture medium containing 100 U penicillin/streptomycin in a 24-well plate (three pieces of the explants per well). The explants in all treatments were incubated at 28°C for 2 days. The oocyte growth in the ovary explants was determined by measuring the diameter of oocytes after haematoxylin and eosin staining. Briefly, the ovary pieces were fixed in 20 volumes of Davidson's fixative (33% v/v ethanol, 22% v/v formaldehyde, 11% v/v acetic acids) for 48 hr before processed by paraffin embedding and sectioning into tissue section of 5 μm thickness. The tissue sections were subsequently stained by haematoxylin and eosin, and the image was visualized and photographed under a light microscope. The oocyte growth was determined by two parameters, oocyte diameter and percentage of perinucleolar oocytes (%PO). The diameter of oocytes was measured as previously described (Ayub & Ahmed, 2002; Yano, 1988) using AxioVision Rel 4.8 program (Carl Zeiss). The PO was identified as the oocyte with diameter of approximately 30–70 μm, and having nucleolus located at the nuclear envelop. The %PO was calculated by the number of perinucleolar oocytes × 100 divided by total number of oocyte cells in the ovary section.

2.5 | Effect of rGIH on oocyte growth in ovary explant culture

Ovary explant culture was prepared as described above, and then three pieces of the explant were cultured in 1 ml of well-mixed 200 ng of rGIH in the culture medium supplemented with 100 U penicillin/streptomycin in each well of a 24-well plate. The ovary explant culture was then incubated at 28°C for 2 days. The ovary pieces were proceeded to oocyte growth determination as described above.

2.6 | Statistical analysis

The data were statistically analysed by ANOVA using SPSS program (IBM, SPSS statistics 20). The time course of *Vg* expression in rGIH-treated primary ovarian cells was analysed by two-way ANOVA with Bonferroni's test for pairwise comparison. Oocyte growth was analysed by randomized complete block design (RCBD) one-way ANOVA or two-way ANOVA due to variation of individual shrimp used for ovarian explant preparation.

3 | RESULTS

3.1 | Verification of inhibitory effect of recombinant GIH on Vg expression

The 97 amino acid residues of the mature GIH used for rGIH expression were showed in Figure 1a. The rGIH was expressed from the yeast, *P. pastoris*, and subsequently purified following the purification procedure of Treerattrakool et al., 2014) (Figure 1b). In addition, the rGIH was also proven by Western blot analysis with anti-GIH mAb (Treerattrakool et al., 2014). The purified rGIH was validated for its activity to suppress *Vg* synthesis in vitro. The *Vg* mRNA level was significantly reduced by approximately 50% in rGIH-treated ovarian cells at 24 hr after the treatment compared with that in PBS-treated cells. Furthermore, the decrease of *Vg* expression in the rGIH-treated cells was prolonged to 48 hr after treatment (Figure 2).

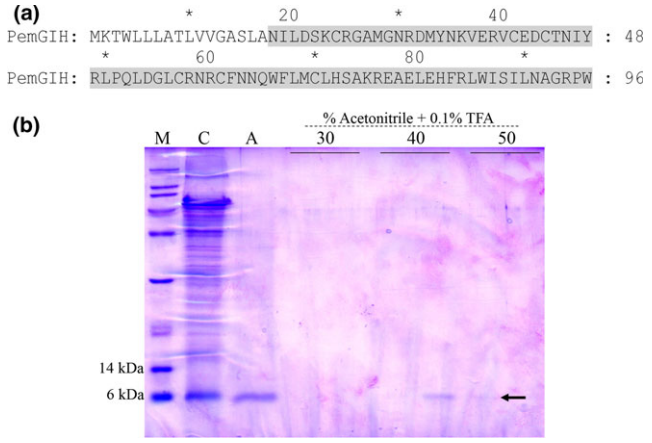

FIGURE 1 rGIH amino acid sequence and its purification. (a) The amino acid sequences corresponding to *Penaeus monodon*'s mature GIH (GenBank Accession No. ABG33898) used for the expression of rGIH in *Pichia pastoris* are shaded in grey. (b) The SDS-PAGE was used to determine a purification pattern of rGIH peptide. The "C" and "A" represent culture medium containing rGIH and 40%–50% w/v saturated ammonium sulphate precipitated rGIH respectively. The precipitated rGIH was purified via Sep-Pak C-18 column, and it was eluted with different concentrations (30%–50% v/v) of acetonitrile containing 0.1% TFA. An arrow indicated the purified rGIH eluted in the fraction of 40%–50% acetonitrile. The "*" indicates the position of amino acid at 10 residues interval

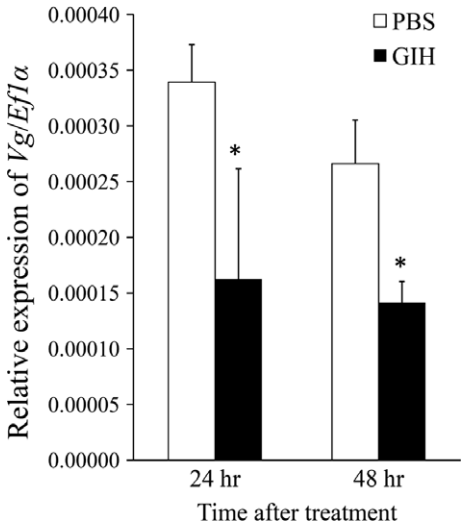

FIGURE 2 Validation of rGIH activity on *Vg* inhibition in *Penaeus monodon*'s primary ovarian cells. The primary ovarian cells prepared from previtellogenic ovary of *P. monodon* were treated with 200 ng of rGIH or buffer for 24 hr and 48 hr ($n = 6$). *Vg* expression was determined by relative quantification real-time PCR. Bars and error bars represent mean and SEM respectively. Asterisk is significant difference between group at $p < .05$ by Bonferroni's test

3.2 | Calcium ionophore induces the release of putative gonad-stimulating factor (GSF) from thoracic ganglia

To study whether the release of putative GSF from thoracic ganglia is under the influence of GIH or not, the ex vivo induction of GSF release was confirmed by a pharmaceutical agent, calcium ionophore (A23187). The ovary explants were incubated, either alone or together with thoracic ganglia explants, in the culture medium containing 5 μM A23187 for 2 days. The result showed that the percentage of PO (%PO) was significantly increased from 48.4 ± 2.8% in the PBS-treated ovary explants that were culture with thoracic ganglia to 64.7 ± 5.8% in the A23187-treated cocultured explants. By contrast, no significant difference of % PO was observed between the PBS and A23187 treatment in the ovary explants that were cultured alone in the absence of thoracic ganglia (Figure 3a). Similarly, oocyte diameter was significantly increased in A23187-treated ovary explants that were cultured with thoracic ganglia (37.7 ± 1.7 μm) compared with that of the PBS-treated explants (31.1 ± 0.8 μm), whereas no significant change in oocyte diameter was observed between the two treatments when the ovary explants were cultured alone (Figure 3b). The result suggested that A23187 can stimulate the release of GSF from thoracic ganglia and therefore can be used as the assay system to study the effect of GIH on GSF release from thoracic ganglia.

3.3 | Effect of rGIH on the release of putative GSF from thoracic ganglia

The influence of GIH on stimulation of GSF release was investigated in the ovary explant culture using A23187 to induce the release of putative GSF from thoracic ganglia. Similar to the result of previous experiment, the addition of A23187 did not affect oocyte growth when the ovary explants were cultured alone, but significantly increased %PO and oocyte diameter of the ovary explants that were incubated with thoracic ganglia (Figure 4, light grey bar). However, when 200 ng of rGIH was added to the A23187-treated culture of ovary explants with thoracic ganglia, similar level of oocyte growth stimulation (Figure 4, black bar) to that without rGIH was still obtained implying that the release of GSF from thoracic ganglia by A23187 was independent of GIH activity. Interestingly, incubation of the ovarian explants alone with rGIH or rGIH mixed with A23187 (Figure 4, dark grey and black bars, respectively) could stimulate oocyte growth regardless of the vitellogenin-inhibiting function of rGIH. For example, %PO was increased from 12.4 ± 1.8% in the PBS-treated ovary explants to 16.7 ± 1.5% and 16.2 ± 1.6% in ovary explants that were incubated with rGIH only and with both rGIH and A23187 respectively (Figure 4a). Similarly, a significant increase in oocyte diameter was also induced by the incubation with rGIH, either alone or in the presence of A23187 (Figure 4b).

3.4 | Confirmation of oocyte growth stimulation activity of rGIH

To verify the effect of rGIH on oocyte growth, the ovary explant culture was incubated either with rGIH or with PBS for 48 h, and oocyte growth as determined by %PO and oocyte diameter of both groups were compared. The result in Figure 5 showed that the %PO (26.3 ± 2.3%) and oocyte diameter (26.0 ± 0.7 μm) of the ovary

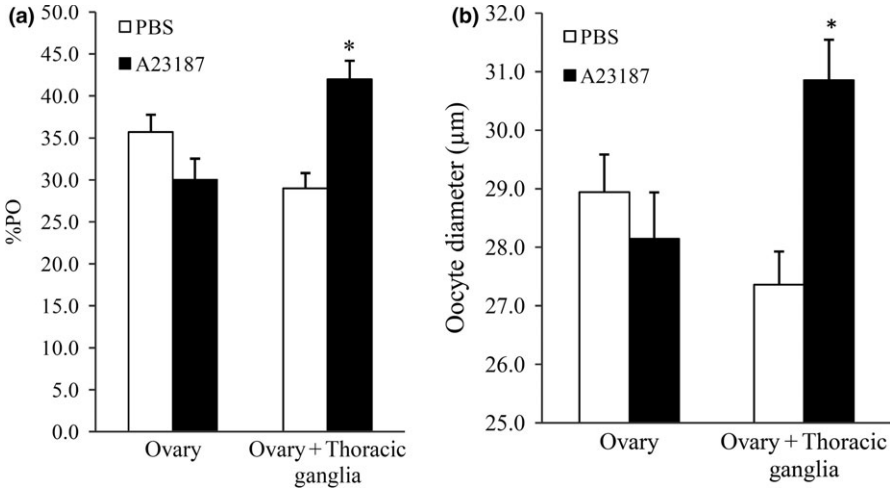

FIGURE 3 Effect of A23187-induced putative GSF release from thoracic ganglia on oocyte growth. The ovary explants of previtellogenic shrimp that were cultured alone or with thoracic ganglia were treated with 5 μm A23187 or PBS for 48 hr. The oocyte growth in the ovary explants of each treatment was determined by % PO (a) and oocyte diameter measurement (b). Bars and error bars represent mean and SEM of two independent experiments respectively. Asterisk is significant difference within a group at $p < .05$ by Bonferroni's test

explants were significantly increased after 48 hr incubation with rGIH when compared with those in the PBS-treated explants (17.7 ± 2.2%PO and 23.2 ± 0.7 μm oocyte diameter respectively). The representative of ovary sections from rGIH and PBS-treated ovarian explants indicating PO and CNO was shown in Figure 5c. This result affirms the activity of rGIH to stimulate oocyte growth that was observed in the previous experiment.

4 | DISCUSSION

Several factors are known to mediate hormonal control of ovarian development in shrimp such as peptide hormones, steroid hormones and neurotransmitters (Subramoniam, 2011). Gonad-inhibiting hormone (GIH), a neuropeptide belonging to the crustacean hyperglycemic hormone (CHH) family, that was mainly expressed at X-organ sinus gland complex in crustacean eyestalk is well-studied in its function to inhibit vitellogenin (Vg) synthesis (Chen et al., 2014; Edomi et al., 2002; Treerattrakool et al., 2008). Recently, a recombinant GIH of *P. monodon* (rGIH) was successfully expressed as a secreted protein in the yeast *P. pastoris* and exhibited a dose-dependent *Vg* inhibition activity where about 50% inhibition of *Vg* expression in primary ovarian cells was achieved within 24 hr when supplied with 11.5 nM (approximately 100 ng/ml) rGIH. In addition, a monoclonal antibody against rGIH could markedly compromise the inhibitory function of rGIH on *Vg* expression (Treerattrakool et al., 2014). Our result here consistently confirmed the suppression of *Vg* expression in primary ovarian cells after treated with 200 ng/ml rGIH; this suppression could be prolonged to 48 hr (Figure 1).

One mechanism of action of GIH on Vg inhibition has been hypothesized to occur through the inhibition of putative gonad-stimulating factor (GSF) synthesis and/or secretion (Nagaraju, 2011). In vertebrates, induction of vertebrate gonadotrophin secretion including follicle-stimulating hormone (FSH) and luteinizing hormone (LH) from pituitary gland was demonstrated in vitro by a pharmaceutical agent, a calcium ionophore (A23187) (Chuknyiska, Blackman & Roth, 1987; Kile & Nett, 1994; Simpson, Vernom, Jones & Rush, 1989). Similarly, A23187 was also able to induce the release of

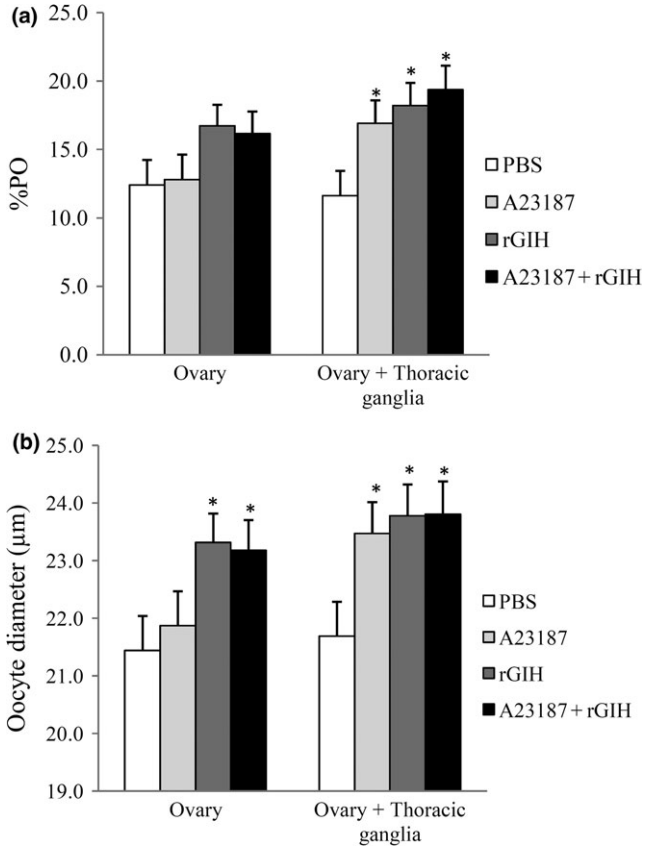

FIGURE 4 Effect of rGIH on A23187-induced putative GSF from thoracic ganglia. The ovary explants of previtellogenic shrimp cultured either in the presence or the absence of thoracic ganglia were treated with PBS, A23187, rGIH and rGIH mixed with A23187 for 48 hr. Oocyte growth activity, % PO (a) and oocyte diameter (b), was used to determine the effect of putative GSF secretion. Bars and error bars represent mean and SEM ($n = 5$) respectively. Asterisks represent significant difference between groups compared to PBS treatment at $p < .05$ by RCBD one-way ANOVA, and pairwise comparison by least significant difference test

putative GSF from brain and thoracic ganglia in the crayfish, *P. clarkii* (Sarojini et al., 1995). Our study showed that A23187 treatment could stimulate oocyte growth in the ovary explant of *P. monodon*

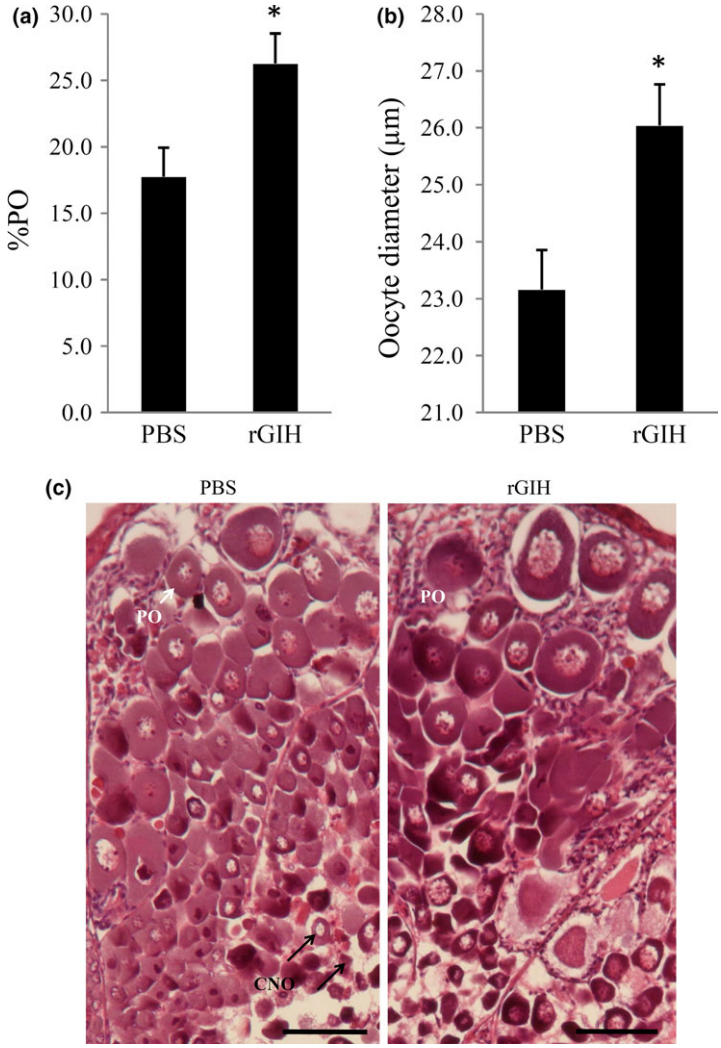

FIGURE 5 Effect of rGIH on oocyte growth in *Penaeus monodon*'s ovary explants. The ovary explants of previtellogenic shrimp treated with 200 ng of rGIH or PBS for 48 hr were determined for their oocyte growth by % PO (a) and oocyte diameter measurement (b). Bars and error bars represent mean and SEM ($n = 5$) respectively. Asterisks depict significant difference between group as analysed by at $p < .05$ by RCBD one-way ANOVA. (c) Haematoxylin and eosin staining of ovarian section after treatment with rGIH. The ovary explants culture treated with rGIH or PBS was fixed, processed, sectioned and stained by H&E. Chromatin nucleolar oocyte (CNO) and perinucleolar oocyte (PO) are depicted by black and white arrows respectively. The rGIH-treated ovary explants contained higher proportion of PO with longer diameter than those treated with PBS. Bars indicate scale of 50 μM

only when it was cultured with thoracic ganglia, but not when the ovary explant was cultured alone (Figure 3a,b). This suggested that A23187, by itself, did not affect oocyte growth, but was able to induce the release of putative GSF from thoracic ganglia, which subsequently stimulated oocyte growth in ovary explants. Thus, we further investigated whether GIH regulates putative GSF release from thoracic ganglia by A23187 induction.

The recombinant GIH (rGIH) protein was produced as a secreted protein from *P. pastoris* and exhibited in vitro activity in inhibition of *Vg* expression in primary ovarian cells (Figure 2) similar to that reported previously by Treerattrakool et al. (2014). Therefore, the rGIH in this study was functionally active. To ensure that the effect of rGIH on the inhibition of GSFs release, if there is any, would be clearly detected, the doubled concentration of the rGIH compared to the previous study (Treerattrakool et al., 2014) was used. The addition of rGIH to the A23187-treated ovary explants cultured with thoracic ganglia gave comparable level of oocyte growth to that without rGIH (Figure 4a,b) suggesting that rGIH may not suppress *Vg* expression through interfering with the release of GSF from thoracic ganglia as previously hypothesized. In addition, incubation with only rGIH in the absence of A23187 was sufficient to induce oocyte growth in the ovary explants that were cultured with thoracic ganglia and, more interestingly, even in the ovary explants alone (Figure 4a,b). Our result here suggested that GIH itself may also contain an unconventional oocyte growth stimulating activity.

We further confirmed the stimulatory activity of rGIH on oocyte growth by culturing ovary explants from previtellogenic *P. monodon* in the presence of rGIH for 48 hr. The result consistently showed that rGIH could induce oocyte growth in the treated ovary explants (Figure 5a,b). A number of studies have suggested the existence of substances with gonad-stimulating activity in brain and thoracic ganglia of crustaceans. For instances, an increase of Vg level in the haemolymph of kuruma prawn, *P. japonicas* was induced by injection of thoracic ganglia extract (Yano, 1992). Vitellogenesis in the shrimp *Paratya compressa* was also stimulated by the extract from brain and thoracic ganglia (Takayanagi et al., 1986). Because GIH expression was not limited only to the eyestalk, but it was also expressed in brain and thoracic ganglia in several crustaceans such as *P. monodon*, *L. vannamei* and *N. norvegicus* (Chen et al., 2014; Edomi et al., 2002; Treerattrakool et al., 2008), our result thereby suggested that GIH might be one of the

factors in thoracic ganglia that is responsible for oocyte growth stimulation in previtellogenic ovary. At previtellogenic stage, high level of GIH (approximately 15 ng/ml in average) was detected in the haemolymph and significantly declined in vitellogenic stage in *P. monodon* and the lobster, *H. americanus* (De Kleijn et al., 1998; Urtgam et al., 2015). This reflects the important function in vitellogenesis inhibition during previtellogenic phase of ovarian development in crustaceans. On the other hand, the abundance of GIH in previtellogenic stage suggests that the hormone may be involved in oocyte growth and follicular development that are primarily required before yolk synthesis in the early stage of ovarian development. Our result agreed well with this assumption and, thus, demonstrated an in vitro dual function of GIH that is required during previtellogenic stage; these should be further confirmed by in vivo study in the shrimp. The suppression of *Vg* synthesis at this stage may be necessary to allow oocyte growth and prepare for vitellogenin accumulation in higher vitellogenic stages.

The release of putative GSF from its synthesis and/or storage sites was known to be regulated by neurotransmitters such as dopamine and serotonin. Sarojini, Nagabhushanam and Fingerman (1996) demonstrated in *P. clarkii* that serotonin stimulated a release of putative GSF to induce oocyte growth whereas dopamine repressed it (Sarojini et al., 1996). Whether or not the stimulation of oocyte growth by GIH is under control of these neurotransmitters is not known. Therefore, the detailed mechanism of GIH regulation and its receptor at potential targets such as ovary and thoracic ganglia remains to be elucidated to unravel the control of ovarian development in shrimp.

5 | CONCLUSION

Our study revealed that GIH did not affect the release of putative GSF from thoracic ganglia by A23187 but, by itself, exhibited oocyte growth stimulation. This is the first report of the dual role played by GIH during previtellogenic stage of ovarian development, that is stimulation of oocyte growth and inhibition of *Vg* expression in vitro, and needs to be verified by in vivo study. This knowledge will benefit hormonal manipulation scheme for future improvement of reproduction in female shrimp.

ACKNOWLEDGMENTS

The authors would like to thank Miss Somjai Wongtripop (Shrimp Genetics Improvement Center, Surat Thani, Thailand) for providing the shrimp samples. We are thankful to Ms. Chawewan Chimwai, Mrs. Suparp Hongthong and Ms. Pannee Thongboonsong for their technical assistance. This work was supported by Thailand Research Fund (BRG5880005 to AU, DBG5980011 to SP), Mahidol University Research Grant and the Office of the Higher Education Commission and Mahidol University under the National Research Universities Initiative. PS is the recipient of the student fellowship by the Royal Golden Jubilee Ph.D. Program.

REFERENCES

Ayub, Z., & Ahmed, M. (2002). A description of the ovarian development stages of penaeid shrimps from the coast of Pakistan. *Aquaculture Research*, *33*, 767–776.

Chang, E. S. (2001). Crustacean hyperglycemic hormone family: Old paradigms and new perspectives. *American Zoologist*, *41*, 380–388.

Charniaux-Cotton, H. (1985). Vitellogenesis and its control in malacostracan crustacea. *American Zoologist*, *25*, 197–206.

Chen, T., Zhang, L. P., Wong, N. K., Zhong, M., Ren, C. H., & Hu, C. Q. (2014). Pacific white shrimp (*Litopenaeus vannamei*) vitellogenesis-inhibiting hormone (VIH) is predominantly expressed in the brain and negatively regulates hepatopancreatic vitellogenin (VTG) gene expression. *Biology of Reproduction*, *90*(47), 1–10.

Chuknyiska, R. S., Blackman, M. R., & Roth, G. S. (1987). Ionophore A23187 partially reverses LH secretory defect of pituitary cells from old rats. *American Journal of Physiology*, *253*, 233–237.

De Kleijn, D. P. V., Jansen, K., Waddy, S., Hegeman, R., Lai, W., Martens, G., & Van Herp, F. (1998). Expression of the crustacean hyperglycaemic hormones and the gonad-inhibiting hormone during the reproductive cycle of the female American lobster *Homarus americanus*. *Journal of Endocrinology*, *156*, 291–298.

De Kleijn, D. P. V., Sleutels, F. J. G. T., Martens, G. J. M., & Van Herp, F. (1994). Cloning and expression of mRNA encoding prepro-gonad-inhibiting hormone (GIH) in the lobster *Homarus americanus*. *FEBS Letter*, *353*, 255–258.

Edomi, P., Azzoni, E., Mettulio, R., Pandolfelli, N., Ferrero, E. A., & Giulianini, P. G. (2002). Gonad-inhibiting hormone of the Norway lobster (*Nephrops norvegicus*): cDNA cloning, expression, recombinant protein production, and immunolocalization. *Gene*, *284*, 93–102.

Kile, J. P., & Nett, T. M. (1994). Differential secretion of follicle-stimulating hormone and luteinizing hormone from ovine pituitary cells following activation of protein kinase A, protein kinase C, or increased intracellular calcium. *Biology of Reproduction*, *50*, 49–54.

Nagaraju, G. P. C. (2011). Reproductive regulators in decapod crustaceans: An overview. *Journal of Experimental Biology*, *214*, 3–16.

Sarojini, R., Nagabhushanam, R., & Fingerman, M. (1995). A neurotransmitter role for red-pigment-concentrating hormone in ovarian maturation in the red swamp crayfish *Procambarus clarkii*. *Journal of Experimental Biology*, *198*, 1253–1257.

Sarojini, R., Nagabhushanam, R., & Fingerman, M. (1996). In vitro inhibition by dopamine of 5-hydroxytryptamine-stimulated ovarian maturation in the red swamp crayfish, *Procambarus clarkii*. *Experientia*, *52*, 707–709.

Simpson, W. G., Vernom, M. E., Jones, H. M., & Rush, M. E. (1989). The role of calcium in gonadotropin-releasing hormone induction of follicle-stimulating hormone release by the pituitary gonadotrope. *Endocrine Research*, *15*, 355–373.

Subramoniam, T. (2011). Mechanisms and control of vitellogenesis in crustaceans. *Fisheries Science*, *77*, 1–21.

Takayanagi, H., Yamamoto, Y., & Takeda, N. (1986). An ovary-stimulating factor in the shrimp, *Paratya compressa*. *Journal of Experimental Zoology*, *240*, 203–209.

Treerattrakool, S., Boonchoy, C., Urtgam, S., Panyim, S., & Udomkit, A. (2014). Functional characterization of recombinant gonad-inhibiting hormone (GIH) and implication of antibody neutralization on induction of ovarian maturation in marine shrimp. *Aquaculture*, *428–429*, 166–173.

Treerattrakool, S., Panyim, S., Chan, S. M., Withyachumnarnkul, B., & Udomkit, A. (2008). Molecular characterization of gonad-inhibiting hormone of *Penaeus monodon* and elucidation of its inhibitory role in vitellogenin expression by RNA interference. *FEBS Journal*, *275*, 970–980.

Tseng, D. Y., Chen, Y. N., Kou, G. H., Lo, C. F., & Kuo, C. M. (2001). Hepatopancreas is the extraovarian site of vitellogenin synthesis

in black tiger shrimp, *Penaeus monodon*. *Comparative Biochemistry and Physiology Part A: Molecular & Integrative Physiology*, *129*, 909–917.

Urtgam, S., Treerattrakool, S., Roytrakul, S., Wongtripop, S., Prommoon, J., Panyim, S., & Udomkit, A. (2015). Correlation between gonad-inhibiting hormone and vitellogenin during ovarian maturation in the domesticated *Penaeus monodon*. *Aquaculture*, *437*, 1–9.

Von Stetina, J. R., & Orr-Weaver, T. L. (2011). Developmental control of oocyte maturation and egg activation in metazoan models. *Cold Spring Harbor Perspectives in Biology*. https://doi.org/101101/cshperspect.a005533.

Yano, I. (1988). Oocyte development in the kuruma prawn *Penaeus japonicus*. *Marine Biology*, *99*, 547–553.

Yano, I. (1992). Effect of thoracic ganglion on vitellogenin secretion in kuruma prawn, *Penaeus japonicus*. *Bulletin National Research Institute of Aquaculture*, *21*, 9–14.

How to cite this article: Sathapondecha P, Panyim S, Udomkit A. In vitro study of a putative role of gonad-inhibiting hormone in oocyte growth stimulation in *Penaeus monodon*. *Aquac Res*. 2017;00:1–8. https://doi.org/10.1111/are.13407

Manuscript Details

Manuscript number	DCI_2018_282
Title	Suppression of Argonautes compromises viral infection in Penaeus monodon
Article type	Full Length Article

Abstract

Argonaute (Ago) proteins, the catalytic component of an RNA-induced silencing complex (RISC) in RNA interference pathway, function in diverse processes, especially in antiviral defense and transposon regulation. So far, cDNAs encoding four members of Argonaute were found in Penaeus monodon (PmAgo1-4). Two PmAgo proteins, PmAgo1 and PmAgo3 shared high percentage of amino acid identity to Ago1 and Ago2, respectively in other Penaeid shrimps. Therefore, the possible roles of PmAgo1 and PmAgo3 in shrimp antiviral immunity were characterized in this study. The level of PmAgo1 mRNA expression in shrimp hemolymph was stimulated upon YHV challenge, but not with dsRNA administration. Interestingly, silencing of either PmAgo1 or PmAgo3 using sequence-specific dsRNAs impaired the efficiency of PmRab7-dsRNA to knockdown shrimp endogenous PmRab7 expression. Inhibition of yellow head virus (YHV) replication and delayed mortality rate were also observed in both PmAgo1- and PmAgo3-knockdown shrimp. In addition, silencing of PmAgo3 transcript, but not PmAgo1, revealed partial inhibition of white spot syndrome virus (WSSV) infection and delayed mortality rate. Therefore, our study provides insights into PmAgo1and PmAgo3 functions that are involved in a dsRNA-mediated gene silencing pathway and play roles in YHV and WSSV replication in the shrimp.

Keywords	RNA interference; yellow head virus; white spot syndrome virus; double-stranded RNA; shrimp
Taxonomy	Gene Silencing, Molecular Biology
Manuscript category	Invertebrate

Corresponding Author	Apinunt Udomkit
Corresponding Author's Institution	Mahidol University
Order of Authors	Teerapong Ho, Sakol Panyim, Apinunt Udomkit
Suggested reviewers	Anchalee Tassanakajon, Maria Carla Saleh, Gregory Warr, Craig Browdy

Submission Files Included in this PDF

File Name [File Type]

cover letter.docx [Cover Letter]

Highlights.docx [Highlights]

Manuscript-27-6-2018.doc [Manuscript File]

Figure 1.jpg [Figure]

Figure 2.jpg [Figure]

Figure 3.jpg [Figure]

Figure 4.jpg [Figure]

Figure 5.jpg [Figure]

Figure 6.jpg [Figure]

Figure S1.pdf [Figure]

Figure S2.pdf [Figure]

To view all the submission files, including those not included in the PDF, click on the manuscript title on your EVISE Homepage, then click 'Download zip file'.

Suppression of Argonautes compromises viral infection in *Penaeus monodon*

Teerapong Ho[a], Sakol Panyim[a,b] and Apinunt Udomkit [a,*]

[a]*Institute of Molecular Biosciences, Mahidol University, Phutthamonthon 4 Road, Salaya, Nahkon Pathom 73170, Thailand*

[b]*Department of Biochemistry, Faculty of Science, Mahidol University, Rama VI Road, Bangkok 10400, Thailand*

[*] Corresponding author

Tel: +(66) 2 441 9003-7 ext 1236 Fax: +(66) 2 441 1013

E-mail: apinunt.udo@mahidol.ac.th

Abstract

Argonaute (Ago) proteins, the catalytic component of an RNA-induced silencing complex (RISC) in RNA interference pathway, function in diverse processes, especially in antiviral defense and transposon regulation. So far, cDNAs encoding four members of Argonaute were found in *Penaeus monodon* (*PmAgo1-4*). Two PmAgo proteins, PmAgo1 and PmAgo3 shared high percentage of amino acid identity to Ago1 and Ago2, respectively in other Penaeid shrimps. Therefore, the possible roles of PmAgo1 and PmAgo3 in shrimp antiviral immunity were characterized in this study. The level of *PmAgo1* mRNA expression in shrimp hemolymph was stimulated upon YHV challenge, but not with dsRNA administration. Interestingly, silencing of either *PmAgo1* or *PmAgo3* using sequence-specific dsRNAs impaired the efficiency of *PmRab7*-dsRNA to knockdown shrimp endogenous *PmRab7* expression. Inhibition of yellow head virus (YHV) replication and delayed mortality rate were also observed in both *PmAgo1*- and *PmAgo3*-knockdown shrimp. In addition, silencing of *PmAgo3* transcript, but not *PmAgo1*, revealed partial inhibition of white spot syndrome virus (WSSV) infection and delayed mortality rate. Therefore, our study provides insights into *PmAgo1*and *PmAgo3* functions that are involved in a dsRNA-mediated gene silencing pathway and play roles in YHV and WSSV replication in the shrimp.

Keywords

RNA interference; yellow head virus; white spot syndrome virus; double-stranded RNA; shrimp

1. Introduction

Multiple innate defenses including cellular and humoral immune reactions and RNA interference (RNAi) of invertebrates were wildly known as host defense mechanisms against microbial infection. In shrimp, discoveries of several molecules related to both cellular (encapsulation, coagulation, and melanization) and humoral (Toll, Immune deficiency (IMD) and JAK/STAT pathway) immune reactions reveal the existence of innate immune activities to fight against invading pathogens (Borregaard et al., 2000; Hoffmann et al., 1999). In addition, RNAi is also known as one of the potent antiviral immunities in many organisms such as mammals, plants, insects and shrimp (Robalino et al., 2004; Wang et al., 2006; Zambon et al., 2006). The RNAi pathway is triggered by different classes of small regulatory RNAs originating from either endogenous transcripts or exogenous dsRNAs such as small-interfering RNA (siRNA), microRNA (miRNA) and piwi-interacting RNA (piRNA). These small RNAs serve as guide sequences to direct the formation of an RNA-induced silencing complex (RISC), which contains an Argonaute (Ago) family protein as the catalytic core, to regulate viral replication by specific cleavage of the corresponding viral mRNA or translation inhibition (Aliyari et al., 2008).

Regarding their structural features, four domains are identified in a bilobate architecture of Ago proteins; one lobe with N and PAZ domains and the other lobe with MID and PIWI domains. Based on crystal structure analysis, the N domain takes part in unwinding of small RNA duplex (Kwak and Tomari, 2012), while a specific binding pocket on the PAZ domain binds to the 3' end of small RNA duplex (Lingel et al., 2003; Ma et al., 2004). The 5' phosphate of small RNAs is held onto the Ago protein by the MID domain (Kiriakidou et al., 2007; Till et al., 2007). A catalytic motif Asp-Asp-His (DDH) in the PIWI domain is responsible for the endonucleolytic activity (Song et al., 2004; Wang et al., 2008).

Multiple members of the Argonaute family exist in a wide range of organisms and are highly conserved among species. Ago proteins can be separated according to their phylogenetic relationships into Ago and Piwi subfamilies (Chen and Meister, 2005; Hammond et al., 2000; Janowski et al., 2006; Leebonoi et al., 2014; Yigit et al., 2006). Members of the Ago subfamily mediate post-transcriptional gene regulation by associating with either miRNA or siRNA. Piwi subfamily proteins are germ cell specific Argonautes associating with piRNAs, which behave as a small RNA-based immune system to safeguard genome integrity against transposon movement in germ cells and to control spermatogenesis and germ cell differentiation (Kalmykova et al., 2005; Kuromochi et al., 2004). In addition, another class of Argonaute proteins, a worm-specific Argonaute (WAGO), was exclusively found in the nematodes where they play a role in RNAi pathway to mediate a variety of cellular processes (Yigit et al., 2006). Numbers of Argonaute genes are different among organisms, ranging from a single member in *Schizosaccharomyces pombe* to twenty-seven members in *Caenorhabditis elegans* (Hock and Meister, 2008). So far, Ago2 of *Drosophila* and human were demonstrated to possess slicer activity (Meister et al., 2004; Miyoshi et al., 2005) and mediate antiviral defense via RNAi cleavage mechanism (Chen et al., 2011a; Van et al., 2006).

To date, at least two Ago subfamily members were identified and characterized in Penaeid shrimps. In *Litopenaues vannamei*, two Argonaute genes, *LvAgo1* and *LvAgo2* were identified; only *LvAgo2* was involved in siRNA mediated post-transcriptional gene silencing (Chen et al., 2011b; Labreuche et al., 2010). Likewise, *MjAgo1* and *MjAgo2* were found in *Masupenaeus japonicus*. MjAgo1 play important role in antiviral response in the shrimp (Huang and Zhang, 2012), while MjAgo2 acts as a key protein in viral siRNA biogenesis and function (Huang and Zhang, 2013). These studies suggest that Argonaute 2 proteins were

essential for the functional siRNA-associated RISC and play a role in antiviral defense via siRNA-mediated viral mRNA degradation in the shrimp.

Interestingly, cDNAs encoding four types of the Ago subfamily proteins were reported in the black tiger shrimp, *Penaeus monodon* (*PmAgo1-4*). From phylogenetic analysis, PmAgo1 is clustered in the same group with LvAgo1 and MjAgo1, and was demonstrated for its important function in effective RNAi pathway in the primary culture of lymphoid cells (Dechklar et al., 2008). PmAgo3 was classified into the same group of Argonaute 2 proteins in penaeid shrimp i.e. LvAgo2 and MjAgo2, and was shown to be involved in the pathway of dsRNA-mediated gene silencing (Phetrungnapha et al., 2013). In addition, PmAgo2 and PmAgo4 were classified in the same cluster, but located on a separate branch from PmAgo3. The expression of *PmAgo2* was responsive to both viral and bacterial infections, and was also activated upon dsRNA and ssRNA administration (Yang et al., 2014). All members of *PmAgos*, except *PmAgo4* are expressed ubiquitously in all shrimp tissues. Interestingly, *PmAgo4* displays a gonad-specific expression similar to that of the Piwi subfamily. The gonad-specific *PmAgo4* was suggested to be involved in the protection of shrimp genome against transposons invasion (Leebonoi et al., 2014). Although accumulating evidences have demonstrated that *PmAgos* could exhibit diverse-functions, no report has thus far indicated the actual function of Argonaute proteins for innate immunity in shrimp compared to model organisms such as *Drosophila*. In this study, we reported the possible involvement of *PmAgo1* and *PmAgo3*, homologs of DmAgo1 and DmAgo2, respectively in the mechanism of dsRNA-mediated gene silencing. Moreover, the involvement of *PmAgo1* and *PmAgo3* in shrimp antiviral immunity was also characterized. Functional analysis of *PmAgo1* and *PmAgo3* in the RNAi mechanism for shrimp antiviral defense will provide a basis for further development of effective strategies to control viral diseases in the economically important Penaeid shrimp.

2. Materials and methods

2.1 Animals

Live adolescent black tiger shrimp (approximately 10-15 g body weight) were purchased from shrimp farms around the central area of Thailand. They were first screened for yellow head virus (YHV) and white spot syndrome virus (WSSV) infection by RT-PCR as previously described (Attasart et al., 2009; Yodmuang et al., 2006). The virus-free shrimp were used in all experiments. Shrimp were gradually acclimatized to the laboratory condition in 10 ppt (parts per thousand) sea water with aeration for 2 days. They were also fed with commercial shrimp feed (CP, Thailand) twice a day for a few days before setting the experiment.

2.2 Viral stock preparation

To obtain fresh viral stock of YHV and WSSV, crude viruses were injected into the healthy virus-free shrimps. After 48 h, the hemolymph was drawn from moribund shrimp, and the viruses were then purified and determined for viral titer as previously described by Assavalapsakul et al., 2003. Appropriate dilutions of the viral stock (100-fold and 10-fold for YHV and WSSV, respectively) that gave complete mortality within 3 days post-infection (dpi) were freshly prepared before use.

2.3 Detection of gene transcripts by reverse transcription-polymerase chain reaction (RT-PCR)

Gills were dissected from individual shrimp and homogenized in TRI-REAGENT® (Molecular Research Center), while hemolymph was collected and subsequently mixed with TRI-REAGENT®. Total RNA was isolated according to the manufacturer's protocol. The concentration and purity of the extracted total RNA was examined by Nanodrop® ND-1000 spectrophotometer (Nanodrop Technologies). First strand cDNA was

reverse-transcribed from 1-2 µg of total RNA priming with PRT-oligo-dT_{16} primer (5'-CCGGAATTCAAGCTTCTAGAGGATCCTTTTTTTTTTTTTTT-3') by Impromp-II™ reverse transcriptase (Promega) using the following condition: 25 °C for 5 min, 42 °C for 60 min, and 70 °C for 15 min.

One microliter of the first strand cDNA was used as a template to examine mRNA expression. Multiplex-PCR with two primer pairs was applied to determine the expression of the mRNA of interest and *β-actin* mRNA (internal control) simultaneously. The reaction contains the standard components according to Tag DNA polymerase's protocol (Thermo scientific). *PmAgo1* transcript was amplified with PmAgo1-F and PmAgo1-R primers using the following condition: 94°C for 5 min, 2 cycles of 94°C for 1 min, 60°C for 1 min, 72°C for 1 min and additional 30 cycles of 94°C for 1 min, 55°C for 1 min, 72°C for 1 min (Phetrungnapha et al., 2013). The final extension was performed at 72°C for 7 min. Amplification of *PmAgo3*, *PmRab7*, *YHV-helicase (YHV-Hel)* and WSSV *vp28* mRNAs were carried out with specific primer pairs and specific conditions as previously described (Attasart et al., 2009; Ongvarrasopone et al., 2008; Phetrungnapha et al., 2013; Yodmuang et al., 2006). In the experiment, two *β-actin* PCR products of either 550 bp or 350 bp were amplified with the same forward primers (Actin-F) and different reverse primers, Actin-R or Actin-R2, respectively. The oligonucleotide sequences of Actin primers and specific conditions are previously described by Posiri et al., 2013.

2.4 Double-stranded RNA (dsRNA) production

The hair-pin dsRNA precursor was produced by *in vivo* bacterial expression system as described by Ongvarrasopone et al., 2007. The recombinant plasmids pET17b-st-*PmAgo1* (previously construct in our laboratory), pET17b-st-*PmAgo3* (Phetrungnapha et al., 2013), pET17b-st-*PmRab7* (Ongvarrasopone et al., 2008) and pET3a-st-*GFP* (kindly provided by Asst. Prof.Witoon Tirasophon) harboring the cassette for producing the hair-pin dsRNA of

corresponding genes were used to transform ribonuclease III-deficient *Escherichia coli* strain HT115 (DE3). The expression of hair-pin dsRNAs were induced with 0.4 mM IPTG for 4 h with shaking. The hair-pin dsRNAs were extracted by ethanol extraction method (Posiri et al., 2013) before dissolving in 150 mM NaCl. The concentration and purity of the hair-pin dsRNAs were monitored by agarose gel electrophoresis and Nanodrop® ND-1000 spectrophotometer. The hair-pin dsRNAs were verified by RNase digestion assay as described previously (Posiri et al., 2013).

2.5 Analysis of *PmAgo1 expression* in response to dsRNA or virus injection

Alteration in *PmAgo*1 transcript level in shrimp hemolymph was investigated upon either dsRNA or viral injections. Shrimp, approximately 10 g body weight (b.w.) were injected with *GFP*-dsRNA at 2.5 μg g^{-1} b.w. or challenged with 50 μl of the 10^{-2} dilution of YHV stock. After that, the hemolymph was collected from individual shrimp from each group (n = 5 and 10 for *GFP*-dsRNA and YHV injected group, respectively) at 0, 3, 6, 9, 12, 24, 36, 48 and 72 hours post-injection (hpi) for determination of *PmAgo1* mRNA expression by RT-PCR. Multiplex amplification of *PmAgo*1 and the internal control, *β-actin* transcripts was carried out by specific primers for each gene as described in 2.3, and the PCR products were subsequently analyzed by agarose gel electrophoresis. The Scion image analysis program was applied to quantify the band intensity of *PmAgo1* PCR product normalized with that of *β-actin*, and presented as mean ± standard error of mean (SEM) as relative expression levels of *PmAgo1*. The significant difference of relative *PmAgo1* expression level ($p < 0.05$) between each time point was analyzed by sample T-Test.

2.6 Investigation of the effect of *PmAgo1* and *PmAgo3* knockdown on the efficiency of RNAi

P. monodon (approximately 10 g b.w.) were injected with *PmAgo1*- or *PmAgo3*-dsRNA at 2.5 μg g^{-1} b.w. Either 150 mM NaCl or *GFP*-dsRNA was injected into shrimp as control groups. At 2 days-post injection, the hemolymph sample from shrimp in each group (n = 5) was collected to determine the expression levels of *PmAgo1* and *PmAgo3*. Subsequently, *PmRab7*-dsRNA was injected into *PmAgo* knocked-down shrimp at 0.63 μg g^{-1} b.w. to suppress *PmRab7* mRNA expression. Expression of *PmRab7* was determined by multiplex RT-PCR analysis as described in 2.3 at 0, 24, 48 and 72 h post *PmRab7*-dsRNA injection.

2.7 Biological assay for antiviral function of *PmAgo1* and *PmAgo3*

Shrimps (approximately 10 g b.w.) were injected with 25 μg g^{-1} b.w of *PmAgo1-, PmAgo3*- or *GFP*-dsRNA (5–10 shrimp per group). The hemolymph was collected at 48 h post-dsRNA injection to determine the transcript levels of *PmAgo1 and PmAgo3* as described in 2.3. The shrimp were subsequently injected with 50 μl of either the 100 fold diluted YHV or 10 fold diluted WSSV stock. Shrimps injected with 150 mM NaCl alone or NaCl following with viruses were used as negative and positive control groups, respectively. Multiplex RT-PCR analysis of *helicase* gene of YHV (*hel*) or *Vp28* gene of WSSV was performed to determine viral mRNA expression relative to that of *actin* in the shrimp at 0, 36, and 48 h post viral injection. PCR detection of WSSV genome was also performed to determine the level of WSSV genome. In addition, mortality of individual shrimp in each group was also recorded.

3. Results

3.1 Expression of *Ago1* in *P. monodon* upon YHV and *GFP*-dsRNA administration

Because the two isoforms of *Ago1* in *P. monodon*, *PemAgo1* (Dechklar et al., 2008) and *PmAgo1* (Unajak et al., 2006) contain the same coding sequences and cannot be differentiated by the RT-PCR detection, they were collectively referred to as *PmAgo1* in this study. In order to determine whether *PmAgo1* expression is correlated to its possible role in antiviral immunity and dsRNA mediated gene silencing as reported earlier, the expression of *PmAgo1* in response to YHV injection or GFP-dsRNA in the hemolymph of shrimp at various time points was determined by multiplex RT-PCR**.** Successful YHV infection was confirmed at 72 hpi by the detection of YHV *helicase* gene expression in the hemolymph of individual shrimp. The result in **Figure 1A** revealed that the expression levels of *PmAgo1* in YHV injected shrimp gradually increased from 0 hpi to the highest level of approximately 2-fold with significant difference ($p < 0.05$) at 9 hpi before continuously decreasing until 72 hpi. On the other hand, *PmAgo1* expression in shrimp hemolymph at every time point post-*GFP*-dsRNA injection was rather constant throughout the course of the experiment **(Figure 1B)**. These data demonstrated that *PmAgo1* expression was activated by YHV, but not by dsRNA administration.

3.2 Silencing of *PmAgo1* and *PmAgo3* by specific dsRNAs

To study the function of *PmAgo1* and *PmAgo3*, their expression was first suppressed by dsRNA-mediated gene silencing approach. The injection of *PmAgo1*-dsRNA significantly suppressed *PmAgo1* transcript level ($p < 0.05$) approximately 60% and 50% on day 2 and day 4 post-injection, respectively. More than 95% suppression of *PmAgo3* transcript was found in the hemolymph after one day post-*PmAgo3*-dsRNA injection, and this level of suppression lasted for at least 3 days (**Figure S1).** Moreover, *PmAgo1*-dsRNA did not have effect on *PmAgo3* expression and *vice versa* **(Figure 2A and 2B)**. Therefore, these dsRNAs were able to efficiently and specifically suppress *PmAgo1* and *PmAgo3* expression, and thus could be used for further functional analysis of both *PmAgo*s.

3.3 Impairment of RNAi-mediated *PmRab7* repression in *PmAgo*-knockdown shrimp

To investigate possible involvement of *PmAgo1* and *PmAgo3* in dsRNA-mediated RNAi pathway, the efficiency of *PmRab7*-dsRNA to repress shrimp endogenous *PmRab7* mRNA expression was studied in *PmAgo*-knockdown shrimp. The silencing of *PmAgo1* and *PmAgo3* expression in shrimp hemolymph was confirmed on day 2 after injected with corresponding dsRNAs compared with that in the control shrimp injected with NaCl or an unrelated *GFP*-dsRNA **(Figure S2)**, whereas the expression of *PmRab7* among each group was not dramatically different **(Figure 3; Day0)**. Shrimp in each group were then injected with *PmRab7*-dsRNA, and *PmRab7* expression was determined at 24 h interval after *PmRab7*-dsRNA injection. The result in **Figure 3** showed the complete suppression of *PmRab7* mRNA expression in both control groups (NaCl or *GFP*-dsRNA injection followed by *PmRab7*-dsRNA) at 24, 48 and 72 h post-*PmRab7*-dsRNA injection. Interestingly, the expression of *PmRab7* could be detected in *PmAgo1*- and *PmAgo3*-knockdown shrimp to a certain extent, but significantly different ($p < 0.05$) from the control shrimp, at all time-points from 24 to 72 h after injected with *PmRab7*-dsRNA indicating that dsRNA-mediated *PmRab7* suppression in *PmAgo*-knockdown shrimp was not as efficient as that in the control shrimp.

3.4 Effect of *PmAgo1 and PmAgo3* knockdown on viral infection in shrimp

To investigate the function of *PmAgo1 and PmAgo3* on virus infection, viral replication and shrimp mortality after YHV or WSSV challenge in *PmAgo*-knockdown shrimp were determined compared with that in the control groups (NaCl or *GFP*-dsRNA injcetion). The expression of *PmAgo1* and *PmAgo3* was knocked down by the injection of specific dsRNA two days before YHV challenge. The YHV-*hel* transcript could be detected in the hemolymph of both control groups at 48 hours post-YHV injection (hpi), but not in the hemolymph of *PmAgo1*-knockdown shrimp (**Figure 4A)**. In addition, the control shrimp that

had been injected with NaCl or GFP-dsRNA prior to YHV challenge started to die after 84 hpi, and the cumulative mortality reached 100% at 108 hpi, whereas the mortality of *PmAgo1*-knockdown shrimp was observed after 120 h post-YHV challenge and reached 100% at 138 hpi (**Figure 4B)**. Similarly, barely detectable level of YHV-*hel* and delayed cumulative mortality rate upon YHV challenge was also observed in *PmAgo3*-knockdown shrimp when compared with the control groups (**Figure 5A and 5B**). The detection of YHV-*hel* gene in the gill tissue from all dead shrimp confirmed that the shrimp were infected with the virus (**Figure 4C and 5**C).

Since WSSV is one of major viruses that cause high mortality in the shrimp, the role of *PmAgo1* and *PmAgo3* in WSSV infection was also investigated. The result showed that the levels of WSSV *vp28* transcript as well as WSSV genomic DNA in *PmAgo1*-knockdown shrimp infected with WSSV was comparable to that in both control groups that were injected with either NaCl or GFP-dsRNA prior to viral challenge **(Figure 6A and 6B)**. In addition, the cumulative mortality rate of the shrimp in all groups was not different; shrimp started to die after 36 h, and all were dead by 48 h **(Figure 6C)**. By contrast, lower levels of WSSV *vp28* transcript, notably with undetectable level in two out of five shrimp, and lower amounts of viral DNA genome in the pleopod were detected in *PmAgo3*-knockdown shrimp at 36 h post-WSSV infection compared with that in both control groups **(Figure 6A and 6B)**. Moreover, the delay in the cumulative mortality rate in *PmAgo3*-knockdown shrimp was observed upon WSSV challenge when compared to the control groups **(Figure 6C)**. The WSSV *vp28* transcript could be detected in gill tissue from dead shrimp in all groups confirming that the shrimp died of WSSV infection **(Figure 6D)**.

4. Discussion

Four types of Argonaute protein were previously identified in *P. monodon*. They are all classified as the Ago subfamily. Nevertheless, the mechanism underlying the Ago-related antiviral immunity in shrimp remains largely unknown. In this study, functional significance of *PmAgo1* and *PmAgo*3 on YHV and WSSV replication and their role in dsRNA-mediated post-transcriptional gene silencing were characterized.

Expression of key proteins in the effective innate antiviral RNAi mechanism was usually stimulated by exogenous RNAs (Choudhary et al., 2007; Garbutt and Reynolds, 2012; Phetrungnapha et al., 2013; Yang et al., 2014). Injection of dsRNA could induce expression of *dicer-2* and *argonaute-2* in tobacco hornworm (Garbutt and Reynolds, 2012). In *Neurospora crassa*, the induction of dicer (DCL-2) and argonaute (QDE-2) expression by dsRNA resulted in an increase in the efficiency of dsRNA-mediated RNAi pathway (Choudhary et al., 2007). These evidences suggested that *dicer-2* and *argonaute-2* are involved in dsRNA-mediated gene silencing pathway. Up-regulation of the expression of genes encoding core RNAi proteins e.g. *Dcr2*, *Ago2* and *Ago3* and associated components such as *TRBP*, *TSN* and *Mov-10* upon dsRNA challenge were also demonstrated in penaeid shrimps (Li et al., 2013; Phetrungnapha et al., 2012, 2013, 2015; Yang et al., 2013, 2014). In addition, suppression of *HsAgo2* by *HsAgo2*-siRNA in Human Embryonic Kidney 293 cells (HEK-293) impeded the efficiency of RNAi mechanism to knock-down histone deacetylase 2 (HDAC2) by specific HDAC2-siRNA (Naoghare et al., 2011). Similarly, silencing of *PmAgo1* and *PmAgo3* expression by specific dsRNAs in this study reduced the efficiency of *PmRab7* mRNA suppression by *PmRab7*-dsRNA, indicating the involvement of PmAgo1 and PmAgo3 in dsRNA-mediated gene silencing process. These results strongly supported the study of Dechklar et al., 2008 where repression of *Ago1* reduced the competency of 5HT-dsRNA in suppressing 5HT gene in *P. monodon*'s Oka cells. In addition, the knockdown of *PmTSN* or *MjTRBP* expression by specific dsRNA in shrimp also impaired the efficiency of

dsRNA/siRNA mediated gene silencing (Phetrungnapha et al., 2012; Wang et al., 2012). Previous reports on the Argonaute-interacting proteins in shrimp revealed that argonaute-2 of *L. vannamei* and *M. japonicus* bound to dicer-2 and TRBP1, respectively. These Ago2 complexes played a role in dsRNA/siRNA-mediated sequence-specific RNAi process while argonaute-1 primarily functioned in a miRNA pathway (Chen et al., 2011b; Huang and Zhang, 2013). However, the interacting proteins and small RNAs associated with either PmAgo1 or PmAgo3 need to be identified to confirm the precise mechanism of each PmAgo in the RNAi pathway.

Previous studies in other species demonstrated that the responsive expression of *Ago* transcripts upon virus infection enhanced the effective RNAi antiviral defense (Sun et al., 2009; Várallyay et al., 2010). For instance, the increased expression of *Nb*Ago1 mRNA in Cymbidun ringspot virus (CymRSV) infected *Nicotiana benthamiana* and the accumulation of argonaute-1 protein enhanced the RNAi antiviral activity by reducing the levels of CymRSV accumulation in the plant (Várallyay et al., 2010). In addition, high levels of *MjAgo1A* and *MjAgo1B* transcript were accumulated upon WSSV infection in *M. japonicus* (Huang and Zhang, 2012). Similarly, our result showed that the increased levels of *PmAgo1* expression was noticed in the haemolymph of YHV-infected shrimp. This phenomenon was also observed in YHV-infected lymphoid organ (Unajak et al., 2006) indicating a possible involvement of PmAgo1 in antiviral mechanism. Up-regulation of argonaute 2 (GrAgo2) transcripts were exhibited in grass carp reovirus-infected rare minnow *Gobiocypris rarus* (Su et al., 2009). Likewise, the infection of tomato yellow leaf curl virus in tomato, *Solanum lycopersicum* induced the expression of dicers and Agos (Bai et al., 2012). In *P. monodon*, Yang et al., 2014 demonstrated that *PmAgo2* mRNA expression was escalated by WSSV challenge while the expression of *PmAgo3* and *PmAgo4* was not altered in YHV infected shrimp (Leebonoi et al., 2014; Phetrungnapha et al., 2013). Virus infection in Penaeid

shrimps could also evoke other RNAi components such as LvDicer-1, LvDrosha and FcTRBP (Huang et al., 2012; Wang et al., 2009; Yoa et al., 2010). Nonetheless, the responsive expression of *PmAgos* upon viral challenge may not necessarily specify PmAgos' function in antiviral defense. Whether or not PmAgos take part in RNAi antiviral defense in shrimp was therefore further characterized in this study.

The function of Argonaute proteins in RNAi-mediated antiviral defense in invertebrates was generally demonstrated by an increase in susceptibility to viruses in *Ago*-knockdown animals (Huang and Zhang, 2012). For instance, the hypersensitivity to *Drosophila* C virus infection and high viral RNA accumulation were presented in *DmAgo2* mutant drosophila comparing to wild type and *DmAgo1* mutant flies (Van et al., 2006). A significant increase of viral loads was also observed in the shrimp, in which the expression of RNAi machinery e.g. *Ago1*, *dicer-1*, *TRBP* and *Mov10* had been knocked down (Huang and Zhang, 2012; Phetrungnapha et al., 2015; Su et al., 2008; Wang et al., 2012). Therefore, the functional significant of *PmAgo1* and *PmAgo3* in RNAi antiviral mechanism were investigated by determination the level of viral transcript and cumulative mortality in *PmAgos*-suppressed shrimp comparing to the control groups.

In general, once the hosts are infected by RNA viruses, the dsRNA replicative intermediates of the viruses are recognized by Dicer and cleaved into viral-derived siRNAs (viRNAs). The complex between viRNAs and Ago proteins in the RISC subsequently trigger the activity of RNA silencing-mediated antiviral immunity (Molnar et al., 2005; Pantaleo et al., 2007; Parameswaran et al., 2010; Weng et al., 2015). However, some viruses could express viRNAs that interfered with host gene expression and promoted viral infection (Adkar-purushothama et al., 2015; Wang et al., 2016). For example, the expression of two callose synthase genes in tomato plant was down-regulated by an siRNA derived from potato spindle tuber viroid leading to the accumulation of viroids and the severity of disease (Adkar-

purushothama et al., 2015). Likewise, siRNAs derived from Cucumber mosaic virus (CMV) Y satellite RNA (Y-sat) could decrease the expression *chlI* gene in the chlorophyll synthesis pathway, and enhanced the yellowing symptom in tobacco plants (Smith et al., 2011). Our results revealed that inhibition of YHV replication and delay mortality were noticeably observed in *PmAgo1*- and *PmAgo3*-knockdown shrimp when compared with that in both control groups (injection with either NaCl or *GFP*-dsRNA prior to viral challenge). These evidences suggest that the positive single-stranded YHV might produce viRNAs that were subsequently loaded into either PmAgo1 or PmAgo3 RISC to regulate cellular gene expression of shrimp, and accounted for promoting viral replication and disease severity. However, the gene required for YHV replication, whose expression was affected by YHV-derived small RNA in the shrimp needed to be further identified.

In addition to RNA viruses, a number of DNA viruses could also produce viral-derived small RNAs. For example, viRNAs derived from shrimp DNA virus, WSSV were reported in Penaeid shrimps (Huang and Zhang, 2013), and they required shrimp Ago2 protein for the effective function in response to WSSV infection (Yang et al., 2014). Our results also showed that the replication of WSSV in *P. monodon* was suppressed in *PmAgo3*-knockdown shrimp, but not in *PmAgo1*-knockdown shrimp suggesting that PmAgo3 might play an important role in both DNA and RNA virus replication in the shrimp. The preference for each Ago protein in response to RNA and DNA viruses is not surprising as it has been demonstrated that *Arabidopsis* Ago1 and Ago2 played a major role in the anti-RNA viral response (Dzianott et al., 2012; Garcia-Ruiz et al., 2015; Jaubert et al., 2011; Wang et al., 2011), while Ago4 functions in an antiviral activity against several RNA (Bhattacharjee et al., 2009; Hamera et al., 2012) and DNA viruses (Raja et al., 2008, 2014). Nevertheless, what defines these preferential antiviral activities in shrimp is still elusive.

In conclusion, the function in antiviral immunity of *PmAgo1* and *PmAgo3* of *P. monodon* was reported in this study. The elevated *PmAgo1* expression in the hemolymph upon YHV challenge suggests its association with shrimp antiviral response. Suppression of *PmAgo*s by specific dsRNA indicated that *PmAgo1* was preferentially required for YHV replication, whereas *PmAgo3* has more extensive effect on the replication of both YHV and WSSV. Our findings expand an understanding in Argonaute-associated RNA silencing mechanism and antiviral defense in the Penaeid shrimp.

Acknowledgments

We thank Ms. Chawewan Chimwai and Ms. Pannee Thongboonsong for technical assistance. This work was supported by the Thailand Research Fund (BRG5880005 to AU, DBG5980011 to SP) and Mahidol University Research Grant. A student fellowship is granted to TH by the Royal Golden Jubilee Ph.D. Program, Thailand Research Fund.

References

Adkar-purushothama, C.R., Brosseau, C., Giguère, T., Sano, T., Moffett, P., Perreault, J.P., 2015. Small RNA derived from the virulence modulation region of the *Potato spindle tuber viroid* silences *callose synthase* genes of tomato plants. Plant Cell. 27, 2178-2194.

Aliyari, R., Wu, Q., Li, H.W., Wang, X.H., Li, F., Green, L.D., Han, C.S., Li, W.X., Ding, S.W., 2008. Mechanism of induction and suppression of antiviral immunity directed by virus-derived small RNAs in *Drosophila*. Cell Host. Microbe. 4, 387–397.

Assavalapsakul, W., Smith, D.R., Panyim, S., 2003. Propagation of infectious yellow head virus particles prior to cytopathic effect in primary lymphoid cell cultures of *Penaeus monodon*. Dis. Aquat. Org. 55, 253-258.

Attasart, P., Kaewkhaw, R., Chimwai, C., Kongphom, U., Namramoon, O., Panyim, S., 2009. Inhibition of white spot syndrome virus replication in *Penaeus monodon* by combined silencing of viral rr2 and shrimp PmRab7. Virus Res. 145, 127-133.

Bai, M., Yang, G.S., Chen, W.T., Mao, Z.C., Kang, H.X., Chen, G.H., Yang, Y.H., Xie, Y.B., 2012. Genome-wide identification of Dicer-like, Argonaute and RNA-dependent RNA polymerase gene families and their expression analyses in response to viral infection and abiotic stresses in *Solanum lycopersicum*. Gene 501, 52-62.

Bhattacharjee, S., Zamora, A., Azhar, M.T., Sacco, M.A., Lambert, L.H., Moffett, P., 2009. Virus resistance induced by NB-LRR proteins involves Argonaute4-dependent translational control. Plant J. 58, 940–951.

Borregaard, N., Elsbach, P., Ganz, T., Garred, P., Svejgaard, A., 2000. Innate immunity: from plants to humans. Immunol. Today 21, 68-70.

Chen, P.Y., Meister, G., 2005. MicroRNA-guided posttranscriptional gene regulation. Biol. Chem. 386, 1205-1218.

Chen, S., Chahar, H.S., Abraham, S., Wu, H., Pierson, T.C., Wang, X.A., Manjunath, N., 2011a. Ago-2-mediated slicer activity is essential for anti-flaviviral efficacy of RNAi. PLoS One 6, e27551.

Chen, Y.H., Jia, X.T., Zhao, L., Li, C.Z., Zhang, S., Chen, Y.G., Weng, S.P., He, J.G., 2011b. Identification and functional characterization of Dicer2 and five single VWC domain proteins of *Litopenaeus vannamei*. Dev. Comp. Immunol. 35, 661-671.

Choudhary, S., Lee, H.C., Maiti, M., He, Q., Cheng, P., Liu, Q., Liu, Y., 2007. A double-stranded-RNA response program important for RNA interference efficiency. Mol. Cell. Biol. 27, 3995–4005.

Dechklar, M., Udomkit, A., Panyim, S., 2008. Characterization of Argonaute cDNA from *Penaeus monodon* and implication of its role in RNA interference. Biochem. Biophys. Res. Commun. 367, 768-774.

Dzianott, A., Sztuba-Solinska, J., Bujarski, J.J., 2012. Mutations in the antiviral RNAi defense pathway modify Brome mosaic virus RNA recombinant profiles. Mol. Plant Microbe Interact. 25, 97–106.

Garbutt, J.S., Reynolds, S.E., 2012. Induction of RNA interference genes by double-stranded RNA; implications for susceptibility to RNA interference. Insect Biochem. Mol. Biol. 42, 621–628.

Garcia-Ruiz, H., Carbonell, A., Hoyer, J.S., Fahlgren, N., Gilbert, K.B., Takeda, A., Giampetruzzi, A., Garcia Ruiz, M.T., McGinn, M.G., Lowery, N., Martinez Baladejo, M.T., Carrington, J.C., 2015. Roles and Programming of *Arabidopsis* ARGONAUTE Proteins during Turnip Mosaic Virus Infection. PLoS Pathog. 11, e1004755.

Hamera, S., Song, X., Su, L., Chen, X., Fang, R., 2012. Cucumber mosaic virus suppressor 2b binds to AGO4-related small RNAs and impairs AGO4 activities. Plant J. 69, 104–115.

Hammond, S.M., Bernstein, E., Beach, D., Hannon, G.J., 2000. An RNA-directed nuclease mediates post-transcriptional gene silencing in *Drosophila* cells. Nature 404, 293-296.

Hock, J., Meister, G., 2008. The Argonaute protein family. Genome Biol. 9, 210.

Hoffmann, J.A., Kafatos, F.C., Janeway, C,A,, Ezekowitz, R.A., 1999. Phylogenetic perspectives in innate immunity. Science 284, 1313-1318.

Huang, T., Xu, D., Zhang, X., 2012. Characterization of shrimp Drosha in virus infection. Fish Shellfish Immunol. 33, 575-581.

Huang, T., Zhang, X., 2012. Contribution of the argonaute-1 isoforms to invertebrate antiviral defense. PLoS One 7, e50581.

Huang, T., Zhang, X., 2013. Host defense against DNA virus infection in shrimp is mediated by the siRNA pathway. Eur. J. Immunol. 43, 137-146.

Janowski, B.A., Huffman, K.E., Schwartz, J.C., Ram, R., Nordsell, R., Shames, D.S., Minna, J.D., Corey, D.R., 2006. Involvement of AGO1 and AGO2 in mammalian transcriptional silencing. Nat. Struct. Mol. Biol. 13, 787-792.

Jaubert, M.J., Bhattacharjee, S., Mello, A.F., Perry, K.L., Moffett, P., 2011. AGO2 mediates RNA silencing anti-viral defenses against Potato virus X in *Arabidopsis*. Plant Physiol. 156, 1556–1564.

Kalmykova, A.I., Klenov, M.S., Gvozdev, V.A., 2005. Argonaute protein PIWI controls mobilization of retrotransposons in the *Drosophila* male germline. Nucleic Acids Res. 33, 2052-2059.

Kiriakidou, M., Tan, G.S., Lamprinaki, S., De Planell-Saguer M., Nelson, P.T., Mourelatos, Z., 2007. An mRNA m(7)G cap binding-like motif within human Ago2 represses translation. Cell 129, 1141—1151.

Kuramochi-Miyagawa, S., Kimura, T., Ijiri, T.W., Isobe, T., Asada, N., Fujita, Y., Ikawa, M., Iwai, N., Okabe, M., Deng, W., Lin, H., Matsuda, Y., Nakano, T., 2004. Mili, a mammalian member of piwi family gene, is essential for spermatogenesis. Development. 131, 839-849.

Kwak, P.B., Tomari, Y., 2012. The N domain of Argonaute drives duplex unwinding during RISC assembly. Nat. Struct. Mol. Biol. 19, 145-151.

Labreuche, Y., Veloso, A., de la Vega, E., Gross, P.S., Chapman, R.W., Browdy, C.L., Warr, G.W., 2010. Non-specific activation of antiviral immunity and induction of RNA interference may engage the same pathway in the Pacific white leg shrimp *Litopenaeus vannamei*. Dev. Comp. Immunol. 34, 1209-1218.

Leebonoi, W., Sukthaworn, S., Panyim, S., Udomkit, A., 2014. A novel gonad-specific Argonaute 4 serves as a defense against transposons in the black tiger shrimp *Penaeus monodon*. Fish Shellfish Immunol. 42, 280-288.

Lingel, A., Simon, B., Izaurralde, E., Sattler, M., 2003. Structure and nucleic-acid binding of the *Drosophila* Argonaute 2 PAZ domain. Nature 426, 465-469.

Li, X., Yang, L., Liang, S., Fu, M., Huang, J., Jiang, S., 2013. Identification and expression analysis of Dicer2 in black tiger shrimp (*Penaeus monodon*) responses to immune challenges. Fish Shellfish Immunol. 35, 1-8.

Ma, J.B., Ye, K., Patel, D.J., 2004. Structural basis for overhang-specific small interfering RNA recognition by the PAZ domain. Nature 429, 318-322.

Meister, G., Landthaler, M., Patkaniowska, A., Dorsett, Y., Teng, G., Tuschi, T., 2004. Human Argonaute2 mediates RNA cleavage targeted by miRNAs and siRNAs. Mol. Cell. 15, 185-197.

Miyoshi, K., Tsukumo, H., Nagami, T., Siomi, H., Siomi, M.C., 2005. Slicer function of *Drosophila* Argonautes and its involvement in RISC formation. Genes Dev. 19, 2837-2848.

Molnar, A., Csorba, T., Lakatos, L., Varallyay, E., Lacomme, C., Burgyan, J., 2005. Plant virus-derived small interfering RNAs originate predominantly from highly structured single-stranded viral RNAs. J. Virol. 79, 7812–7818.

Naoghare, P.K., Tak, Y.K., Kim, M.J., Han, E., Song, J.M., 2011. Knock-Down of Argonaute 2 (AGO2) Induces Apoptosis in Myeloid Leukaemia Cells and Inhibits siRNA-Mediated Silencing of Transfected Oncogenes in HEK-293 Cells. Basic Clin. Pharmacol. Toxicol. 109, 274–282.

Ongvarrasopone, C., Chanasakulniyom, M., Sritunyalucksana, K., Panyim, S., 2008. Suppression of PmRab7 by dsRNA inhibits WSSV or YHV infection in shrimp. Mar. Biotechnol (NY). 10, 374-381.

Ongvarrasopone, C., Roshorm, Y., Panyim, S., 2007. A simple and cost effective method to generate dsRNA for RNAi studies in invertebrates. Science Asia. 33, 35-39.

Pantaleo, V., Szittya, G., Burgyán, J., 2007. Molecular bases of viral RNA targeting by viral small interfering RNA-programmed RISC. J. Virol. 81, 3797–3806.

Parameswaran, P., Sklan, E., Wilkins, C., Burgon, T., Samuel, M.A., Lu, R., Ansel, K.M., Heissmeyer, V., Einav, S., Jackson, W., Doukas, T., Paranjape, S., Polacek, C., dos Santos, F.B., Jalili, R., Babrzadeh, F., Gharizadeh, B., Grimm, D., Kay, M., Koike, S., Sarnow, P., Ronaghi, M., Ding, S.W., Harris, E., Chow, M., Diamond, M.S., Kirkegaard, K., Glenn, J.S., Fire, A.Z., 2010. Six RNA viruses and forty-one hosts: viral small RNAs and modulation of small RNA repertoires in vertebrate and invertebrate systems. PLoS Pathog. 6, e1000764.

Phetrungnapha, A., Ho, T., Udomkit, A., Pamyim, S., Ongvarrasopone, C., 2013. Molecular cloning and functional characterization of Argonaute-3 gene from *Penaeus monodon*. Fish Shellfish Immunol. 35, 874-882.

Phetrungnapha, A., Kondo, H., Hirono, I., Panyim, S., Ongvarrasopone, C., 2015. Molecular cloning and characterization of Mj-MOV10, a putative RNA helicase involved in RNAi of Kuruma shrimp. Fish Shellfish Immunol. 44, 241-247.

Phetrungnapha, A., Panyim, S., Ongvarrasopone, C., 2012. A Tudor staphylococcal nuclease from *Penaeus monodon*: cDNA cloning and its involvement in RNA interference. Fish Shellfish Immunol. 31, 373-380.

Posiri, P., Ongvarrasopone, C., Panyim, S., 2013. A simple one-step method for producing dsRNA from *E. coli* to inhibit shrimp virus replication. J. Virol. Methods. 188, 64-69.

Raja, P., Jackel, J.N., Li, S., Heard, I.M., Bisaro, D.M., 2014. Arabidopsis double-stranded RNA binding protein DRB3 participates in methylation-mediated defense against geminiviruses. J. Virol. 88, 2611–2622.

Raja, P., Sanville, B.C., Buchmann, R.C., Bisaro, D.M., 2008. Viral genome methylation as an epigenetic defense against geminiviruses. J. Virol. 82, 8997–9007.

Robalino, J., Browdy, C.L., Prior, S., Metz, A., Parnell, P., Gross, P., Warr, G., 2004. Induction of antiviral immunity by double-stranded RNA in a marine invertebrate. J. Virol. 78, 10442-10448.

Smith, N.A., Eamens, A.L., Wang, M.B., 2011. Viral small interfering RNAs target host genes to mediate disease symptoms in plants. PLoS Pathog. 7, e1002022.

Song, J.J., Smith, S.K., Hannon, G.J., Joshua-Tor, L., 2004. Crystal structure of Argonaute and its implications for RISC slicer activity. Science 305, 1434-1437.

Su, J., Oanh, D.T., Lyons, R.E., Leeton, L., Van Hulten, M.C., Tan, S.H., Song, L., Rajendran, K.V., Walker, P.J., 2008. A key gene of the RNA interference pathway in the black tiger shrimp, *Penaeus monodon*: identification and functional characterization of Dicer-1. Fish Shellfish Immunol. 24, 223-233.

Su, J., Zhu, Z., Wang, Y., Jang, S., 2009. Isolation and characterization of Argonaute2: A key gene of the RNA interference pathway in the rare minnow, *Gobiocypris rarus*. Fish Shellfish Immunol. 29, 164-170.

Sun, Q., Choi, G.H., Nuss, D.L., 2009. A single Argonaute gene is required for induction of RNA silencing antiviral defense and promotes viral RNA recombination. Proc. Natl. Acad. Sci. U S A. 106, 17927–17932.

Till, S., Lejeune, E., Thermann, R., Bortfeld, M., Hothorn, M., Enderle, D., Heinrich, C., Hentze, M.W., Ladurner, A.G., 2007. A conserved motif in Argonaute-interacting proteins mediates functional interactions through the Argonaute PIWI domain. Nat. Struct. Mol. Biol. 14, 897–903.

Unajak, S., Boonsaeng, V., Jitrapakdee, S., 2006. Isolation and characterization of cDNA encoding Argonaute, a component of RNA silencing in shrimp (*Penaeus monodon*). Comp. Biochem. Physiol. B Biochem. Mol. Biol. 145, 179-187.

Van Rij, R. P., Saleh, M. C., Berry, B., Foo, C., Houk, A., Antoniewski, C., Andino, R., 2006. The RNA silencing endonuclease Argonaute 2 mediates specific antiviral immunity in *Drosophila melanogaster.* Genes Dev. 20, 2985–2995.

Várallyay, É., Válóczi, A., Ágyi, Á., Burgyán, J., Havelda, Z., 2010. Plant virus-mediated induction of miR168 is associated with repression of argonaute1 accumulation. EMBO J. 29, 3507–3519.

Wang, J., Tang, Y., Yang, Y., Ma, N., Ling, X., Kan, J., He, Z., Zhang, B., 2016. Cotton Leaf Curl Multan Virus-Derived Viral Small RNAs Can Target Cotton Genes to Promote Viral Infection. Front Plant Sci. 7, 1162.

Wang, S., Chen, A.J., Shi, L.J., Zhao, X.F., Wang, J.X., 2012. TRBP and eIF6 homologue in *Marsupenaeus japonicus* play crucial roles in antiviral response. PLoS One 7, e30057.

Wang, S., Liu, N., Chen, A.J., Zhao, X.F., Wang, J.X., 2009. TRBP homolog interacts with eukaryotic initiation factor 6 (eIF6) in *Fenneropenaeus chinensis*. J. Immunol. 182, 5250-5258.

Wang, X.B., Jovel, J., Udomporn, P., Wang, Y., Wu, Q., Li, W.X., Gasciolli, V., Vaucheret, H., Ding, S.W., 2011. The 21-nucleotide, but not 22-nucleotide, viral secondary small

interfering RNAs direct potent antiviral defense by two cooperative Argonautes in *Arabidopsis thaliana*. Plant Cell. 23, 1625–1638.

Wang, X.H., Aliyari, R., Li, W.X., Li, H.W., Kim, K., Carthew, R., Atkinson, P., Ding, S.W., 2006. RNA interference directs innate immunity against viruses in adult *Drosophila*. Science 312, 452-454.

Wang, Y., Sheng, G., Juranek, S., Tuschl, T., Patel, D.J., 2008. Structure of the guide-strand-containing argonaute silencing complex. Nature 456, 209-213.

Weng, K.F., Hsieh, P.T., Huang, H.I., Shih, S.R., 2015. Mammalian RNA virus-derived small RNA: biogenesis and functional activity. Microbes Infect. 17, 557–563.

Yang, L., Li, X., Huang, J., Zhou, F., Su, T., Jiang, S., 2013. Isolation and characterization of homologous TRBP cDNA for RNA interference in *Penaeus monodon*. Fish Shellfish Immunol. 34, 704-711.

Yang, L., Li, X., Jiang, S., Qiu, L., Zhou, F., Liu, W., Jiang, S., 2014. Characterization of Argonaute2 gene from black tiger shrimp (*Penaeus monodon*) and its responses to immune challenges. Fish Shellfish Immunol. 36, 261-269.

Yao, X., Wang, L., Song, L., Zhang, H., Dong, C., Zhang, Y., Qiu, L., Shi, Y., Zhao, J., Bi, Y., 2010. A Dicer-1 gene from white shrimp *Litopenaeus vannamei*: expression pattern in the processes of immune response and larval development. Fish Shellfish Immunol. 29, 565-570.

Yigit, E., Batista, P.J., Bei, Y., Pang, K.M., Chen, C.C., Tolia, N.H., Joshua-Tor, L., Mitani, S., Simard, M.J., Mello, C.C., 2006. Analysis of the C. elegans Argonaute family reveals that distinct Argonautes act sequentially during RNAi. Cell 127, 747-757.

Yodmuang, S., Tirasophon, W., Roshorm, Y., Chinnirunvong, W., Panyim, S., 2006. YHV-protease dsRNA inhibits YHV replication in *Penaeus monodon* and prevents mortality. Biochem. Biophys. Res. Commun. 341, 351-356.

Zambon, R.A., Vakharia, V.N., Wu, L.P., 2006. RNAi is an antiviral immune response against a dsRNA virus in *Drosophila melanogaster*. Cell Microbiol. 8, 880-889.

Figure legends

Figure 1 *PmAgo1* expression in response to yellow head virus (YHV) and GFP-dsRNA administration

Multiplex RT-PCR was used to determine the expression of *PmAgo1* in the hemolymph of *P. monodon* at different time points after injected with either 50 µl of 100-fold dilution of purify YHV lysate (A; n=10) or *GFP*-dsRNA at 2.5 µg g^{-1} shrimp (B; n=5). The bar-graphs represent expression level of *PmAgo1* normalized with that of *β-actin* as analyzed by Scion image analysis program. Each bar represents mean ± SEM. Asterisk indicates significant difference from 0 hpi ($p < 0.05$).

Figure 2 Suppression of *PmAgo1* and *PmAgo3* transcripts by dsRNA

P. monodon were injected with 2.5 µg g^{-1} shrimp b.w. of either *PmAgo1*-dsRNA (dsPmAgo1) or *PmAgo3*-dsRNA (dsPmAgo3). The expression of *PmAgo*s in the hemolymph was determined by multiplex RT-PCR at 2 days post-injection comparing with that in shrimp injected with NaCl and GFP-dsRNA as the control groups. The levels of *PmAgo1* and *PmAgo3* transcripts in the hemolymph of shrimp in each group were analyzed by agarose gel electrophoresis together with the internal control *β-actin* transcript. The histograms show the relative expression of *PmAgo1* (A) and *PmAgo3* (B) normalized with that of *β-actin* as

measured by Scion image analysis program. Each bar represents mean ± SEM (n=5). Asterisks (*) indicate the significant difference ($p < 0.05$) between *PmAgo1*-dsRNA or *PmAgo3*-dsRNA injection groups and the control groups at each time point.

Figure 3 Impairment of *PmRab7* silencing by *Rab7*-dsRNA in *PmAgo1*- and *PmAgo3*-knockdown shrimp

The expression of *PmAgo1* and *PmAgo3* was suppressed by the injection of *PmAgo1*- or *PmAgo3*-dsRNA at 2.5 μg g^{-1} b.w., whereas NaCl and *GFP*-dsRNA injection were used as the controls. Two days following the dsRNA injection, shrimp in each group were subsequently injected with *PmRab7*-dsRNA (0.6 μg g^{-1} shrimp b.w.), and the expression of *PmRab7* in the hemolymph was determined at 0, 24, 48 and 72 h post-*PmRab7*-dsRNA injection (upper panel). *β-actin* was detected as an internal control. Numbers represent individual shrimp. The histograms (lower panel) show the relative expression of *PmRab7* normalized with that of *β-actin* as measured by Scion image analysis program. Each bar represents mean ± SEM (n=5). Asterisks (*) indicate the significant difference ($p < 0.05$) between *PmAgo1*-dsRNA (dsPmAgo1) or *PmAgo3*-dsRNA (dsPmAgo3) injection groups and the control groups at each time point.

Figure 4 Effect of *PmAgo1* knockdown on YHV replication and cumulative mortality in shrimp upon YHV infection

Suppression of *PmAgo1* expression was carried out by *PmAgo1*-dsRNA injection with NaCl and *GFP*-dsRNA injection as controls. On day 2 after injected with dsRNA, shrimp were subsequently challenged with YHV, and the expression of YHV *helicase* gene (YHV-

hel) in the hemolymph of *PmAgo1*-knockdown shrimp (dsPmAgo1+YHV) and the control shrimp (NaCl+YHV, dsGFP+YHV) was detected by multiplex RT-PCR compared with that of *β-actin* at 0, 36 and 48 hours post YHV infection (n=5 at each time point) (A). Mortality of individual shrimp in each group was also recorded, and presented as cumulative percent mortality (B). Virus infection in the shrimp was verified by detection of YHV-*hel* mRNA in gill tissue from dead shrimp in all groups (C).

Figure 5 Effect of *PmAgo3* knockdown on YHV replication and cumulative mortality in shrimp upon YHV infection

Suppression of *PmAgo3* expression was carried out by *PmAgo3*-dsRNA injection with NaCl and *GFP*-dsRNA injection as controls. The *PmAgo3*-knockdown shrimp were infected with YHV (dsPmAgo3+YHV), and the expression of YHV-*hel* gene in the hemolymph was detected by multiplex RT-PCR compared with that of control shrimp (NaCl+YHV, dsGFP+YHV) at 0, 36 and 48 hours post YHV infection (n=5 at each time point) (A). *β-actin* transcript was determined as internal control. Mortality of individual shrimp in each group was also recorded, and presented as cumulative percent mortality (B). Expression of YHV-*hel* mRNA in gill tissue from dead shrimp was examined to confirm virus infection in the shrimp (C).

Figure 6 WSSV replication and shrimp mortality upon WSSV infection in *PmAgo1*- and *PmAgo3*-knockdown *P. monodon*

P. monodon were injected with either 2.5 μg g^{-1} shrimp of *PmAgo1*-dsRNA, *PmAgo3*-dsRNA, *GFP*-dsRNA or 150 mM NaCl (n = 5 in each group) 2 days prior to WSSV challenge. WSSV replication in *PmAgo1*-knockdown shrimp (dsPmAgo1+WSSV), *PmAgo3*-knockdown shrimp (dsPmAgo3+WSSV) comparing with control shrimp (NaCl+WSSV and

dsGFP+WSSV) was determined by both RT-PCR detection of WSSV *Vp28* mRNA (A) and PCR amplification of WSSV genomic DNA (B) at 0, 24 and 36 hours post WSSV infection. *β-actin* transcript was determined as an internal control. Mortality of individual shrimp in each group was also recorded, and presented as cumulative percent mortality (C). WSSV infection in all dead shrimp was confirmed by RT-PCR of WSSV-vp28 mRNA in the gill tissue (D).

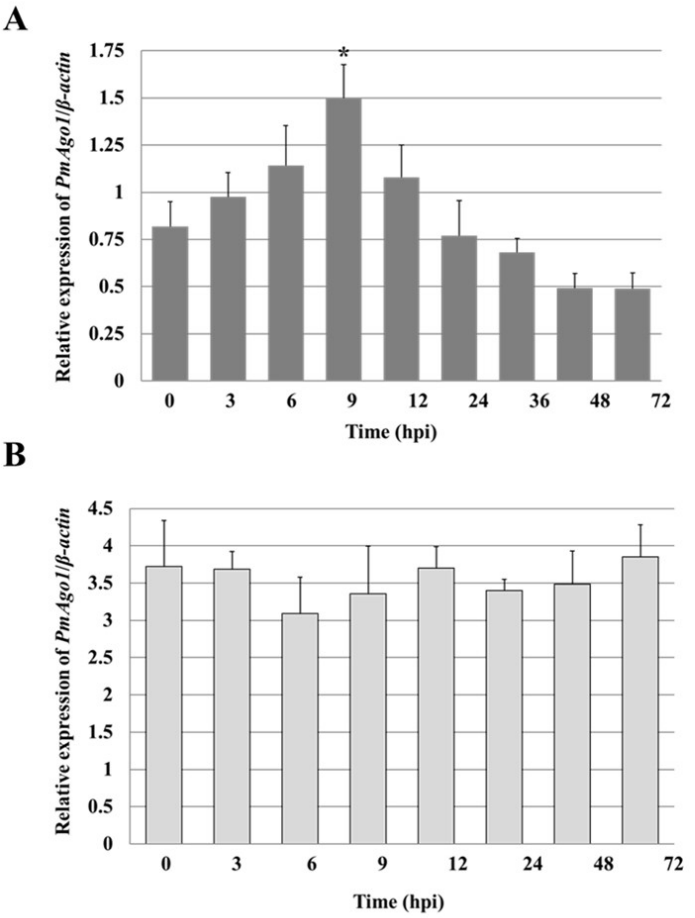
A
Relative expression of PmAgo1/β-actin
1.75
1.5
1.25
1
0.75
0.5
0.25
0
*
0
3
6
9
12
24
36
48
72
Time (hpi)
B
Relative expression of PmAgo1/β-actin
4.5
4
3.5
3
2.5
2
1.5
1
0.5
0
0
3
6
9
12
24
48
72
Time (hpi)

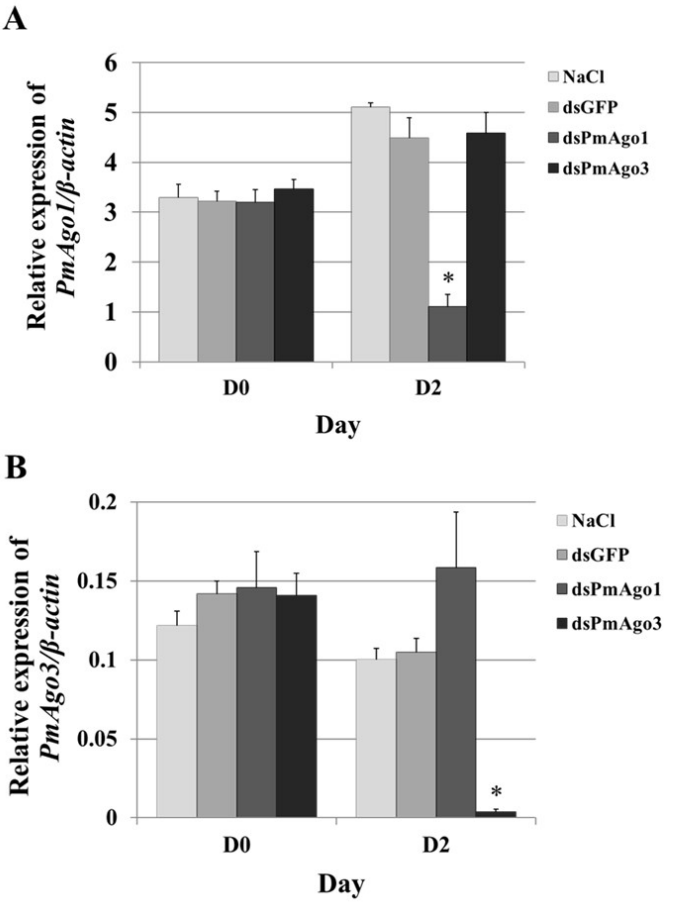
A
Relative expression of PmAgo1/β-actin
6
5
4
3
2
1
0
*
D0
D2
Day
NaCl
dsGFP
dsPmAgo1
dsPmAgo3
B
Relative expression of PmAgo3/β-actin
0.2
0.15
0.1
0.05
0
*
D0
D2
Day
NaCl
dsGFP
dsPmAgo1
dsPmAgo3

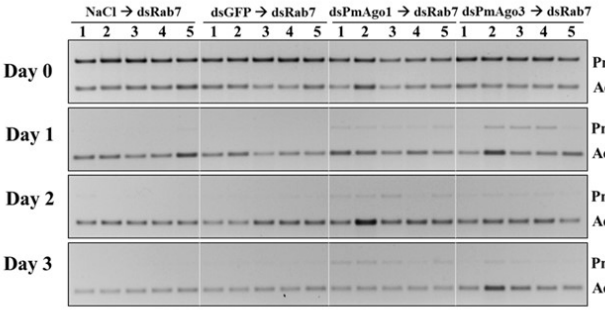
NaCl → dsRab7
dsGFP → dsRab7
dsPmAgo1 → dsRab7
dsPmAgo3 → dsRab7
1 2 3 4 5 1 2 3 4 5 1 2 3 4 5 1 2 3 4 5
Day 0
Day 1
Day 2
Day 3
PmRab7
Actin

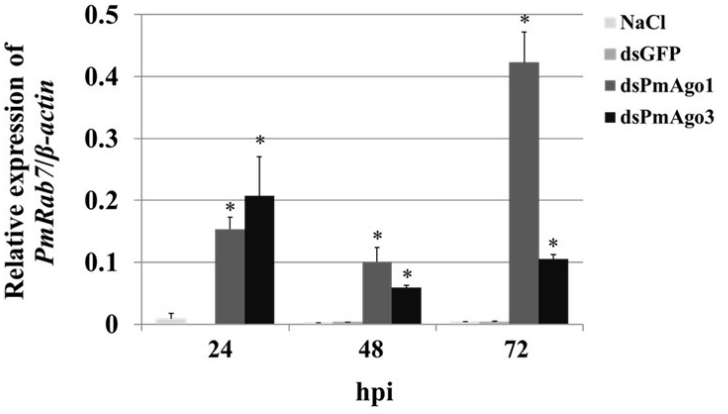
Relative expression of
PmRab7/β-actin
0.5
0.4
0.3
0.2
0.1
0
24
48
72
hpi
NaCl
dsGFP
dsPmAgo1
dsPmAgo3

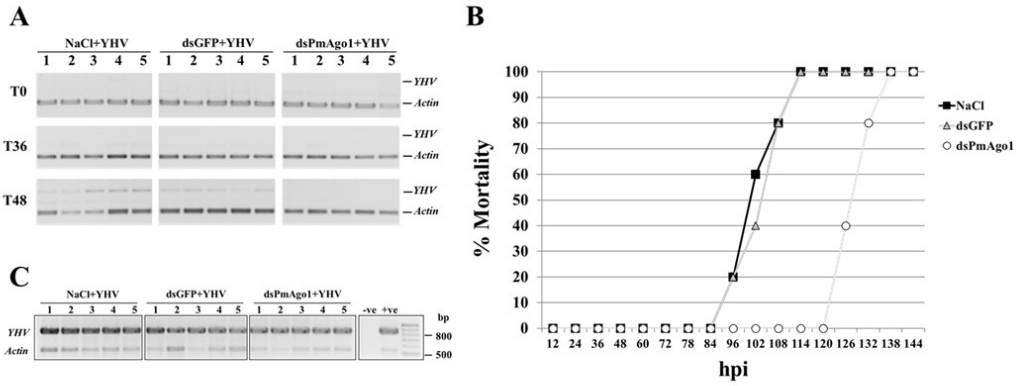
A
NaCl+YHV
dsGFP+YHV
dsPmAgo1+YHV
1 2 3 4 5
T0
T36
T48
YHV
Actin
B
% Mortality
hpi
NaCl
dsGFP
dsPmAgo1
C
-ve +ve
bp
800
500

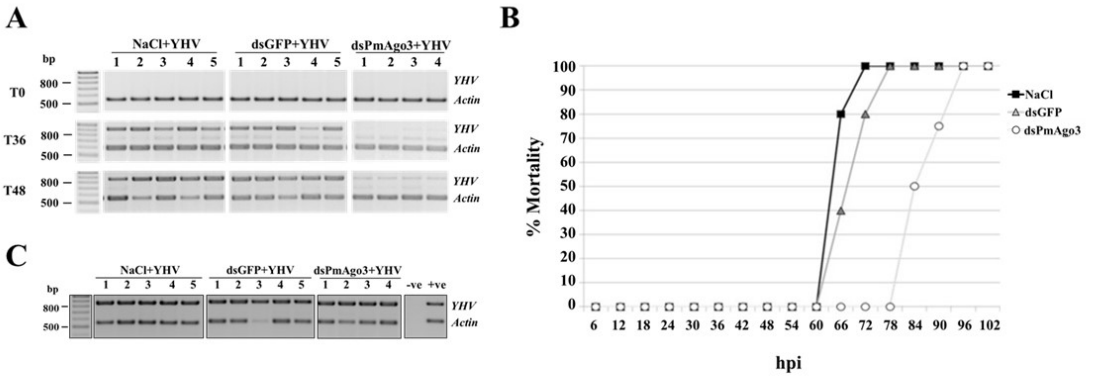
A
NaCl+YHV
dsGFP+YHV
dsPmAgo3+YHV
bp
1 2 3 4 5
1 2 3 4 5
1 2 3 4
T0
T36
T48
800
500
YHV
Actin
B
% Mortality
100
90
80
70
60
50
40
30
20
10
0
6 12 18 24 30 36 42 48 54 60 66 72 78 84 90 96 102
hpi
NaCl
dsGFP
dsPmAgo3
C
NaCl+YHV
dsGFP+YHV
dsPmAgo3+YHV
-ve +ve
YHV
Actin

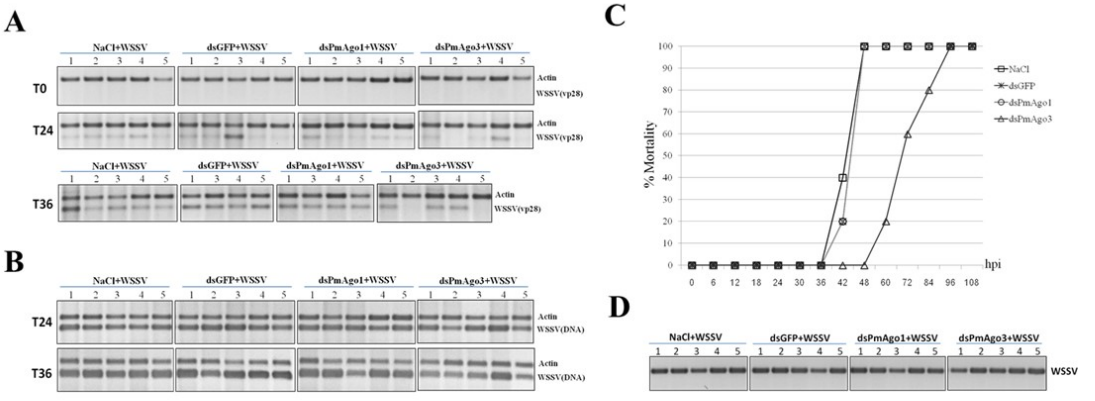
A
NaCl+WSSV
dsGFP+WSSV
dsPmAgo1+WSSV
dsPmAgo3+WSSV
1 2 3 4 5
T0
T24
T36
Actin
WSSV(vp28)
B
Actin
WSSV(DNA)
C
% Mortality
hpi
0 6 12 18 24 30 36 42 48 60 72 84 96 108
NaCl
dsGFP
dsPmAgo1
dsPmAgo3
D
WSSV

Figure S1

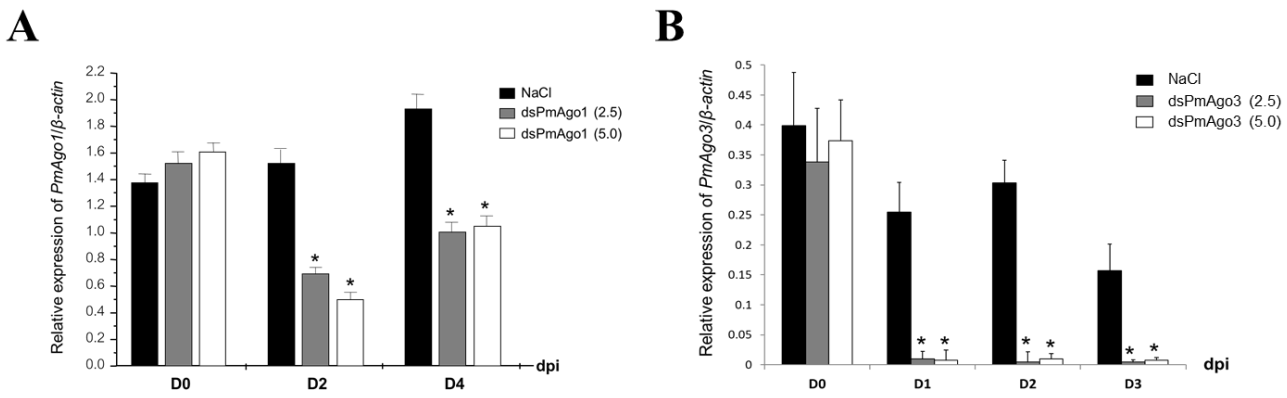

Figure S1 Suppression of *PmAgo1* and *PmAgo3* transcript by dsRNA in the hemolymph of *P. monodon*

Shrimp were injected with 2.5 and 5 µg g-1 shrimp of PmAgo1-dsRNA (n=7) or PmAgo3-dsRNA (n=5). Shrimp injected with NaCl were used as a control group. The expression of PmAgo1 in the hemolymph was determined by multiplex RT-PCR at 0, 2 and 4 days post-injection, whereas PmAgo3 expression was determined at 0, 1, 2 and 3 days post-injection. The histograms show the relative expression of *PmAgo1* and *PmAgo3* normalized with that of β-actin as measured by Scion image analysis program. Each bar represents mean ± SEM. Asterisks (*) indicate the significant difference ($p < 0.05$) between PmAgo1-dsRNA (dsPmAgo1) or PmAgo3-dsRNA (dsPmAgo3) injected groups and the control group at each time point.

Figure S2

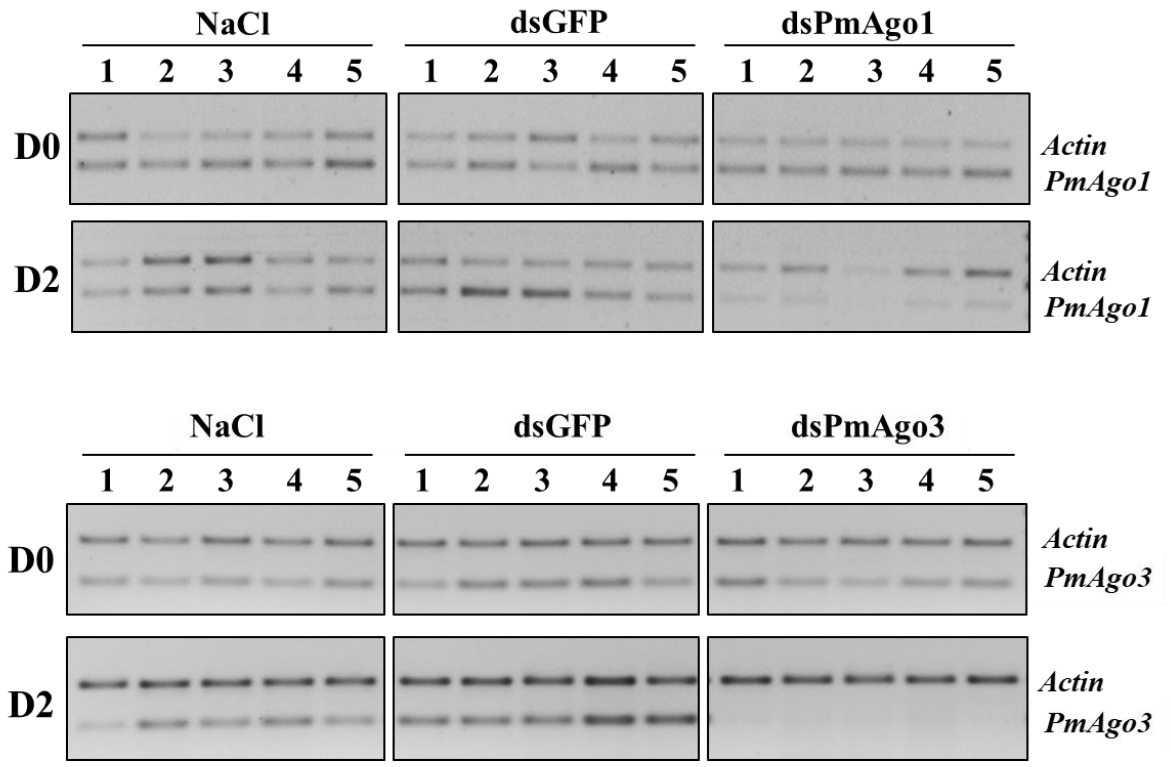

Figure S2 Verification of *PmAgo1* and *PmAgo3* knockdown by dsRNA prior to *PmRab7*-dsRNA injection

The expression of *PmAgo1* (upper panel) and *PmAgo3* (lower panel) in the hemolymph of *P. monodon* at 0 and 2 days after injected with *PmAgo1*- or *PmAgo3*-dsRNA, respectively at 2.5 µg g^{-1} was detected by multiplex RT-PCR compared with that in the control groups injected with either NaCl or *GFP*-dsRNA. The shrimp were subsequently injected with *PmRab7*-dsRNA (0.6 µg g^{-1} shrimp) to determine the effect of *PmAgo1* and *PmAgo3* knockdown on *PmRab7* suppression by *PmRab7*-dsRNA.

Manuscript Details

Manuscript number	AQUA_2018_1144
Title	Piwi controls transposon expression and spermatogenesis in Penaeus monodon
Article type	Research Paper

Abstract

Piwi proteins comprise a subfamily of Argonaute that plays a major role in germline development by association with a distinct class of small RNAs called Piwi interacting RNA (piRNA). Although the functions of Piwi in the development of germline cells as well as transposon regulation were reported in a number of mammalians and insects, developmental expression and function of Piwi subfamily in crustaceans is poorly known. This study is aimed at cloning and characterization of a Piwi cDNA in the black tiger shrimp, Penaeus monodon. The cDNA encoding a Piwi protein of P. monodon (PmPiwi) was obtained by rapid amplification of cDNA ends (RACE). The PmPiwi1 coding cDNA contains 2,811 nt encoding a putative protein of 936 amino acids, and was specifically expressed in testis and ovary, suggesting its possible function in gametogenesis. RNAi experiment showed that suppression of PmPiwi1 expression led to a significant up-regulation of retrotransposon gypsy2 and DNA element transposon mariner in shrimp testis. Investigation of the function of PmPiwi1 in spermatogenesis by sperm count showed significantly lower number of sperms in the spermatophore sac of PmPiwi1-knockdown shrimp compared with that in the control shrimp. Our study thus reported for the first time the cDNA encoding a Piwi protein in the shrimp P. monodon. Its roles in controlling transposons and spermatogenesis as implied by the results in this study will be important for understanding sperm development and could be useful for the improvement of reproduction in male shrimp in the future.

Keywords	Penaeus monodon; Piwi; piRNA; transposon; reproduction
Taxonomy	Gene Expression Control, Transposon
Manuscript category	Genetics

Corresponding Author	Apinunt Udomkit
Corresponding Author's Institution	Mahidol University
Order of Authors	Suchitraporn Sukthaworn, Sakol Panyim, Apinunt Udomkit
Suggested reviewers	Mikiko Siomi, Uthairat Na-Nakorn, Kenneth Söderhäll, Ikuo Hirono

Submission Files Included in this PDF

File Name [File Type]

cover letter.docx [Cover Letter]

Highlights.docx [Highlights]

manuscipt .doc [Manuscript File]

Figure 1.pptx [Figure]

Figure 2.pptx [Figure]

Figure 3.pptx [Figure]

Figure 4.pptx [Figure]

Figure 5.pptx [Figure]

Figure 6.pptx [Figure]

Tables.docx [Table]

To view all the submission files, including those not included in the PDF, click on the manuscript title on your EVISE Homepage, then click 'Download zip file'.

Piwi controls transposon expression and spermatogenesis in *Penaeus monodon*

Suchitraporn Sukthaworn[1], Sakol Panyim[1, 2], Apinunt Udomkit[1,*]

[1] Institute of Molecular Biosciences, Mahidol University, Salaya Campus, Nakhon Pathom 73170, Thailand

[2] Department of Biochemistry, Faculty of Sciences, Mahidol University, Rama VI Road, Bangkok 10400, Thailand

* Corresponding author

Telephone +66 2 441 9003 ext. 1236

Fax +66 2 441 1303

E-mail apinunt.udo@mahidol.ac.th

Abstract

Piwi proteins comprise a subfamily of Argonaute that plays a major role in germline development by association with a distinct class of small RNAs called Piwi interacting RNA (piRNA). Although the functions of Piwi in the development of germline cells as well as transposon regulation were reported in a number of mammalians and insects, developmental expression and function of Piwi subfamily in crustaceans is poorly known. This study is aimed at cloning and characterization of a *Piwi* cDNA in the black tiger shrimp, *Penaeus monodon*. The cDNA encoding a Piwi protein of *P. monodon* (PmPiwi) was obtained by rapid amplification of cDNA ends (RACE). The *PmPiwi1* coding cDNA contains 2,811 nt encoding a putative protein of 936 amino acids, and was specifically expressed in testis and ovary, suggesting its possible function in gametogenesis. RNAi experiment showed that suppression of *PmPiwi1* expression led to a significant up-regulation of retrotransposon *gypsy2* and DNA element transposon *mariner* in shrimp testis. Investigation of the function of *PmPiwi1* in spermatogenesis by sperm count showed significantly lower number of sperms in the spermatophore sac of *PmPiwi1*-knockdown shrimp compared with that in the control shrimp. Our study thus reported for the first time the cDNA encoding a Piwi protein in the shrimp *P. monodon*. Its roles in controlling transposons and spermatogenesis as implied by the results in this study will be important for understanding sperm development and could be useful for the improvement of reproduction in male shrimp in the future.

Keywords:

Penaeus monodon; Piwi; piRNA; transposon; reproduction

1. Introduction

Argonaute is a central protein component of an RNA-induced silencing complex (RISC) in a small RNA-mediated gene silencing pathway called RNA interference (RNAi). Argonaute protein family is characterized by the presence of two major conserved domains: the PAZ domain that binds specifically to small non-coding RNAs, and the PIWI domain that forms a catalytic triad Asp-Asp-His (DDH) required for the cleavage of a target mRNA that is complementarily bound to the small RNA (Carmell *et al.*, 2002; Niraj and Leemor, 2006; Peters and Meister, 2007; Olina *et al.*, 2018). Phylogenetic analysis classifies proteins in the Argonaute family into Ago and Piwi subfamilies. The Ago subfamily is ubiquitously expressed and normally functions in association with small interfering RNAs (siRNAs) and/or micro RNAs (miRNAs). In contrast to the Ago subfamily, Piwi proteins exhibit a germline-specific expression pattern and bind to a distinct class of small RNA called PIWI-interacting RNAs or piRNAs in germline cells (Carmell *et al.*, 2002; Peters and Meister, 2007; Seto *et al.*, 2007; Sheu-Gruttadauria and MacRae, 2017).

Piwi proteins and their small RNA partners, piRNAs are implicated in transcriptional gene expression, post-transcriptional gene regulation and transposon silencing that are important during germline development, particularly in spermatogenesis and oogenesis (Vagin *et al.*, 2006; Akkouche *et al.*, 2017; Marie *et al.*, 2017). Loss of *piwi* causes defects in germ cell development in diverse organisms (Houwing *et al.*, 2007; Ma *et al.*, 2017a). Piwi is most studied in *Drosophila*, whose genome codes for three Piwi members; Piwi, Aubergine (Aub) and Argonaute 3 (Ago3). Both Aub and Ago3 are cytoplasmic proteins that are restrictedly expressed in the germline granules called a nuage (Macdonald, 2001; Nagao et al., 2010; Huang et al., 2014). *Aub*-deficient flies displayed male sterility and maternal effect lethality (Schmidt, 1999; Sahin *et al.*, 2016; Ma *et al.*, 2017b). By contrast, *Drosophila*'s Piwi seems to be predominantly expressed in the nucleus and is necessary for self-renewing

division of germline stem cells in both males and females (Cox *et al.*, 1998; Cox, 2000; Gonzalez *et al.*, 2015). The depletion of Piwi led to infertility and axis specification defects in the developing egg chambers (Cox *et al.*, 1998). In the mouse, *Mus musculus,* three members of Piwi have been identified namely Miwi, Mili and Miwi2. Miwi and Mili are expressed in both testis and oocyte. They are involved in meiotic regulation of spermatogenesis and oocyte development (Kuramochi-Miyagawa, 2001; Kuramochi-Miyagawa *et al.*, 2004; Ding *et al.*, 2013; Kabayama *et al.*, 2017). On the other hand, Miwi2 is expressed in both germ cells and somatic cells, and is essential for maintaining germ-line stem cells (Carmell *et al.*, 2007; Wasserman *et al.*, 2017). Similarly, the two Piwi proteins of zebrafish, Ziwi and Zili, are essential for germ line maintenance. Ziwi is abundantly expressed during both mitotic and early meiotic stages of germ cell differentiation, while Zili is involved in germ cell differentiation similar to the mouse Miwi2 (Houwing *et al.*, 2007; Saskia Houwing, 2008). Like in other organisms, the expression of two Piwi proteins in the silkworm *Bombyx mori*, Siwi and BmAgo3, was found in germline cells. Both of them are abundantly expressed in testes and ovaries indicating that they might be involved in spermatogenesis and oogenesis in *B. Mori* (Kawaoka *et al.*, 2008). Similarly, the regulation of spermatogenesis and oogenesis in the honey bee, *Apis mellifera* is regulated by two *piwi*-like genes, Am-*aub* and Am-*ago3* (Liao *et al.*, 2010). Recently, genes encoding three crustacean Piwi proteins have been first identified in the crab *Portunus trituberculatus*. All of *P. trituberculatus*' *piwi* genes were expressed in adult testis, thus suggesting their functions during spermatogenesis (Xiang *et al.*, 2014).

Recent studies have shown that piRNAs are central players in transposon silencing, which is particularly important for germ cell differentiation and genome maintenance during germline developmental process (Chambeyron *et al.*, 2008; De Fazio *et al.*, 2011; Teixeira *et al.*, 2017). The piRNAs are primarily derived from transposons and other repeated elements

by a proposed ping-pong model that involves the three Piwi proteins in *Drosophila* (Saito *et al.*, 2006; Wang and Elgin, 2011; Wang *et al.*, 2015; Webster *et al.*, 2015). The Piwi proteins are important for controlling transposon mobilization in germ cells. For examples, loss-of-*miwi*,-*mili* and -*miwi2* mice exhibited transposon activation in germline that consequently resulted in germ cells deficiency (Carmell *et al.*, 2007; Kabayama *et al.*, 2017). In *Drosophila*, Piwi controlled expression and mobilization of retrotransposons. Mutation of *piwi* deregulates retrotransposon expression in the germline that finally led to embryonic defects (Kalmykova *et al.*, 2005; Akkouche *et al.*, 2017; Teixeira *et al.*, 2017). Although Piwi proteins have been extensively studied in diverse organisms, but Piwi in crustacean is less known. To help fulfill our knowledge in the control of gonad development in this large subphylum of arthropods, we cloned and characterized a cDNA encoding a member of Piwi proteins from the black tiger shrimp, *Penaeus monodon*. The expression of *PmPiwi* during gonad developmental stage, its function in controlling transposon expression and regulating spermatogenesis in the male germline of *P. monodon* were also investigated.

2. Materials and methods

2.1 Penaeus monodon samples

P. monodon were kindly provided by Shrimp Genetic Improvement Center, Surat Thani, Thailand. Male shrimps at three different maturation stages were used in this study: adolescent or immature shrimp about 4 months old or approximately 20 g bodyweight (bw) were defined as those forming spermatophores without sperm inside; sub-adult male shrimp were about 6 months of age with approximately 40 g bw; and adult male shrimp were over 10 months old. Female shrimp were divided into five reproductive maturation stages based on histochemical staining with hematoxylin and eosin according to Tan-Fermin and Pudadera, 1989 (Tan-Fermin and Pudadera, 1989).

2.2 Cloning of a full-length Piwi cDNA of P. monodon (PmPiwi1)

Total RNA was extracted from the testis of *P. monodon* by TriSolution Plus Reagent (GMbiolab) as described in the manufacturer's protocol. Approximately 2 μg of total RNA were used for cDNA synthesis by incubating with 0.5 μM of oligo dT primer in a volume of 5 μl followed by incubating at 70°C for 5 min and cooling on ice for 5 min. Then, the mixture containing 5X Improm pt II™ reaction buffer, 3 mM $MgCl_2$, 0.5 mM each dNTP, and 1 μl of Impromt II™ reverse transcriptase (Promega) was added, and the reaction was continued at 42°C for 60 min, then at 70°C for 15 min. One microliter of the cDNA was used as a template for amplification of the partial *Piwi* cDNA with specific primers PIWI-F4 and PIWI-R4 (Table 1) at 95°C for 5 min followed by 35 cycles of 95°C for 30 sec, 57°C for 30 sec, and 68°C for 30 sec.

The 3' end of *PmPiwi1* cDNA were obtained from the oligo-dT-primed first strand cDNA by 3' RACE. The first amplification was performed with 3RACE1 primer designed from the partial Piwi cDNA obtained above and oligo-dT reverse primer. Subsequently, the nested PCR was performed using 3' inner primer 3RACE2 and PM1 primer. The PCR profile for 3'RACE was as follows; initial denaturation at 95°C for 5 min, annealing at 55°C for 30 sec and extension at 68°C for 2 min 30 sec for 35 cycles using *Taq* DNA polymerase (NEB® Inc.).

For 5' RACE, the first strand cDNA was synthesized using specific reverse primer of PmPiwi1 (5RACE-R1), followed by tailing of poly A at its 3' end using terminal deoxynucleotidyl transferase (Promega). The 5' cDNA of *PmPiwi1* was obtained by three rounds of 5'RACE using the following temperature profile: initial denaturation at 95°C for 5 min, annealing at 55°C for 30 sec and extension at 68°C for 2 min 30 sec for 35 cycles using *Taq* DNA polymerase (NEB® Inc.). Schematic diagrams of 3' and 5' RACE amplification are

shown in Fig. 1, and all primers together with their nucleotide sequences are shown in Table 1.

The entire coding region of *PmPiwi1* was obtained by amplification with coding-F and coding-R primers using Expand High Fidelity enzyme (Roche) in a 25 µl reaction containing 1X Expand High Fidelity buffer with $MgSO_4$, 0.352 mM dNTP and 0.3 µM each primer. The amplification was carried out using the following temperature profile; denaturation at 94°C for 10 sec, annealing at 50°C for 30 sec and extension at 68°C for 2 min for 10 cycles, followed by the second round of amplification with 25 cycles of denaturation at 94°C for 15 sec, annealing at 50°C for 30 sec and extension at 68°C for 2 min 20 sec. All the primers used and their nucleotide sequences are listed in Table 1. The amplified fragments were purified and cloned into pGEM®-T easy (Promega). The nucleotide sequences were determined by automated DNA sequencing (1st BASE DNA Sequencing Services, Singapore) and analyzed by Blast program (http://www.ncbi.nlm.nih.gov/blast).

2.3 Determination of PmPiwi1 expression in P. monodon

Adult male and female *P. monodon* (approximately 100 g bw) were used for tissue distribution determination. Several tissues such as brain, gill, hepatopancreas, heart lymphoid, abdominal nerve cord, throracic ganglia, testis, vas deferens, spermatophore and ovary were dissected and sliced into small pieces. About 100 mg of each tissue were homogenized in Trisolution Plus Reagent (GMbiolab), Approximately 2 µg of total RNA from each tissue were used for cDNA synthesis with oligo dT as described above. The *PmPiwi1* mRNA expression was determined by cDNA amplification with Coding-F1 and 5RACE-R5 primers by *Taq* DNA polymerase (NEB® Inc.) in a 25 µl PCR reaction using the PCR profile as previously described for the amplification of *PmPiwi1* coding cDNA. Actin was used as an internal control. All primers were shown in Table 1.

The mRNA expression levels of *PmPiwi1* in the ovary and testis at different developmental stages were determined by real-time PCR using KAPA SYBR® FAST qPCR kit (Kapa Biosystems) according to the manufacturer's protocol. The fluorescent signal was detected by Eppendorf Realplex (Eppendorf) machine. Relative expression level of *PmPiwi1* was compared with that of the reference gene (elongation factor 1 alpha: *Ef1*□), and the data was analyzed by $2^{-\Delta\Delta CT}$ method.

2.4 Double-stranded RNA preparation

The recombinant plasmid harboring the PAZ domain region of *PmPiwi1* cDNA was used as a template for *PmPiwi1* dsRNA production. The dsRNA was synthesized as a stem-loop precursor in *Escherichia coli* expression system. The template of the sense (stem) strand was amplified with sense-*Xba* I-F and sense-*Hind* III-R primers, whereas the anti-sense (stem-loop) strand template was amplified with anti-*Xho* I-F and anti-*Hind* -R primers. The reaction was performed by 30 cycles of denaturation at 95°C for 2 min, annealing at 55°C for 30 min and extension at 72°C for 1 min using *Pfu* DNA polymerase (Thermo scientific). The sense and anti-sense template fragments were sequentially cloned into pET17b vector at the restriction sites corresponding to their termini. The pET17b vector harboring *PmPiwi1* dsRNA template was expressed in *E. coli* strain HT115 with 0.4 mM IPTG induction at 37°C for 4 hr. The *PmPiwi1* dsRNA was extracted by TriSolution Plus Reagent with the addition of 5 ng RNaseA to digest host single strand RNA and the loop region of the stem-loop dsRNA precursor. The quality of dsRNA was determined by RNase digestion assay with RNaseA and RNaseIII.

2.5 In vivo silencing of PmPiwi1

In order to investigate the function of *PmPiwi1*, its expression was first suppressed by dsRNA-mediated silencing. To demonstrate the potency of dsRNA to knockdown *PmPiwi1* expression in the shrimp, male *P. monodon* approximately 50 g bw were injected with

PmPiwi1-dsRNA (dsPiwi1) at 2.5 μg.g^{-1} shrimp bw in a volume of 100 μl. Shrimp injected with 150 mM NaCl were used as a control group. The shrimp were injected twice on day 0 and day 7. Testes were collected on day14 after the first injection to determine silencing effect of dsRNA by detecting transcript levels of *PmPiwi1* in the testis by RT-PCR with specific primers as shown in Table 1.

2.6 Effect of PmPiwi1 silencing on transposon expression level

The consequence of *PmPiwi1* silencing on transposon expression was determined in the testis of *PmPiwi1*-silenced shrimp on day 14 after the first dsRNA injection. Three types of transposon elements i.e. two LTR-retrotransposons; *gypsy1* (Accession no. HF548819), *gypsy2* (Accession no. HF548820.1) and DNA element transposon *mariner* (partially cloned in our laboratory, unpublished data) were examined. The expression level of each transposon was determined by real-time PCR with specific primers for each element as shown in Table 1 using KAPA SYBR® FAST qPCR kit (Kapa Biosystems) according to the manufacturer's protocol. The fluorescent signal was detected by Eppendorf Realplex (Eppendorf) machine. *Ef1α* was used as reference gene, and the data was analyzed by $2^{-\Delta\Delta CT}$ method.

2.7 Determination of sperm numbers in PmPiwi1-silenced shrimp

According to Jiang SG., et al 2009 (Jiang *et al.*, 2009), spermatophores and sperms in male *P. monodon* were first detected at 157 days of age or about 21.7 g bw. To ensure the formation of spermatophore, male shrimp approximately 40 g bw was used to determine the function *PmPiwi1* in spermatogenesis. The shrimp were divided into 2 groups; the first group was injected with *GFP*-dsRNA (dsGFP) as a control group, and the second group was injected with dsPiwi1 (n=4 each). The dsRNA was injected at a dose of 2.5 μg.g^{-1} shrimp bw into the hemocoel at the base of the fifth pleopod. Previous study reported that

spermatogenesis was related to molting cycle in *P. monodon*, and the newly formed spermatophores could be observed around day 3 after molt. Therefore, to investigate the function of *PmPiwi1*, male shrimps were injected on day 3 after molting (molting stage C-D0), and tissues (testes and spermatophores) were collected on day 3 after the next molt. One of the two spermatophores (the left one) was collected and homogenized in 1 ml of Ca^{2+}-free seawater (370 mM NaCl, 15 mM KCl, 8.5 mM H_3BO_3, 4.75 mM NaOH, 20 mM $MgSO_4.7H_2O$, pH 7.4) at 4° C. Then, 25 µl of sperm suspension were mixed with 0.4% trypan blue and incubated at room temperature for 5 min. After that, 15 µl of the mixture were dropped on a hemacytometer, and the number of sperms were counted under light microscope. Data were analyzed using SPSS program. Differences between groups was analyzed by t-test at $P<0.05$ as statistical significance.

3. Results

3.1 Cloning and characterization of Piwi1 cDNA in P. monodon

The full-length nucleotide sequence of *PmPiwi1* cDNA was obtained by RACE strategy. The combined *PmPiwi1* cDNA fragment is 2,988 bp in length with a 66 bp 5'UTR, a putative 2,811 bp coding region and a 111 bp 3' UTR (Accession no. MH279567). The continuous reading frame of *PmPiwi1* was verified by RT-PCR. The deduced amino acid sequence of PmPiwi1 contains 936 residues with a predicted molecular weight of 105.31 kDa and a theoretical isoelectric point of 9.36. Identification of conserved domains by ScanProsite program (prosite.expazy.org/scanprosite) revealed that PmPiwi1 contains the signature PAZ and PIWI domains of the Argonaute family (Fig. 1). The predicted catalytic residues Asp-Asp-His (DDH) were also present at the C-terminal PIWI domain of PmPiwi1 similar to other members of the Argonaute family.

The percentage of similarity among PmPiwi1 and their homologues in other species are shown in table 2. Most of the similarities lay in the conserved PAZ and PIWI domains.

Phylogenetic tree analysis revealed that PmPiwi1 was classified into the same group as insect Ago3, and closely clustered with Piwi1 of the crab *P. trituberculatus* (Fig. 2).

3.2 Expression of PmPiwi1 in P. monodon

The expression of *PmPiwi1* mRNA in *P. monodon* tissues was determined by RT-PCR. High levels of *PmPiwi1* transcript were detected in the testis and, at a lower level, in the ovary but was not detected in other tissues (Fig. 3A).

In order to investigate further whether or not the expression of *PmPiwi1* in the ovary changes upon ovarian development, the levels of *PmPiwi1 t*ranscript in the ovary at different developmental stages were determined by real-time PCR. The result in Fig. 3B showed that the expression levels of *PmPiwi1*were not significantly different throughout ovarian development from stage 0 to stage IV. In male shrimp, the expression levels of *PmPiwi1* in the testis was rather constant from immature to adult shrimp (Fig. 3C).

3.3 Function of PmPiwi1 in transposon suppression

The efficiency of *PmPiwi1* silencing by specific dsRNA was investigated in the testis of *P. monodon*. The injection with double dosages of dsPiwi1 at 2.5 $\mu g.g^{-1}$ bw on day 0 and day 7 showed the highest suppression of *PmPiwi1*, approximately 96%, at 14 days post-injection (dpi.) (Fig. 4A). The expression of other *Agos* of *P. monodon* was not affected by dsPiwi1 (Fig. 4B), indicating the specificity of dsPiwi1 to knockdown its target transcript.

To determine the influence of *PmPiwi1* silencing on transposon expression in shrimp testis, the expression of *PmPiwi1* was suppressed by dsPiwi1 for 14 days as described above. The transcript levels of three types of transposons including two *gypsy*-like elements and a *mariner*-like element in *PmPiwi1*-knockdown shrimp were determined by real-time PCR. The results showed that the expression level of *gypsy1* was slightly increased, while *gypsy2* and *mariner*-like elements were significantly up-regulated in *PmPiwi1*-knockdown shrimp when compared with the control (Fig. 5).

3.4 Effect of PmPiwi1-knockdown on spermatogenesis in P. monodon

To investigate the function of *PmPiwi1* in sperm production, male shrimp were injected with dsPiwi1 at 2.5 μg.g^{-1} bw on day 3 after molt, and the testes and spermatophores were collected on day 3 after the next molting. The efficiencies of *PmPiwi1* knockdown in this experiment (Fig. 6A) were comparable to the previous experiment. The numbers of sperm deposited in the spermatophores of *PmPiwi1*-knockdown shrimp were significantly reduced when compared with that in the dsGFP-injected and the control group (Fig. 6B). Moreover, the spermatophores of *PmPiwi1*-knockdown shrimp were apparently smaller than that of the control groups (Fig. 6C).

4. Discussion

A cDNA encoding Piwi protein in the black tiger shrimp, *P. monodon* was identified and characterized. The alignment of the deduced amino acid sequences revealed that PmPiwi1 contained the conserved PAZ and PIWI domains, which are signature of the Argonaute family. Similarly to the PAZ domain of the Ago subfamily that forms a specific binding module for the 2-nt 3' overhang of small RNAs generated by RNase III-like enzyme such as Dicer, the PAZ domain of the PIWI subfamily forms a binding pocket that anchors the exonuclease-trimmed 3’ end of piRNAs (Matsumoto *et al.*, 2016). The PIWI domain has similar fold to RNaseH with the catalytic triad DDH that is essential for slicing activity of the Ago subfamily (Niraj and Leemor, 2006; Peters and Meister, 2007; Olina *et al.*, 2018). In *Drosophila*, all three members of the PIWI subfamily (Ago3, Aub and Piwi) also possess the conserved DDH residues in their PIWI domain. Whereas the nuclease catalytic triad of Ago3 and Aub was essential for the piRNA biogenesis pathway via the ping-pong cycle, it did not seem to be required for the function of *Drosophila*’s Piwi in repressing transcription of its targets (Rozhkov *et al.*, 2013). The PIWI domain of PmPiwi1 also contained the conserved

DDH residues, indicating that PmPiwi1 could form a nuclease catalytic triad, possibly for cleavage of the substrate RNA complementary to the bound piRNAs.

One feature that distinguishes Piwi proteins from the Ago subfamily proteins is the presence of putative asymmetric dimethylated arginine residues (arginine-glycine/RG, arginine-alanine/RA) or symmetrically dimethylated arginine (sDMA) composing of arginine flanked by glycine (GRG) or alanine (GRA or ARG) repeats at the N-terminal region (Kirino *et al.*, 2009; Vagin *et al.*, 2009). Arginine methylation is an important post-transcriptional modification that mediates protein-protein interaction. Piwi proteins were reported to associate with multiple members of the Tudor protein family through sDMA methylation, which are necessary for piRNA function in transposon silencing and gametogenesis in both flies and mice (Nishida *et al.*, 2009; Vagin *et al.*, 2009; Kirino *et al.*, 2010; Mathioudakis *et al.*, 2012). The deduced PmPiwi1possesses multi-arginine methylation sites at the N-terminus, suggesting the potential to form heterodimeric complex with Tudor proteins and play role in the operation of piRNA pathway during germline development of the shrimp.

The restricted gonad expression of *PmPiwi1* conforms to the expression and the role in germline development, a conserved function of Piwi proteins across species. Different types of Piwi may display distinct expression profiles during sperm development suggesting that they have diverse functions in different phases of spermatogenesis. For example, in the murine *Mus musculus*, Miwi2 was restricted expressed only in the testis (Carmell *et al.*, 2007) whereas Miwi and Mili were detected in both testis and oocyte (Deng, 2002; Ding *et al.*, 2013; Kabayama *et al.*, 2017). Miwi is expressed from meiotic spermatocytes to elongating spermatids (Deng, 2002), whereas Mili is expressed from 3 dpp mitotically arrested prenatal germline stem cell to round spermatids(Kuramochi-Miyagawa *et al.*, 2004; Unhavaithaya *et al.*, 2009). *Miwi*-deficient mice show spermatogenesis arrest at early spermiogenic stage while *Mili*-deficient mice are terminally blocked at zygotene or early

pachytene stages of meiotic prophase I (Deng, 2002; Kuramochi-Miyagawa *et al.*, 2004; Grivna *et al.*, 2006; Beyret and Lin, 2011). Miwi2 is detected from day 15.5 dpc to 3 dpp in mitotically arrested prenatal germline stem cells (Aravin *et al.*, 2008). In addition, Miwi2 was also found in Sertoli cells, which are somatic supporting cells within seminiferous tubules (Carmell *et al.*, 2007). *Miwi2* mutants not only displayed a meiotic progression defect in early prophase of meiosis I but also seemed to affect mitotic germ cell maintenance(Wasserman *et al.*, 2017). In addition, Miwi and Mili proteins were detected in mouse oocyte, implicating that it may also function in oocyte development (Ding *et al.*, 2013; Kabayama *et al.*, 2017). In *P. monodon*, the significant decrease in the number of sperms in spermatophore of *PmPiwi1*-knockdown shrimp compared with that in the control shrimp indicated the function of *PmPiwi1* during spermatogenesis. Since *PmPiwi1* transcript was detected in the testis but not in vas deferens and spermatophore, PmPiwi1 might be directly involved in meiotic regulation in spermatogenesis but not in sperm differentiation or sperm maturation. Although the gonad-specific expression of *PmPiwi1* suggests its function in both sperm and oocyte development, the detail at which steps PmPiwi1 play a role in gametogenesis control in the shrimp remains to be elucidated.

Piwi proteins have important function in the control of transposon in animal germline. *Piwi* knockout resulted in transposon activation, which led to germline defects. For example, derepression and up-regulation of endogenous retrotransposon *copia* was found in *loss-of-Piwi Drosophila* testes. Similarly, *Drosophila Piwi* mutant caused accumulation of *mdg1* transcripts at the apical tip of testes where Piwi protein was not detected (Kalmykova *et al.*, 2005; Brennecke *et al.*, 2007). In the zebrafish, *Zili* mutant resulted in up-regulation of both retrotransposons and DNA transposable element (Saskia Houwing, 2008). The increased expression levels of *gypsy* LTR-retrotransposons and DNA element *mariner* in the *PmPiwi1*-knockdown testis of *P. monodon* in this study suggested the function of *PmPiwi1* in the

control of transposable elements in shrimp testis. Another member of Argonaute proteins, namely PmAgo4, that is highly expressed in *P. monodon*'s germline was also demonstrated to regulate transposable elements in shrimp testis (Leebonoi *et al.*, 2015). Whether or not PmPiwi1 works in cooperation with PmAgo4 to protect shrimp germ cells from deleterious effects of excessive movement of transposable elements during gamete development needs further investigation. In addition, piRNA biogenesis and transposable elements activation in *Drosophila* and mice are known to be regulated by three members of Piwi proteins (Manakov *et al.*; Saito *et al.*, 2006; Brennecke *et al.*, 2007; Rozhkov *et al.*, 2013). Three types of Piwi transcripts were also identified in the crab, *P. trituberculatus* (Xiang *et al.*, 2014). Therefore, identification of additional members of Piwi in *P. monodon* still awaits exploration.

In conclusion, a novel cDNA encoding *PmPiwi1* in *P. monodon* was identified. Its gonad-specific expression was correlated with potential roles in sperm production and regulation of transposable elements in shrimp testis. The possibility that PmPiwi1 functions together with PmAgo4 and other Piwi members to maintain integrity of shrimp germ cells from transposition effects as has been demonstrated in a number of organisms needs to be elucidated.

Acknowledgements

We thank Ms. Somjai Wongtripop (Shrimp Genetic Improvement Center, Thailand) for providing shrimp samples, Ms. Chawewan Chimwai and Ms. Pannee Thongboonsong for technical assistance. This work was supported by the Thailand Research Fund (BRG5880005 to AU, DBG5980011 to SP), National Research Council of Thailand and Mahidol University Research Grant. SS is supported by a scholarship from National Research Council of Thailand.

References

Akkouche, A., Mugat, B., Barckmann, B., Varela-Chavez, C., Li, B., Raffel, R., Pelisson, A., Chambeyron, S., 2017. Piwi Is Required during Drosophila Embryogenesis to License Dual-Strand piRNA Clusters for Transposon Repression in Adult Ovaries. Molecular cell 66, 411-419.

Aravin, A.A., Sachidanandam, R., Bourc'his, D., Schaefer, C., Pezic, D., Toth, K.F., Bestor, T., Hannon, G.J., A piRNA Pathway Primed by Individual Transposons Is Linked to De Novo DNA Methylation in Mice. Molecular cell 31, 785-799.

Aravin, A.A., Sachidanandam, R., Bourc'his, D., Schaefer, C., Pezic, D., Toth, K.F., Bestor, T., Hannon, G.J., 2008. A piRNA Pathway Primed by Individual Transposons Is Linked to De Novo DNA Methylation in Mice. Molecular cell 31, 785-799.

Beyret, E., Lin, H., 2011. Pinpointing the expression of piRNAs and function of the PIWI protein subfamily during spermatogenesis in the mouse. Dev Biol 355, 215-226.

Brennecke, J., Aravin, A.A., Stark, A., Dus, M., Kellis, M., Sachidanandam, R., Hannon, G.J., 2007. Discrete small RNA-generating loci as master regulators of transposon activity in Drosophila. Cell 128, 1089-1103.

Carmell, M.A., Girard, A., van de Kant, H.J., Bourc'his, D., Bestor, T.H., de Rooij, D.G., Hannon, G.J., 2007. MIWI2 is essential for spermatogenesis and repression of transposons in the mouse male germline. Developmental cell 12, 503-514.

Carmell, M.A., Xuan, Z., Zhang, M.Q., Hannon, G.J., 2002. The Argonaute family: tentacles that reach into RNAi, developmental control, stem cell maintenance, and tumorigenesis. Genes & development 16, 2733-2742.

Chambeyron, S., Popkova, A., Payen-Groschene, G., Brun, C., Laouini, D., Pelisson, A., Bucheton, A., 2008. piRNA-mediated nuclear accumulation of retrotransposon transcripts in the Drosophila female germline. Proceedings of the National Academy of Sciences of the United States of America 105, 14964-14969.

Cox, D.N., Chao, A., Baker, J., Chang, L., Qiao, D., Lin, H., 1998. A novel class of evolutionarily conserved genes defined by piwi are essential for stem cell self-renewal. Genes & development 12, 3715-3727.

Cox, D.N., Chao, A, and Lin H,, 2000. *piwi* encodes a nucleoplasmic factor whose activity modulates the number and division rate of germline stem cells. Development 127, 503-514.

De Fazio, S., Bartonicek, N., Di Giacomo, M., Abreu-Goodger, C., Sankar, A., Funaya, C., Antony, C., Moreira, P.N., Enright, A.J., O'Carroll, D., 2011. The endonuclease activity of Mili fuels piRNA amplification that silences LINE1 elements. Nature 480, 259-263.

Deng, W.a.L.H., 2002. *miwi*, a Murine homolog of piwi, encodes a cytoplasmic protein essential for spermatogenesis. Developmental cell 2, 819-830.

Ding, X., Guan, H., Li, H., 2013. Characterization of a piRNA binding protein Miwi in mouse oocytes. Theriogenology 79, 610-615.

Gonzalez, J., Qi, H., Liu, N., Lin, H., 2015. Piwi Is a Key Regulator of Both Somatic and Germline Stem Cells in the Drosophila Testis. Cell Rep 12, 150-161.

Grivna, S.T., Pyhtila, B., Lin, H., 2006. MIWI associates with translational machinery and PIWI-interacting RNAs (piRNAs) in regulating spermatogenesis. Proceedings of the National Academy of Sciences 103, 13415.

Houwing, S., Kamminga, L.M., Berezikov, E., Cronembold, D., Girard, A., van den Elst, H., Filippov, D.V., Blaser, H., Raz, E., Moens, C.B., Plasterk, R.H., Hannon, G.J., Draper, B.W., Ketting, R.F., 2007. A role for Piwi and piRNAs in germ cell maintenance and transposon silencing in Zebrafish. Cell 129, 69-82.

Huang, H., Li, Y., Szulwach, K.E., Zhang, G., Jin, P., Chen, D., 2014. AGO3 Slicer activity regulates mitochondria–nuage localization of Armitage and piRNA amplification. The Journal of Cell Biology 206, 217-230.

Jiang, S.-G., Huang, J.-H., Zhou, F.-L., Chen, X., Yang, Q.-B., Wen, W.-G., Ma, Z.-M., 2009. Observations of reproductive development and maturation of male *Penaeus monodon* reared in tidal and earthen ponds. Aquaculture 292, 121-128.

Kabayama, Y., Toh, H., Katanaya, A., Sakurai, T., Chuma, S., Kuramochi-Miyagawa, S., Saga, Y., Nakano, T., Sasaki, H., 2017. Roles of MIWI, MILI and PLD6 in small RNA regulation in mouse growing oocytes. Nucleic acids research 45, 5387-5398.

Kalmykova, A.I., Klenov, M.S., Gvozdev, V.A., 2005. Argonaute protein PIWI controls mobilization of retrotransposons in the Drosophila male germline. Nucleic acids research 33, 2052-2059.

Kawaoka, S., Minami, K., Katsuma, S., Mita, K., Shimada, T., 2008. Developmentally synchronized expression of two *Bombyx mori* Piwi subfamily genes, SIWI and

BmAGO3 in germ-line cells. Biochemical and biophysical research communications 367, 755-760.

Kirino, Y., Kim, N., de Planell-Saguer, M., Khandros, E., Chiorean, S., Klein, P.S., Rigoutsos, I., Jongens, T.A., Mourelatos, Z., 2009. Arginine methylation of Piwi proteins catalysed by dPRMT5 is required for Ago3 and Aub stability. Nature cell biology 11, 652-658.

Kirino, Y., Vourekas, A., Sayed, N., de Lima Alves, F., Thomson, T., Lasko, P., Rappsilber, J., Jongens, T.A., Mourelatos, Z., 2010. Arginine methylation of Aubergine mediates Tudor binding and germ plasm localization. RNA 16, 70-78.

Kuramochi-Miyagawa, S., et al., 2001. Two mouse *piwi*-related genes; *miwi* and *mili*. Mechanisms of Development 108, 121-133.

Kuramochi-Miyagawa, S., Kimura, T., Ijiri, T.W., Isobe, T., Asada, N., Fujita, Y., Ikawa, M., Iwai, N., Okabe, M., Deng, W., Lin, H., Matsuda, Y., Nakano, T., 2004. Mili, a mammalian member of piwi family gene, is essential for spermatogenesis. Development 131, 839-849.

Leebonoi, W., Sukthaworn, S., Panyim, S., Udomkit, A., 2015. A novel gonad-specific Argonaute 4 serves as a defense against transposons in the black tiger shrimp *Penaeus monodon*. Fish & shellfish immunology 42, 280-288.

Liao, Z., Jia, Q., Li, F., Han, Z., 2010. Identification of two piwi genes and their expression profile in honeybee, *Apis mellifera*. Archives of insect biochemistry and physiology 74, 91-102.

Ma, X., Ji, A., Zhang, Z., Yang, D., Liang, S., Wang, Y., Qin, Z., 2017a. Piwi1 is essential for gametogenesis in mollusk *Chlamys farreri*. PeerJ 23.

Ma, X., Zhu, X., Han, Y., Story, B., Do, T., Song, X., Wang, S., Zhang, Y., Blanchette, M., Gogol, M., Hall, K., Peak, A., Anoja, P., Xie, T., 2017b. Aubergine Controls Germline Stem Cell Self-Renewal and Progeny Differentiation via Distinct Mechanisms. Developmental cell 41, 157-169.e155.

Macdonald, A.N.H.a.P.M., 2001. *aubergine* encodes a Drosophila polar granule component required for pole cell formation and related to elF2C. Development 128, 2823-2832.

Manakov, Sergei A., Pezic, D., Marinov, Georgi K., Pastor, William A., Sachidanandam, R., Aravin, Alexei A., MIWI2 and MILI Have Differential Effects on piRNA Biogenesis and DNA Methylation. Cell Reports 12, 1234-1243.

Marie, P.P., Ronsseray, S., Boivin, A., 2017. From Embryo to Adult: piRNA-Mediated Silencing throughout Germline Development in Drosophila. G3 7, 505-516.

Mathioudakis, N., Palencia, A., Kadlec, J., Round, A., Tripsianes, K., Sattler, M., Pillai, R.S., Cusack, S., 2012. The multiple Tudor domain-containing protein TDRD1 is a molecular scaffold for mouse Piwi proteins and piRNA biogenesis factors. RNA 18, 2056-2072.

Matsumoto, N., Nishimasu, H., Sakakibara, K., Nishida, K.M., Hirano, T., Ishitani, R., Siomi, H., Siomi, M.C., Nureki, O., 2016. Crystal Structure of Silkworm PIWI-Clade Argonaute Siwi Bound to piRNA. Cell 167, 484-497.e489.

Nagao, A., Mituyama, T., Huang, H., Chen, D., Siomi, M.C., Siomi, H., 2010. Biogenesis pathways of piRNAs loaded onto AGO3 in the Drosophila testis. RNA 16, 2503-2515.

Niraj, H.T., Leemor, J.-T., 2006. Slicer and the Argonautes. Nature Chemical Biology 3, 36-43.

Nishida, K.M., Okada, T.N., Kawamura, T., Mituyama, T., Kawamura, Y., Inagaki, S., Huang, H., Chen, D., Kodama, T., Siomi, H., Siomi, M.C., 2009. Functional involvement of Tudor and dPRMT5 in the piRNA processing pathway in Drosophila germlines. The EMBO journal 28, 3820-3831.

Olina, A.V., Kulbachinskiy, A.V., Aravin, A.A., Esyunina, D.M., 2018. Argonaute Proteins and Mechanisms of RNA Interference in Eukaryotes and Prokaryotes. Biochemistry (Moscow) 83, 483-497.

Peters, L., Meister, G., 2007. Argonaute proteins: mediators of RNA silencing. Molecular cell 26, 611-623.

Rozhkov, N.V., Hammell, M., Hannon, G.J., 2013. Multiple roles for Piwi in silencing Drosophila transposons. Genes & development 27, 400-412.

Sahin, H.B., Karatas, O.F., Specchia, V., Tommaso, S.D., Diebold, C., Bozzetti, M.P., Giangrande, A., 2016. Novel mutants of the aubergine gene. Fly 10, 81-90.

Saito, K., Nishida, K.M., Mori, T., Kawamura, Y., Miyoshi, K., Nagami, T., Siomi, H., Siomi, M.C., 2006. Specific association of Piwi with rasiRNAs derived from retrotransposon and heterochromatic regions in the Drosophila genome. Genes & development 20, 2214-2222.

Saskia Houwing, E.B.a.R.F.K., 2008. Zili is required for germ cell differentiation and meiosis in zebrafish. The EMBO journal 27, 2702-2711.

Schmidt, A., et al., 1999. Genetic and molecular characterization of *sting*, a gene involved in crystal formation and meiotic drive in the male germ line of *Drosophila melanogaster*. Genetics 151, 749-760.

Seto, A.G., Kingston, R.E., Lau, N.C., 2007. The coming of age for Piwi proteins. Molecular cell 26, 603-609.

Sheu-Gruttadauria, J., MacRae, I.J., 2017. Structural Foundations of RNA Silencing by Argonaute. Journal of Molecular Biology 429, 2619-2639.

Tan-Fermin, J.D., Pudadera, R.A., 1989. Ovarian maturation stages of the wild giant tiger prawn, *Penaeus monodon Fabricius*. Aquaculture 77, 229-242.

Teixeira, F.K., Okuniewska, M., Malone, C.D., Coux, R.X., Rio, D.C., Lehmann, R., 2017. piRNA-mediated regulation of transposon alternative splicing in the soma and germ line. Nature 552, 268-272.

Unhavaithaya, Y., Hao, Y., Beyret, E., Yin, H., Kuramochi-Miyagawa, S., Nakano, T., Lin, H., 2009. MILI, a PIWI-interacting RNA-binding protein, is required for germ line stem cell self-renewal and appears to positively regulate translation. The Journal of biological chemistry 284, 6507-6519.

Vagin, V.V., Sigova, A., Li, C., Seitz, H., Gvozdev, V., Zamore, P.D., 2006. A distinct small RNA pathway silences selfish genetic elements in the germline. Science 313, 320-324.

Vagin, V.V., Wohlschlegel, J., Qu, J., Jonsson, Z., Huang, X., Chuma, S., Girard, A., Sachidanandam, R., Hannon, G.J., Aravin, A.A., 2009. Proteomic analysis of murine Piwi proteins reveals a role for arginine methylation in specifying interaction with Tudor family members. Genes & development 23, 1749-1762.

Wang, S.H., Elgin, S.C., 2011. Drosophila Piwi functions downstream of piRNA production mediating a chromatin-based transposon silencing mechanism in female germ line. Proceedings of the National Academy of Sciences of the United States of America 108, 21164-21169.

Wang, W., Han, B.W., Tipping, C., Ge, D.T., Zhang, Z., Weng, Z., Zamore, P.D., 2015. Slicing and Binding by Ago3 or Aub Trigger Piwi-Bound piRNA Production by Distinct Mechanisms. Molecular cell 59, 819-830.

Wasserman, G.A., Szymaniak, A.D., Hinds, A.C., Yamamoto, K., Kamata, H., Smith, N.M., Hilliard, K.L., Carrieri, C., Labadorf, A.T., Quinton, L.J., Ai, X., Varelas, X., Chen, F., Mizgerd, J.P., Fine, A., O'Carroll, D., Jones, M.R., 2017. Expression of Piwi protein MIWI2 defines a distinct population of multiciliated cells. J Clin Invest 127, 3866-3876.

Webster, A., Li, S., Hur, Junho K., Wachsmuth, M., Bois, Justin S., Perkins, Edward M., Patel, Dinshaw J., Aravin, Alexei A., 2015. Aub and Ago3 Are Recruited to Nuage through Two Mechanisms to Form a Ping-Pong Complex Assembled by Krimper. Molecular cell 59, 564-575.

Xiang, D.F., Zhu, J.Q., Hou, C.C., Yang, W.X., 2014. Identification and expression pattern analysis of Piwi genes during the spermiogenesis of *Portunus trituberculatus*. Gene 534, 240-248.

Figure legends

Fig. 1 Cloning of *PmPiwi1* cDNA by RACE and deduced amino acid sequence of PmPiwi1

A) A diagram for 5' and 3' RACE of *PmPiwi1* cDNA. B) The deduced amino acid sequence of PmPiwi1 is shown in one-letter symbol under corresponding codons. The PAZ and PIWI domains are highlighted in light gray and dark gray, respectively. The catalytic DDH residues are depicted by black highlight.

Fig. 2 Phylogenetic relationship among Piwi proteins.

Phylogenetic tree of Piwi proteins was constructed by Mega4 Program using the neighbor-joining distance analysis. The amino acid sequences analyzed include Piwi proteins of *B. mori*: SIWI (AB372006), BmAgo3 (AB372007).; *D. melanogaster*: DmPiwi (AAF53043.1), DmAub (AG18944.1), DmAgo3 (ABO27430.1); *A. mellifera*: AmAub (GQ444142), AmAgo3 (GQ444137); *P. trituberculatus*: Pt-PIW1 (KC203335), Pt-PIWI2 (KC203336), Pt-PIWI3 (KC203337); *D. rerio*: Ziwi (NP899181.1), Zili (NP001073668.2); *M. musculus*: Miwi (AAL3104.1), Mili (BAA93706.1), Miwi2 (AAN75583.1). Bootstrap values from 1000 replicates are indicated at the nodes.

Fig. 3 Expression profile of *PmPiwi1* in *P. monodon*

A) Tissue distribution of *PmPiwi1* expression in *P. monodon*. The mRNA transcript levels of *P. monodon* in eyestalk ganglia (Es), brain (Bn), gill (Gl), haemolymph (Hl), hepatopancreas (Hp), lymphoid organ (Lp), abdominal nerve cord (Nc), throracic ganglia (Tg), testis (Tt), sperm duct or vas deferens (Vd), spermatophore sac (Ss) and ovary (Ov) were detected by semi-quantitative RT-PCR. The level of actin transcript (550 bp) was also detected as an internal control. The pictures show the inverted images of ethidium bromide stained agarose gels. B) The expression levels of *PmPiw1* in shrimp ovaries at different

stages of ovarian development i.e. undeveloped stage (stage O), pre-developed stage (stage I), early-developed stage (stage II), late developed stage (stage III) and mature stage (stage IV) were determined by real-time PCR (n = 4 each). Expression levels of *PmPiwi1* relative to that of *EF1α* were analyzed by $2^{-\Delta\Delta Ct}$ method and presented as mean ±SEM. C) The expression levels of *PmPiwi1* in the testis of adolescent or immature, sub-adult and adult *P. monodon* (n = 4 each) were determined by RT-PCR and analyzed as mentioned above.

Fig.4. Efficiency of *PmPiwi1* suppression by dsPiwi1.

A) The *PmPiwi1* transcript levels in the testis of dsPiwi1-injected *P. monodon* at 14 dpi were determined by RT-PCR comparing to that of the control (NaCl injected shrimp). *Actin* transcript was amplified as an internal control. The intensity of each band of *PmPiwi1* and *actin* transcripts on the ethidium bromide-stained agarose gel (upper panel) was determined by Scion-Image program and used for the calculation of the relative expression levels of *PmPiwi1* and *actin* as shown in bar graph (lower panel). B) Specificity of *PmPiwi1* suppression by dsPiwi1 is demonstrated by determination of the expression levels of *PmAgo1*, *PmAgo3* and *PmAgo4* cDNAs in dsPiwi1-injected shrimp compared with the control. An asterisk indicates statistical difference between groups as determined by Turkey's test of independent sample t-test from SPSS program ($p<0.05$).

Fig.5. Transposon expression in the testis of *PmPiwi1*-knockdown *P. monodon*.

The expression of *PmPiwi1* in the testis of *P. monodon* was suppressed by the injection of dsPiwi1 as determined by RT-PCR compared to that of the control (NaCl injected shrimp). Actin transcript was amplified as an internal control (upper panel). The expression levels of three types of transposons (*gypsy1*, *gypsy2* and *mariner*-like elements) in the testis of *PmPiwi1*-knockdown shrimp and the control (NaCl-injected shrimp) were determined by

real-time PCR (lower panel). Expression level of each transposon relative to that of *Ef1α* was analyzed by $2^{-\Delta\Delta Ct}$ method and shown as mean ±SEM (n = 6). Asterisk indicates statistical difference between the *PmPiwi1*-knockdown and NaCl-injected groups as analyzed by *t*-test from SPSS program ($p<0.05$).

Fig 6. Numbers of sperms in *PmPiwi1*-knockdown *P. monodon*

DsPiwi1 was injected into male *P. monodon* at 2.5 μg.g^{-1} bw on day 3 after molt, and the testes and spermatophores were collected on day 3 after the next molt. Shrimp injected with dsGFP were used as a control group. A) The efficiency of dsPiwi1 to knockdown *PmPiwi1*expression in the testis was determined by RT-PCR compared to the control shrimp. B) The numbers of sperms in the spermatophore of *PmPiwi1*-knockdown and the control shrimp were counted using the hemacytometer under microscope. Asterisk indicates statistical difference of sperm numbers between both groups as determined by One-way ANOVA from SPSS program ($\rho<0.05$). C) Morphology of spermatophore of the *PmPiwi1*-knockdown shrimp (dsPmPiwi1) and dsGFP-injected shrimp (control) was compared.

A

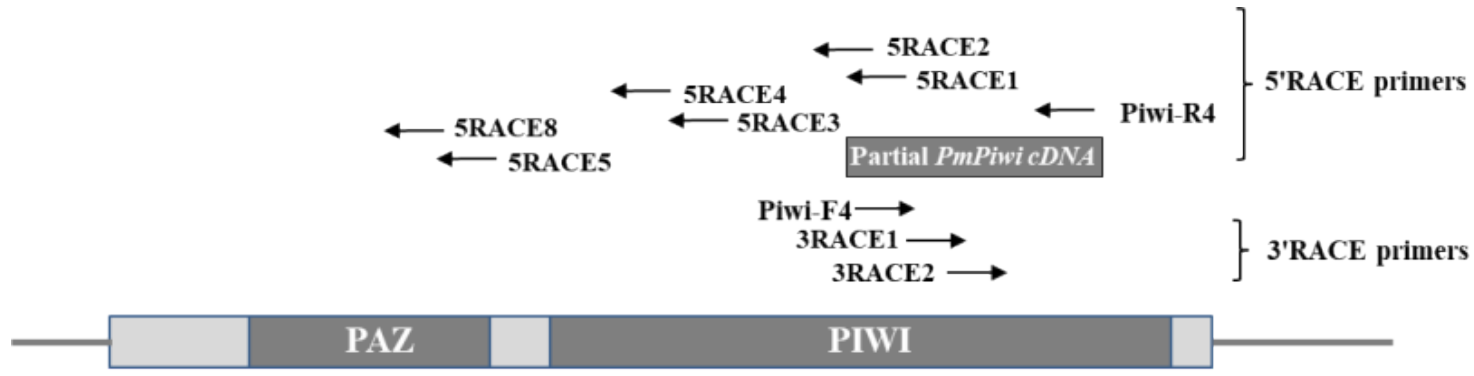

B

```
aacatttgattaccggagaaaaagaccattgaaggacagcagagtgactgacattcaggcagcacaatggatggggacccaactccacca     90
                                                                  M  D  G  D  P  T  P  P
ctgcctcctatgggcaggggggggacgggggggcagctatcttgcgggcactccagtcctcgtctcggcagccaggcacagctggctctagt    180
 L  P  P  M  G  R  G  G  R  G  A  A  I  L  R  A  L  Q  S  S  S  R  Q  P  G  T  A  G  S  S
ctgcccggtcagcaaccagctttgcctccacctgttgtgacgggaggagcaggagttcagtccccagagtgctcaggagcctcggccctg    270
 L  P  G  Q  Q  P  A  L  P  P  P  V  V  T  G  G  A  G  V  Q  S  P  E  C  S  G  A  S  A  L
tcttcccctaggagtcccagcagctccagcattgggtcatcggggagcagccgcggggccctcctgtaccacctgatcaagcagaagagc    360
 S  S  P  R  S  P  S  S  S  S  I  G  S  S  G  S  S  R  G  A  L  L  Y  H  L  I  K  Q  K  S
ggccacaaagctgactcacttcagtctcccttgggggacagttcttctgtggtgccaaagagggcaaaaggacgtggccgtgcggagatc    450
 G  H  K  A  D  S  L  Q  S  P  L  G  D  S  S  S  V  V  P  K  R  A  K  G  R  G  R  A  E  I
ctgcaggcactcaaggtgggctcgctcacatctctcccaggagccaaacctctgagagcagacatgcaagactctagctcacaatcctca    540
 L  Q  A  L  K  V  G  S  L  T  S  L  P  G  A  K  P  L  R  A  D  M  Q  D  S  S  S  Q  S  S
tctgttacggaaagcatgcagcaactgaacatttctgagccccaagagcgcgaggctgtcgtgaacagagggacaagtggattgaagttc    630
 S  V  T  E  S  M  Q  Q  L  N  I  S  E  P  Q  E  R  E  A  V  V  N  R  G  T  S  G  L  K  F
tctgctacatcaagctggatccgactctcagtgaaccctgaaaaggcagtgtttgagtatgaagtcaaatttgaacctcaggtcgatgct    720
 S  A  T  S  S  W  I  R  L  S  V  N  P  E  K  A  V  F  E  Y  E  V  K  F  E  P  Q  V  D  A
cggaacctgcgcttccaccttctcggcactcagagggaaaagctgggatctgtcaagagctttgatggtgtaatgctctggcttccaaca    810
 R  N  L  R  F  H  L  L  G  T  Q  R  E  K  L  G  S  V  K  S  F  D  G  V  M  L  W  L  P  T
catttacctaatgagatcagcattttccaagtcccccaccccatcacgaaagaaaccatgaccatgaaggtgatattcaagaagcgcacc    900
 H  L  P  N  E  I  S  I  F  Q  V  P  H  P  I  T  K  E  T  M  T  M  K  V  I  F  K  K  R  T
tccatggacaagtgcgtccagctttacaatgtcctgtttggccgcatcatgaggatcctcaagatggccagagtgggccagaattactat    990
 S  M  D  K  C  V  Q  L  Y  N  V  L  F  G  R  I  M  R  I  L  K  M  A  R  V  G  Q  N  Y  Y
gctcccagtggatccgtccttgttccgcagcacaagctagagatctggcctgggtatgtaactgctgcgcattatagggaaggcggcgtt   1080
 A  P  S  G  S  V  L  V  P  Q  H  K  L  E  I  W  P  G  Y  V  T  A  A  H  Y  R  E  G  G  V
atgctgtgtgtcgatgtgtcacatagggtcctgcgcacacaaacctgttatgagataatgtctgaaatatttaacaatcgccgaggccag   1170
 M  L  C  V  D  V  S  H  R  V  L  R  T  Q  T  C  Y  E  I  M  S  E  I  F  N  N  R  R  G  Q
ttcaaggaccacgtgattaaggctctggtgggaagcattgttctcacacgctacaacaacaaaacttatcgcattgatgacatcctcttc   1260
 F  K  D  H  V  I  K  A  L  V  G  S  I  V  L  T  R  Y  N  N  K  T  Y  R  I  D  D  I  L  F
gacaagaatcctaggtcgaccttcaccaactcgaaggaggaggaggtgtgttacatggactattacaagaatgcatataacatcactatc   1350
 D  K  N  P  R  S  T  F  T  N  S  K  E  E  E  V  C  Y  M  D  Y  Y  K  N  A  Y  N  I  T  I
aaggacccacagcaacctcttctgctccacagagtgcgaaagaaggaattgaaagaccagggcacgaccaagtttctgtgcctgatccca   1440
 K  D  P  Q  Q  P  L  L  L  H  R  V  R  K  K  E  L  K  D  Q  G  T  T  K  F  L  C  L  I  P
gagctatgctacatgacaggcttgacggacgacatgcgttctgatttccgggtcatgaaggacattgcgcaacacactcgcatcacgcct   1530
 E  L  C  Y  M  T  G  L  T  D  D  M  R  S  D  F  R  V  M  K  D  I  A  Q  H  T  R  I  T  P
aatgtcaggcatgcctctctcagaacctttgtcaggaatgtcaatggatcctcagaagcttggcaggtcttggctgattggggcttagct   1620
 N  V  R  H  A  S  L  R  T  F  V  R  N  V  N  G  S  S  E  A  W  Q  V  L  A  D  W  G  L  A
ctcgacgatgacactttcacaatggaagggcgaattctgacccctgagacgatccactttggttcgagggaagtgcctgggacggaaagt   1710
 L  D  D  D  T  F  T  M  E  G  R  I  L  T  P  E  T  I  H  F  G  S  R  E  V  P  G  T  E  S
gcagactgggggagggagtcggccagagaaaaagtgatcgtgcctatcgacctacggccacagtgctggcagatcttcttctcggcgagg   1800
 A  D  W  G  R  E  S  A  R  E  K  V  I  V  P  I  D  L  R  P  Q  C  W  Q  I  F  F  S  A  R
gatgaggcgcgcgtcctcaagttctcagagatgatccgacaagtcacacgctccatgggcattcaggtggggcctcctcagatgatccgc   1890
 D  E  A  R  V  L  K  F  S  E  M  I  R  Q  V  T  R  S  M  G  I  Q  V  G  P  P  Q  M  I  R
ctcccagatgacaggatcgagacttatgtcaacgggatcaagcagcatttccatgataggctacagctggcagttatcatcttcccagcc   1980
 L  P  D  D  R  I  E  T  Y  V  N  G  I  K  Q  H  F  H  D  R  L  Q  L  A  V  I  I  F  P  A
cagcgtgaggatcggtattcagctgtgaagcgtctggcctgtgtggatcttggcttgccgacacagtgcattaactcacgcaccatcagc   2070
 Q  R  E  D  R  Y  S  A  V  K  R  L  A  C  V  D  L  G  L  P  T  Q  C  I  N  S  R  T  I  S
caggagaacaaactgcgctctgtcacacagaagattgcactgcagatcaattgcaagttgggtggggagctgtgggctctcaagatcccc   2160
 Q  E  N  K  L  R  S  V  T  Q  K  I  A  L  Q  I  N  C  K  L  G  G  E  L  W  A  L  K  I  P
atgacaggacttatggtatgtggtgtggatgtgtaccacgaccctgtccgtcgtggggcctctgtggtaggctttgtggcatcaaccaac   2250
 M  T  G  L  M  V  C  G  V  D  V  Y  H  D  P  V  R  R  G  A  S  V  V  G  F  V  A  S  T  N
cagacgctgacccggtggttttcgcatgtcaacttccagcatcccggtgatgagatcgtccatggcctcaagatctcactcctacaggcc   2340
 Q  T  L  T  R  W  F  S  H  V  N  F  Q  H  P  G  D  E  I  V  H  G  L  K  I  S  L  L  Q  A
ctcaggcattaccataagcaacaccactccctcccccgcaccatcatcatctaccgcgacggcgtgagcgagggccagatgcgggtagtg   2430
 L  R  H  Y  H  K  Q  H  H  S  L  P  R  T  I  I  I  Y  R  D  G  V  S  E  G  Q  M  R  V  V
gaggagcacgagctgccccagctggccaccatcttccagcacttcgactcgaacgagcccaagttctccttcgtcatcgtgcagaagaag   2520
 E  E  H  E  L  P  Q  L  A  T  I  F  Q  H  F  D  S  N  E  P  K  F  S  F  V  I  V  Q  K  K
atcagcaccaggatcttcgcctcactgaattccgagctggacaaccctccaccgggatccatcatcgaccacggcatcacgcatcgttat   2610
 I  S  T  R  I  F  A  S  L  N  S  E  L  D  N  P  P  P  G  S  I  I  D  H  G  I  T  H  R  Y
tggtatgacttcttcctggtgtcccagcatgtgcgacagagcaccgtggcgcccacacactatgtcgtcctccgtgacggcgggaacctc   2700
 W  Y  D  F  F  L  V  S  Q  H  V  R  Q  S  T  V  A  P  T  H  Y  V  V  L  R  D  G  G  N  L
gaggtggacaatatgcagaggctggcatacaaactcacgcacctctattacaactggcccggaactgttcgggtgccggcgccgtgtcag   2790
 E  V  D  N  M  Q  R  L  A  Y  K  L  T  H  L  Y  Y  N  W  P  G  T  V  R  V  P  A  P  C  Q
atgcacataaactagcttttgtcgacgggcagaatgtgaggaaggaaccttcggatacactctgtgacaagctcttcttcctctgaagt   2880
 Y  A  H  K  L  A  F  V  D  G  Q  N  V  R  K  E  P  S  D  T  L  C  D  K  L  F  F  L  *
ggtgtctgttctcagccgaaaaatagagagaaaaaagaaaaaaagaccatgagaacagagcaagggaaaggtaaaaggttaaaaaaaaga   2970
aaatgtgaaagtgagacc                                                                          2988
```

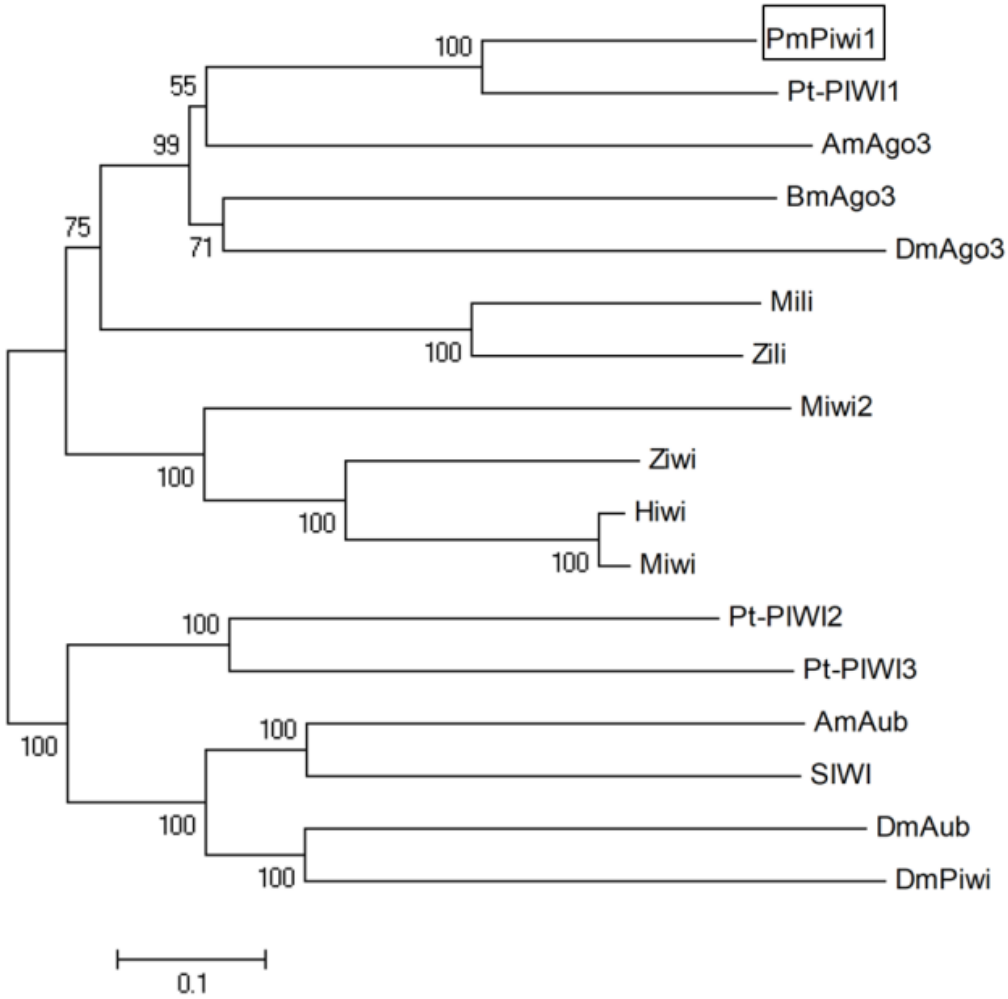
PmPiwi1
Pt-PIWI1
AmAgo3
BmAgo3
DmAgo3
Mili
Zili
Miwi2
Ziwi
Hiwi
Miwi
Pt-PIWI2
Pt-PIWI3
AmAub
SIWI
DmAub
DmPiwi
100
55
99
75
71
100
100
100
100
100
100
100
100
100
100
0.1

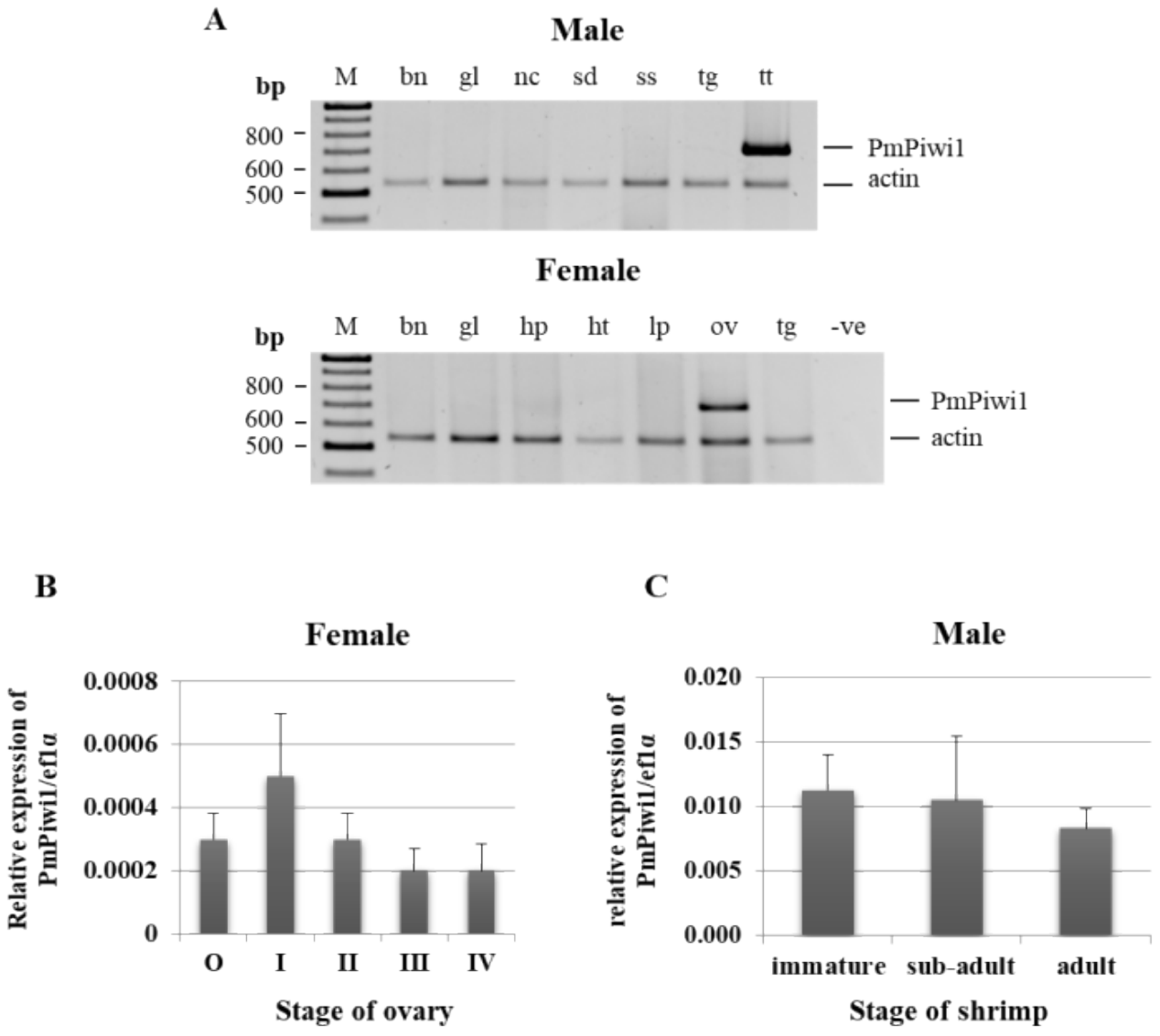
A
Male
bp
M
bn
gl
nc
sd
ss
tg
tt
800
600
500
PmPiwi1
actin
Female
bp
M
bn
gl
hp
ht
lp
ov
tg
-ve
800
600
500
PmPiwi1
actin
B
Female
Relative expression of PmPiwi1/ef1α
0.0008
0.0006
0.0004
0.0002
0
O
I
II
III
IV
Stage of ovary
C
Male
relative expression of PmPiwi1/ef1α
0.020
0.015
0.010
0.005
0.000
immature
sub-adult
adult
Stage of shrimp

A

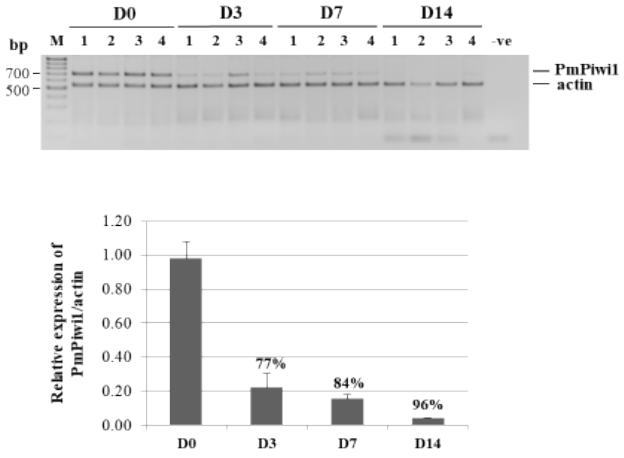
D0
D3
D7
D14
bp
M 1 2 3 4 1 2 3 4 1 2 3 4 1 2 3 4 -ve
700
500
PmPiwi1
actin
Relative expression of PmPiwil/actin
1.20
1.00
0.80
0.60
0.40
0.20
0.00
77%
84%
96%
D0
D3
D7
D14

B

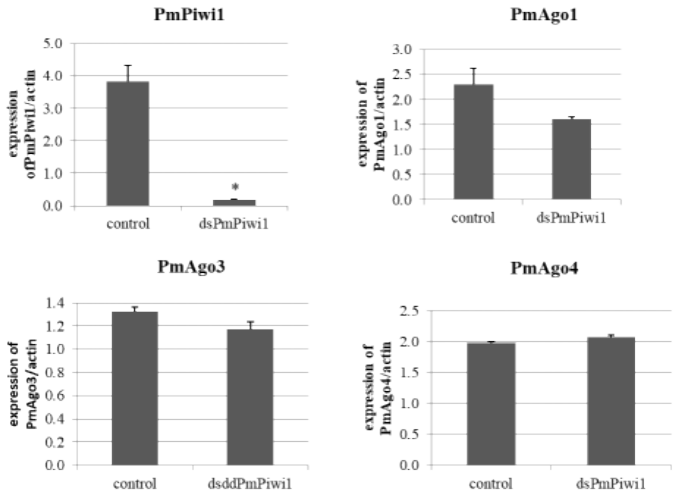
PmPiwi1
expression ofPmPiwil/actin
5.0
4.0
3.0
2.0
1.0
0.0
*
control
dsPmPiwi1
PmAgo1
expression of PmAgo1/actin
3.0
2.5
2.0
1.5
1.0
0.5
0.0
control
dsPmPiwi1
PmAgo3
expression of PmAgo3/actin
1.4
1.2
1.0
0.8
0.6
0.4
0.2
0.0
control
dsddPmPiwi1
PmAgo4
expression of PmAgo4/actin
2.5
2.0
1.5
1.0
0.5
0.0
control
dsPmPiwi1

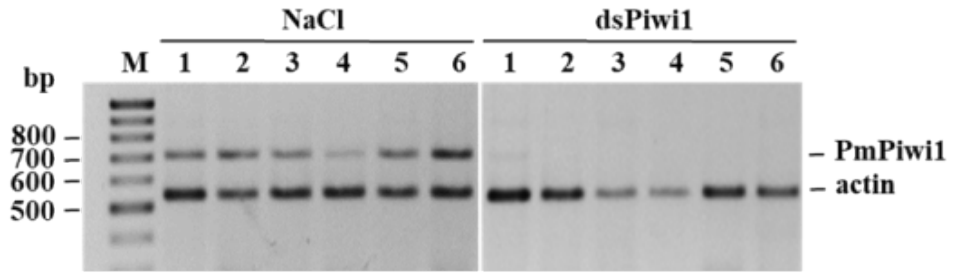
NaCl
dsPiwi1
M 1 2 3 4 5 6 1 2 3 4 5 6
bp
800
700
600
500
PmPiwi1
actin

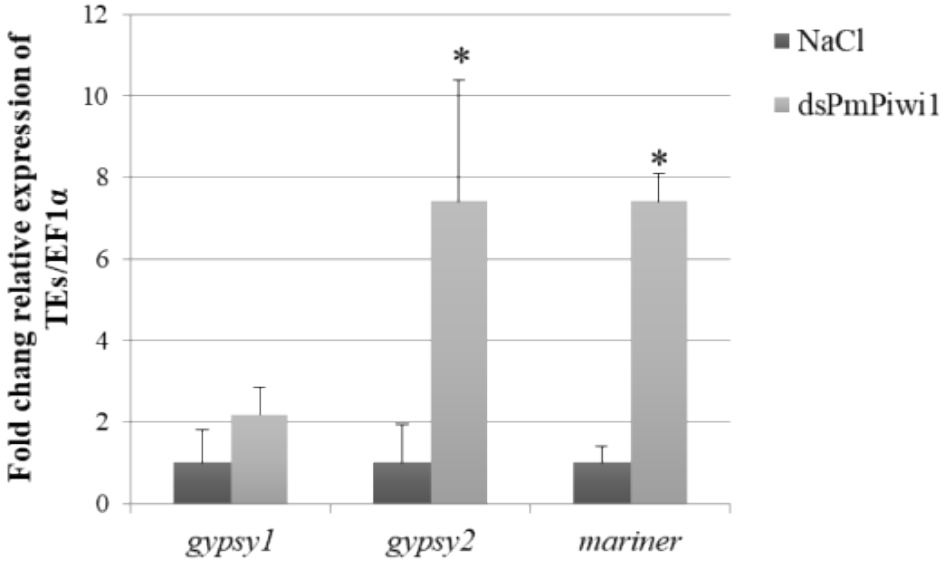
Fold chang relative expression of TEs/EF1α
12
10
8
6
4
2
0
*
*
NaCl
dsPmPiwi1
gypsy1
gypsy2
mariner

A

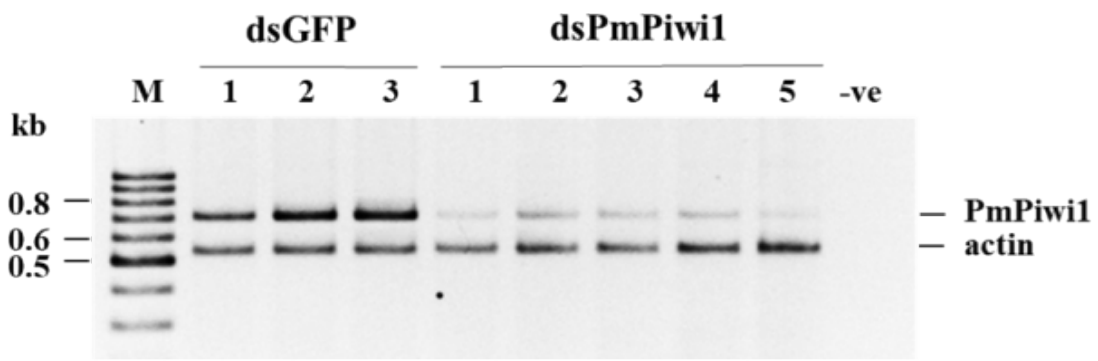
dsGFP
dsPmPiwi1
M
1
2
3
1
2
3
4
5
-ve
kb
0.8
0.6
0.5
PmPiwi1
actin

B

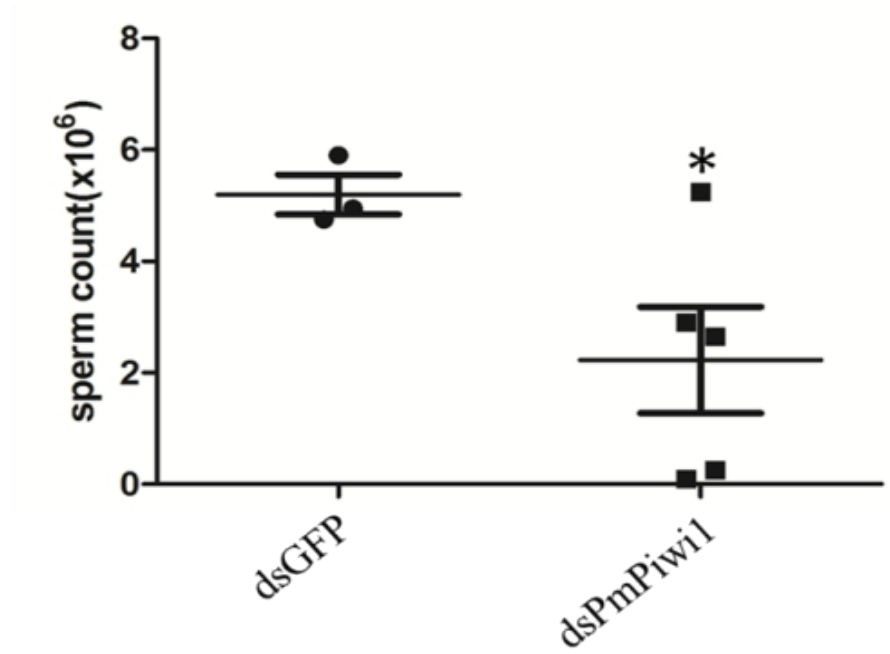
sperm count(x10^6)
8
6
4
2
0
*
dsGFP
dsPmPiwi1

C

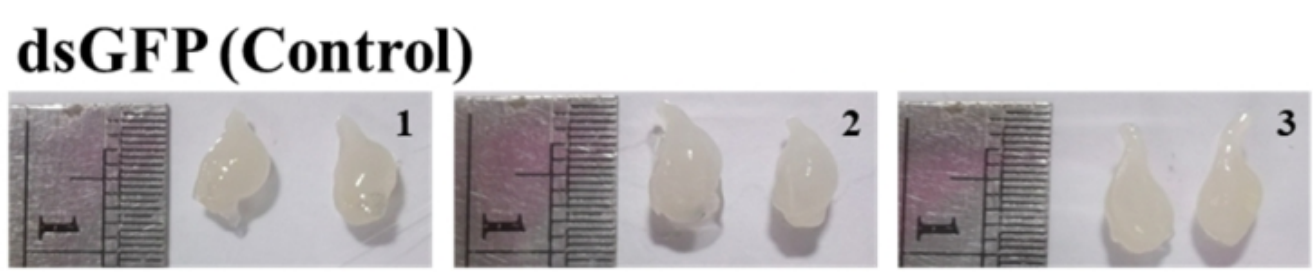
dsGFP (Control)
1
2
3

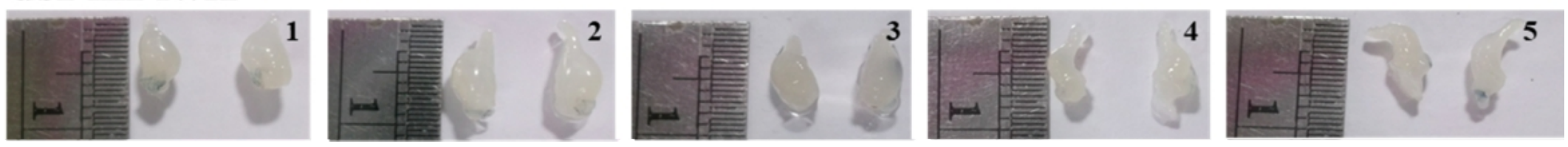
dsPmPiwi1
1
2
3
4
5

Table 1 Primers used in this study and their nucleotide sequences

Primer name	Primer sequence (5' to 3')	Experiment
oligo dT	CCGGAATTCAAGCTTCTAGAGGATCCTTT TTTTTTTTTTTTT	Cloning, mRNA expression and detection of PmPiwi1 knockdown
PM1	CCGGAATTCAAGCTTCTAGAGGATCC	
Actin-F	GACTCGTACGTGGGCGACGAG	
Actin-R	AGCAGCGGTGGTCATCTCCTGCTC	
Piwi-F4	TACCGCGACGGCGTGAGCGAG	
Piwi-R4	CAAAAGCTAGTTTATGTGCAT	
5RACE1	TAACGAGCGTGATGCCGTCGTG	
5RACE2	CGAGTCGAAGTGCTGGAAGA	
5RACE3	AATACCGATCCTCACGCTGG	
5RACE4	ATGGAGCGTGTGACTTGTCG3	
5RACE5	GAGGATCCATTGACATTCCTGAC	
5RACE8	GCCAGATCTCTAGCTTGTGC	
Piwi1-3RACE1	GATCAGCACCAGGATCTT	
Piwi1-3RACE2	TGGCCTCAAGATCTCACTCC	
Coding-F1	ATGAAGGTGATATTCAGGAAGCG	
Coding-F2	ATGGATGGGGACCCAACTCC	
Coding-R	TCAGAGGAAGAAGAGCTTGTCA	
Sense-XbaI-F	GCTCTAGACCACGTGATTAAGGCTCTGG	dsRNA-PmPiwi1 synthesis
Sense-HindIII-R	CCCAAGCTTGGATCCATTGACATTCCTGAC	
dsPAZ-anti-XhoI-F	CCGCTCGAGCCACGTGATTAAGGCTCTGG	
dsPAZ-anti-Hind-R	CCCAAGCTTTGTCATGTAGCATAGCTCTGG	
MarinerF	CGGTTGGGAGAATAGGCAAATCA	Transposable elements expression
MarinerR	CCTTACAAACTGACGTTGATGGC	
GyPemo1bF	CTACAGCACCAACAACGTCCAA	
GyPemo1bR	CGTTTCCTCAAGCTGTATGAGGTG	
GyPemo2F	GATGCCTCAAACCTCGGGCT	
GyPemo2R	AGTGACGGAGGGCCCATGTG	
EF1αF	GAACTGCTGACCAAGATCGACAGG	
EF1αR	GAGCATACTGTTGGAGGTCTCCA	

Table 2 Percentage of similarity between *P. monodon* Piwi1 and other homologues

		***P. monodon*'s Piwi1**		
		ORF	**PAZ domain**	**PIWI domain**
P. trituberculatus	Piwi-1	59.6	65.2	74.7
	Piwi-2	33.2	45.7	46.6
	Piwi-3	29.7	41.3	44.9
B. mori	Siwi	29.4	42.4	40.6
	Ago3	40.1	33.9	54.3
A. mellifera	Aub	29.2	32.5	43.2
	Ago3	40.5	42.4	53.2
D. melanogaster	Piwi	29.1	36.3	38.7
	Aub	29.0	30.3	38.7
	Ago3	35.5	43.5	50.0
M. musculus	Miwi	34.4	37.4	44.7
	Mili	35.8	33.0	52.7
	Miwi2	29.0	47.8	38.7
D. rerio	Ziwi	36.3	42.4	51.2
	Zili	34.7	44.1	51.0